EDGEWOOD
RESEARCH, DEVELOPMENT & ENGINEERING CENTER
U.S. ARMY CHEMICAL AND BIOLOGICAL DEFENSE COMMAND

ERDEC-CR-114
(GC-TR-93-2194)

IMPROVED FILTRATION MATERIALS AND MODELING

Amanda B. Brady
Charles L. Dawson, III
Michele M. Farris
Stephen E. Harper
Narasimhan Sundaram
David K. Friday

GEO-CENTERS, INC.
Newton Centre, MA 02159

June 1994

Approved for public release; distribution is unlimited.

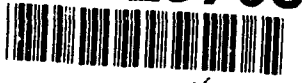

Aberdeen Proving Ground, MD 21010-5423

Disclaimer

The findings in this report are not to be construed as an official Department of the Army position unless so designated by other authorizing documents.

REPORT DOCUMENTATION PAGE

Form Approved
OMB No. 0704-0188

1. AGENCY USE ONLY *(Leave blank)*	2. REPORT DATE	3. REPORT TYPE AND DATES COVERED
	1994 June	Final, 90 Aug - 93 Aug

4. TITLE AND SUBTITLE

Improved Filtration Materials and Modeling

5. FUNDING NUMBERS

C-DAAA15-90-C-1056

6. AUTHOR(S)

Brady, Amanda B.; Dawson, Charles L., III; Farris, Michele M.; Harper, Stephen E.; Sundaram, Narasimhan; and Friday, David K.

7. PERFORMING ORGANIZATION NAME(S) AND ADDRESS(ES)

GEO-CENTERS, Incorporated, 7 Wells Avenue,
Newton Centre, MA 02159

8. PERFORMING ORGANIZATION REPORT NUMBER

ERDEC-CR-114
(GC-TR-93-2194)

9. SPONSORING/MONITORING AGENCY NAME(S) AND ADDRESS(ES)

DIR, ERDEC,* ATTN: SCBRD-RTE, APG, MD 21010-5423

10. SPONSORING/MONITORING AGENCY REPORT NUMBER

11. SUPPLEMENTARY NOTES

COR: Dr. David E. Tevault, SCBRD-RTE, (410) 671-8400

(Continued on page ii)

12a. DISTRIBUTION/AVAILABILITY STATEMENT

Approved for public release; distribution is unlimited.

12b. DISTRIBUTION CODE

13. ABSTRACT *(Maximum 200 words)*

This report highlights the important results obtained during the performance period of Contract No. DAAA15-90-C-1056. The reported results are divided into the following five major subject areas: (1) single component isotherm, (2) multi-component isotherm, (3) breakthrough/rate processes, (4) Pressure Swing Adsorption (PSA), and (5) other results. Within each subject area, significant results are highlighted and supported with a brief discussion. The letter-number identifier following each highlight corresponds to an appendix that contains the GEO-CENTERS quarterly report which gives a more detailed discussion of that particular highlight. Referring to the quarterly report also gives specific references for obtaining further background information.

14. SUBJECT TERMS		15. NUMBER OF PAGES
Adsorption	PSA	248
Isotherm	Air purification	16. PRICE CODE

17. SECURITY CLASSIFICATION OF REPORT	18. SECURITY CLASSIFICATION OF THIS PAGE	19. SECURITY CLASSIFICATION OF ABSTRACT	20. LIMITATION OF ABSTRACT
UNCLASSIFIED	UNCLASSIFIED	UNCLASSIFIED	UL

11. SUPPLEMENTARY NOTES (Continued)

*At the time this work was started, ERDEC was known as the U.S. Army Chemical Research, Development and Engineering Center, and the Contracting Officer's Representative was assigned to the Research Directorate.

PREFACE

The work described in this report was authorized under Contract No. DAAA15-90-C-1056. This work was started in August 1990 and completed in August 1993.

The use of trade names or manufacturers' names in this report does not constitute an official endorsement of any commercial products. This report may not be cited for purposes of advertisement.

This report has been approved for release to the public. Registered users should request additional copies from the Defense Technical Information Center; unregistered users should direct such requests to the National Technical Information Service.

Acknowledgment

The authors gratefully acknowledge the many administrative contributions of Billie Little. Her preparation, editing, and proof-reading of manuscripts are appreciated.

Blank

TABLE OF CONTENTS

APPENDICES

Blank

IMPROVED FILTRATION MATERIALS AND MODELING

1.0 INTRODUCTION

This report highlights the important results obtained during the performance period of Contract # DAAA 15-90-C-1056, "Improved Filtration Materials and Modeling". The results are divided into the following five major subject areas: namely, (1) single component isotherm, (2) multi-component isotherm, (3) breakthrough/rate processes, (4) Pressure Swing Adsorption (PSA), and (5) other results. Within each subject area, significant results are highlighted and supported with a brief discussion. The letter-number identifier (e.g. A-1, A-2, etc.) following each highlight corresponds to an appendix that contains the relevant GEO-CENTERS quarterly report. The quarterly report gives a more detailed discussion of that particular highlight. Referring to the quarterly report also gives specific references for obtaining further background information.

2.0 TECHNICAL RESULTS AND DISCUSSION

2.1 Single Component Isotherm

- PFCBa adsorption equilibria on three different adsorbents are measured. (A-1)

Single component isotherms for perfluorocyclobutane (PFCBa) were measured on BPL carbon, ASC carbon, and 13X molecular sieve. Results of this study demonstrated that there are significant differences in PFCBa capacities for each adsorbent. Over certain concentration ranges, the capacity of BPL carbon is more than twice that of the 13X.

- Effect of impregnants on adsorption capacity is shown using two different adsorbates on substrate, ASC and ASC-T carbons. (A-2)

Adsorption isotherms of two adsorbates, R-113 and PFCBa, were measured on three adsorbents. Results showed that the impregnation process does not significantly affect the heat of adsorption, but it does reduce the adsorption capacity. This study also showed that ASC isotherms may be predicted from substrate isotherms by modifying the saturation capacity of a slightly different version of the Modified Antoine Equation.

- The water isotherm system is modified to maintain a more stable challenge RH. (A-2)

Room temperature excursions resulted in condensation in lines to the adsorbent samples. Modifications to the water isotherm apparatus were made to minimize these problems and prevent condensation from forming on the adsorbent sample.

- Major modifications to the procedure for preparing 13X molecular sieve for isotherm measurements yield reproducible data. (A-3)

Isotherm data for PFCBa on Davison 13X molecular sieve showed a considerable amount of scatter. It was determined that the likely reason was due to small amounts of adsorbed water. The operating procedures were modified to remove residual water collected on the 13X during the weighing process. This new procedure produced nearly duplicate PFCBa/13X isotherms.

- The volumetric isotherm system is modified to improve reproducibility and accuracy of data measurements. (A-4)

The adsorbent sample holder was placed in a temperature controlled water bath to minimize the effects of room temperature changes on the results. Changes in room temperature of 1-2 K result in isotherm loadings which can easily be detected with this system. A program was written in Pascal which provides for user defined mass injections and computer controlled isotherm temperatures.

- Isotherms measured at 25°C for R-113 on a super-activated carbon and BPL cross at about 5.0 mg/liter vapor-phase concentration. (A-4)

Water isotherms measured for each carbon indicate that the super-activated carbon has a total pore capacity almost twice that of the BPL carbon. This is consistent with nitrogen BET surface area results. However, R-113 isotherm data measured at 25°C show that the isotherms for BPL and the super-activated carbon cross at a vapor-phase concentration of about 5.0 mg/liter. Below 5.0 mg/liter the capacity of the BPL carbon is larger. There are significant system design implications in this result.

- R-22 BPL isotherm data are measured. (A-6)

Isotherm data for R-22 on BPL carbon were measured and compared to previously measured data for PFCBa and R-113 on BPL activated carbon to demonstrate the effect of boiling point on adsorption capacity at a given partial pressure. For example, for a vapor-phase concentration of 100 mg/m^3, the loading of R-113 (b.p. = 47°C) is about 10 times that of PFCBa (b.p. = -5°C), and the loading of PFCBa is about 10 times that of R-22 (b.p. = -40°C).

- Isotherm data for R-113 on 13X molecular sieve are measured at 25°C. (A-6)

The loading of R-113 showed only a small increase (0.10 to 0.15 g/g) over more than 2 orders of magnitude of vapor-phase concentration (1,000 to 100,000 mg/m^3). The design implication is that systems employing 13X may be overwhelmed at high feed concentrations, since the adsorption capacity does not increase appreciably with increasing vapor-phase concentrations.

- R-22 isotherm data measured on 13X molecular sieve at three temperatures. (A-7)

Isotherm data measured for R-22 on 13X at 25°C, 50°C, and 75°C were compared to isotherm data at the same temperature for R-22 on BPL carbon. This marked the first time that 13X showed a higher capacity for a chemical vapor than BPL. It also demonstrated that volatile, polar gases may require an adsorbent other than carbon. This was the first evidence that multiple adsorbents (layered beds) would be needed to provide protection against the broad spectrum of chemical threats.

- R-11 isotherms are measured on BPL carbon at three temperatures. (A-8)

Results show unusually high loadings for the high vapor-phase concentrations employed. There is a suspicion that the calibration for the R-11 is not accurate over the full range of vapor-phase concentrations employed.

- Flame Ionization Detector (FID) response is more sensitive at higher R-11 concentrations. (A-9)

These results explained the anomalous behavior observed for the R-11/BPL system in quarterly report number 08. Modification of the calibration function used to convert area counts to mass of chemical in the closed-loop circulation system was required. R-11 is the only chemical used which behaves this way with the FID.

- UOP 13X molecular sieve is found to be far superior to the Davison 13X. (A-9)

To this point during the contract, all experiments using 13X molecular sieve were performed with the Davison 13X molecular sieve. Results of Guild PSA full-scale testing with UOP 13X showed dramatically better performance than the lab-scale results with the Davison 13X. Isotherm experiments in the laboratory using R-11 as the adsorbate confirmed that the

capacity of the UOP 13X is about two times greater than the Davison 13X over the range of concentrations used in the PSA experiments.

Single Component Isotherm Reference List

1. Mahle, J.J., Buettner, L.C., and Friday, D.K., "Measurement and Correlation of the Adsorption Equilibria of Refrigerant Vapors on Activated Carbon", Ind. Eng. Chem. Chem. Res., Submitted May 1993.

2. Sundaram, N., "A Modification of the Dubinin Isotherm", *Langmuir*, Vol. 9, No. 6, (1993).

3. Carlile, D.C., Buettner, L.C., Tevault, D.E., and Friday, D.K., "CFC-113 Adsorption Equilibrium Data on ASC Whetlerite and BPL Carbon", 1992 ERDEC Conference on Chemical Defense given Nov 17, 1992.

4. Sundaram, N., Friday, D.K., Buettner, L.C., and Mahle J.J. "Development of a Pore-Filling Adsorption Equilibrium Model", 1992 ERDEC Conference on Chemical Defense given Nov 17, 1992.

5. Mahle, J.J., Buettner, L.C., and Friday, D.K. "A Gravimetric Technique for Measurement of Isotherms of Strongly Adsorbed Vapors", 1992 ERDEC Conference on Chemical Defense given Nov 17, 1992.

6. Mahle, J.J., Friday D.K., Mann, R., and Yousef, H. "Interpretation of Adsorption Isotherm Hysteresis for an Activated Charcoal Using Stochastic Pore Networks", CRDEC-TR-407, September 1992.

7. Carlile, D.L. and Friday, D.K., "1,1,2 Trichloro-1,2,2-Triflouroethane (CFC-113) and Water Isotherm Measurements on Impregnated and Unimpregnated Activated Carbons", CRDEC-TR-349, July 1992.

8. Brady, A. B., Friday, D. K., Carlile, D. L., and Buettner, L. C., "Adsorption Equilibria for Simulant Vapors on 13X Molecular Sieve", Proceedings of the 1991 U.S. Army Chemical Research, Development and Engineering Center Scientific Conference on Chemical Defense Research, 19-22 November, 1991.

9. Wang, C . C., Buettner, L. C., Carlile, D. L, and Friday, D. K., "Single Component Isotherm Measurement with the Cahn Microbalance", Proceedings of the 1991 U.S. Army Chemical Research, Development and Engineering Center Scientific Conference on Chemical Defense Research, 19-22 November, 1991.

10. Mahle, J. J., Buettner, L. C., Friday, D. K., and Rossin, J., "New Reactive Adsorbent Development Program: Mechanistic Studies", CRDEC TR-324, CONFIDENTIAL Report, September 1992.

11. Friday, D. K., Mahle, J. J., Buettner, L. C., Carlile, D. L., and Brady, A. B., "Adsorption Equilibria of CFC-113 and PFCB on Impregnated and Unimpregnated Adsorbents", Proceedings of the 1990 U.S. Army Chemical Research, Development and Engineering Center Scientific Conference on Chemical Defense Research, 13-16 November, 1990.

2.2 Multi-Component Isotherm

- R-113 isotherm data are measured on BPL carbon at three different relative humidities. (A-4)

These represented the initial results using the multi-component isotherm system with cryogenic recovery to quantify loadings. R-113 data was measured at 60%, 70%, and 80% RH over about two orders of magnitude of R-113 vapor-phase concentration.

- The Miller-Nelson is replaced with a temperature-controlled sparging unit for more precise RH control. (A-5)

A sparging unit was designed and assembled to fit into a temperature-controlled water bath. By setting the temperature of the water bath and using a mass flow controller to meter the sparging gas (usually nitrogen), precise control of the feed dew point was achieved. Swings in the RH that are a natural consequence of the Miller-Nelson control scheme were eliminated.

- The multi-component system is reconfigured to improve operating efficiency. (A-8)

Two four-way valves were installed in the system to facilitate the calibration portion of the experimental procedure. Problems with inconsistent and erroneous results prompted a complete system rebuild for more effective troubleshooting. In addition, work was performed

to insure that the four-way valves are switched in the correct sequence when changing to the next step in the procedure.

- PFCBa and water on BPL carbon data are measured. (A-9)

PFCBa isotherms were measured over four orders of magnitude of PFCBa vapor-phase concentrations at 80% RH, 60% RH, 40% RH and dry (about -40°C dew point) conditions. The results for the PFCBa under dry conditions matched well with the PFCBa/BPL carbon isotherms measured using the single component system. The data measured at the three RH's demonstrated the dramatic effect of co-adsorbed water. For example, at a PFCBa concentration of 1.0 mg/liter, the loading of PFCBa at 80% RH is only 0.0006 g/g, or about 100 times lower than the loading of PFCBa under dry conditions. Even at 60% RH, the PFCBa loading is less than 20% of the dry PFCBa loading.

- PFCBa/water isotherm data measured on UOP 13X. (A-10)

Initial isotherm experiments were performed on UOP 13X and compared with PFCBa data on BPL. Dry UOP 13X and dry BPL carbon have about the same adsorption capacity between PFCBa vapor-phase concentrations of 1.0 mg/liter and 10.0 mg/liter. Below about 0.5 mg/liter, the adsorption capacity of 13X falls precipitously. Thus, even under dry conditions, 13X would not be expected to perform well against chemicals which adsorb similar to PFCBa. Preliminary studies at different RH's demonstrate that 13X capacity is severely reduced at 20% RH.

- Internal leaks in four-way valves result in inaccurate water loadings. (A-11)

Unrealistic water loadings were measured in several experiments. A series of trouble-shooting experiments were conducted to identify the source(s) of the problem. It was determined that water was entering the "closed-loop" desorption system through internal leaks in the four-way valves located above and below the bed. The leak problem was solved by placing two-way valves on the challenge side of the two four-way valves in question and closing them during the desorption and analysis phases. A careful examination of the circulating pump also revealed a small leak, so the pump was replaced.

Multi-Component Isotherm Reference List

1. Farris, M.M., Dawson, C.L. and Friday, D.K., "Multi-Component Adsorption Equilibria for Perfluorocyclobutane (PFCBa) and Water on BPL Carbon", 1992 ERDEC Conference on Chemical Defense given Nov 17, 1992.

2. Matuszko, R. A., Friday, D. K., and Lamontagne, R. A., "Prediction of Binary Vapor Adsorption for a Hexane-Water Mixture on Activated Carbons", Proceedings of the 1991 U.S. Army Chemical Research, Development and Engineering Center Scientific Conference on Chemical Defense Research, 19-22 November, 1991.

2.3 Breakthrough/Rate Processes

- Axial dispersion is identified as a major contributor to the spreading of the adsorption wave in single-pass systems. (A-2)

A study was conducted using R-113 on BPL carbon to determine the controlling rate processes in shallow-bed adsorbers (e.g., gas masks). Adsorption isotherms, internal particle mass transfer rates and external particle mass transfer rates for R-113 and BPL carbon were measured and correlated. Results of breakthrough experiments indicate that axial dispersion contributes significantly to the premature breakthrough observed in shallow-bed adsorbers.

- The breakthrough apparatus is modified to maintain a constant temperature. (A-3)

Room temperature fluctuations affected the breakthrough results to the extent that axial dispersion coefficients could not be reliably calculated. An important modification to the system was made to keep the bed at a constant temperature. Breakthrough data measured using the temperature control system were much more consistent.

- The first phase of axial dispersion work is completed. (A-4)

Three important conclusions are generated from a study of axial dispersion using three different challenge vapors on BPL carbon. These conclusions are: (1) Axial dispersion can control the breadth of the breakthrough curve even for deep beds, (2) If one employs the Fickian model, then the axial dispersion coefficient is a function of the shape of the adsorption isotherm. In addition, the Fickian model cannot represent the breakthrough behavior of very strongly adsorbed vapors, and (3) Axial dispersion is affected by the bed diameter under certain

conditions, with smaller diameter beds exhibiting sharper breakthrough curves (smaller axial dispersion coefficients) than larger diameter beds.

- Axial dispersion may not be effectively characterized in PSA systems using the Fickian model. (A-8)

Problems with the Fickian model surfaced again. For systems with a reasonable axial dispersion coefficient and a moderate cycle time (30 seconds), model results showed that the concentration at the bed inlet did not reach the feed concentration. This initiated an effort to characterize dispersion in a more rigorous manner using a physically correct mathematical description.

Breakthrough/Rate Processes Reference List

1. Mahle, J.J. and Friday, D.K. "Axial Dispersion Effects on the Breakthrough Behavior of Favorably Adsorbed Vapors", *Recents Progres en Genie des Procedes*, No. 17, Volume 5, Adsorption Processes for Gas Separation, (1991).

2. Mahle, J. J., Buettner, L. C., and Friday, D. K., "Modelling Axial Dispersion in Shallow Bed Filters", Proceedings of the 1990 U.S. Army Chemical Research, Development and Engineering Center Scientific Conference on Chemical Defense Research, 13-16 November, 1990.

3. Newton, R. A. and D. K. Friday, "Breakthrough Times of Cyanogen Chloride on Layered and Mixed Beds of ASC Whetlerite", Proceedings of the 1990 U.S. Army Chemical Research, Development and Engineering Center Scientific Conference on Chemical Defense Research, 13-16 November, 1990.

4. Mahle, J. J., Friday, D. K., and Buettner, L. C., "A Methodology to Evaluate the Performance of Shallow-Bed Adsorbers", American Institute of Chemical Engineers' Annual National Meeting, Chicago, IL, November, 1990.

2.4 Pressure Swing Adsorption (PSA)

- BPL is shown to be much better than Davison 13X using R-113 as the challenge vapor. (A-2)

Initial PSA experiments measuring product, purge, and feed concentrations demonstrated that Davison 13X was much poorer than BPL. There was immediate breakthrough of R-113 in the product for the 13X experiment, while no measurable product concentration (about 5 mg/m^3) was detected for the BPL system until four hours. Periodic-state product concentrations were 1200 mg/m^3 for the 13X and 150 mg/m^3 for the BPL.

- Apparatus and procedures are developed to accurately measure an overall material balance. (A-3)

Internal leaks in 3-way valves used to direct flows caused feed material to exit the system in the purge without passing through the adsorbing bed. This problem was solved by re-packing valves and instituting a program to periodically replace the valve packings. Surge tanks were placed on the product and purge streams to help average the concentration fluctuations caused by changing pressures.

- The effect of conditioning time (water loading), purge to product ratio, and chemical vapor on the performance of a system using only 13X as the adsorbent is demonstrated. (A-4)

Experiments were performed with a PFCBa challenge. Initial experiments demonstrated that PSA systems using only 13X could suffer a large decrease in performance with long conditioning times. A comparison of system performance against PFCBa and R-113 under identical operating conditions using 13X was conducted. Results showed that PFCBa began breakthrough 200 minutes prior to the R-113. The effect of the purge to product flow ratio was studied using PFCBa on 13X with 15 minutes of pre-conditioning. Two purge to product ratios, 0.855 and 1.21, were used with the larger purge showing a dramatic improvement in performance. This was the first data measured which showed the sensitivity of system performance to the purge to product ratio.

- The in-bed sampling system is constructed (A-4) and used to measure data. (A-5)

A new sampling system was developed to measure in-bed vapor-phase concentrations during PSA cycles. The system is the first of its kind. For those experiments where no chemical is measured in the product, in-bed concentration measurements provide critical design information. Experiments were performed using R-113 on BPL carbon to examine the effects of the purge to product ratio.

- The PSA mathematical model is modified to include axial dispersion. (A-5)

At this time it was thought that differences between model results and measured data could be attributed to axial dispersion. Math model results show that breakthrough times and separation efficiencies can be greatly affected by the value of the axial dispersion coefficient.

- PSA parametric study is performed using R-113/BPL system. (A-7)

Three important PSA parameters were systematically investigated using a challenge vapor of about 4.0 mg/liter of R-113 to beds packed with 12x30 mesh BPL carbon. These parameters were: (1) pressure ratio, (2) purge to product flow ratio, and (3) cycle time. It was found that the system performance was most sensitive to the purge to product flow ratio over the range of conditions tested. The pressure ratio had a much greater effect on performance between 3:1 and 4:1 than it did between 4:1 and 5:1. The cycle time results showed only relatively small changes in performance between cycle times of 20 seconds and 3 minutes. The best system performance was obtained using a cycle time of 60 seconds. These results proved that the cycle time, in particular a shorter cycle time, is <u>not</u> a viable method of improving protection capability of a PSA system.

- The PSA mathematical model is improved by adding an energy balance and a correct physical description of the two-step cycle. (A-7)

Temperature profiles measured during PSA cycles led to changes in the PSA math model code. A differential energy balance was added to the model along with some equations to correctly simulate the pressurization and blowdown portions of the two-step cycle. Initial model results showed only small temperature changes. An overall calculation of energies from gas compression and decompression were consistent with the model results. An investigation into the phenomena responsible for the observed temperature behavior was initiated.

- Air adsorption/desorption is shown to be primarily responsible for measured temperature swings during PSA cycles. (A-8)

Using a series of different packings and feed gases, it was determined that air adsorbing and desorbing during the pressurization and blowdown steps was responsible for the observed temperature swings during PSA cycles. These temperature swings could be as large as 15°C, and were shown to have a dramatic effect on system performance. This required that the PSA math model correctly characterize air adsorption in order to successfully describe PSA system performance.

- PSA experiments are performed using R-11 on BPL and 13X molecular sieve. (A-8)

Experiments using each adsorbent showed that the BPL carbon provided superior protection against R-11 than the 13X. For example, at a bed depth of 20 cm, the breakthrough time for the BPL system was approximately 7 times longer than that of the 13X-based system.

- The solution method for the PSA mathematical model is changed. (A-8)

Up to this point, orthogonal collocation was used to solve the partial differential equations which comprise the material and energy balances and rate processes. However, this method gives rise to solutions which oscillate at low concentrations. The concentrations where these oscillations begin are typically close to, or even higher than, the concentrations of military interest. It was decided that an alternative solution method should be used.

- PSA results demonstrate dramatic performance differences between UOP 13X and Davison 13X. (A-9)

A side-by-side comparison of the UOP 13X and Davison 13X was performed using the laboratory-scale PSA system under identical operating conditions. For the Davison 13X, there is almost an immediate breakthrough of R-22 at 10 cm, while for the UOP 13X, breakthrough does not occur at 10 cm until 300 minutes (600 cycles). R-22 is measured in the product for the Davison 13X after about 225 minutes. For the UOP 13X, R-22 is not detected in the product until about 2775 minutes!

- The behavior of water vapor in PSA systems using BPL carbon and UOP 13X is characterized. (A-9)

Experiments were performed using water as the feed chemical. Water vapor concentrations were measured using a thermal conductivity detector. Results demonstrate that water quickly reaches a periodic-state with BPL carbon and that a significant separation can be achieved. For the conditions used in this study, the ratio of the product water vapor concentration to the feed water vapor concentration is less than 0.1. Results also showed that the RH is reduced from the feed of 80% to less than 40% RH between the 5-cm and 10-cm bed depths. Similar experiments were performed using UOP 13X. It was shown that the depth of water penetration into a bed of 13X is critically dependent on the purge flow rate. It was also demonstrated that increasing the purge flow could clean up adsorbent which had been contaminated with water. These results were the first to demonstrate that 13X could be used in a PSA system, providing the purge flow rate was high enough.

- Water behavior in PSA systems using UOP 13X is examined at higher feed pressures. (A-10)

A study of PSA performance using water/13X was conducted to determine if higher feed pressures (and, by definition, higher pressure ratios) could provide a significant improvement in system performance. Using temperature measurements to infer the presence of contaminants, it was demonstrated that higher pressures do not significantly improve performance. The main benefit of a higher feed pressure is that less absolute column volumes of gas are needed to effectively desorb material during the purge step.

- R-11/BPL carbon experiments are performed to correlate temperature swings with the mass transfer front. (A-11)

These data constitute some of the most important results of the contract effort. Experiments were performed using R-11 on BPL carbon. In-bed concentration measurements were correlated with the magnitude of the temperature change at a given axial position in the bed. The conditions for the experiment and the sampling procedures are given in the quarterly report. Two critical results were observed. First, a direct correlation between the position of the advancing mass-transfer front and the reduction of the temperature swings was observed. Second, a slight rise in the temperature swings was measured just prior to the first measurable concentration at each axial position.

PSA Reference List

1. Mahle, J.J., Friday, D.K., and LeVan, M.D.,"Preliminary Pressure Swing Adsorption for Air Purification Math Model in Support of Armored Vehicle Applications", ERDEC-TR-082, June 1993.

2. Mahle, J.J., Buettner, L.C., Friday, D.K., and Brady, A.B.,"Laboratory Scale Pressure Swing Adsorption System", ERDEC-TR-067, May 1993.

3. Brady, A.B., Dawson, C.L., and Friday, D.K., "Measurement of In-Bed Temperature Profiles During Pressure Swing Adsorption Cycles", 1992 ERDEC Conference on Chemical Defense given Nov 17, 1992.

4. Friday, D.K., Brady, A.B., Mahle, J.J., and Buettner, L.C., "A Parametric Study of PSA for Air Purification Applications", 1992 ERDEC Conference on Chemical Defense given Nov 17, 1992.

5. Mahle, J.J., Friday, D.K., Sundaram, N., and LeVan, M.D., "Non-Isothermal Behavior of PSA for Air Purification", 1992 ERDEC Conference on Chemical Defense given Nov 17, 1992.

6. Friday, D. K., LeVan, M. D., Mahle, J. J., and Buettner, L. C., "PSA for Air Purification: Experiments and Modeling", accepted (October 1992) for publication in Proceedings of 4th International Conference on the Fundamentals of Adsorption, Kyoto, Japan, May, 1992.

7. Buettner, L. C., Mahle, J. J., Friday, D. K., and Brady, A. B., "Experimental Studies in Pressure Swing Adsorption", Proceedings of the 1991 U.S. Army Chemical Research, Development and Engineering Center Scientific Conference on Chemical Defense Research, 19-22 November, 1991.

8. Sundaram, N., Friday, D. K., and Mahle, J. J., "Pressure Swing Adsorption (PSA) Performance Prediction Model", Proceedings of the 1991 U.S. Army Chemical Research, Development and Engineering Center Scientific Conference on Chemical Defense Research, 19-22 November, 1991.

2.5 Other Results

- LabView is selected as the software of choice for laboratory automation. (A-6)

National Instruments LabView 2 was found to be the best software available which satisfied the two needs established for the laboratory; (1) automate large experimental systems with a variety of input and output types and complicated control and decision-making strategies, and (2) provide users with minimal software experience the platform to design, implement, and maintain these experimental systems.

- Initial Temperature Swing Adsorption (TSA) control program and PSA temperature profiling are developed using LabView 2. (A-7)

Software for the TSA laboratory-scale test system was developed using LabView. This became the first system to use the new software.

- Construction of the laboratory-scale TSA system is completed. (A-7)

A TSA system with in-bed heating was constructed. Hardware and software required to control the power input into the system was developed. Parameters such as cycle time and power input could be fixed by the user.

- A grounding problem is identified in the TSA temperature probes. (A-8)

The design of the power monitoring and control equipment was modified to protect external devices connected to the power controller. A Hall effect current loop was employed to ure the current and associated amplifiers were used to generate the 0-5 V representing the output of the power supply. Both these outputs are completely isolated from potentially us voltages.

- First set of TSA experiments completed. (A-9)

Using a single bed to simulate the operation of a two-bed cycle, the first series of TSA experiments with in-bed heating was conducted. Parameters measured included: (1) in-bed temperatures at 5-cm intervals, (2) voltage and current across the bed, and (3) feed, product and purge concentrations. These results showed that the bed could be placed back on-stream (feed) while it is warm and not result in "bleed-through" of the chemical into the product.

- TSA experiments using R-113/BPL with feed, product, and purge concentrations measured are completed. (A-11)

The hardware and software controlling the TSA system was modified by incorporating the National Instruments SCXI Signal Conditioning System. The system is modular in its configuration, and represents a significant improvement in laboratory automation. TSA experiments were performed with R-113 as the challenge chemical and BPL carbon as the adsorbent. The objective of the experiments was to determine if TSA cycle times on the order of 10 minutes, as opposed to several hours, could be successfully used. An overall material balance was calculated, and it showed that periodic-state was achieved after about 20 cycles. Temperature behavior during cycles also supported this conclusion. Once again, no measurable R-113 was detected in the product. Another significant observation was that the bed resistance tended to increase during the course of the 48-hour experiment. This behavior needs to be better understood.

Other Results Reference List

1. Dawson, C.L., "Designing Experimental Control and Data Acquisition for Air Purification Systems", 1992 ERDEC Conference on Chemical Defense given Nov 17, 1992.

3.0 CONCLUSIONS

The conclusions to be drawn from this research and development effort are:

(1) Isotherm data provides the most important information required to design and evaluate adsorption-based air purification systems.

(2) Time and effort applied to experimental procedures and apparatus design are critical elements for any successful air purification system design program.

(3) Automated data acquisition and control are required to generate and reduce the data necessary to design advanced air purification systems.

(4) Successful PSA design requires that the effect of water vapor on PSA system performance be well characterized.

(5) In-bed temperature swings during PSA cycles provide a unique mechanism for tracking the depth of penetration of contaminant vapors.

(6) TSA with in-bed resistance heating exhibits a great deal of promise as a military air purification technology.

Blank

APPENDIX A-1

QUARTERLY PROGRESS REPORT

GC-PR-2194-01

REPORTING PERIOD:	8/6/90 - 10/31/90
REPORTING DATE:	November 9, 1990
CONTRACT NUMBER:	DAAA15-90C-1056
CONTRACT TITLE:	Improved Filtration Materials and Modeling

Adsorption Measurements

Adsorption equilibria for PFCB on three adsorbents, BPL carbon, ASC carbon and 13X molecular sieve, were measured at three temperatures, 25C, 50C, and 75C. The data were correlated using a modified version of the LeVan-Hackskaylo Equation. The data and the correlation for each system are summarized in Figures 1, 2, and 3. These results clearly show the large difference in capacity between the BPL and 13X. This is important in the design of regenerative air purification systems such as PSA as well as single-pass filters.

Adsorption Apparatus

The apparatus to measure adsorption isotherms for 13X molecular sieve was modified to reduce the water vapor concentration. One important modification was a nitrogen cold trap within the circulation loop to reduce the dew point of the vapor in the closed-loop prior to the start of the experiment. Isotherms measured with the cold trap in place have resulted in consistently higher PFCB loadings. A second significant modification was implementing a control valve to automatically switch back and forth from the bed by-pass mode to the bed challenge during the test. By switching the valve to the bypass position prior to a new injection

of PFCB, the amount of material injected into the closed-loop system can be determined using the GC. The reproducibility of isotherm measurements for 13X molecular sieve has improved greatly as a result of the control valve addition.

Modifications have been made to the water isotherm apparatus which have improved the quality of the measured data. Some of the previous water isotherm measurements have been affected by small changes in room temperature (1-3C) which cause significant deviations in the challenge RH. Several modifications have allowed the system to operate for several days without any major deviations in the inlet RH.

Adsorption Theory

Work is continuing to develop an isotherm correlation that accurately represents the data and has physically meaningful parameters. Currently, we are using the following expression

$$\ln(p) = A' - (B' / C' + T)$$

$$A' = A + \ln(\theta)*[1 + a*(\theta^{0.5})]$$
$$B' = B*\theta + b*(1-\theta)$$
$$C' = C$$
$$\theta = W/W0$$

where A, B, and C are the Antoine parameters for the given adsorbate. Since a primary motivation for this work is to develop a predictive isotherm relationship, several interesting aspects of this correlation need to be mentioned. For the systems we have

considered, the θ term power of 0.5 has produced the lowest variance. For example, when .4 and .6 were tried the variance increased. For the LeVan-Hackskaylo expression power of 1, the variance was about three times greater than the variance for the 0.5 power. We think the 0.5 holds physical significance and we are exploring some possible thermodynamic meanings for the term. Another key feature is that the value of b is directly related to the contribution of surface-adsorbate interactions to the heat of adsorption. The $B\theta$ term accounts for the condensation (adsorbate-adsorbate interactions) contribution to the heat of adsorption. We are also exploring methods to predict the value of b for new chemicals based on relationships derived from similar, measured chemicals.

Multi-component Adsorption

Work has been started to develop multicomponent adsorption equilibria expressions based only on single component data. We are focusing our attention on systems where water is the second component. The CFC-113 and water on BPL system is being used a basis for the development. The initial work has involved using Ideal Adsorbed Solution Theory (IAST) to build a multicomponent adsorption isotherm expression. A problem has arisen because IAST requires that each adsorbate must have the same maximum volumetric adsorption capacity, W0. However, CFC-113 has a W0 (cc/g) of .66 and water has a W0 of .54 on BPL carbon. We are currently working on modifications to the existing IAST theory to account for this difference.

Breakthrough Characterization

Axial dispersion has been determined to be most important in describing the breakthrough behavior of shallow-bed filters. A full experimental study is underway. The results are critical for developing a model for a military PSA air purification system.

FIGURE 1. Correlated Isotherm Data for PFCB on BPL Carbon
at 25, 50 and 76C

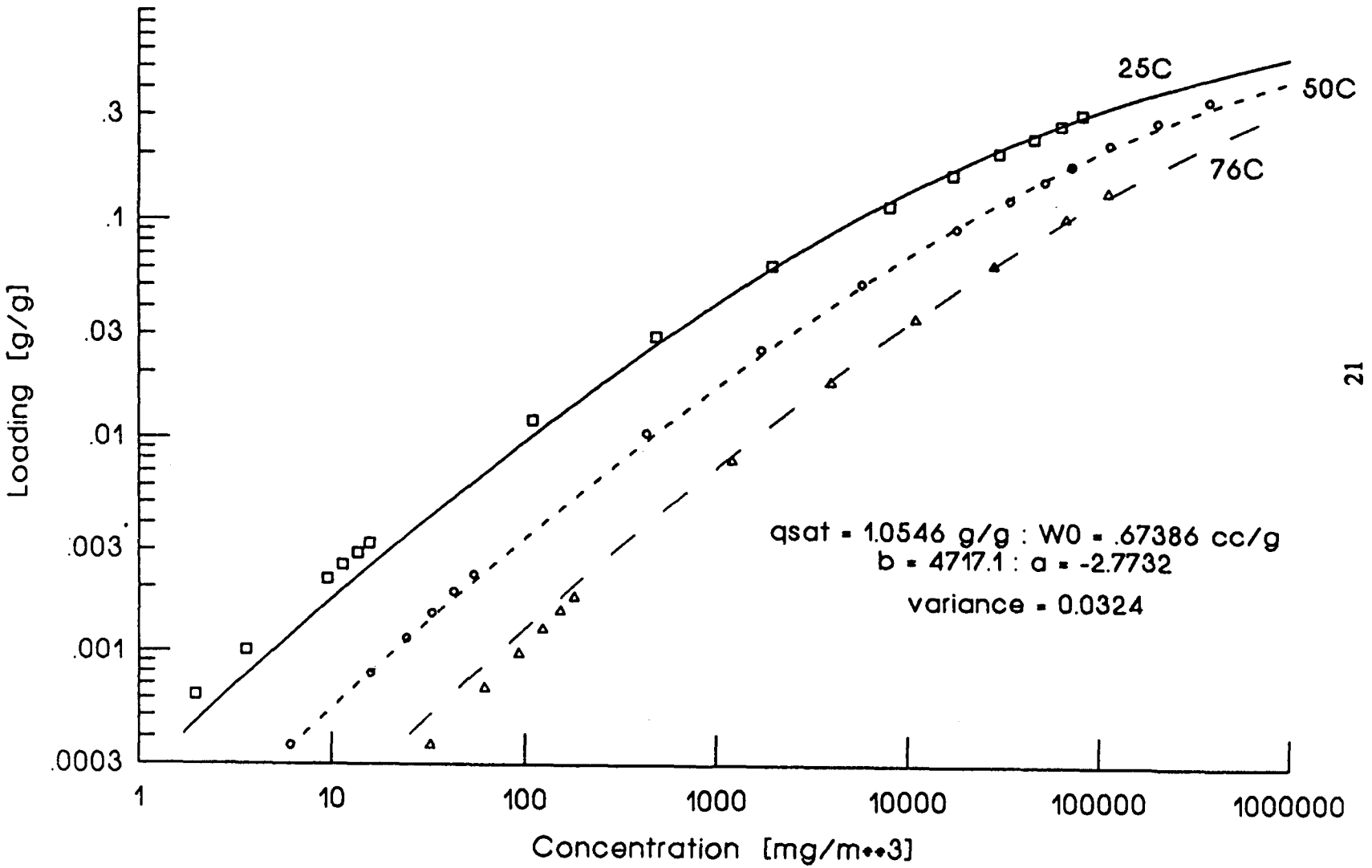

FIGURE 2. Correlated Isotherm Data for PFC3 on ASC Carbon at 25, 50 and 76C

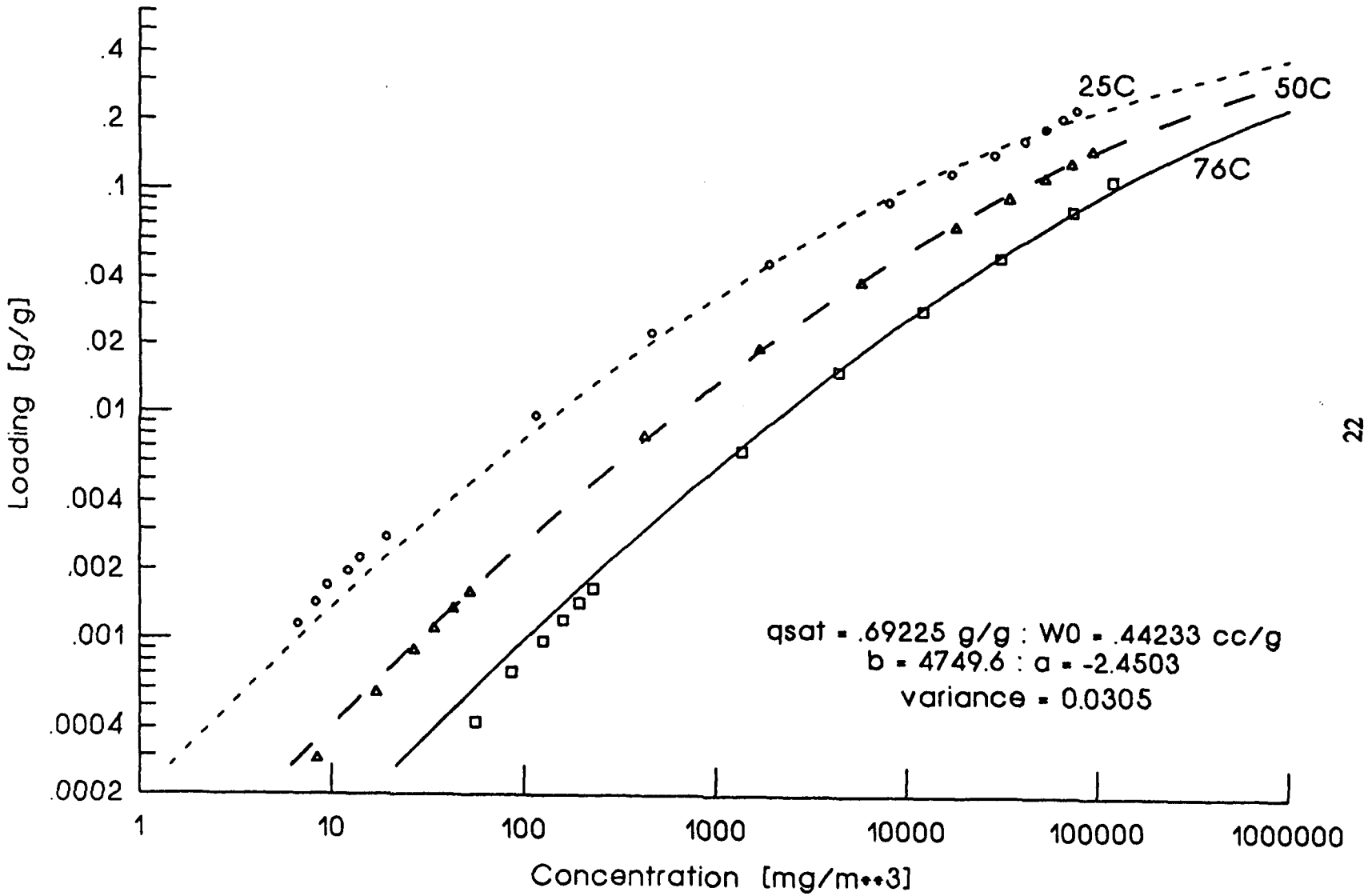

FIGURE 3. Correlated Isotherm Data for PFCB on 13X Molecular Sieve at 25, 49 and 75C

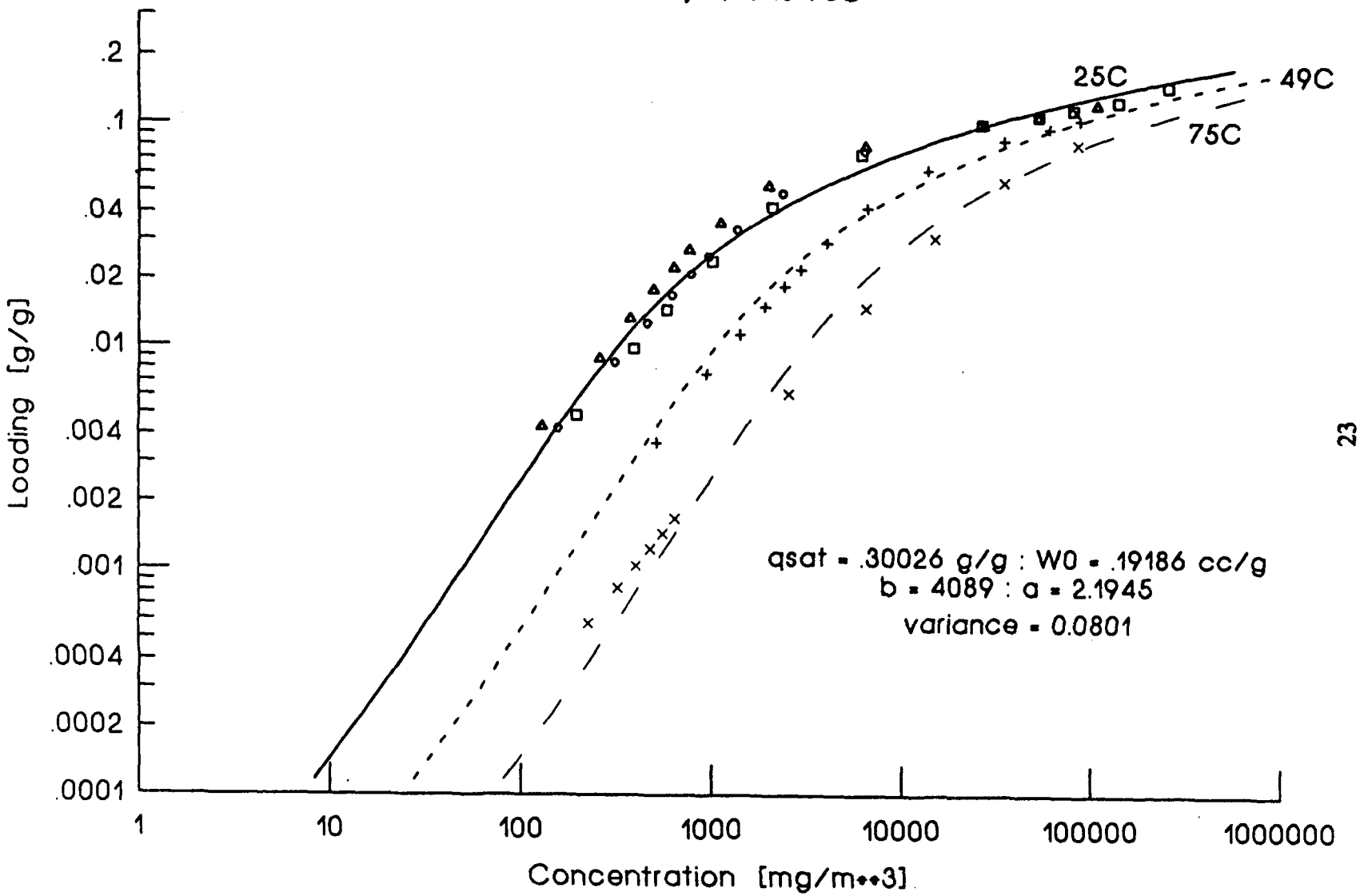

Blank

APPENDIX A-2

QUARTERLY PROGRESS REPORT

GC-PR-2194-02

REPORTING PERIOD:	11/1/90 - 1/31/91
REPORTING DATE:	February 5, 1991
CONTRACT NUMBER:	DAAA15-90-C-1056
CONTRACT TITLE:	Improved Filtration Materials and Modeling

I. Adsorption Measurements

Single Component Measurements and Apparatus

Isotherms at 25C, 50C and 75C were measured for Substrate, ASC and ASC-T carbons using 1,1,2 trichloro, 1,2,2 trifluoroethane (CFC-113) and perfluorocyclobutane (PFCB) as the adsorbates. The data were correlated using the Modified Antoine Equation. Results showed that the impregnation process does not significantly effect the heat of desorption and that ASC isotherms may be predicted from substrate isotherms by reducing W0 (total pore volume) by an appropriate amount. A more detailed analysis is given in the attached November 1990 CRDEC (Appendix A) paper.

In order to verify that adsorbed water or adsorbed oxygen do not effect the CFC-113 isotherms on activated carbon, duplicated runs were made in helium. The results of the runs showed that the isotherms were the same, thus the effects of oxygen, nitrogen and/or trace amounts of water are not important for carbonaceous samples.

Some improvements in the drying procedure used for the 13x molecular sieve were made. Following forty-eight hours in the vacuum oven, the oven is repressurized with dry helium instead of

air. After the sample is allowed to cool, it is weighed and placed in the closed-loop system. Heat tape has been placed around the bed which permits temperatures to reach 170C during the cryogenics phase of the drying procedure. It is hoped that this approach will remove any residual water picked up during the sample-transfer process.

The water isotherm apparatus has been modified to maintain more stable feed RH's when the room temperature changes. This has resulted in more reproducible data. A number of carbon samples have been measured, including all of the carbons used in the impregnation study. We are currently measuring some samples of poor performing ASC carbons provided by PPD.

Multicomponent Measurements and Apparatus

The multicomponent apparatus is almost completed. All of the required hardware is in place. Some additional software development is required to get the system running. We would expect this system to be operational in February.

II. Adsorption Theory

Single Component

We are continuing to utilize the Modified Antoine Equation to correlate measured isotherm data. We are currently investigating some changes in the form to better describe the important physical phenomena. As part of this study, a comparison was made between the Polanyi Potential Theory (PPT) (using the 3-parameter Dubinin-Radushkevitch Equation) versus the Modified Antoine Equation (MAE). Measured isotherm data was correlated for CFC-113 and PFCB on

several different carbons. The results showed that the MAE was superior to the PPT for the CFC-113 (based on variance calculations). However, the PPT produced a slightly better correlation for the PFCB, particularly at very low loadings (<.005 g/g). We are trying to understand how we may use these results to develop an improved MAE.

Multicomponent

We are continuing to work with Rich Matuszko to determine if the Ideal Adsorbed Solution Theory (IAST) may be used to correlate water and CFC-113 isotherms. Preliminary results indicate that the qualitative behavior, i.e. the position and shape of the waves, of breakthrough curves measured at 80% RH can be characterized using this approach. More complicated modifications will certainly be necessary in the future, however, the initial results are encouraging.

III. Breakthrough Studies

Axial dispersion has been identified as a major contributor to the spreading of the adsorption wave in military filters. Emphasis has been placed on understanding and quantifying axial dispersion for single-pass filter design and incorporation into the PSA design model. The attached paper from the Chicago 1990 AIChE Conference (Appendix B) details some of the most important results this quarter.

IV. Pressure Swing Adsorption

Experiments and Apparatus

The PSA apparatus is now operational. Several significant experimental problems have been resolved. Preliminary results show that BPL activated carbon is a much better adsorbent than 13X molecular sieve for air purification applications. Experiments conducted under identical operating conditions gave the following results:

(1) 13X showed immediate breakthrough of CFC-113 while the first measurable concentration (about 1 mg/m^3) for the carbon appeared in approximately four hours.

(2) 13X steady-state product concentration was 1200 mg/m^3 and carbon steady-state product concentration was 150 mg/m^3.

Theory (Mathematical Model)

A new IBM Power Station 520 computer was purchased by the Government. It uses the recently developed Reduced Instruction Set Computing (RISC) technology to greatly improve computational speed. This computer will allow us to develop a more physically correct PSA model more quickly. The first modeling attempts have used PDECOL, a library software package, to solve the mathematical model partial differential equations. However, PDECOL requires the boundary conditions to be in a format that is not compatible with the type of partial differential equations we are solving. With the help of Professor LeVan, we have overcome this problem and now have a working PSA model. We will have initial PSA experiments and math model comparison next quarter.

V. Presentations and Publications

The following presentations and publications were made during this quarter:

(1) November STAS Panel Review

(2) November CRDEC Conference (3 papers)

(3) Chicago AIChE Conference (1 paper)

APPENDIX A

Adsorption Equilibria of CFC-113 and PFCB on Impregnated and Unimpregnated Adsorbents

David K. Friday[1], John J. Mahle[2], Leonard C. Buettner[2], Donna L. Carlile[2], and Amanda B. Brady[1]

[1]GEO-CENTERS, INC., Ft Washington, MD 20744
[2]U.S Army CRDEC, Aberdeen Proving Ground, MD 21010

Abstract

Military air purification systems are subject to a wide range of challenge vapors and environmental conditions. To effectively evaluate new systems and optimize current systems, one must develop a full understanding of all significant processes. One critical element of any program to predict filter performance is an accurate, thermodynamically consistent, description of the adsorption equilibria relationships of volatile, reactive challenge vapors.

Adsorption equilibria (isotherms) for two simulants, 1,1,2 trichloro, 1,2,2 trifluoroethane (CFC-113) and perfluorocyclobutane (PFCB), are measured on impregnated and unimpregnated adsorbents using an automated system developed at CRDEC. Isotherm data are correlated using a Modified Antoine Equation developed by Hackskaylo and LeVan which has been shown to be particularly effective for heterogeneous adsorbents. The effect the impregnation process has on filter performance is investigated by identifying thermodynamic changes in the adsorbent. A method using the simulant isotherms to predict the adsorption behavior of the toxic, reactive vapors is developed.

Introduction

Any program to design improved military air purification systems requires a complete understanding of the adsorption equilibria behavior of the toxic vapors of interest. For toxic vapors which are volatile and reactive, measuring adsorption equilibria is a difficult problem. For example, if one tries to measure the adsorption isotherm of cyanogen chloride on ASC or ASC-T carbons, chemical reactions occur which are quantitatively indistinguishable from the adsorption process. This study develops an approach to predict the adsorption isotherm of a toxic, reactive vapor on an impregnated adsorbent.

Adsorption equilibria (isotherms) for two simulant vapors, 1,1,2 trichloro, 1,2,2 trifluoroethane (CFC-113) and perfluorocyclobutane (PFCB), are measured using three adsorbents; (1) unimpregnated, activated carbon substrate, (2) ASC Whetlerite made from the substrate in (1), and (3) ASC-T made from the ASC in (2). Isotherms are measured using an automated system developed at CRDEC and correlated using a Modified Antoine Equation. Results indicate that the adsorption equilibria of the simulant on the unimpregnated carbon may be used to predict the adsorption equilibria of the simulant on the impregnated carbons. This implies that the adsorption equilibria of the toxic, reactive vapor may be predicted on the impregnated adsorbent using isotherms of the toxic vapor on the unimpregnated substrate.

Theory

To effectively utilize the measured isotherm data in a design application, one must develop a correlation function that accurately reflects the measured data and both correctly interpolates between and extrapolates beyond the measured data points. The correlation function chosen for this effort is a modification of a relationship proposed by Hackskaylo and Levan (Langmuir, Vol. 1, page 97, 1985),

$$\ln(p) = A' - B' / (C' + T) \qquad (1)$$

where,

$$A' = A + \ln(\theta)*(1 + a1*\theta^{0.5}) \qquad (2)$$

$$B' = B + b1*(1 - \theta) \qquad (3)$$

$$C' = C \qquad (4)$$

$$\theta = W/W0 \qquad (5)$$

A,B, and C are the Antoine parameters for the vapor of interest, p is the vapor pressure of the adsorbate in torr, T is the isotherm temperature in K and W0 is the saturation capacity of the adsorbent in cc adsorbate per g of dry adsorbent. W is calculated from the measured loading (g adsorbate per g adsorbent) by multiplying by the liquid phase density, ρ_L (g/cc).

This function was chosen for several reasons. The function possesses thermodynamically consistent limits, becoming the vapor pressure versus temperature relationship when W = W0 and reducing to Henry's Law, (i.e., W = K*p, where K is the Henry's Law constant) at very low values of W. The isosteric heat of adsorption, λ, can be calculated using the Clausius-Claperyon Equation,

$$\lambda = -RT^2 \quad (\partial \ln(p) / \partial T) \text{ at constant } \theta \qquad (6)$$

to give

$$\lambda = - RT^2 \left(B' / (C' + T)^2 \right) \qquad (7)$$

where b1 is the only adjustable parameter that effects λ. The physical meaning of a1 has not been fully resolved at this time, however, one can infer that it is related to the entropy of adsorption.

Experiments

Materials

Chemicals

1. 1,1,2 trichloro, 1,2,2 trifluoroethane (CFC-113)
2. Perfluorocyclobutane (PFCB)

Adsorbents

1. Unimpregnated, activated carbon (Substrate)
2. Substrate impregnated with 11-13% (by weight) salts of Cr, Cu and Ag (ASC)
3. ASC impregnated with 2-3% by weight triethylenediamine (TEDA) (ASC-T)

Apparatus and Procedure

Shown in Figure 1 is a schematic diagram of the closed-loop apparatus used to measure adsorption isotherm data. A brief description of the procedure used to measure an isotherm will be given.

After drying and weighing the adsorbent, it is placed into the closed-loop system. The system is pressure tested to check for leaks before each experiment is started. Several calibration checks for the Flame Ionization Detector (FID) detector in the gas chromatograph (GC) are also performed. The isotherm temperature is established using an injection heater, a thermocouple and a temperature controller. When the bed temperature stabilizes, a computer program is initiated to measure an entire isotherm (usually 15-25 points) automatically.

Valve #1 (V1) is rotated to inject liquid adsorbate into the circulating loop while Valve #2 (V2) is the bypass position.

For experiments with PFCB (a gas at ambient conditions), the injection system is kept under pressure to insure that the injection loop fills with liquid. After a short equilibration time, the concentration in the circulating vapor is measured using the GC and the amount of material injected into the system is calculated by multiplying the vapor concentration times the circulating loop volume. Valve#2 is turned to the bed feed position. After forty-five minutes, samples of the circulating vapor are measured in ten minute intervals to insure equilibrium is reached. The isotherm point is determined using the vapor concentration determined by the GC and the loading on the adsorbent calculated using

(mass injected - mass in vapor) / mass of dry adsorbent

After each isotherm point is determined, the process is repeated until a pre-set, maximum concentration is reached. At this time, the bed is removed and weighed. The measured loading is compared to the loading calculated for the last isotherm point to verify that the material balance is satisfied. In the experiments presented in this paper, the measured and calculated loadings all agree within 3%.

Results and Discussion

Isotherms for each adsorbate on each adsorbent were measured at three temperatures; 25C, 50C, and 75C. Results were correlated by finding the a1 and b1 which gave the least squares best fit of ln(p).

Shown in Figure 2 is the measured isotherm data and the Modified Antoine Equation correlation for CFC-113 on ASC carbon. The graph is constructed using the natural log of the concentration to emphasize the low concentration region. The results indicate that the correlation fits the data well over the entire range and that the loading dependence on the heat of adsorption, λ, is adequately described by $b1(1-\theta)$.

Figure 3 is a similar plot for PFCB on ASC carbon. Because the loadings of PFCB are much lower, these results are plotted on a log-log scale. The deviation between the measured and predicted values at low loadings (below about 0.005 g/g) is worth discussing in more detail. If one draws a horizontal line at about q = .001 through the data, the distance between the isotherms is directly proportional to the isosteric heat of adsorption (graphically equivalent to Equation 6). Therefore, since the measured data seems to be spread wider apart than the correlation predicts, one may assume the linear loading dependence on λ given by $b1(1-\theta)$

is not adequate. The fact that CFC-113 is described better than the PFCB using the linear loading dependence may be a result of structural differences (linear versus cyclic) or simply that the measurements for PFCB are made much closer to the Henry's Law region than the CFC-113 measurements.

Figures 4 and 5 are the CFC-113 and PFCB measured data for each adsorbent at 25C. For each adsorbate, the results show the similarity of isotherms as the impregnants are added. This information clearly indicates that the isotherm for the impregnated carbon can be predicted from the isotherm of the substrate by using a proportionality factor related to the loss of pore volume.

The results for all six systems (two adsorbates-three adsorbents) are summarized in Table 1.

Table 1. Isotherm parameters and physical constants for CFC-113 and PFCB

Isotherm Parameters

Adsorbent	a1	b1	W0	variance
		CFC-113		
ASC-TEDA	-4.8553	5931	.4205	.0244
ASC	-5.4596	6110	.4278	.0221
Substrate	-5.1143	5936	.6875	.0456
		PFCB		
ASC-TEDA	-2.1706	4680	.3970	.0352
ASC	-2.4503	4750	.4423	.0305
Substrate	-2.7732	4717	.6739	.0324

Physical Constants

	CFC-113	PFCB
MW (g/mol)	187	200
ρ_L(g/cc)	1.565	1.513
Antoine A	15.84	16.362
Antoine B	2532.1	2290.6
Antoine C	-45.67	-31.94

The correlation results for CFC-113 can be used to develop an approach to estimate isotherms of similar, but reactive vapors, on ASC and ASC-T. Since a1 and b1 remain relatively constant, one must only change W0 in an appropriate manner. The correlation results indicate that a toxic vapor

adsorption isotherm on ASC may be estimated using the a1 and b1 obtained from the substrate measurement and a value of W0 about 40% less than the substrate value. The ASC-T isotherms may be estimated using the same a1 and b1 but a value of W0 about 2-4% less than the W0 for ASC. The rules of thumb developed for CFC-113 may also be used estimate PFCB behavior on ASC and ASC-T.

Conclusions

1. The Modified Antoine Equation may be used to estimate adsorption equilibria on impregnated carbons from measured substrate isotherms.
2. A complete description of the PFCB adsorption equilibria requires a more complex modification of the Antoine parameters.

Figure 1 Single Component Isotherm Apparatus

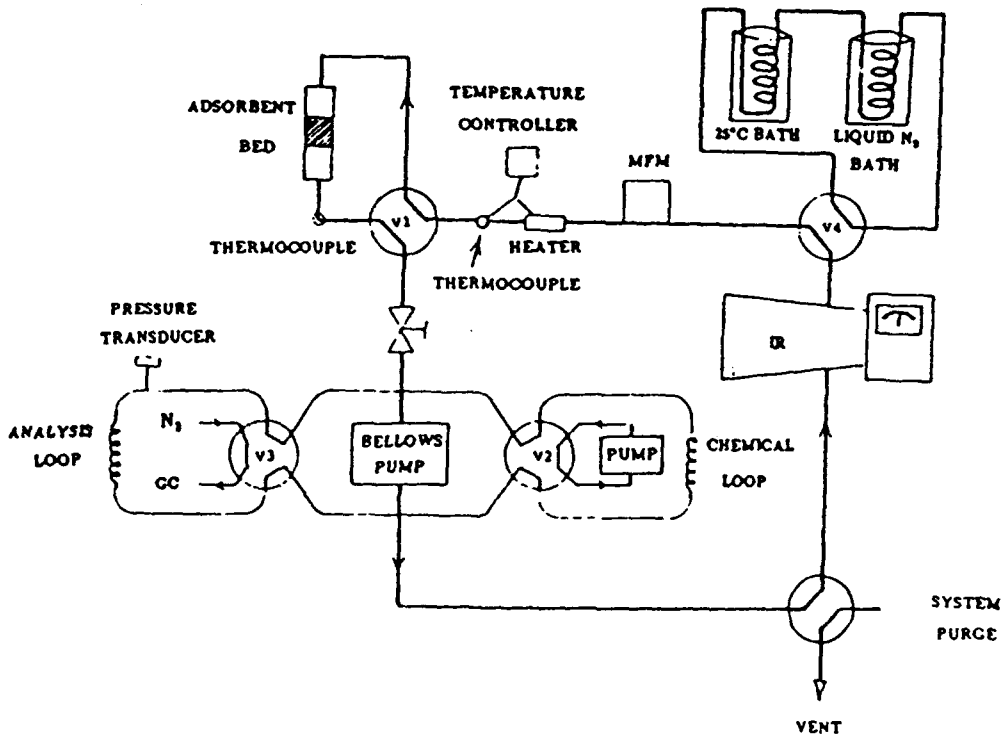

Figure 2 Isotherm Data for CFC-113 on Dry ASC 12x30 at 25, 50 and 75 C

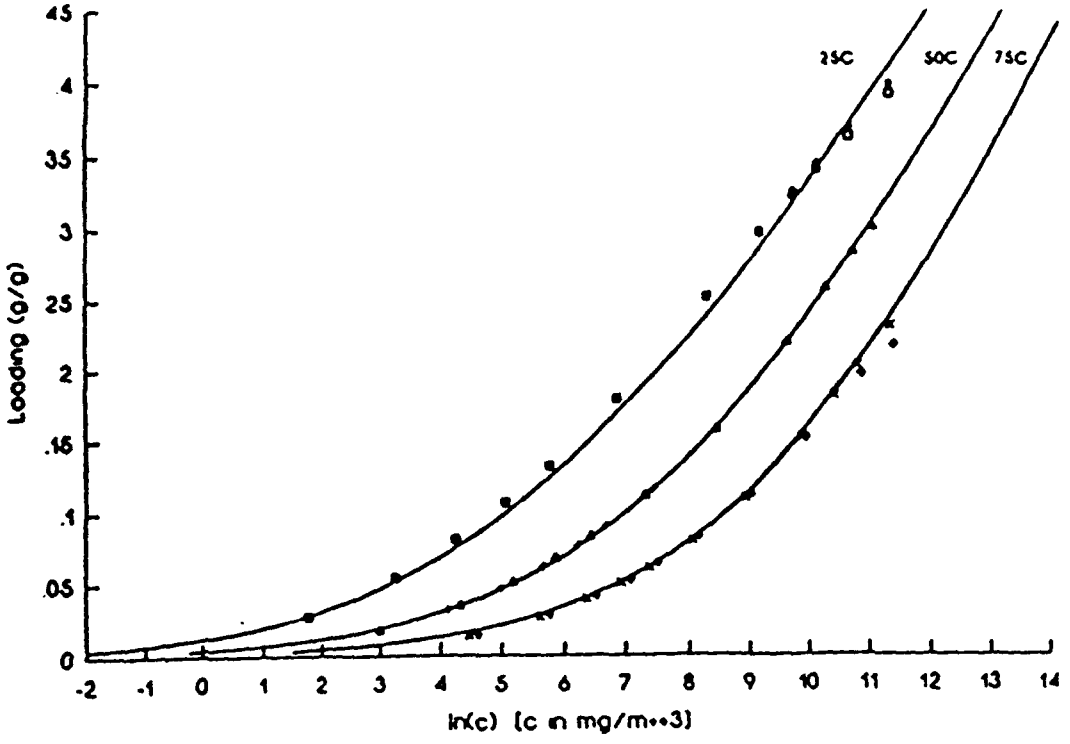

Figure 3. Correlated Isotherm Data for PFC8 on ASC 12x30 Carbon at 25, 50 and 75C

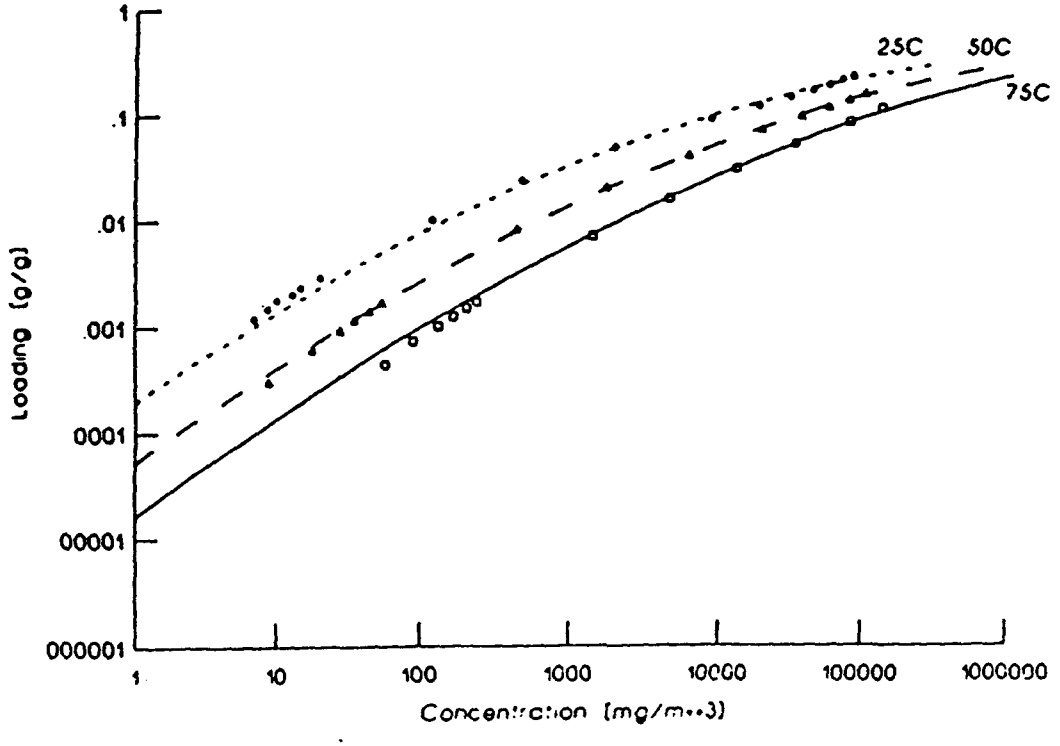

Figure 4 Isotherm Data for CFC-113 on Dry Substrate 9A18-U, ASC 12X30, and ASC-TEDA

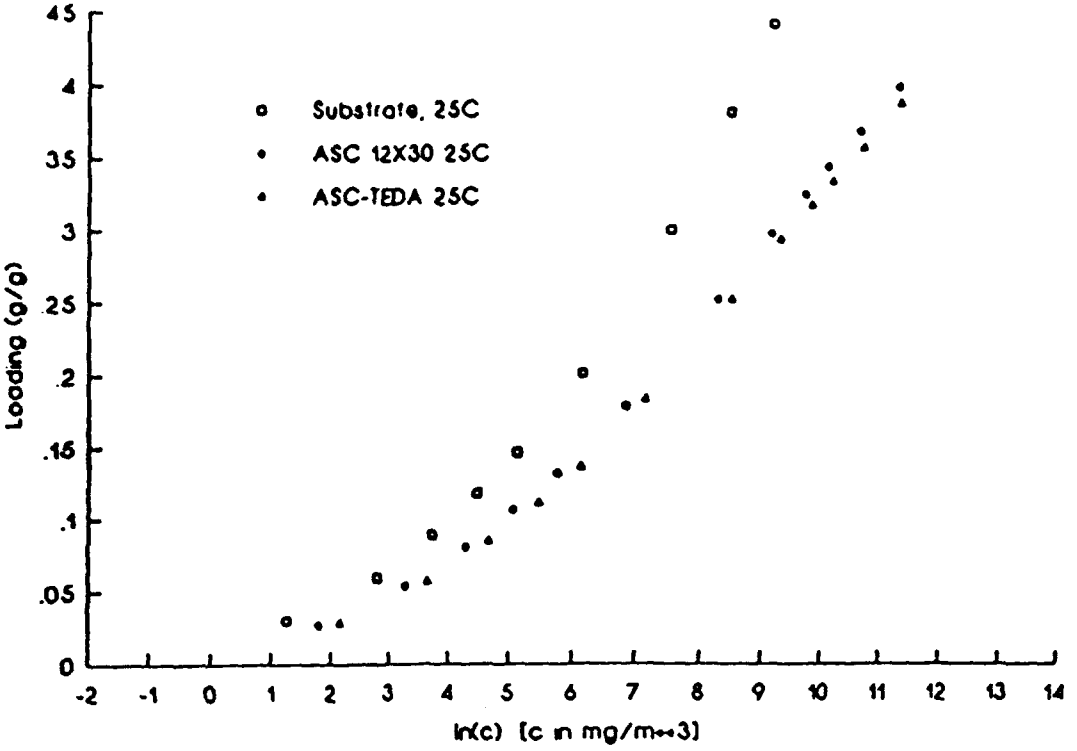

Figure 5. Isotherm Data for PFC8 on Substrate, ASC 12x30 and ASC-Teda at 25C

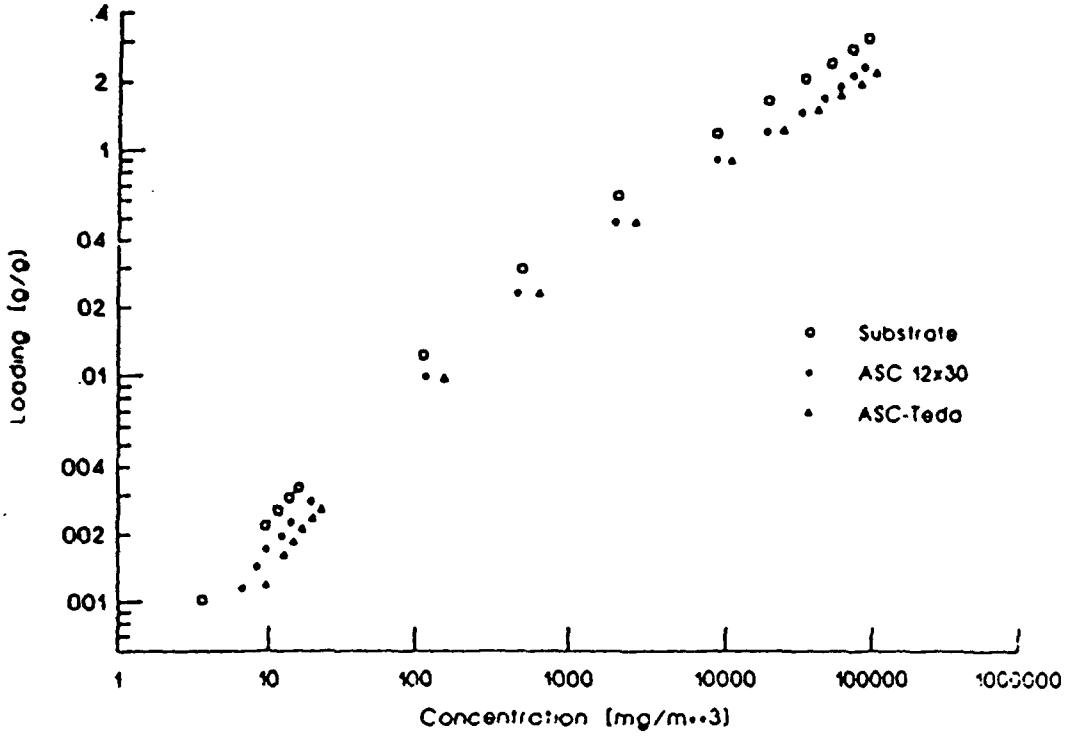

APPENDIX B

A Methodology to Evaluate the Performance of Shallow-Bed Adsorbers

John J. Mahle and Leonard Buettner

U.S. Army CRDEC
Aberdeen Proving Ground, MD 21010

and

David K. Friday

GEO-CENTERS, Inc.
Fort Washington, MD 20744

Presented at the AIChE Annual Meeting

Chicago, IL

November 12, 1990

Introduction

The degree of accuracy required of fixed-bed adsorber models is determined by the intended application. Respiratory filters, the primary application of shallow-bed adsorbers, are designed to minimize pressure drop while providing protection against low concentrations of toxic chemical vapors. For systems such as this it is imperative that adsorption equilibria and all important rate phenomena be understood and quantified.

This work outlines an approach to accurately describe the performance of shallow-bed adsorbers. A test system consisting of CFC-113 (1,1,2 trichlorotriflouroethane) as the adsorbate and BPL activated carbon as the adsorbent is used. The material balance for a cylindrical fixed-bed adsorber is written with a Fickian expression to describe axial dispersion. Adsorption isotherms, internal particle mass transfer rates and external particle mass transfer rates for CFC-113 on BPL carbon are measured and correlated. A breakthrough experiment is performed using a shallow bed (length to diameter ratio less than 1) to determine the axial Peclet number. Results indicate that axial dispersion contributes significantly to the premature breakthrough of shallow-bed adsorbers.

Material Balance

Although the methodology given here is applicable to most adsorption systems, emphasis will be placed on adsorption systems for purification. Only low vapor phase concentrations of the adsorbable component will be considered and isothermal behavior is assumed. Axial dispersion is included in the material balance using a Fickian diffusion term. The appropriate material balance for an isothermal single component system with axial dispersion is

$$\rho_b \frac{\partial q}{\partial t} + \epsilon \frac{\partial c}{\partial t} + \epsilon v \frac{\partial c}{\partial z} - \epsilon D_L \frac{\partial^2 c}{\partial z^2} = 0 \qquad (1)$$

with the following boundary conditions

$$D_L \frac{\partial c}{\partial z} = -v(c - c_o) \quad \text{at} \quad z = 0 \qquad (2)$$

$$\frac{\partial c}{\partial z} = 0 \quad \text{at} \quad z = L \qquad (3)$$

Adsorption Equilibria

Adsorption equilibria for CFC-113 at three different temperatures were measured

using an automated closed-loop system. The data were correlated using a modified form of the isotherm equation given by Hacskaylo and LeVan [1].

$$\ln(p) = A + \ln(\theta)(1+a\theta^{0.5}) - \frac{B\theta + b(1-\theta)}{(C + T)} \tag{4}$$

$$\theta = W/W_o \tag{5}$$

For the function given above, there are three correlation parameters, a, b and W_o. Figure 1 shows the measured data and the correlation values for a, b and W_o. These values were obtained by minimizing the sum of the squares of the errors between the measured ln(p) and the calculated ln(p). Details of the adsorption isotherm apparatus and the theoretical justification of the correlation function will appear in subsequent publications.

Mass Transfer Rates

The mass transfer rate from a flowing fluid stream to particles in packed beds is typically controlled by an external film resistance written as

$$\rho_b \frac{\partial q}{\partial t} = k_v a_s \, (c - c^*) \tag{6}$$

Values for the external mass transfer coefficient, $k_v a_s$, were obtained from the correlation[2]:

$$Sh = 2.0 + 1.1 Re^{0.6} Sc^{1/3} \tag{7}$$

$$k_v = \frac{Sh \, D_m}{2 \, R_p} \tag{8}$$

Intraparticle resistances are expected to be important for systems where material must be transported from the external surface of the particle to an internal site where it adsorbs. The internal diffusion rate is determined by two parallel resistances: namely, a fluid phase resistance (macropore and/or micropore) and a solid (adsorbed) phase resistance. For systems with both large separation factors and high specific surface area adsorbents (both true for the test system), the controlling rate process will be adsorbed phase diffusion[3].

For systems where the isotherm is not highly favorable, an adequate approximation of the internal particle concentration profile may be obtained using a linear driving force expression for the adsorbed phase[4].

$$\frac{\partial q}{\partial t} = k_p a_s (q^* - q) \tag{9}$$

where

$$k_p a_s = \frac{15}{R_p^2} D_e \tag{10}$$

where the surface diffusivity is D_e.

The value of D_e for the test system was measured using a batch system with a large circulation rate to remove the complicating effects of bed dynamics. The material balance for the batch system is given below.

$$\frac{\partial c}{\partial t} = - \frac{\rho_b V_s}{V_f} \frac{\partial q}{\partial t} \tag{11}$$

Equations 9-11 form the mathematical model for the batch uptake system, where D_e is the only adjustable parameter. By comparing measured uptake curves with the results of the model equations appropriate values for the surface diffusivity, D_e, can be obtained. Figure 2 shows the measured batch uptake data for CFC-113 on BPL carbon and the model results using three different values of D_e. The adsorbent particle diameter was 0.1mm (12x30 mesh). Based on these results the appropriate value for D_e was determined to be $1.5 \times 10^{-6} cm^2/s$.

Breakthrough Results and Discussion

The mathematical model for the CFC-113 breakthrough on BPL activated carbon is composed of Equations (1)-(10). The model equations were solved using orthogonal collocation[5] to discretize the spatial dimension and Gear's method[6] to integrate the resulting ordinary differential equations.

The test conditions for the system under consideration are listed in Table 1. All model parameter values, except D_L, were determined from previous experiments and correlations. It was thought that the model could be fully specified, i.e., no adjustable parameters, by determining the value of D_L, *a priori*.

Table 1

Breakthrough System Parameters

Superficial Velocity(cm/s)	12.2
Bed Depth(cm)	2.0
Bed Diameter(cm)	3.0
Particle Diameter(cm)	0.1
FeedConcentration(mg/m ^{3})	4500
EffectiveParticleDiffusivity(cm^2/s)	1.5x10 $^{-6}$
Temperature(C)	25
Adsorbent	BPL Activated Carbon
AdsorbentDensity(g/m ^{3})	4.8x10^5
Adsorbent Void Fraction	0.4
IsothermParameters(p_{sat} in torr)	
a	-5.25
b	6.04x10^3
W_o(cm^3/g)	6.59x10 $^{-1}$

A value of D_L can be calculated using a Peclet number correlation based on the radius of the particle given by Wen and Fan[7]

$$\frac{1}{Pe} = \frac{0.3}{ReSc} + \frac{0.5}{1+3.8/(ReSc)} \tag{12}$$

where

$$Pe = \frac{2R_p v}{D_L} \tag{13}$$

Using the parameter values given in Table 1, the value of D_L calculated using Equations 12 and 13 is 1.2 cm^2/s.

Figure 3 shows a measured breakthrough curve for the CFC-113/BPL test system using the conditions given in Table 1 compared with model results using three values of D_L. Of the three parameters tested, the best fit to the data is obtained using D_L = 7.0 cm^2/s. This value is much larger than the correlated value. One possible explanation for this anomaly is that the correlation was developed for deep beds and is not appropriate for the shallow bed considered in this study.

Figure 4 shows the same breakthrough curves as Figure 3, only plotted on a semi-

log scale to emphasize the effects at low concentrations. To fairly evaluate the model, one can consider a specific application of the model. Assume that it is desired to predict the protection time of a respiratory filter where the maximum concentration allowed in the filter effluent is 10 mg/m^3. Figure 4 shows that when axial dispersion effects are small ($D_L = 1.2$) the predicted protection time is nearly 40% longer (60 minutes versus 85 minutes) than is achieved in the actual system ($D_L = 7.0$). If an accurate estimate of the time a filter could be used safely is a requirement, then axial dispersion must be included.

Figure 5 is a comparison of the relative significance of axial dispersion and internal diffusion. The results are generated from the math model using the values of D_L and D_e indicated on the plot. The boxes correspond to the predicted results where the internal diffusion resistance is negligible, the circles correspond to the test system values, and the triangles correspond to the situation where axial dispersion is very small. The results clearly show that the major contributor to the spreading of the breakthrough curve for the test system is axial dispersion, with the internal diffusion resistance contributing only slightly.

CONCLUSIONS

1. Axial dispersion must be included to accurately model the behavior of the CFC-113/BPL shallow-bed test system considered here.

2. The methodology outlined in this study develops a breakthrough model with only one adjustable parameter, D_L, which describes the data well over three and one-half orders of magnitude.

3. Further work is required to extend the range of axial dispersion correlations to include shallow-bed behavior.

Notation

a_s = surface area to volume ratio ($3/R_p$)
A,B,C = Antoine Equation Coefficients
c = vapor phase concentration
c_o = feed concentration
D_e = effective particle diffusivity
D_L = axial dispersion coefficient
D_m = molecular diffusivity
ϵ = void fraction of packing
k_p = defined by equation 9
k_v = film mass transfer coefficient
L = bed length
q = adsorbed phase concentration
ρ_b = density of adsorbent
R_p = radius of particle
t = time
T = temperature
θ = defined by equation 5
v = interstitial velocity
V_f = volume of batch system
V_s = volume of adsorbent in batch system
W = isotherm pore volume term
W_o = isotherm pore volume saturation term
z = axial coordinate

Literature Cited

1. Hacskaylo, J.J., and Levan, M.D., "Correlation of Adsorption Equilibrium Data Using a Modified Antoine Equation: A New Approach for Pore-Filling Models", Langmuir, 1, 97 (1985).

2. Wakao, N., and Funazkri, T., "Effect of Fluid Dispersion Coefficients On Particle-To-Fluid Mass Transfer Coefficients In Packed Beds", Chem. Eng. Sci., 33, 1375 (1978).

3. Yang, R.T., "Gas Separation by Adsorption Processes", Butterworths Publishers, Boston, 1987.

4. Ruthven, D.M.,"Principles of Adsorption and Adsorption Processes", John Wiley & Sons, New York 1984.

5. Finlayson, B.A., "Nonlinear Analysis in Chemical Engineering", McGraw Hill, New York, 1980.

6. Hindmarsh, A.C., "LSODE and LSODI, Two New Initial-Value Ordinary Differential Equation Solvers", ACM-SIGNUM Newsletter, 1980, 15(4), 10.

7. Wen, C.Y., and Fan, L.T., "Models for Flow Systems and Chemical Reactors", Marcel Dekker, New York, 1975.

Figure 1. Isotherm Data for CFC-113 on Dry BPL at 25, 50 and 75 C

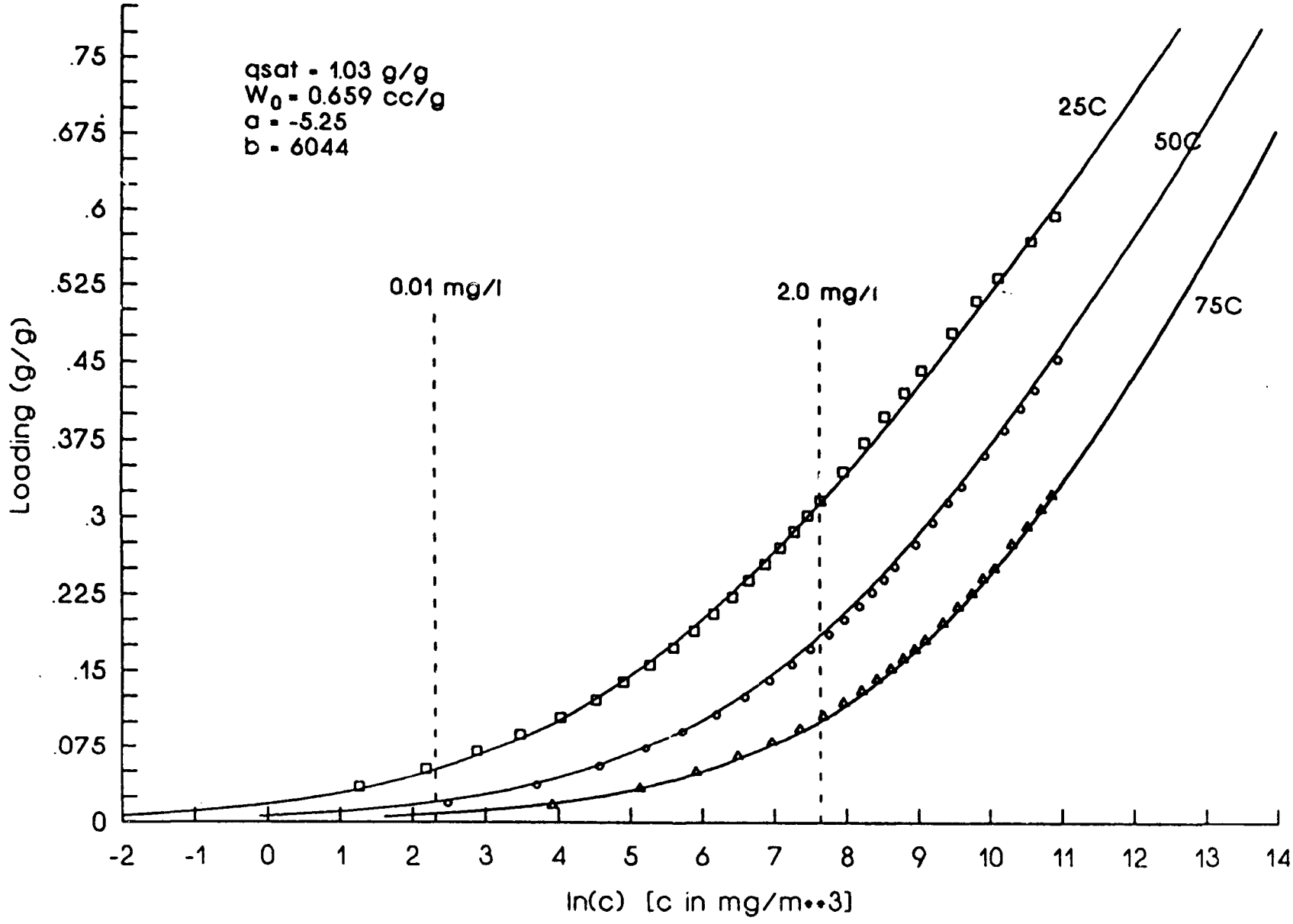

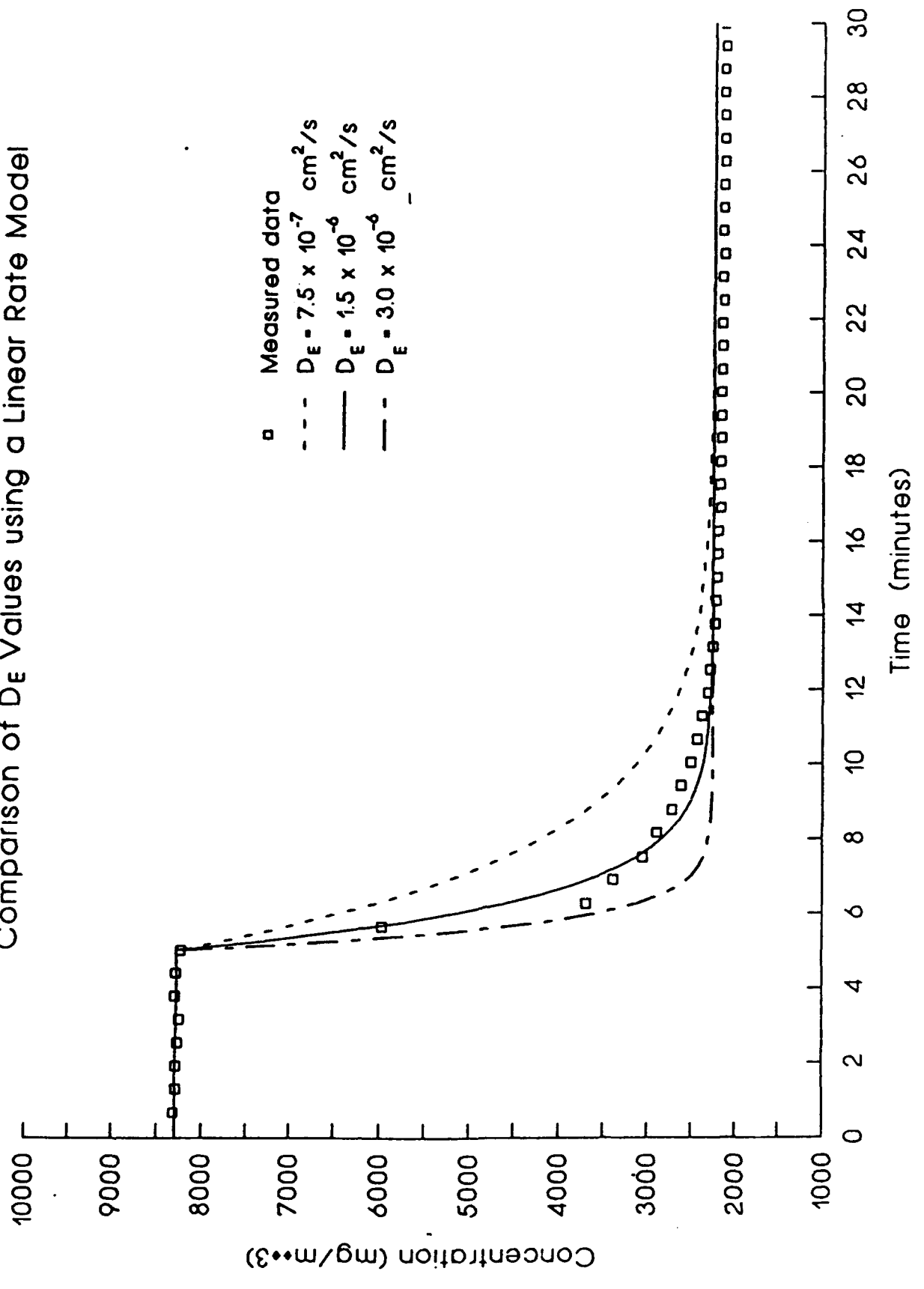
Figure 2. Batch Uptake Curves CFC-113 on Dry BPL Carbon at 25C
Comparison of D_E Values using a Linear Rate Model
Measured data
D_E = 7.5 x 10^{-7} cm^2/s
D_E = 1.5 x 10^{-6} cm^2/s
D_E = 3.0 x 10^{-6} cm^2/s
Concentration (mg/m**3)
10000
9000
8000
7000
6000
5000
4000
3000
2000
1000
0
2
4
6
8
10
12
14
16
18
20
22
24
26
28
30
Time (minutes)

Figure 3. Measured Breakthrough Data for CFC-113 on Dry BPL at 25C Compared to Model Results

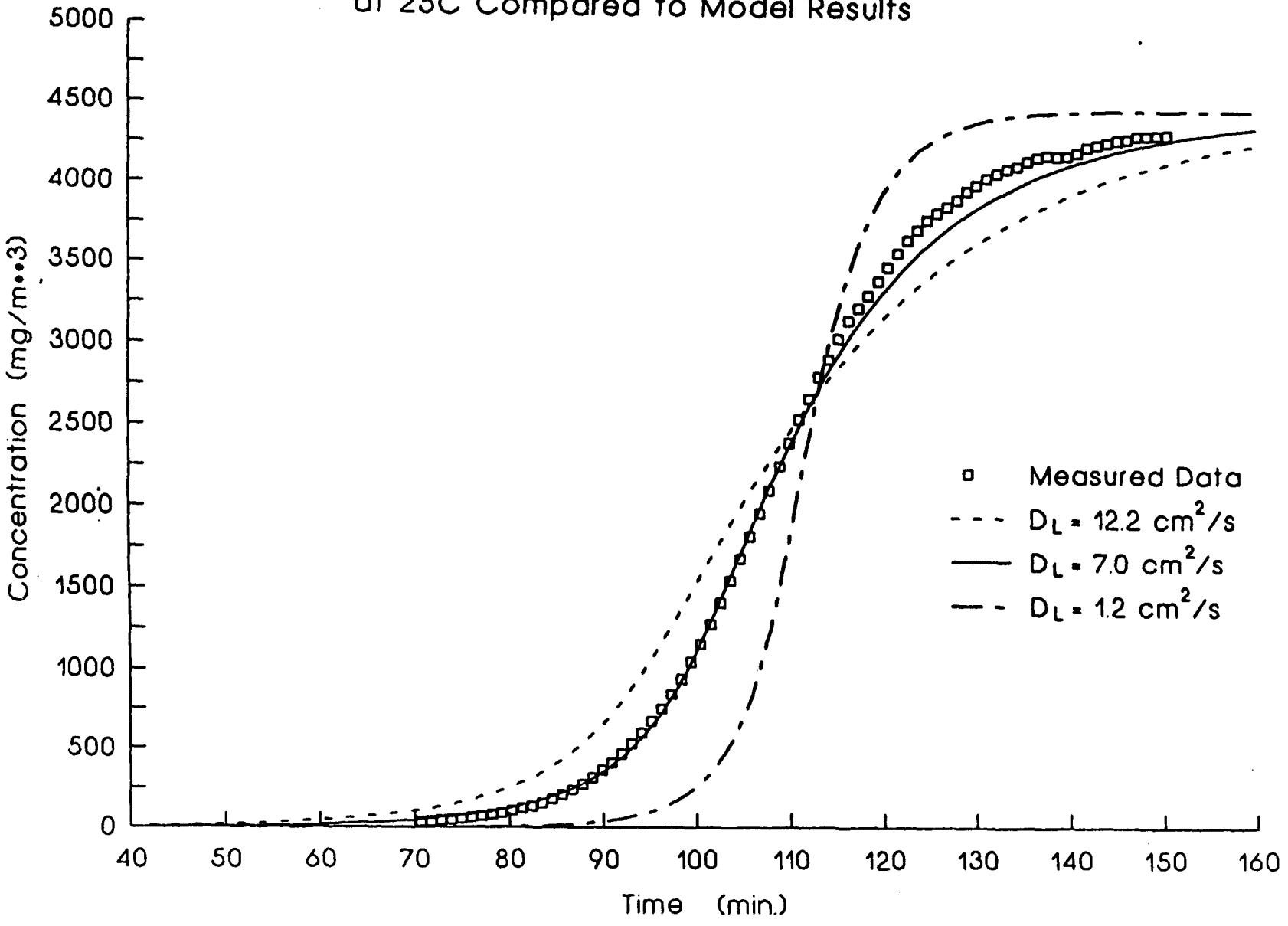

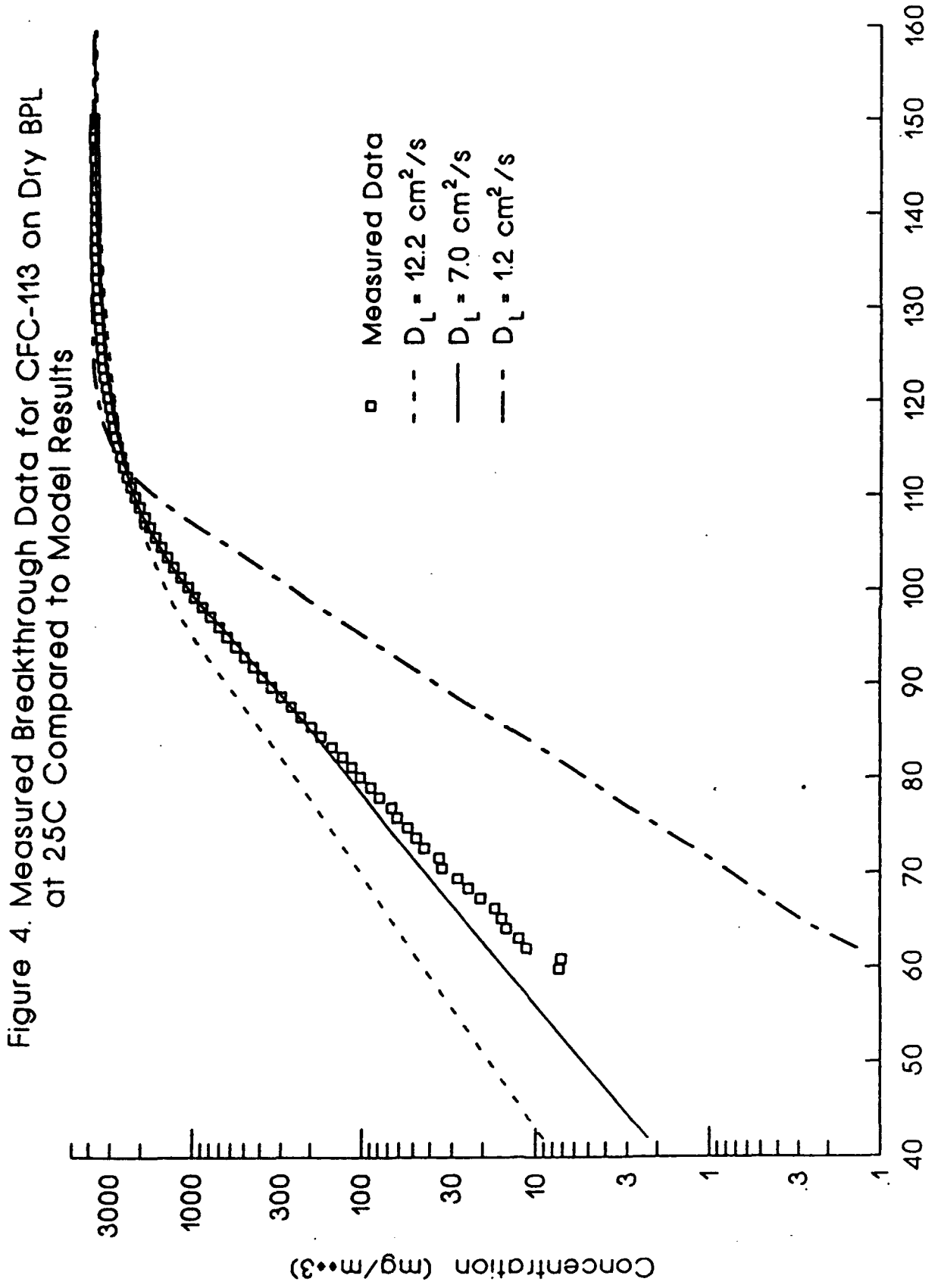

Figure 4. Measured Breakthrough Data for CFC-113 on Dry BPL at 25C Compared to Model Results

Figure 5. Relative Contribution of Dispersion and Internal Diffusion to the Spreading of CFC-113 Breakthrough Curve [Model Results]

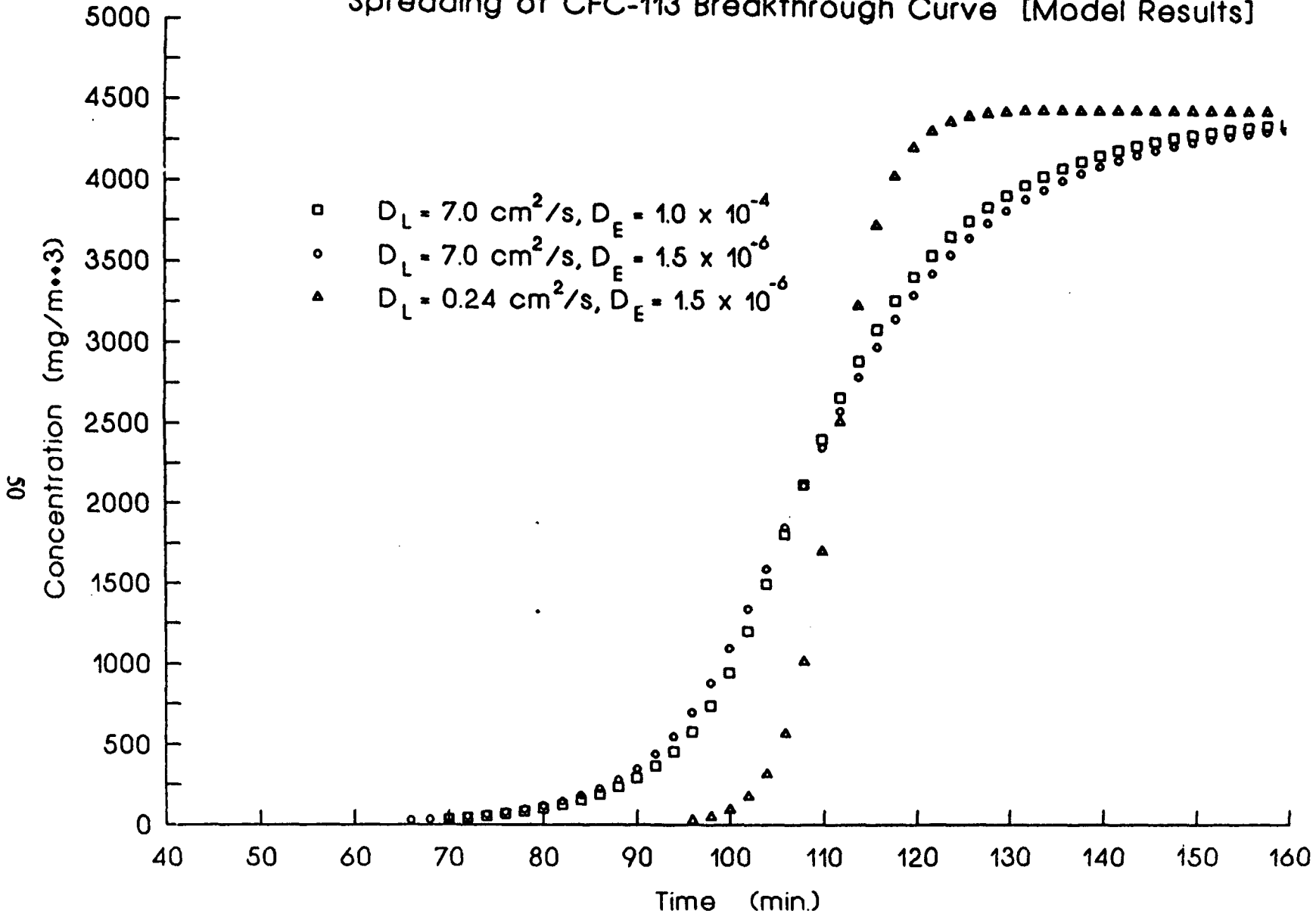

APPENDIX A-3

QUARTERLY PROGRESS REPORT

GC-PR-2194-03

REPORTING PERIOD:	2/1/91 - 4/30/91
REPORTING DATE:	May 15, 1991
CONTRACT NUMBER:	DAAA15-90-C-1056
CONTRACT TITLE:	Improved Filtration Materials and Modeling

I. Adsorption Equilibria

Single Component Measurements and Apparatus

Isotherms at 25C, 50C, 70C and 80C were measured for perfluorocyclobutane (PFCBa) on 13X molecular sieve. The results are presented in Figure 1. The procedure for preparing the molecular sieve pellets for isotherm measurements has been improved. Given below is a summary of the key steps involved.

1. 48 hours in a vacuum oven at 240C
2. Bleed He for 2 hours under vacuum at 240C
3. Turn heat off and bleed He under vacuum for 10 hours
4. Repressurize with He
5. Quickly place a small sample (approximately 1 g) of 13X in the tared sample bed
6. Quickly weigh the sample and place it in the closed-loop isotherm system.
7. Bleed He for 2 hours through the sample which is heated to 175C
8. Close the system and circulate (with the bed at 175C) through a nitrogen bath for 3 hours
9. Isolate sample bed and displace He with PSA effluent air

10. Equilibrate at the desired isotherm temperature and begin isotherm measurement process

The detailed procedure is given to show the problems associated with obtaining fundamental, single-component adsorption data on molecular sieves. We would expect to have to follow similar procedures to perform any fundamental measurement on 13X molecular sieve such as batch-uptake experiments to determine the effective intraparticle diffusivity.

Isotherm data measured at 25C for CFC-113 on 13X are compared with 25C data for PFCB. As shown in Figure 2 , CFC-113 is more favorably adsorbed than PFCB. For reference, at 1.0 mg/l, the loading of CFC-113 is 0.15 g/g and the loading of PFCB is 0.07 g/g.

Shown in Figure 3 is an isotherm of a BPL control carbon and the same BPL carbon treated to make it more hydrophobic. The results of this work clearly show, based on a comparison with control carbon, that the surface treatment did not significantly alter the water adsorption equilibria.

An experimental apparatus designed to measure the saturation capacity of the adsorbent (q_{sat} or W0) was constructed using a Cahn microbalance and preliminary experiments were performed. This system is very similar to the existing single-component isotherm systems in that a known mass of adsorbate is injected into a closed-loop equipped with a circulation pump. However, in this system, the loading q is measured directly using the Cahn balance.

and the vapor phase concentration, c, is calculated by subtracting the amount adsorbed from the amount injected and dividing that number by the loop volume. Shown in Figure 4 is some preliminary data from this apparatus, plotted with data measured using the single component isotherm system. With the Cahn data, the isotherm at 25C for CFC-113 on BPL carbon spans more than 6 decades of concentration, from about 0.003 mg/l to more than 3,000 mg/l. The steep rise observed in the final 6-8 data points probably results from an observed interaction with the vacuum grease. We have replaced the glass fittings with stainless steel to eliminate this problem.

Multicomponent Measurements and Apparatus

The multicomponent isotherm apparatus has been completed. Initial experiments were performed using the single component system of BPL carbon and CFC-113 and the results were within 3% (based on loading) of the values measured using the single component apparatus. A multicomponent point was measured using CFC-113 at 4.0 mg/l and a relative humidity of 75%. However, it was discovered that following the desorption step, the water concentration in the loop decreased slowly over time while the CFC-113 concentration remained constant. The problem has been solved by replacing the IR in the loop with a 3-liter stainless steel vessel. The best guess at this time is that the Teflon present in the IR absorbed the water.

II. Adsorption Theory

Single Component

We recently obtained software from BRL which allows us to quickly correlate isotherm data using the Modified Antoine Equation (MAE). The previous program we used would not work correctly unless the initial parameter values used to start the iterative calculation were very close to the final correlated values.

The initial data measured using the Cahn balance (Figure 3) indicate that the slope of the isotherm on a q vs ln(c) plot does not approach saturation linearly. The current form of the MAE cannot fit the behavior measured with the Cahn balance. We need to investigate the fundamental reasons for this behavior near saturation and make the appropriate changes in the methods used to correlate adsorption equilibria data. This works demonstrates the importance of measuring adsorption equilibria over a very large range of concentrations.

Multicomponent

We are exploring several different approaches to develop rules for describing multi-component adsorption equilibria with only single component isotherm data. One method we explored uses Ideal Adsorbed Solution Theory (IAST) with an excluded volume term to account for the differences in W0 between water and CFC-113. Preliminary results have not been promising. It appears that a more sophisticated approach using techniques to measure and/or estimate liquid phase activity coefficients will have to be developed.

III. Breakthrough Studies

An intensive investigation of axial dispersion has been undertaken during the last quarter (it will completed in about 1 month). As part of this study a major modification to the experimental apparatus was made. The glass bed was replaced by a 1-inch diameter stainless steel bed used in the PSA testing. The bed is wrapped tightly with 1/4 inch copper tubing and temperature controlled water is circulated through the copper tubing. Thermocouples are placed in the system just above the carbon and at a point just below the bottom screen. The stainless steel bed is approximately 35-cm long, and typical carbon bed depths range from 4 to 16 cm. The preliminary results show that the temperature difference between the thermocouples is never more than 1 C. This modification allows us to run isothermally and to maintain better temperature control for 25C experiments even when the room temperature fluctuates (sometimes 5-7C).

IV. Pressure Swing Adsorption

Experiments and Apparatus

A significant problem developed in PSA apparatus. The packing in the three-way valves currently used in the system gradually deform such that leaks from the high pressure side of the valve to low pressure side occur. As a result, a fraction of the feed chemical never passes through the bed since it is discharged directly into the purge. This problem has been resolved in the short term by replacing the valve seats on a regular basis, and in the long term by purchasing poppet valves designed to open and close several million times.

One of our major efforts has focused on obtaining a material balance. This is difficult in PSA systems, since concentrations of purge and product can change considerably during a half cycle and flow measurement devices can be affected by high velocities and pressure waves during pressurization and blowdown. However, we have been able to overcome some of these problems by adding surge tanks for the purge and product flows. Each tank is approximately 30 liters.

For a number of reasons, most related to the ASM program, it was necessary to investigate the performance of PSA systems using 13X molecular sieve. As part of this study, operating conditions were chosen to simulate the performance of a vendor's full-scale unit. Figure 5 shows the results of this study using CFC-113 as the feed chemical. The inlet RH is less than 5% at atmospheric pressure, thus less than 25% at the system pressure of 50 psig. Beds were allowed to equilibrate by operating the PSA system for 16 hours with no feed chemical. These results have two important features. First, the 13X molecular sieve at these operating conditions can provide protection against materials similar to CFC-113 for average feed concentrations (e.g. 2 mg/l) for reasonable time periods (e.g 10-20 minutes). Second, a total material balance at steady can be obtained. Below is the calculation for the material balance at STP.

Theory (Mathematical model)

It is not possible at this time to simulate the CFC-113 or PFCBa on 13X experiments with the math model. This is because water adsorbs so strongly on 13X that the model needs appropriate multi-component adsorption equilibria to produce reasonable predictions. However, a PSA simulation for the 13X-water system was performed using isotherm data from Linde which indicates approximately 1/3 of the bed is saturated with water using the operating conditions given in Figure 5 and a feed concentration of water corresponding to 5% RH. One may conclude that the top 8 cm of the beds used in the experiment depicted in Figure 6 have no capacity for CFC-113 or PFCba.

Figure 1. Isotherm Data for PFCBa on 13X Molecular Sieve at 25, 50, 70 and 80C

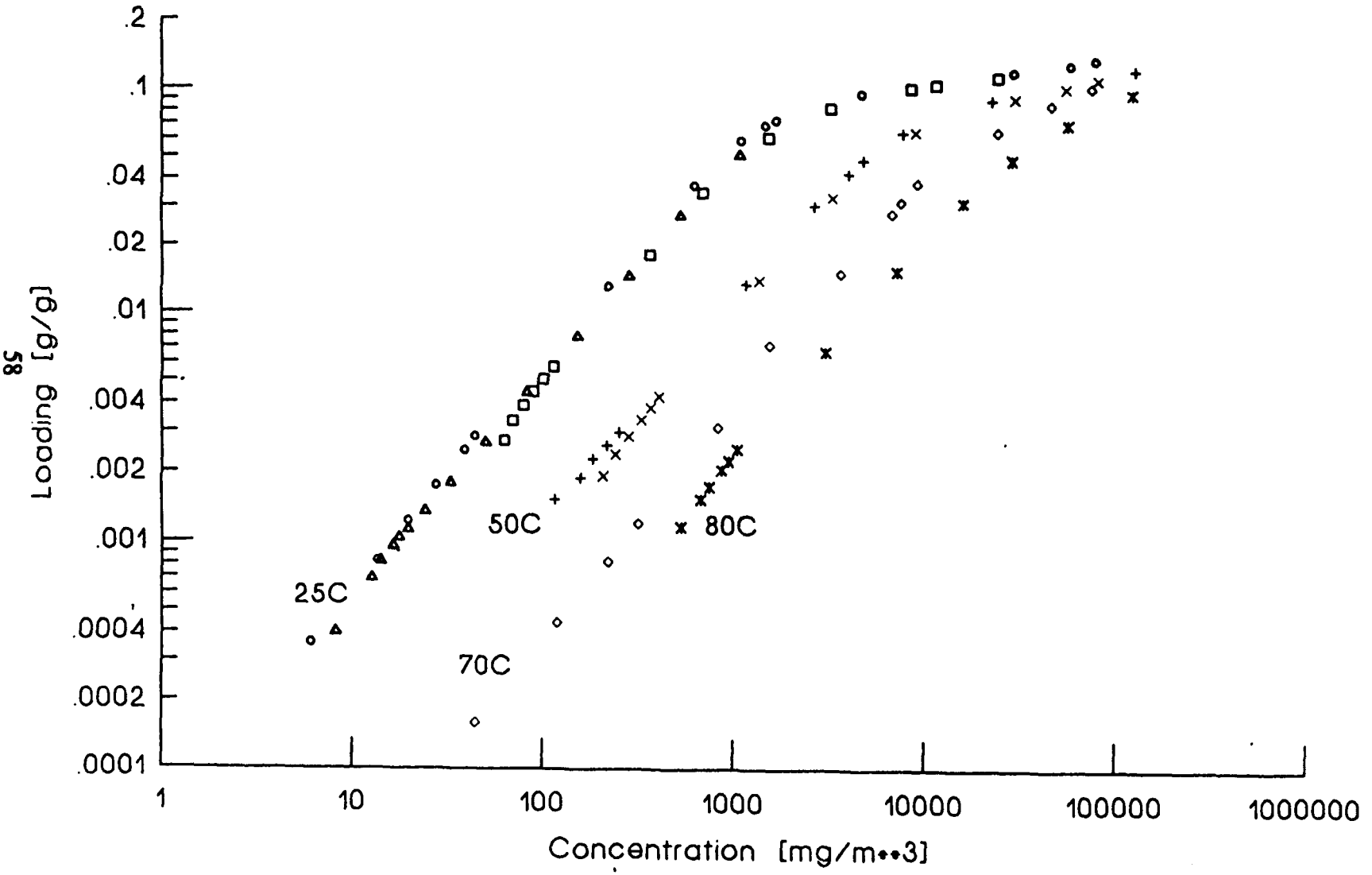

Figure 2. Isotherm Data for PFCBa and CFC-113 on 13X Molecular Sieve at 25C

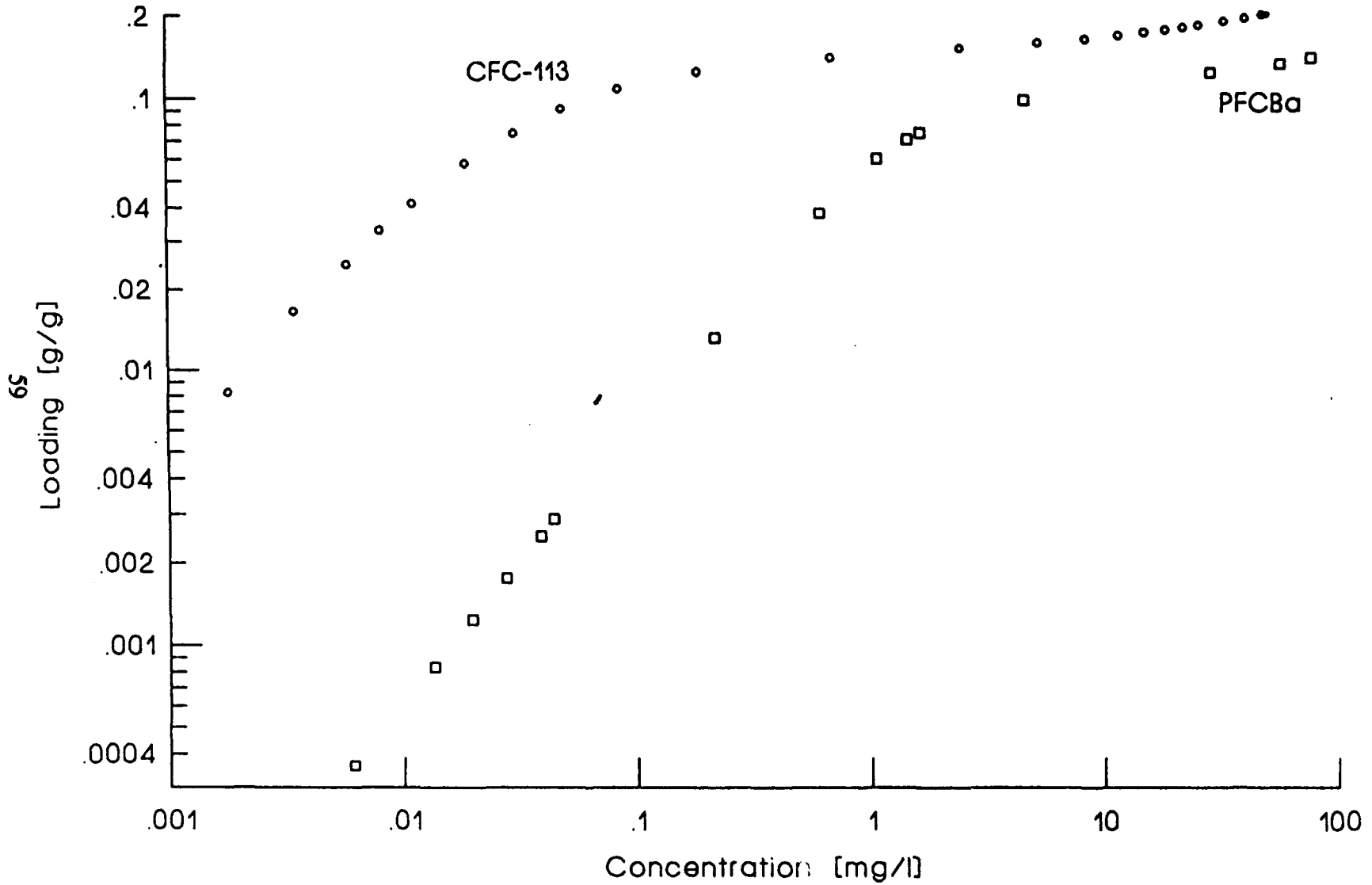

Figure 3. Water Isotherms for BPL and Treated BPL Carbons at 30C

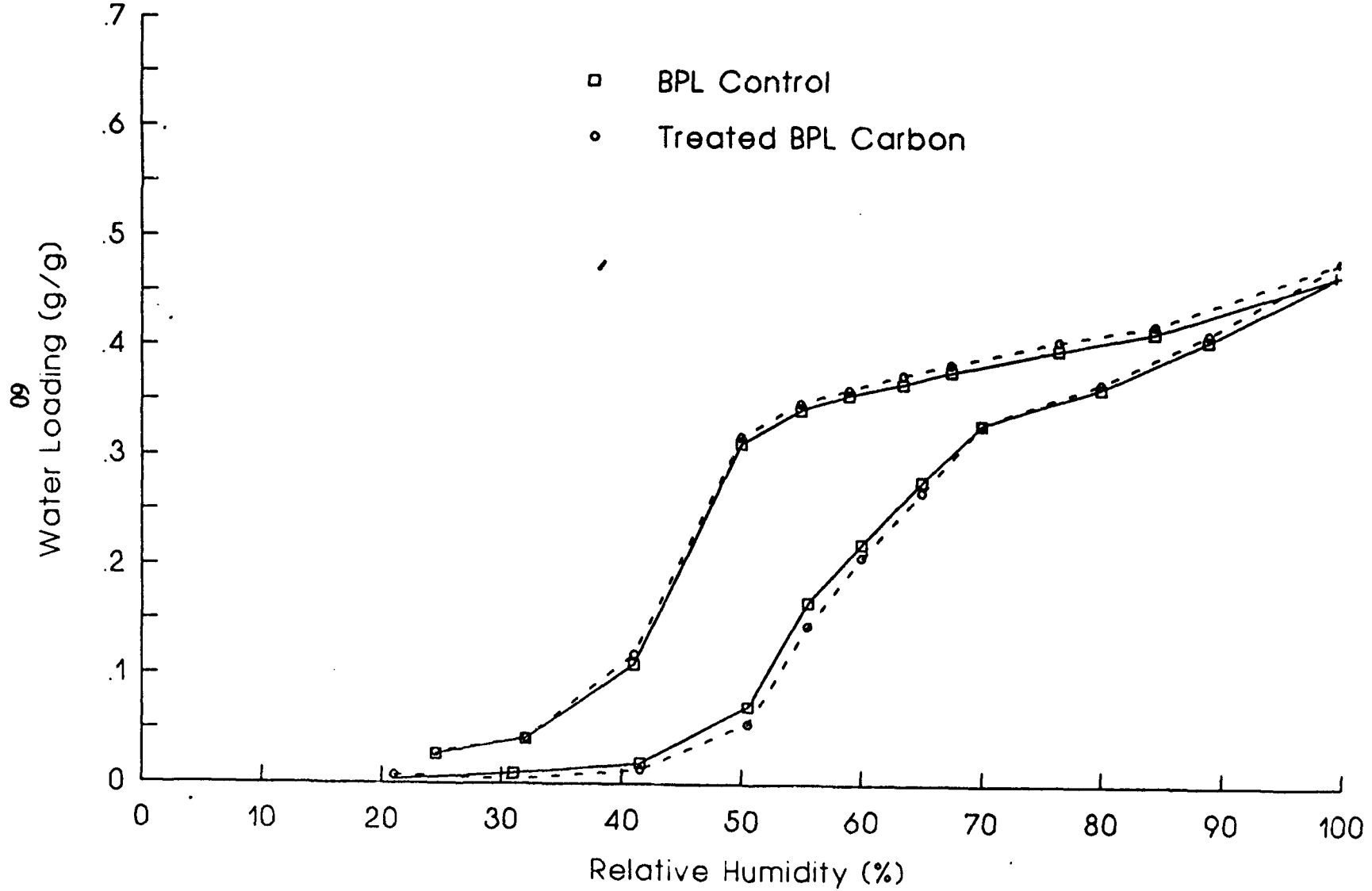

Figure 4. Isotherm Data for Freon 113 on BPL Carbon at 25C

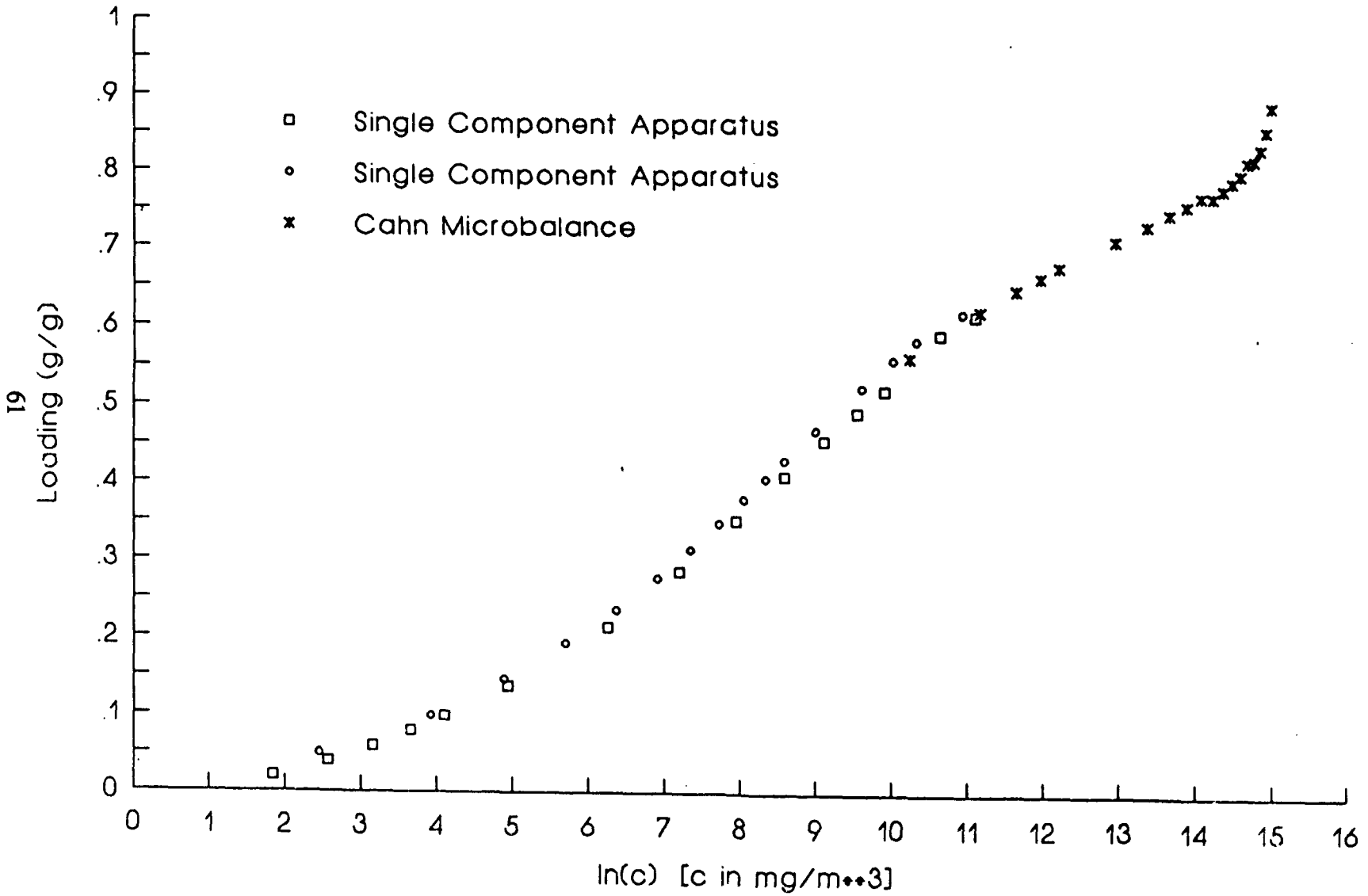

Figure 5. PSA Results for CFC-113 on 13X Molecular Sieve
60s cycle, 24cm bed, 50 psig, 2in diameter

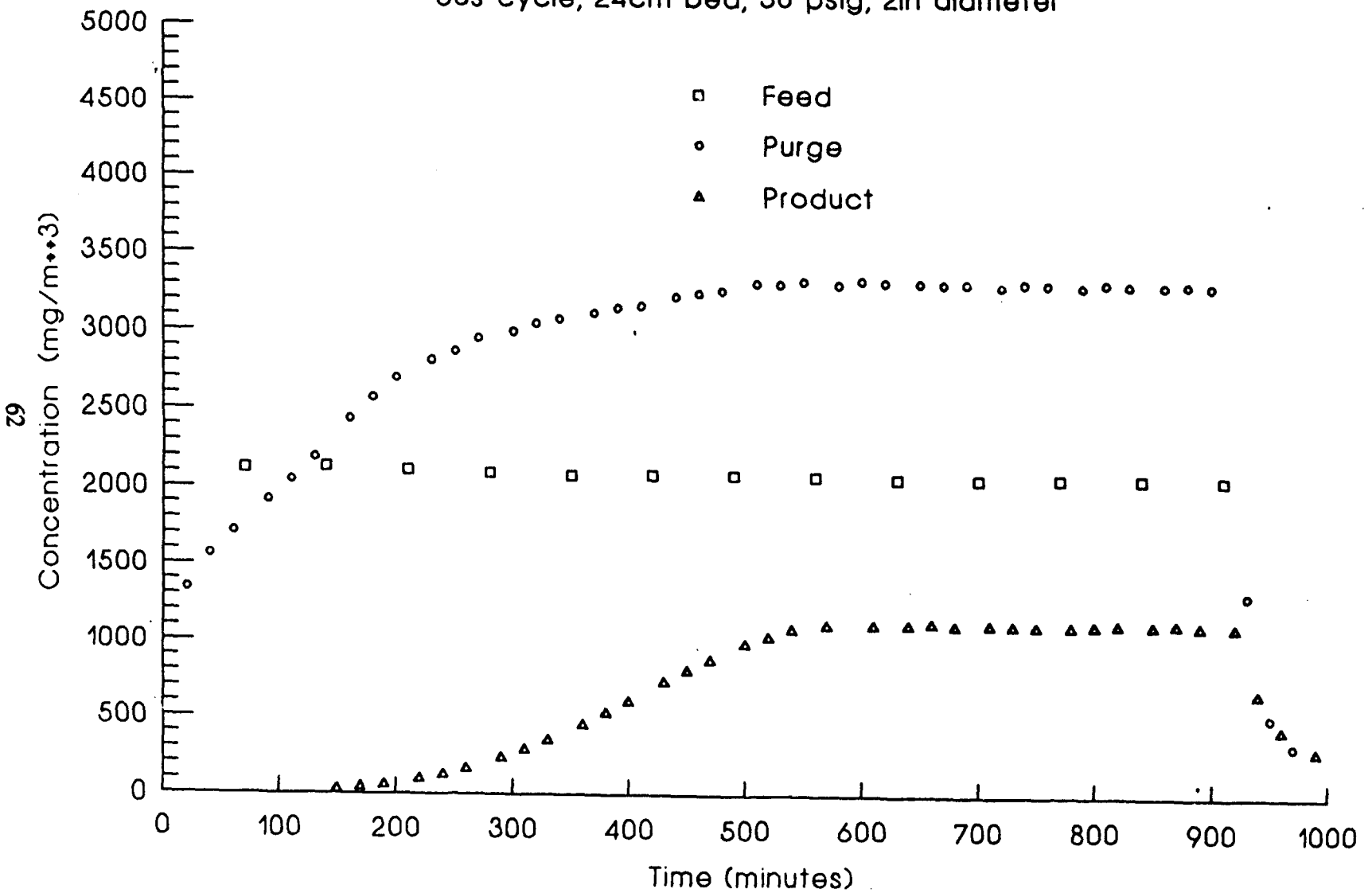

Figure 6. PSA Results for 13X Molecular Sieve
60s cycle, 24cm bed, 50 psig, 2in diameter

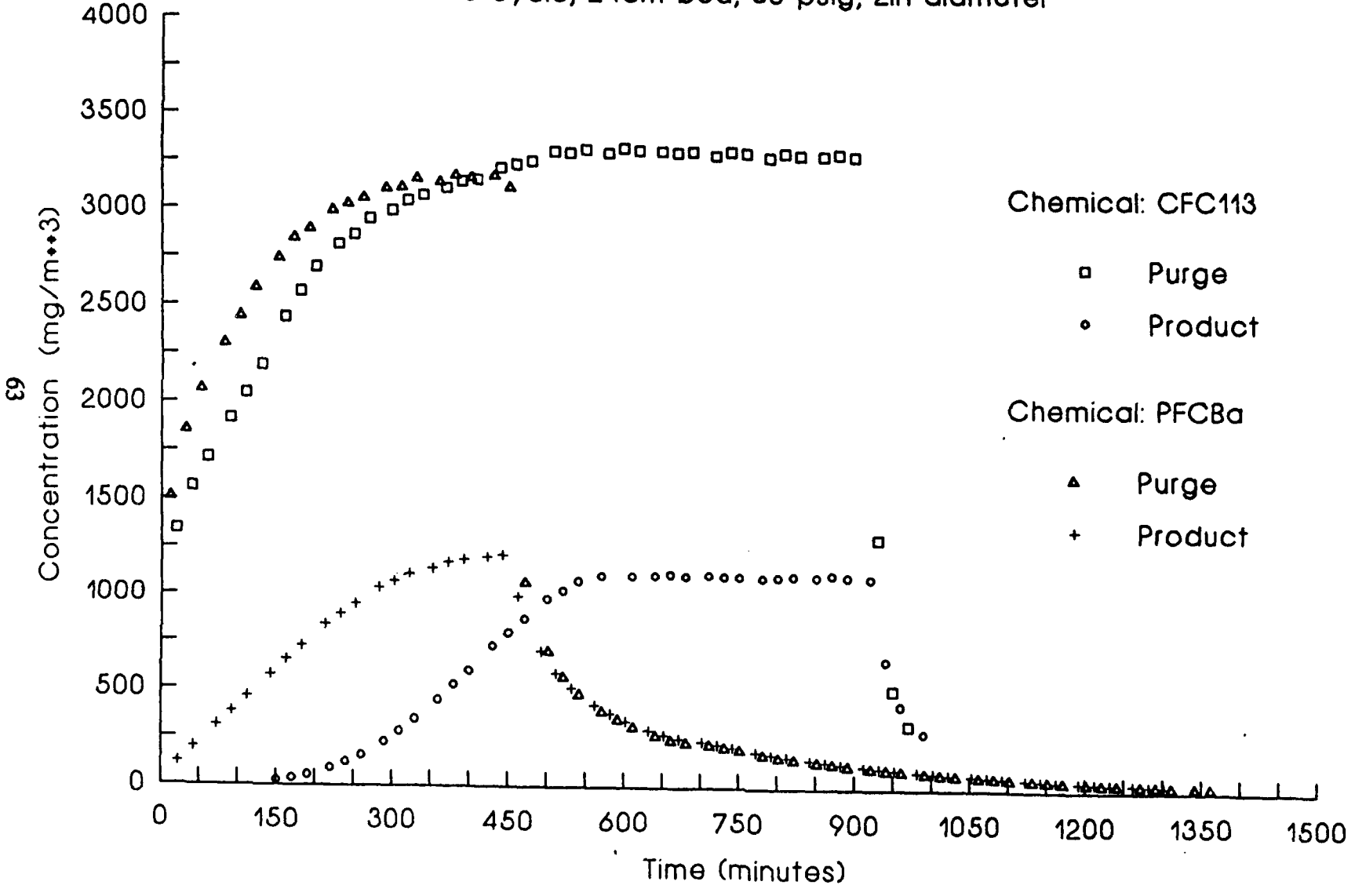

Blank

APPENDIX A-4

QUARTERLY PROGRESS REPORT

GC-PR-2194-04

REPORTING PERIOD:	5/1/91 - 7/31/91
REPORTING DATE:	August 15, 1991
CONTRACT NUMBER:	DAAA15-90-C-1056
CONTRACT TITLE:	Improved Filtration Materials and Modeling

I. Adsorption Equilibria

Single Component Measurements and Apparatus

Temperature control during the course of an isotherm experiment was dependent to a certain degree on the room temperature. We have modified this system to maintain the desired isotherm temperature by submerging the adsorbent bed in a temperature controlled water bath. This change has enabled us to run the 25C experiments successfully even when the room temperature changes from 19C to 27C and back again.

The program controlling the isotherm operation has been converted into Pascal and now runs on the PC. The temperature setpoint for the water bath can be now downloaded from the computer, which allows us to measure multiple isotherms during the same run. This should increase production by reducing the time to measure three isotherms by about 2/3. Shown in Figure 1 are isotherm data for PFCBa on substrate carbon measured with the modified system (approximately 2 days) versus data measured using the old system (approximately 6 days).

Samples of a new superactivated carbon which had been pelletized (MAXSORB) were received from PPD. Water and CFC-113 isotherms were measured and these data were compared to results obtained for BPL carbon. Figures 2 and 3 summarize the results of this study. Note in Figure 3 how the CFC-113 loading on the MAXSORB is less than the BPL at low CFC-113 concentration, but much higher near saturation. This has interesting implications since the breakthrough time of CFC-113 on the BPL at low concentrations could be much longer than the MAXSORB, while at higher concentrations the situation could reverse. The surface area of the MAXSORB by nitrogen BET is about 2 times higher than the BPL. Therefore, if one based performance on surface area measurements, the wrong conclusions would be made at the low CFC-113 concentrations.

Multicomponent Measurements and Apparatus

Experiments were performed using CFC-113 on BPL carbon at 60%, 70% and 80% relative humidity (RH). These results are summarized in Figures 4, 5 and 6. Inconsistencies in the data, particularly the water loadings at 80% are being investigated. One problem identified is that the volume of the analysis loop is too small relative to the amount of water adsorbed. Following desorption and trapping of the adsorption water by liquid nitrogen, the water is allowed to vaporize in the analysis loop. If this loop is not large enough, all of the water cannot vaporize, thus false low loadings may be calculated.

II. Breakthrough Studies

The first phase of the axial dispersion study has been completed. We are presenting an invited paper on the subject in Paris, France on September 11, 1991. Three major conclusions are drawn from this work:

1. Axial dispersion can control the breadth of the breakthrough curve even for deep beds.

2. If one employs the Fickian model, then the axial dispersion coefficient is a function of the shape of the adsorption isotherm. The Fickian model cannot represent breakthrough of very strongly adsorbed vapors.

3. Axial dispersion is affected by the bed diameter under certain conditions, with smaller diameter beds exhibiting sharper breakthrough curves than larger diameter beds.

III. Pressure Swing Adsorption

Experiments and Apparatus

For PSA systems employing 13X molecular sieve as the adsorbent, the effects of adsorbed water can be dramatic. The effect, called "creeping death", results from the adsorbed water wave gradually advancing down the bed after each cycle. Figure 7 shows the effect of creeping death on the PSA system performance against PFCBa using 13X molecular sieve as the adsorbent. Two experiments were run, one where the PSA system was conditioned without chemical for 4 days using a feed of 80% RH air. The second experiment used a bed conditioned for only 15 minutes prior to the introduction of the PFCBa challenge. The difference in the breakthrough curves for the system conditioned 4 days as opposed to 15 minutes is dramatic. After 50 minutes (50 cycles) there is no measurable concentration of PFCBa in the product air of the system conditioned 15 minutes while the product concentration in the bed conditioned 4 days is almost 1000 mg/m^3.

A comparison of adsorbents was performed at 80%RH using CFC-113. The conditions used for the test are given in Figure 8 along with the results. The breakthrough of the CFC-113 occurs almost immediately with 13X Molecular Sieve and reaches its steady state value in a few hours. On the other hand, the system with the BPL carbon adsorbent does not have any measurable CFC-113 in the product until 1700 minutes. This tremendous difference in performance provides a strong argument to choose BPL carbon over 13X for the PSA system.

The breakthrough behavior of PFCBa and CFC-113 on 13X molecular sieve under identical conditions is shown in Figure 9. The PFCBa run was cut short because we ran out of chemical. However, it is clear that the breakthrough of PFCBa begins about 200 minutes prior to the CFC-113. This is to be expected since PFCBa is a more volatile, less strongly adsorbed vapor.

An important system operational parameter is the purge to feed ratio. This is one measure of the efficiency of the system, since high purge to feed ratios imply that most of the purified vapor is discarded via the purge. Shown in Figure 10 are results obtained using 13X molecular sieve and PFCBa at 80% RH. The bed was conditioned 15 minutes prior to the start of the PFCBa challenge. The two ratios employed are 71/154 = 0.461 and 85/155 = 0.548. The breakthrough behavior of the system using the smaller purge to feed ratio shows measurable levels of PFCBa almost immediately, while the first measurable concentration for the high purge to feed occurs at about 70 minutes. Also, the steady state product concentration is higher for the lower purge to feed ratio experiment. The significance of this data is that one must determine the purge to feed ratio that produces the appropriate amount of product yet still provides acceptable protection.

A major modification to the PSA system has been initiated. The in-bed sampling system has been constructed and it should be operational within the next several weeks. This will provide a unique capability to measure vapor phase concentration profiles and track the progression of adsorption waves through the bed. These results will provide valuable data to assess the validity of the mathematical model.

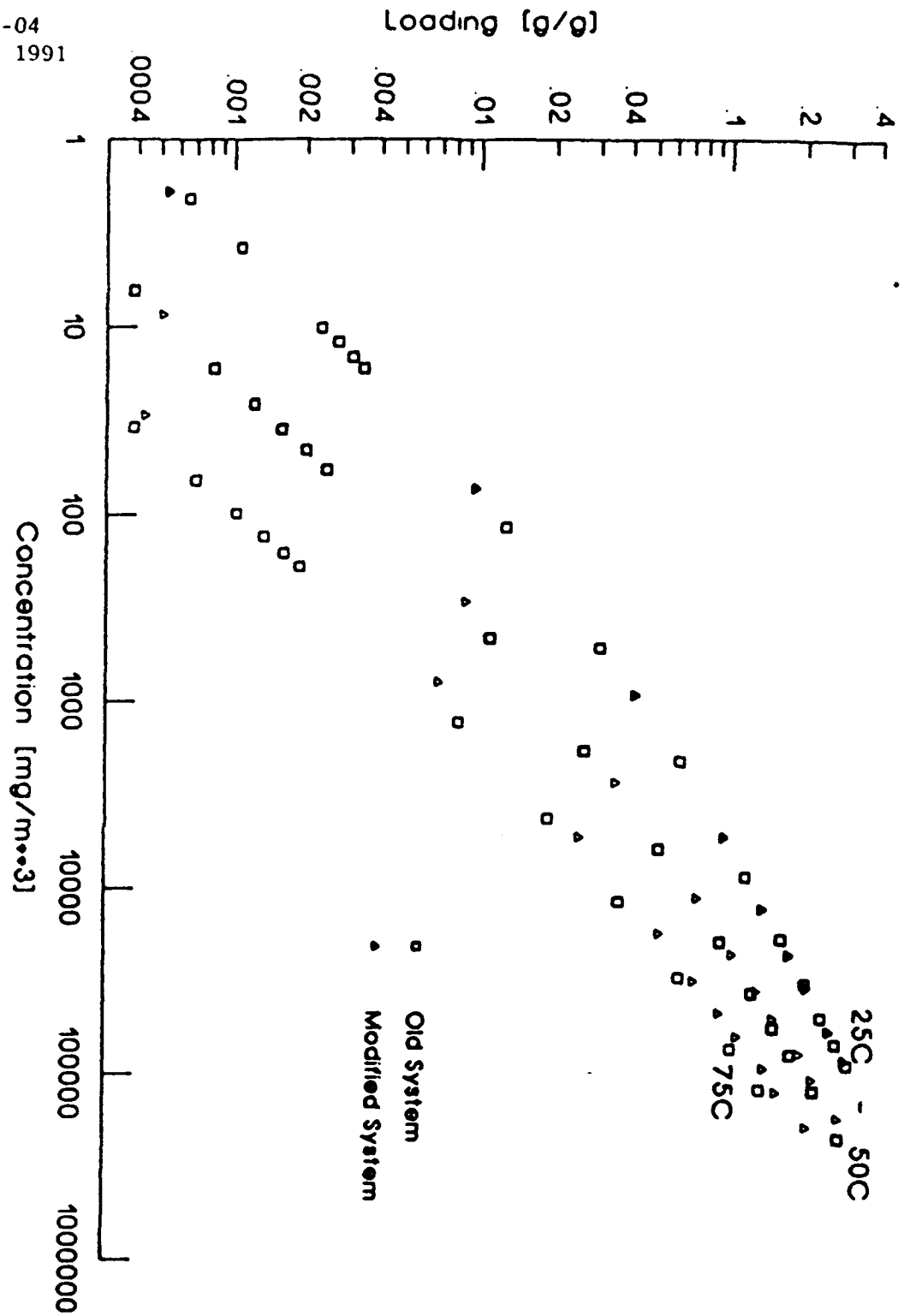

Figure 1. Isotherm Data for PFCBa on 12x30 Substrate (9A18-U) at 25, 50 and 75C

GEO-CENTERS, INC.

Figure 2. Isotherm Data for Water on MAXSORB Carbon at 30C

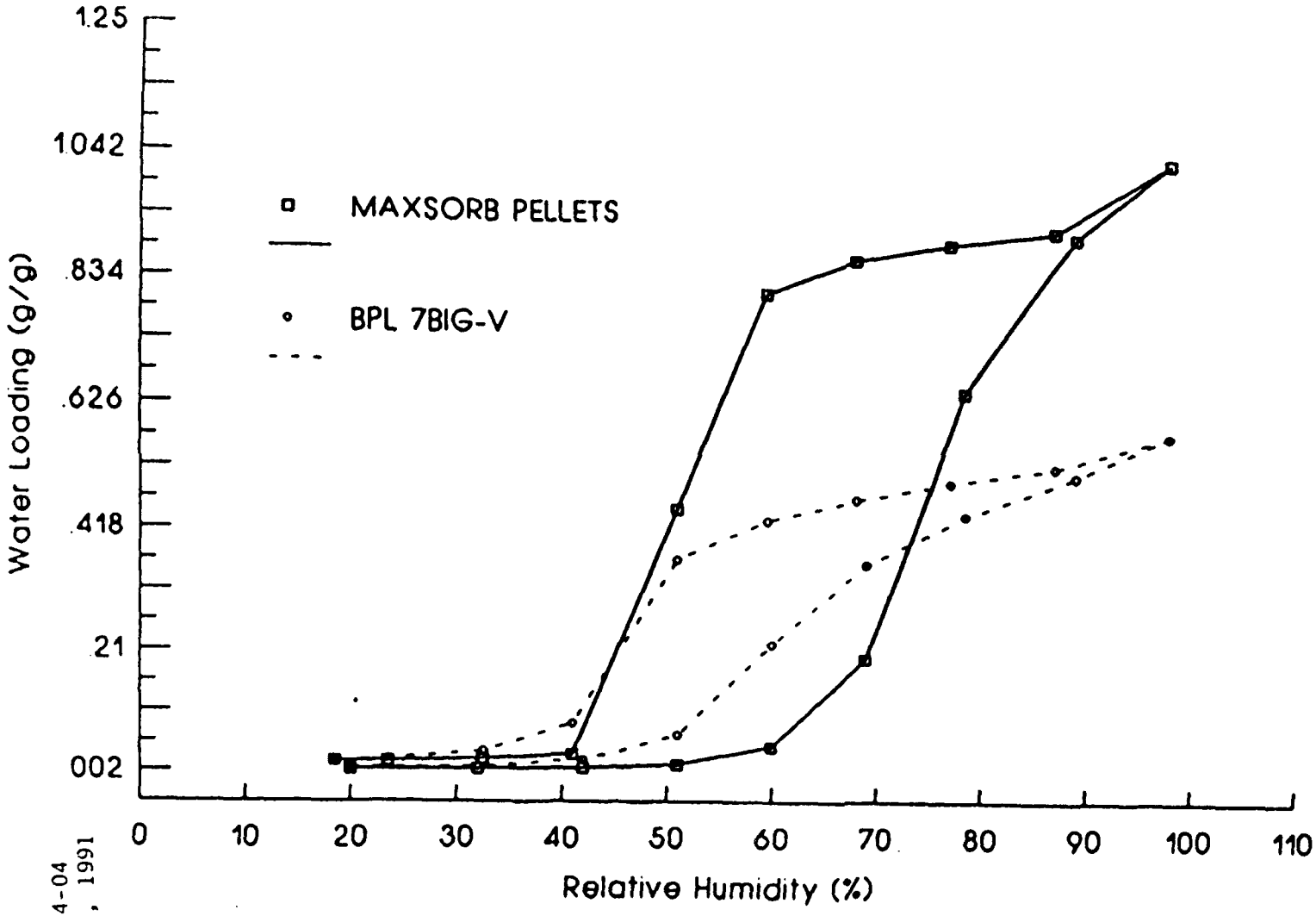

GEO-CENTERS, INC.

71

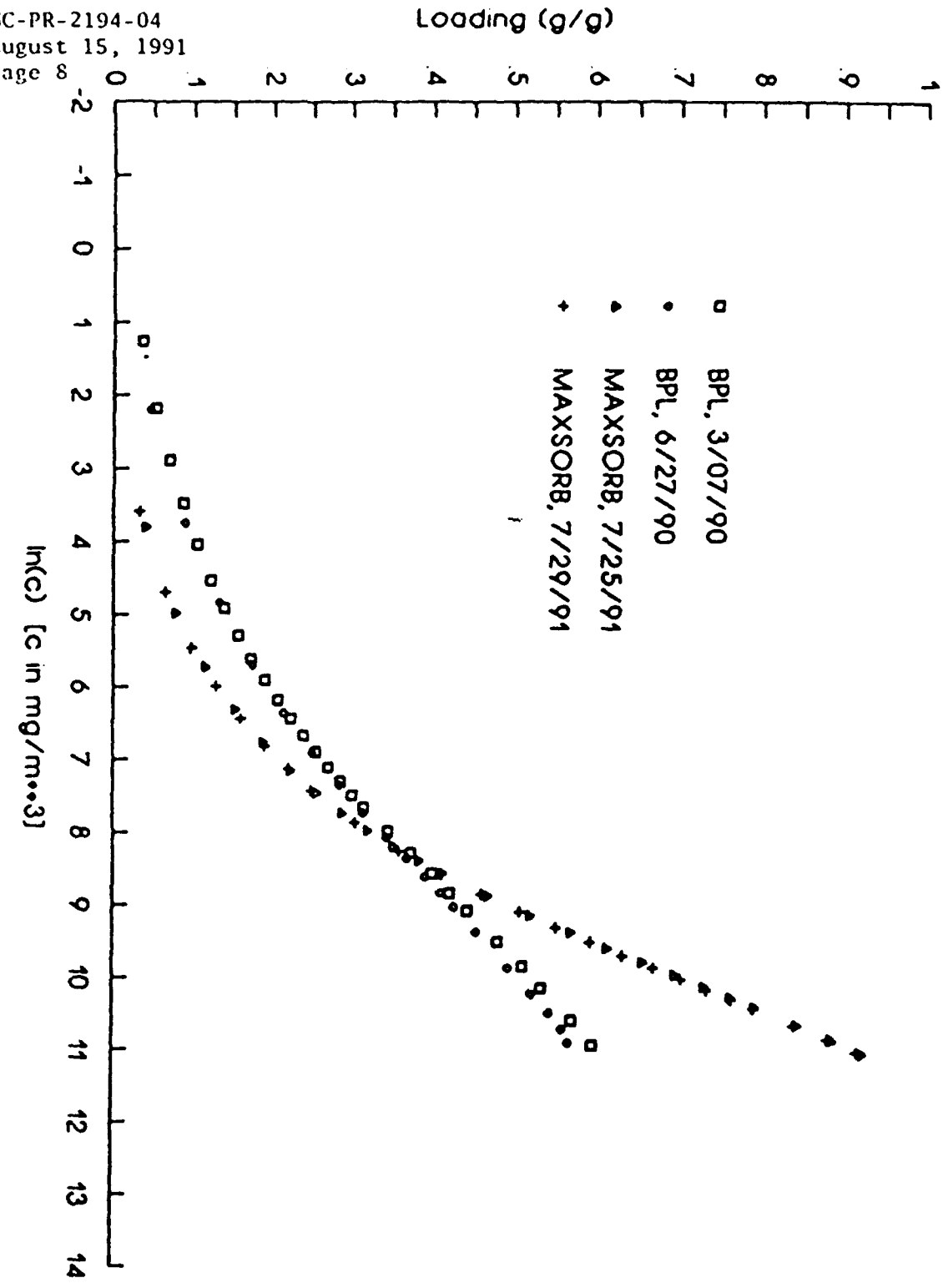

Figure 3. Isotherm Data for CFC113 on Dry BPL(7BIG-V) and MAXSORB Pellets at 25C

GEO-CENTERS, INC.

Figure 4. Multicomponent Isotherm Data for CFC113 on 12x30 BPL at 60% RH and 25C

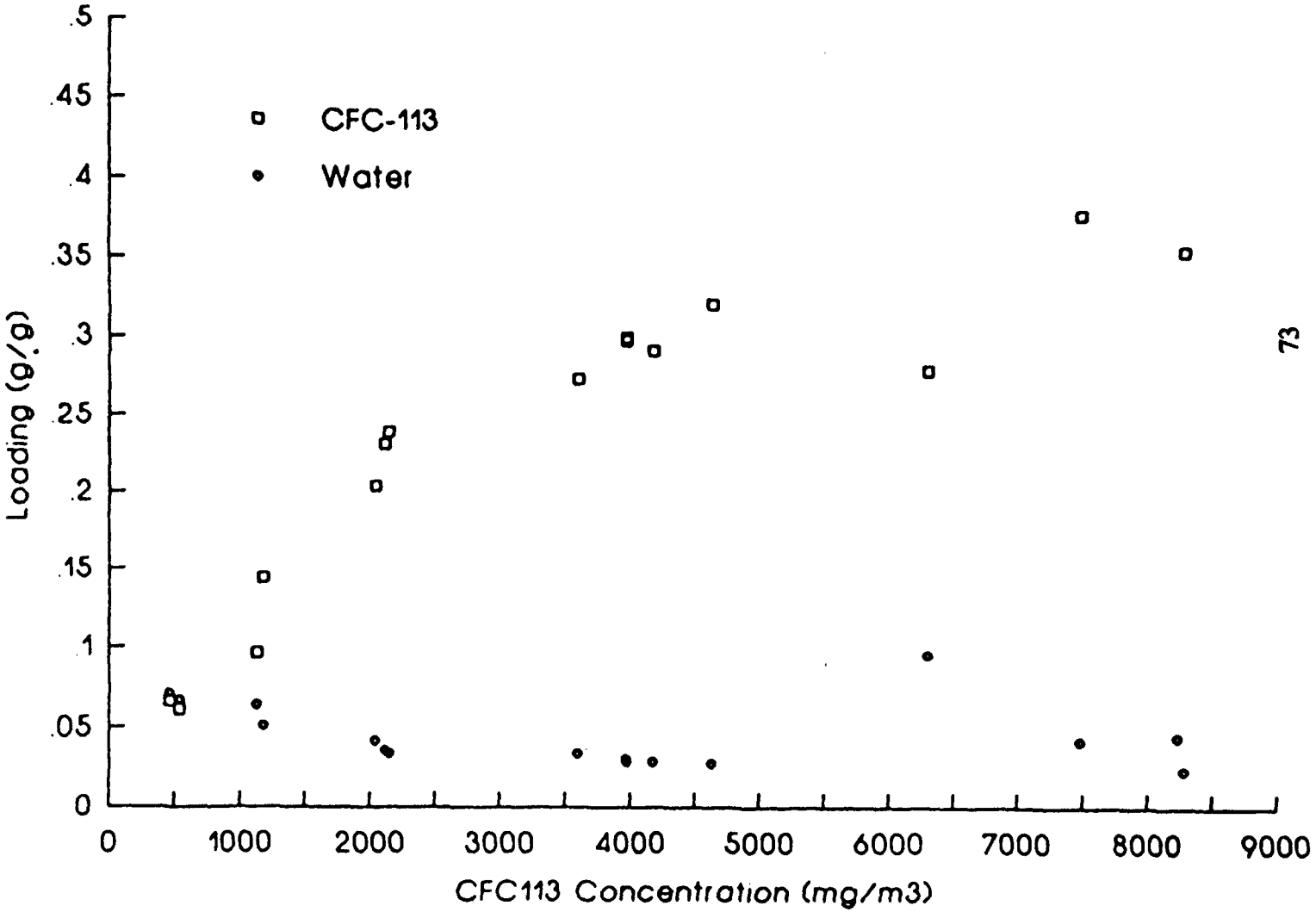

73

Figure 5. Multicomponent Isotherm Data for CFC113 on 12x30 BPL at 70% RH and 25C

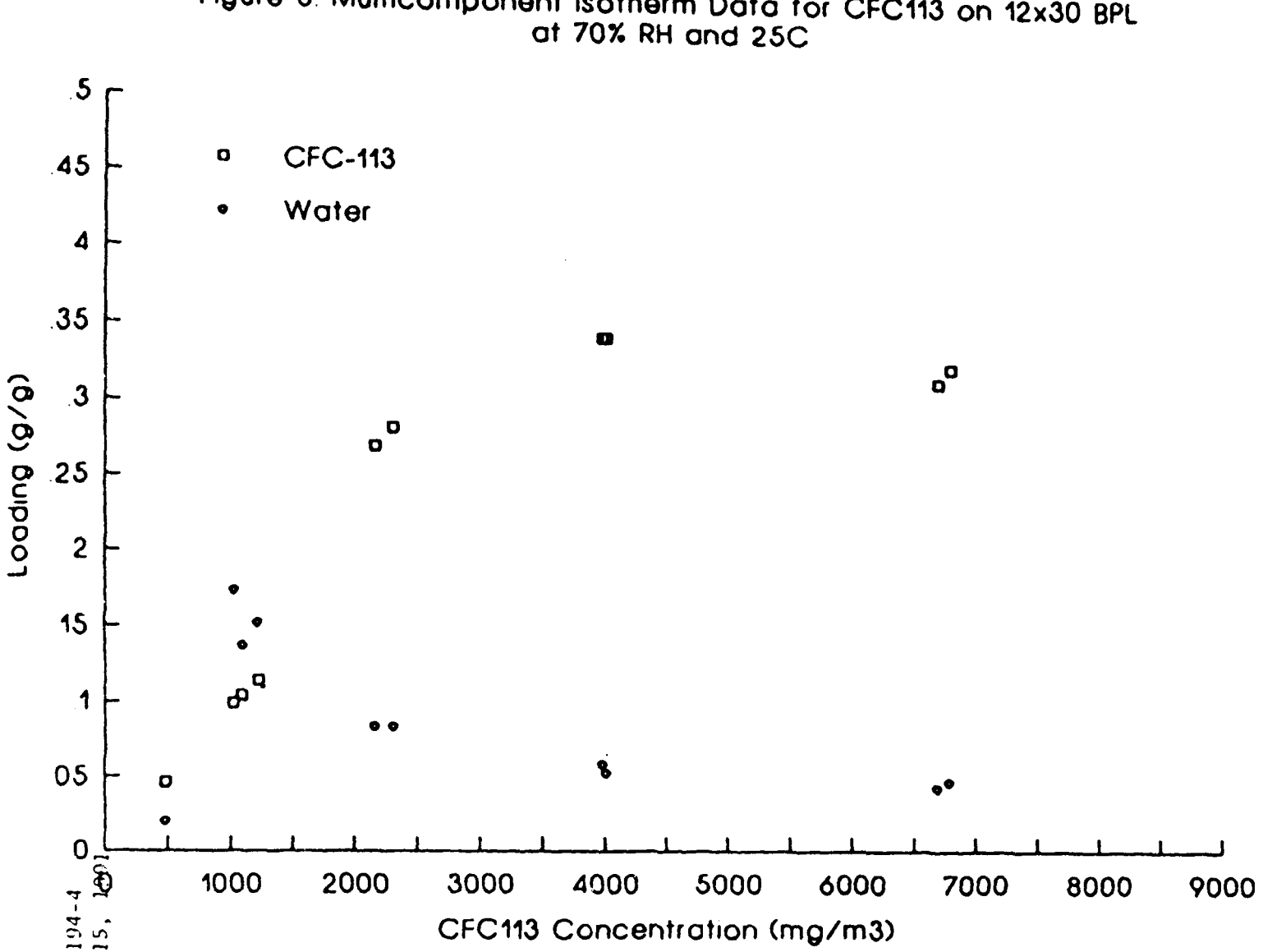

GEO-CENTERS, INC.

74

Figure 6. Multicomponent Isotherm Data for CFC113 on 12x30 BPL at 80% RH and 25C

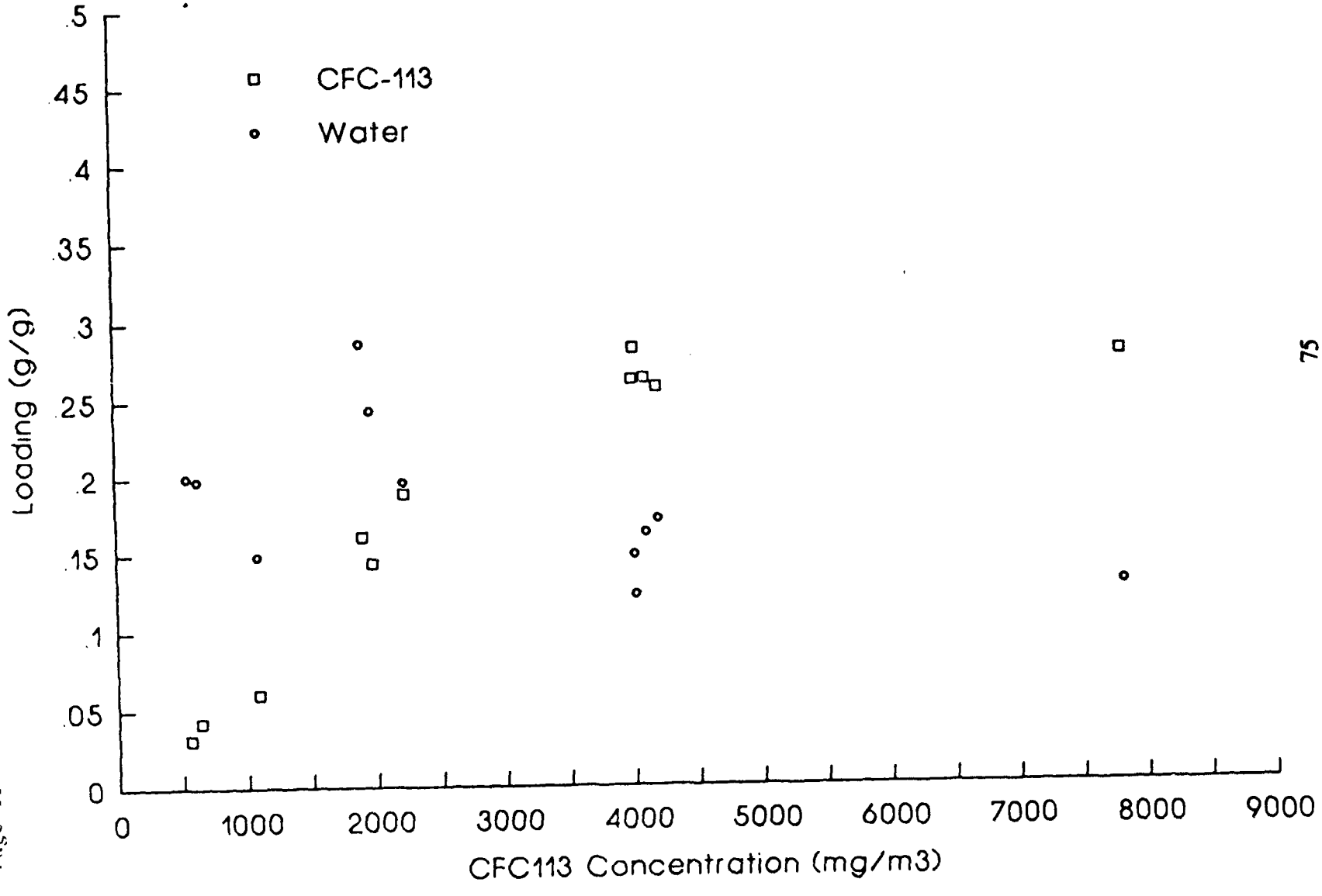

Figure 7. PSA Results for PFCBa on Molecular Sieve
60s cycle, 24cm bed, 2in diameter, 53 psig
Purge 85LPM, Product 70LPM

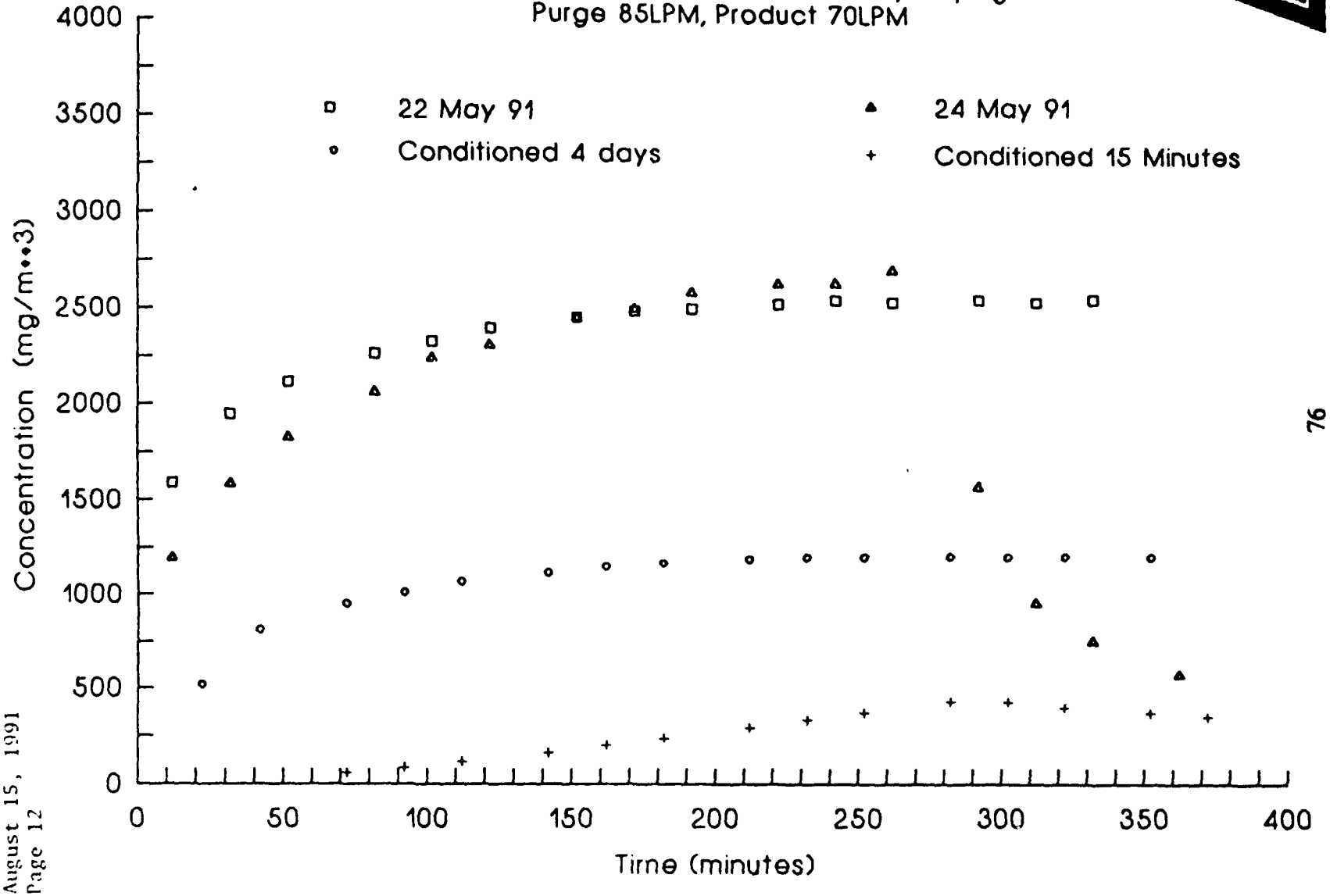

76

Figure 8. PSA Results for CFC-113 at 80%RH
60s cycle, 12cm bed, 50 psig, 2in diameter
Conditioned at 80%RH for 18 Hours
23 July 91 and 18 July 91

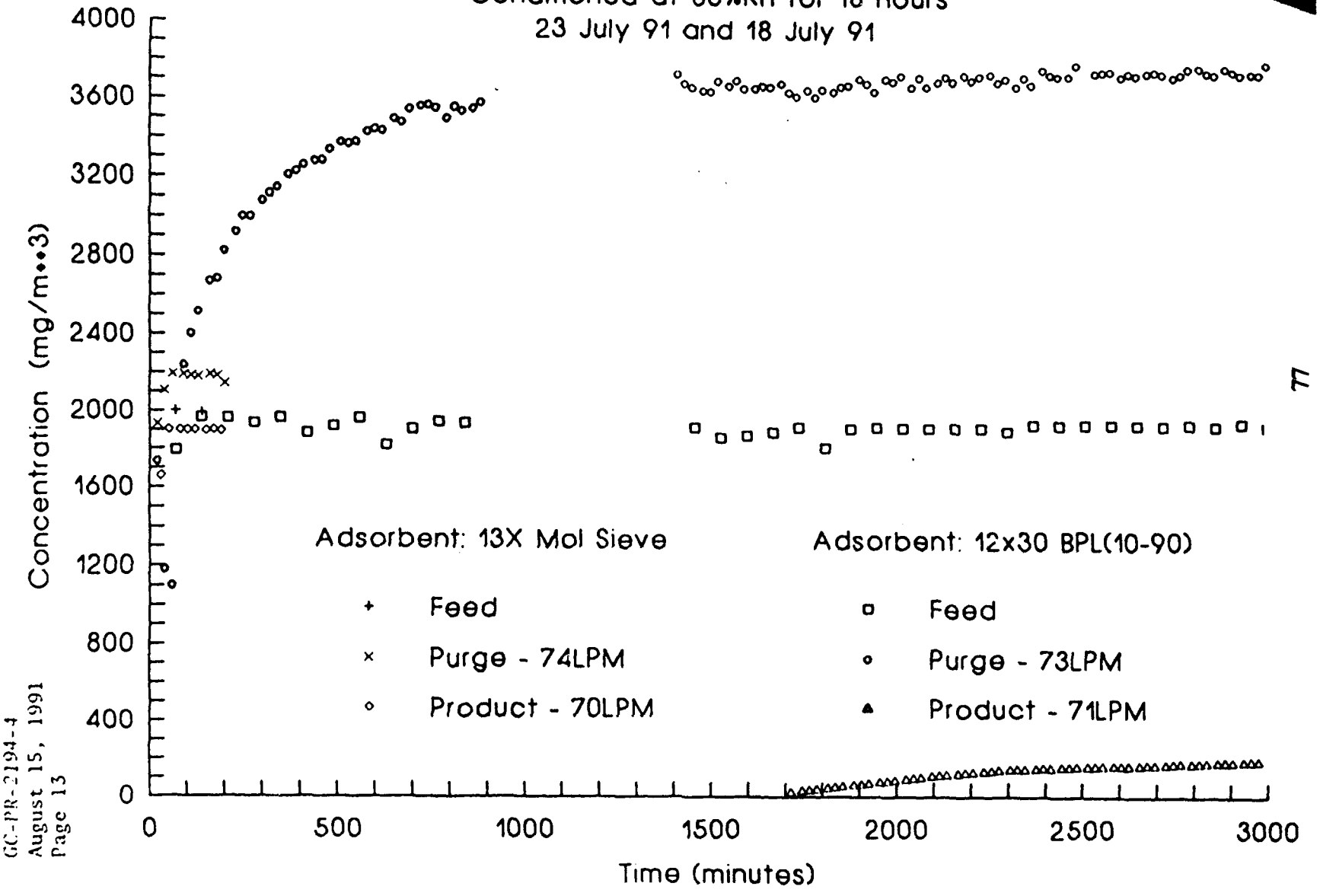

77

Figure 9. PSA Results for 13X Molecular Sieve
60s cycle, 24cm bed, 53 psig, 2in diameter
Purge 85LPM, Product 70LPM

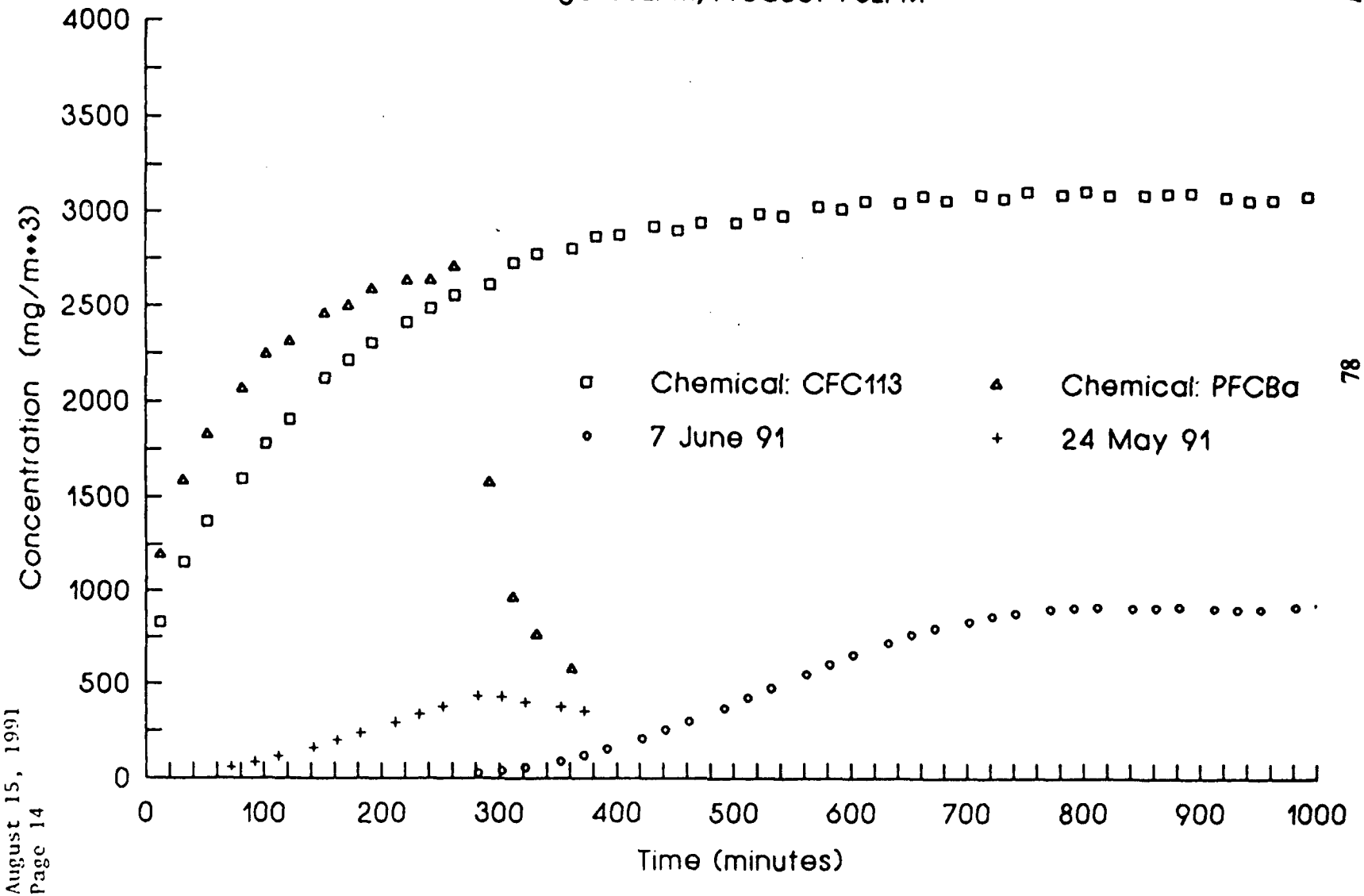

78

Figure 10. PSA Results for PFCBa on 13X Molecular Sieve
Varying Purge to Feed Ratios

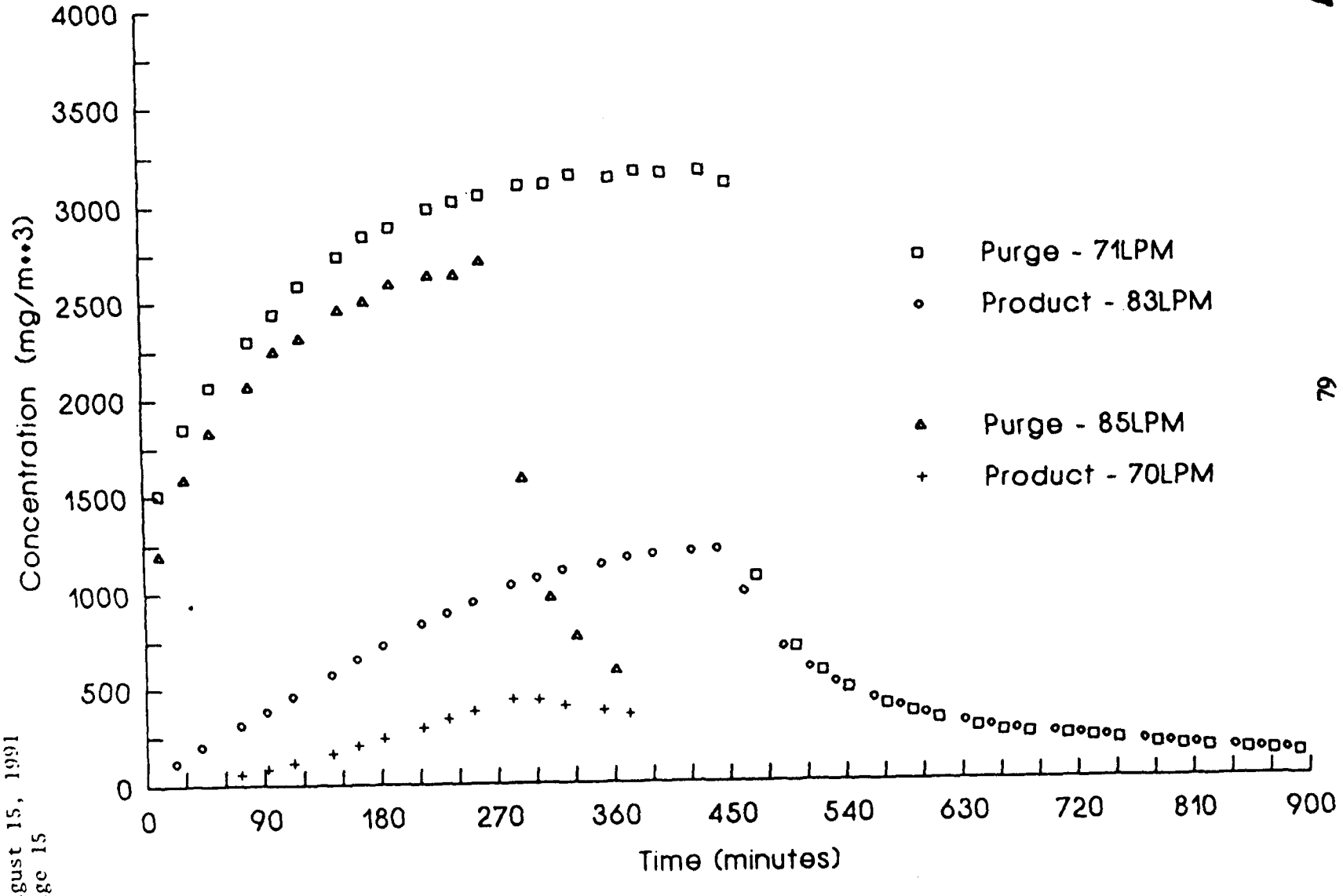

79

Blank

APPENDIX A-5

QUARTERLY PROGRESS REPORT

GC-PR-2194-05

REPORTING PERIOD:	8/1/91 - 10/31/91
REPORTING DATE:	11/15/91
CONTRACT NUMBER:	DAAA15-90-C-1056
CONTRACT TITLE:	Improved Filtration Materials and Modeling

I. Adsorption Equilibria

Single Component Measurements and Apparatus

Several improvements to the system were made during the last quarter. The chemical injection system was modified to produce more repeatable injections of PFCBa. In addition, the computer program which controls the operation has been reconstructed to provide a better user interface and, more importantly, better overall system control. Some specific examples of these improvements include a feed-back temperature control loop and a chemical injection system where the mass of chemical injected for each equilibrium point is closely controlled.

Single component isotherms for PFCBa on BPL activated carbon and 13X molecular sieve are shown in Figures 1 and 2, respectively. These results verify the accuracy and reproducibility of the new system and also point out the advantages of the controlled mass injections. Notice that the data points are evenly spread on the log-log plots. Fewer points are required to obtain the same isotherm information at a given temperature.

Multicomponent Measurements and Apparatus

A major modification was made to the multicomponent system. A sparging system has replaced the Miller-Nelson for relative humidity control. The sparging system consists of three vessels connected in series and submerged in a temperature controlled water bath. By setting the temperature of the bath and the flow rate of nitrogen through the sparger vessels, the desired feed RH to the bed can be established and controlled very precisely. The initial results using this system have been very promising.

II. Breakthrough Studies

An invited paper entitled "Axial Dispersion Effects on the Breakthrough Behavior of Favorably Adsorbed Vapors" was given in Paris, France on September 11, 1991. A copy of this paper, to be published as part of a symposium series, is given in Appendix A.

A major emphasis has been placed on independently determining the axial dispersion coefficient, D_L, for our PSA model (see PSA modeling section). At this time, there is good reason to believe that D_L is a function of pressure. Thus, the value for the feed step is different than the value for the purge step.

The PSA system was used with slight modifications to measure breakthrough curves at PSA feed pressures (30-60 psig). Shown in Figure 3 are the results of an experiment using CFC-113 and 12x30 mesh BPL carbon at 45 psig. The bed depth was 30 cm and the bed diameter was 2 inches. An in-bed sample was taken 5 cm from the bed outlet, i.e. a bed depth of 25 cm. The effluent concentration was measured using an IR analyzer. These results confirm that constant pattern has been achieved. We are in the process of analyzing these data to determine D_L.

After the bed was saturated, the bed was purged using clean air in a counter-current direction. Figure 4 shows the results of the study using all the in-bed probes. These results are used to evaluate D_L during the purge step.

III. Pressure Swing Adsorption

Experiments and Apparatus

The in-bed sampling system is now functional. Shown in Figures 5 and 6 are results from PSA experiments using a cycle time of 1 minute and about 1:1 purge to product flow rates. Only the total flow rate of 171 SLPM versus 150 SLPM are different. These results clearly show the capability of the PSA system to provide protection. In both cases, no product is measured for approximately 300 cycles (300 minutes). Further, operating under a purge to product ratio of 1, the plateau concentrations at 5 and 10 cm into the bed are much smaller than the feed concentration.

Figures 7 and 8 show the results for lower purge to feed ratios. Compare the results in Figure 6 to those in Figure 8. The only difference between the two experiments is the purge to product flow rate ratio. For the purge to product ratio of 1:2 (Figure 8), the breakthrough of each port down the bed almost reaches the plateau value of the previous port. This is in sharp contrast to the results shown in Figure 6 where the plateau levels are greatly reduced. Also, consider the breakthrough time of the 15-cm port in each experiment. For the low purge to product ratio, the breakthrough time is about 1200 minutes (cycles), while for the 1:1 purge to product ratio, the breakthrough time is almost 4000 minutes. This is typical of the change in performance resulting from changes in the purge flow rate.

Math Modeling

Based on the results given in the paper presented in Paris, it is clear that : (1) A quantitative understanding of axial dispersion is required to develop a useful PSA model, and, (2) The axial dispersion coefficient is much larger than correlation values for favorably adsorbed vapors. Figure 9 shows the effect of D_L on the breakthrough time and the plateau concentration achieved within a PSA system. The results presented in Figure 9 are model calculations using the conditions given on the graph.

The PSA model with axial dispersion and all rate resistances takes several hours of computer time to integrate several days of simulation time. We are presently trying to determine if the steady state may be calculated without integrating over time. Shown in Figure 10 are results of a preliminary effort in this area. The data shown are the concentration versus bed depth results at the end of the feed step when the cyclic steady state has been reached. These results are compared with model integration to determine if the steady-state calculational method has any merit. Based on these results, it appears that this approach may be used to determine steady-state profiles for conditions similar to those given in Figure 10. It is not clear at this point if the calculational method is valid for a wide range of parameter values.

Also shown in Figure 10 is the effect of cycle time on the steady-state concentration profile. These results show that for the CFC-113/BPL system, there is not a large difference in system performance for cycle times of 1 and 4 minutes. This is consistent with the input given to us by visiting experts. The cycle time would only appear to be important when material is close to breaking through during the course of the feed step, e.g. shallow beds and high fluid velocities.

IV. Other

Six abstracts have been accepted for presentation at the upcoming CRDEC conference on November 19, 1991.

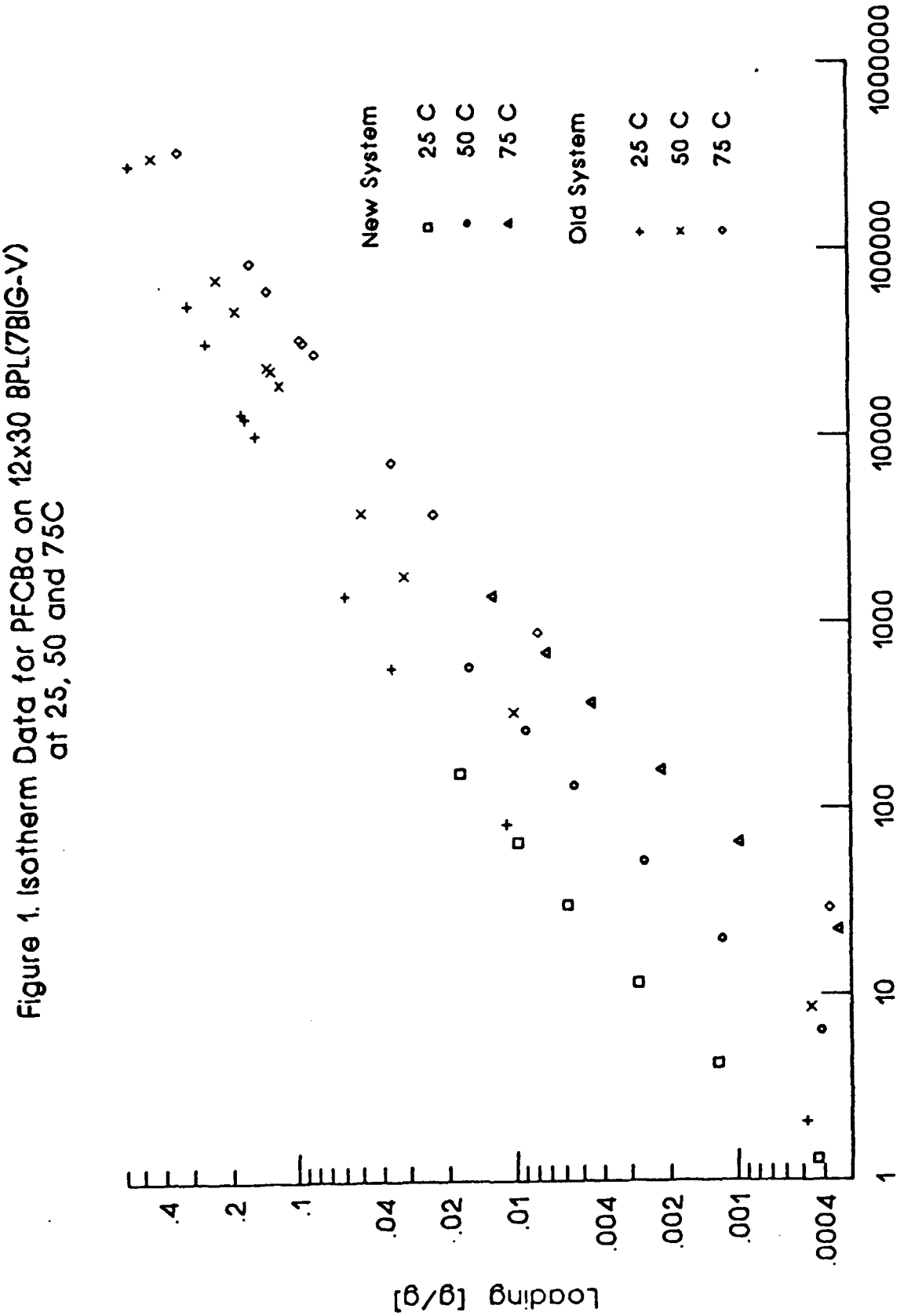
Figure 1. Isotherm Data for PFCBa on 12x30 BPL(7BIG-V)
at 25, 50 and 75C
New System
25 C
50 C
75 C
Old System
25 C
50 C
75 C
Loading [g/g]
.4
.2
.1
.04
.02
.01
.004
.002
.001
.0004
Concentration [mg/m**3]
1
10
100
1000
10000
100000
1000000

Figure 2. Isotherm Data for PFCBa on 13X Molecular Sieve at 25, 50 and 75C

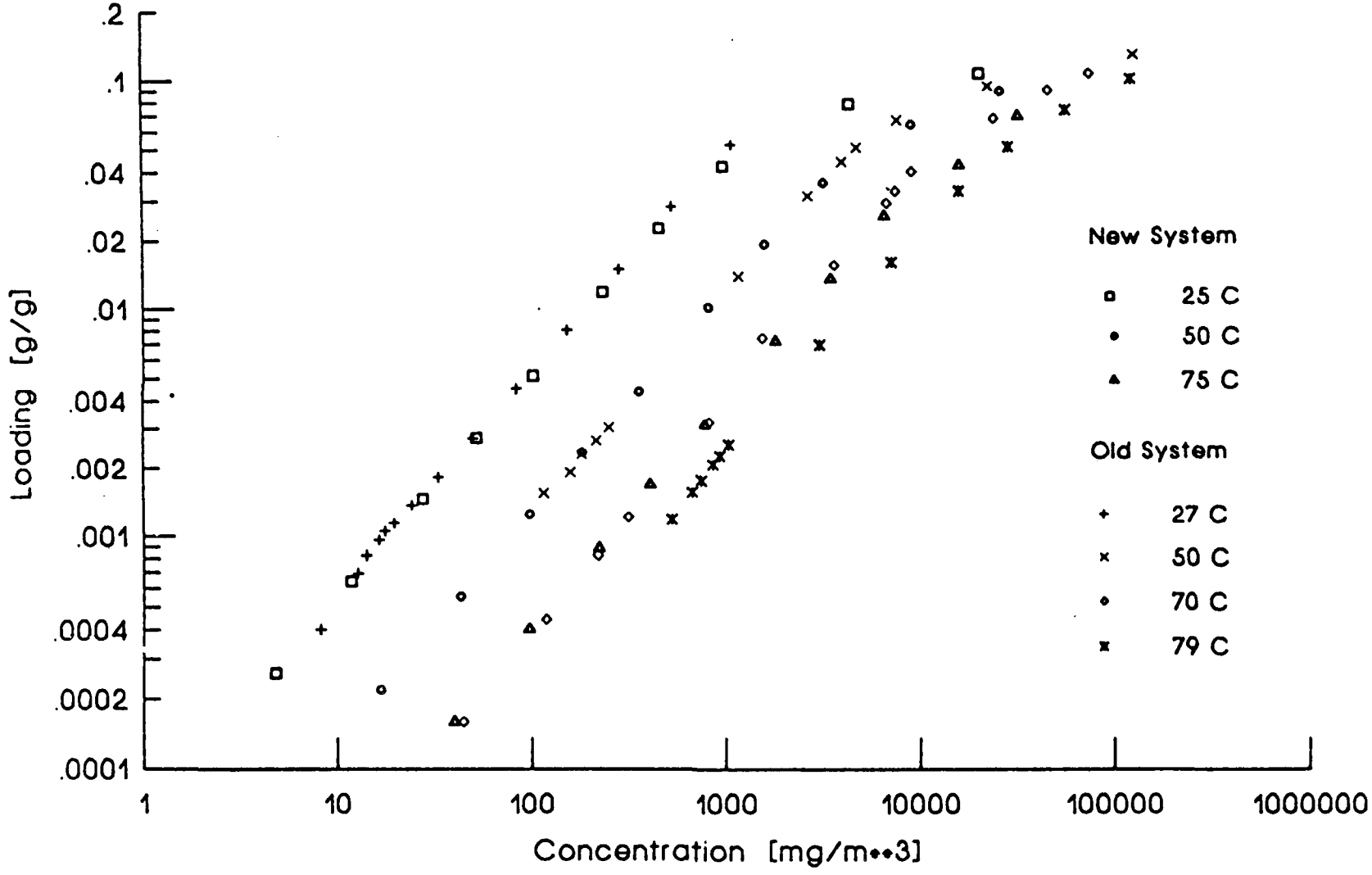

Figure 3. PSA Breakthrough for CFC113 on BPL Carbon
Feed 150LPM

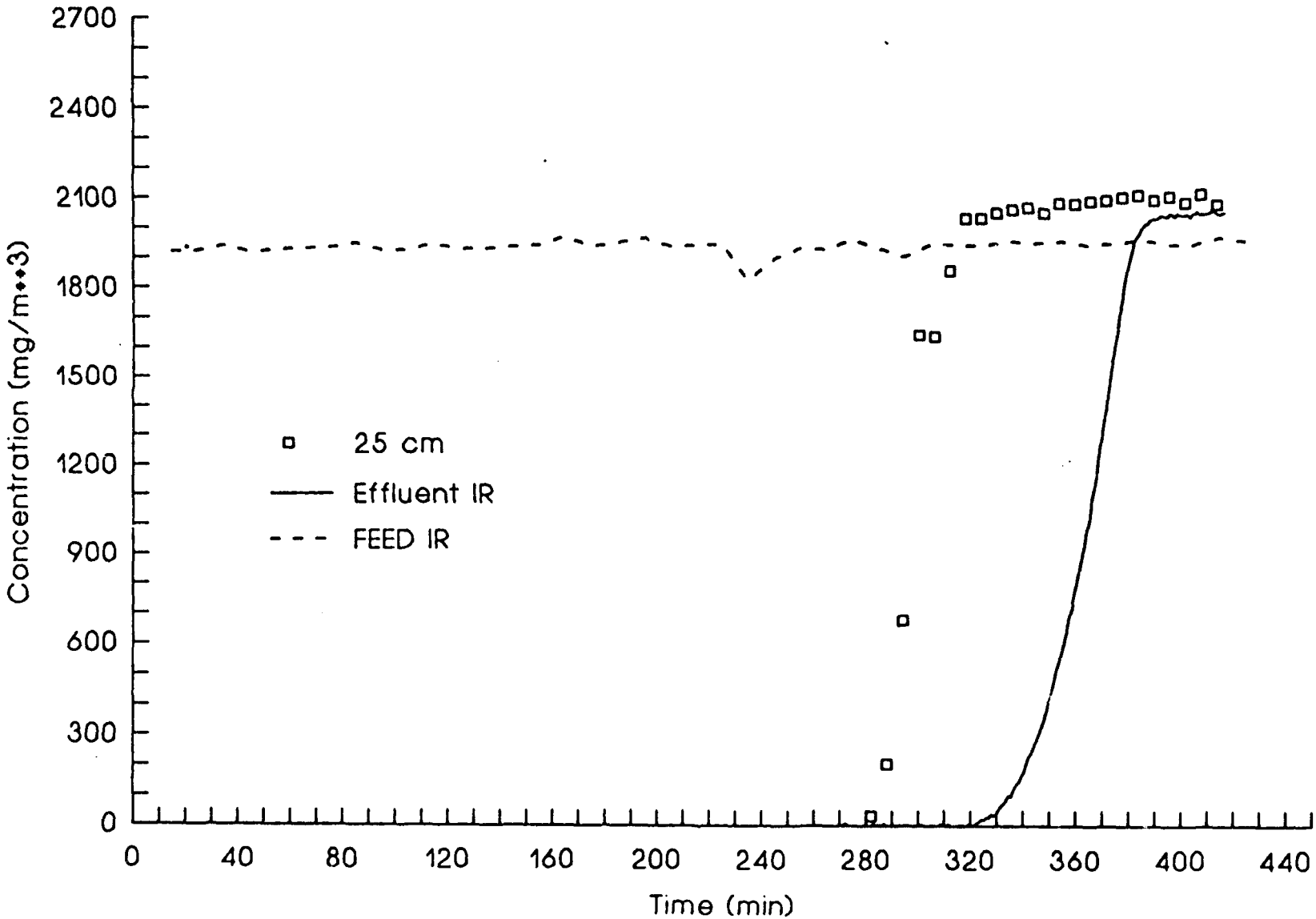

Figure 4. PSA Bed Desorption Curve for CFC113 on BPL Carbon
Purge 80LPM

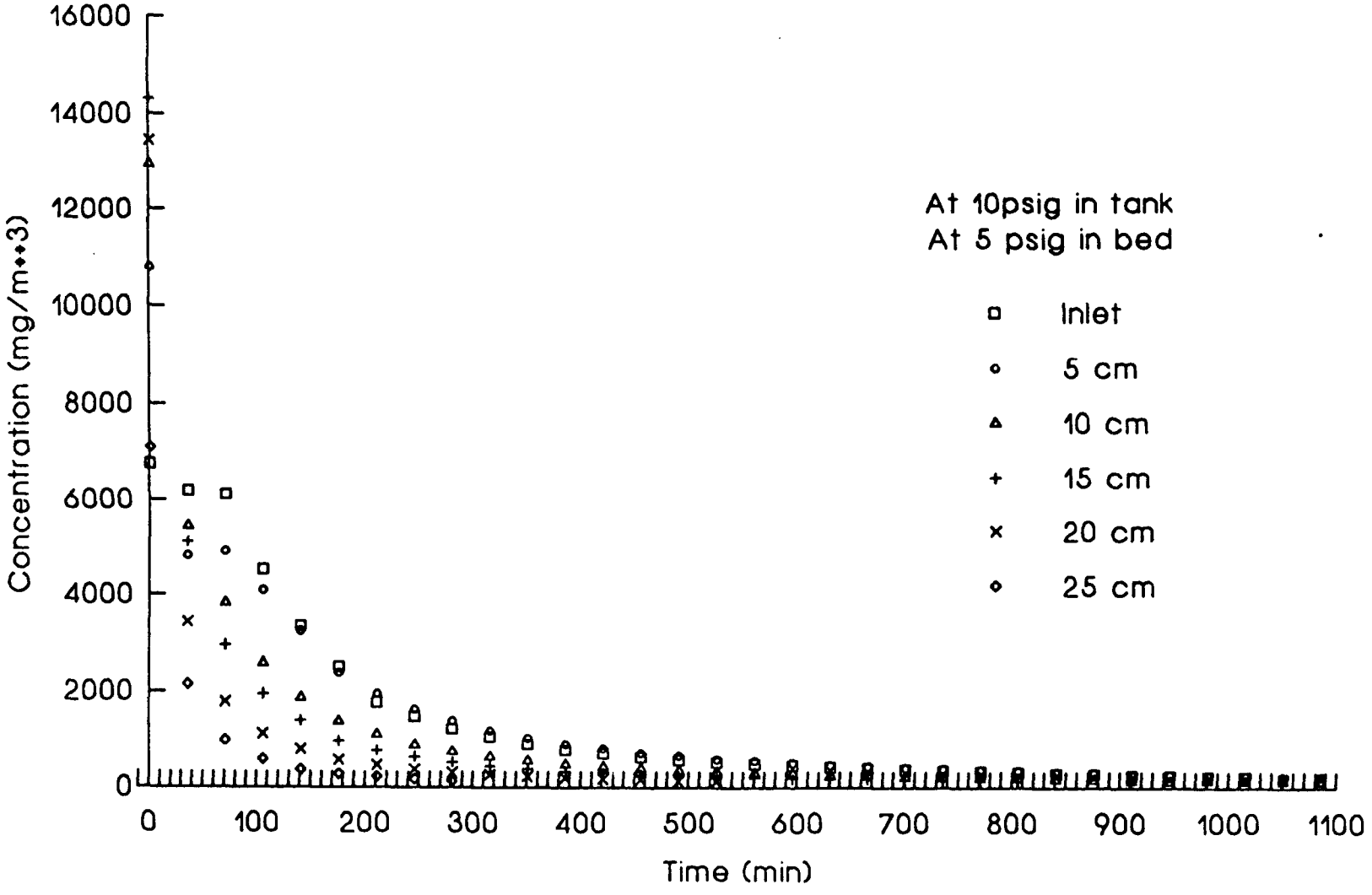

Figure 5. PSA Bed Profile for CFC113 on BPL Carbon
Product 82LPM Purge 89LPM
Feed Pressure = 47 psig

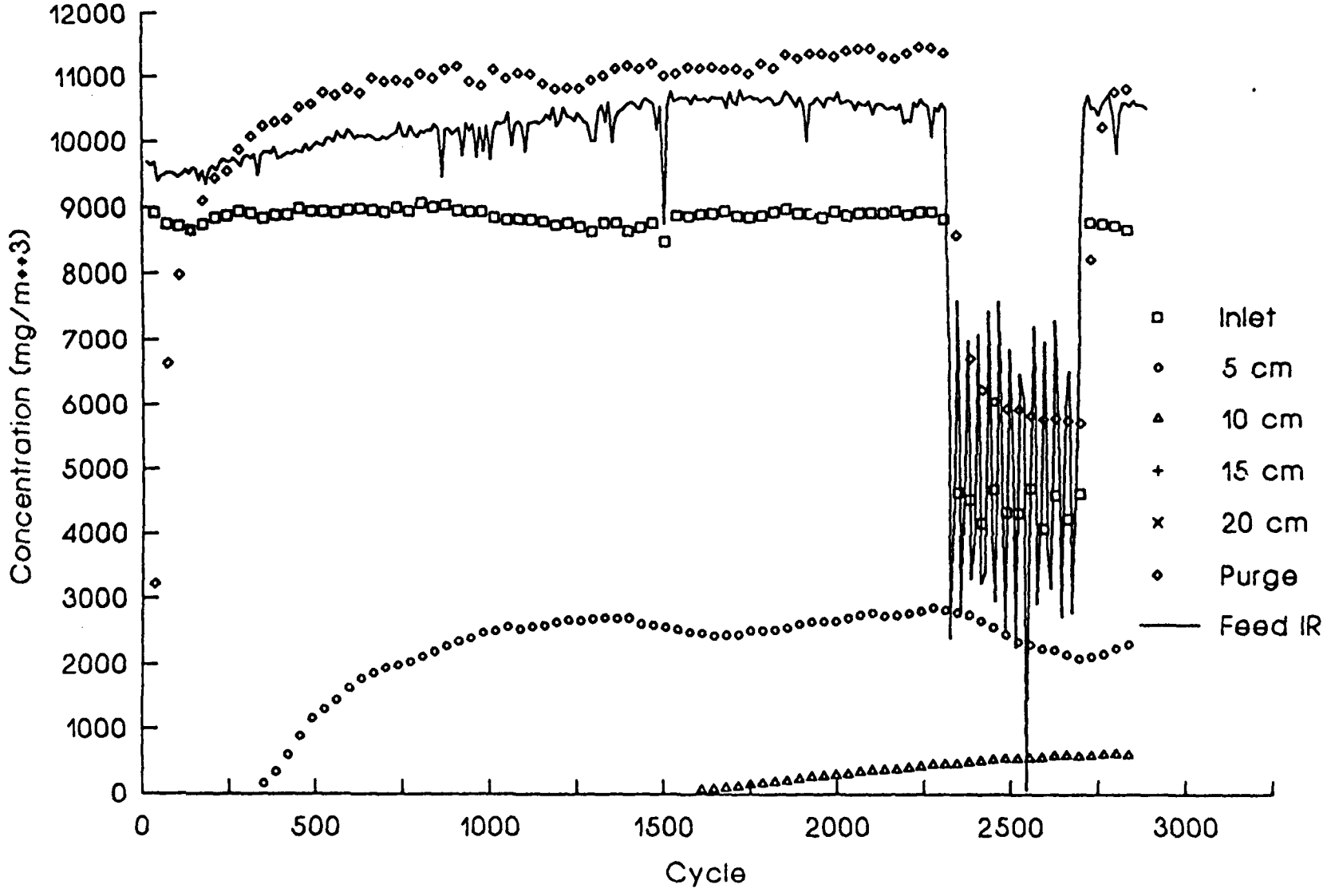

Figure 6. PSA Bed Profile for CFC113 on BPL Carbon
Product 75LPM Purge 75LPM
Feed Pressure = 47.5 psig

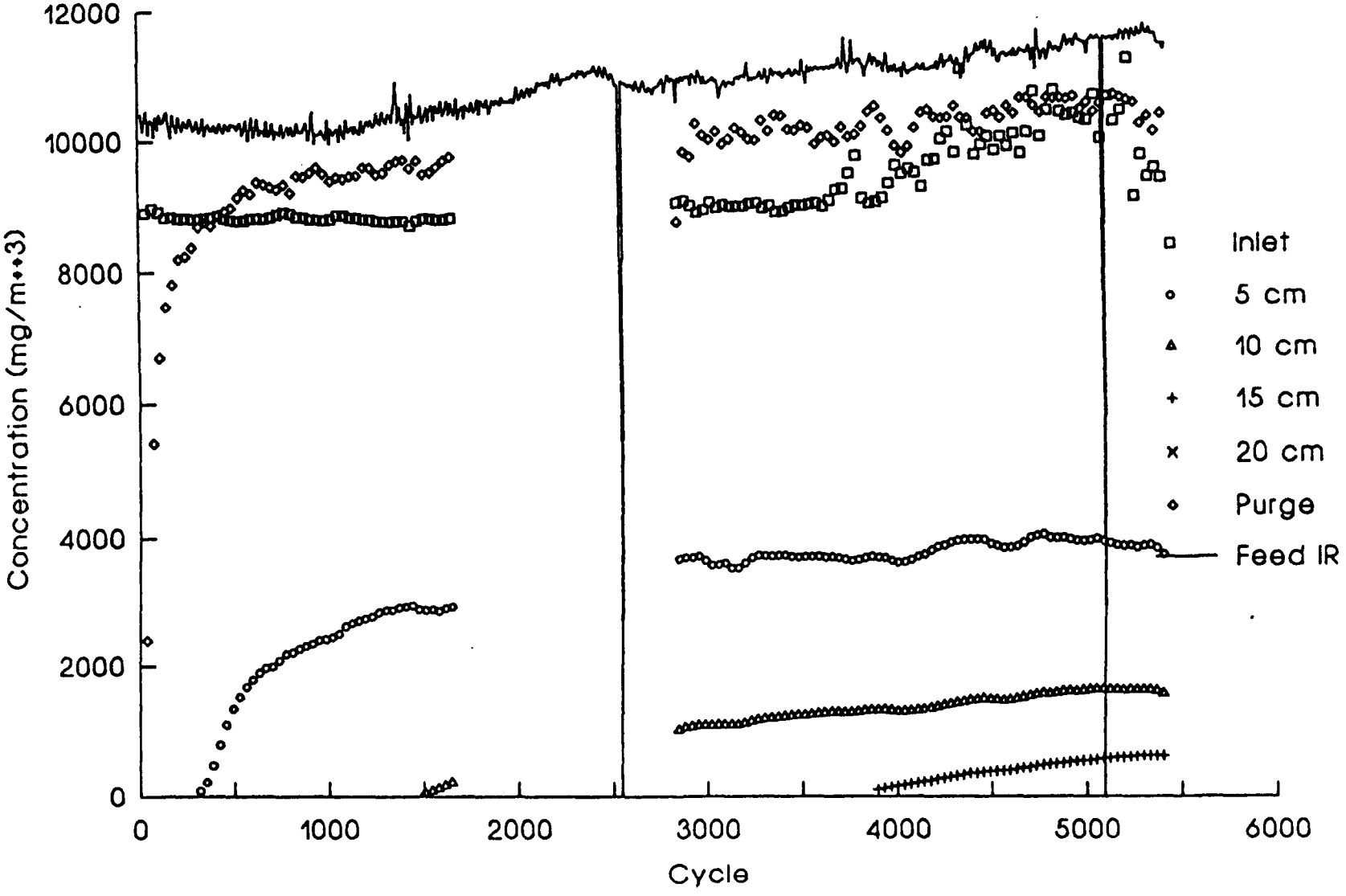

Figure 7. PSA Bed Profile for CFC113 on BPL Carbon
Product 83LPM Purge 52LPM
Feed Pressure = 47 psig

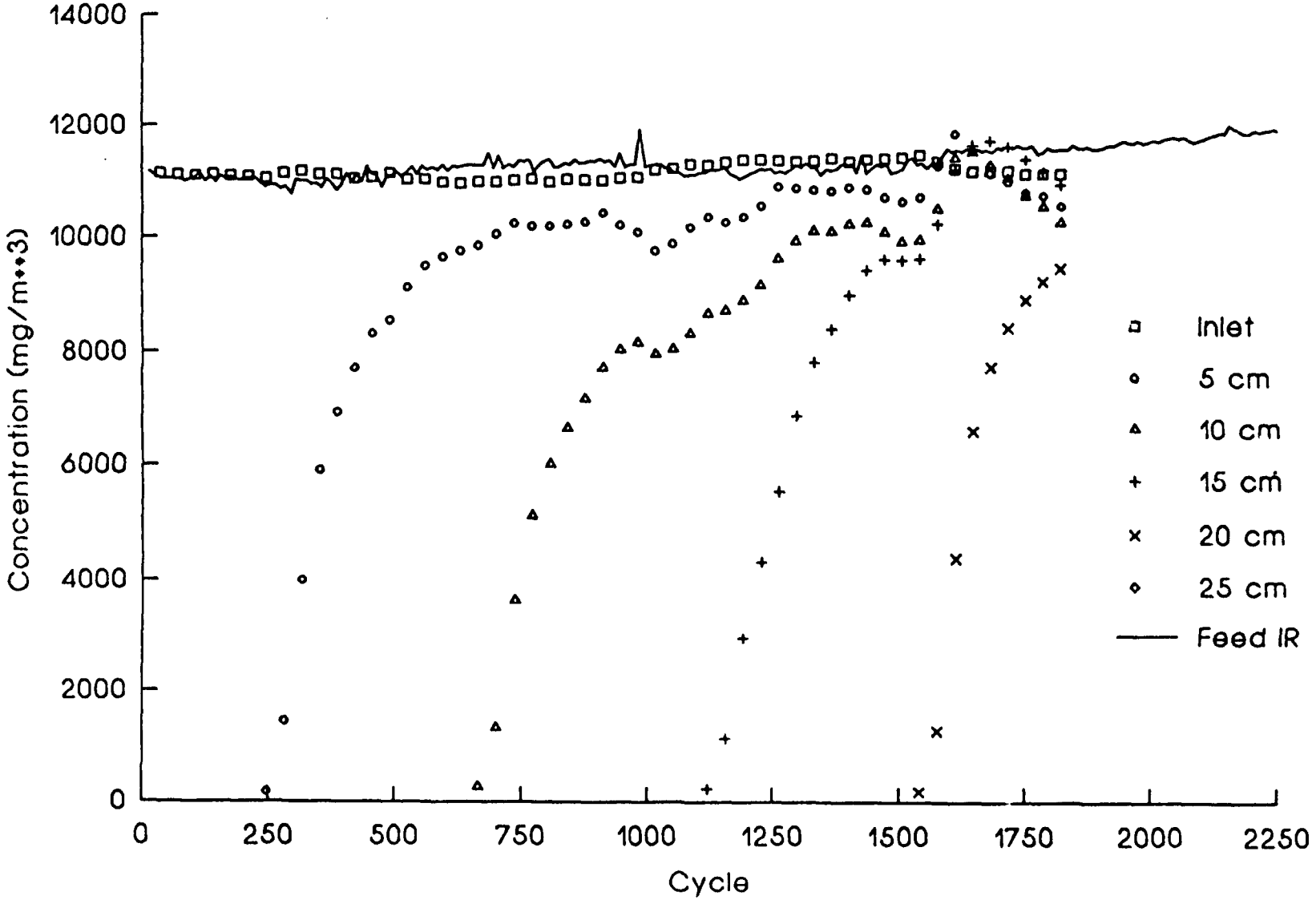

Figure 8. PSA Bed Profile for CFC113 on BPL Carbon
Product 100LPM Purge 50LPM
Feed Pressure = 48 psig

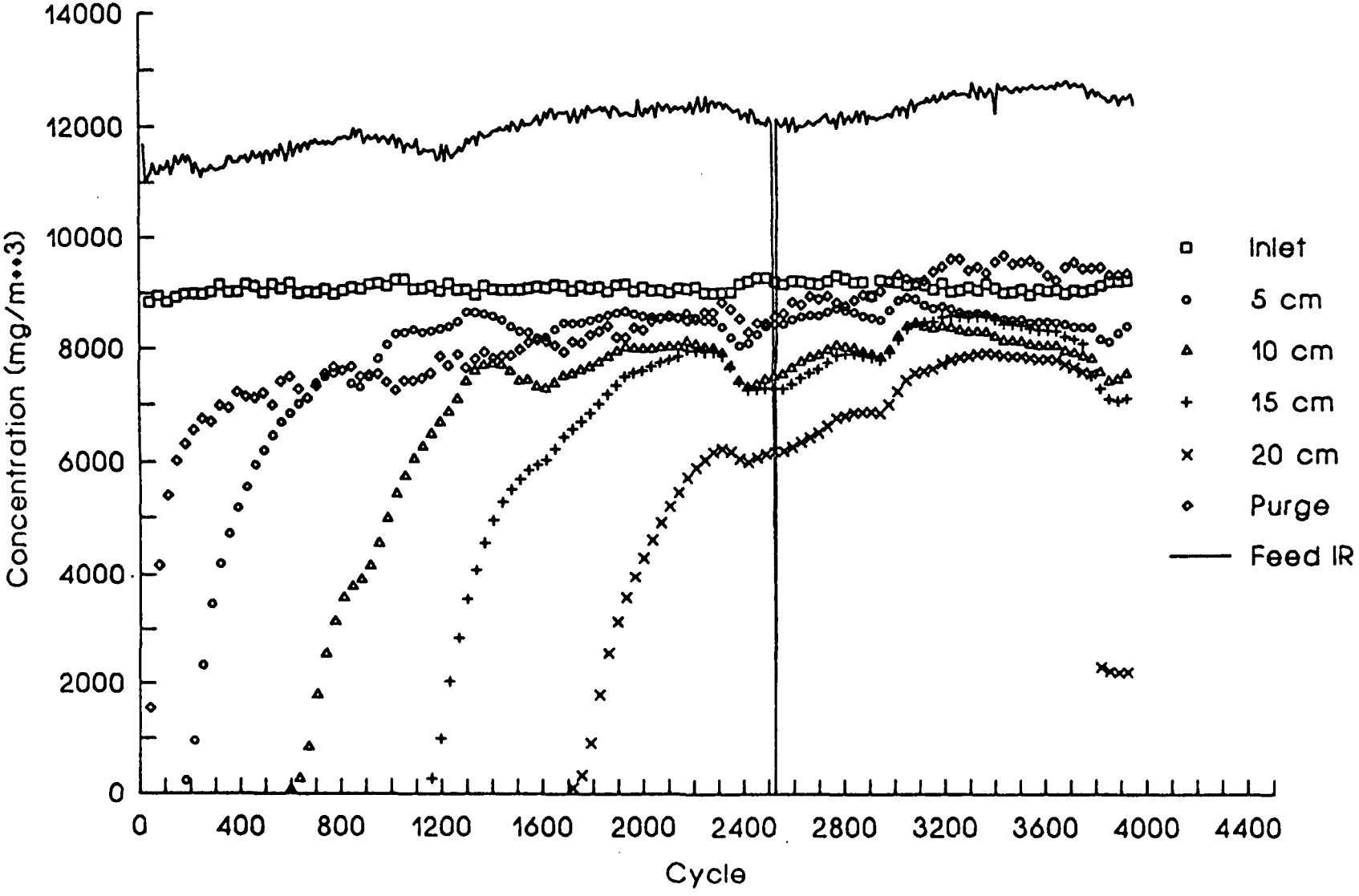

Figure 9. Effect of Axial Dispersion Coefficient on PSA Breakthrough Profile

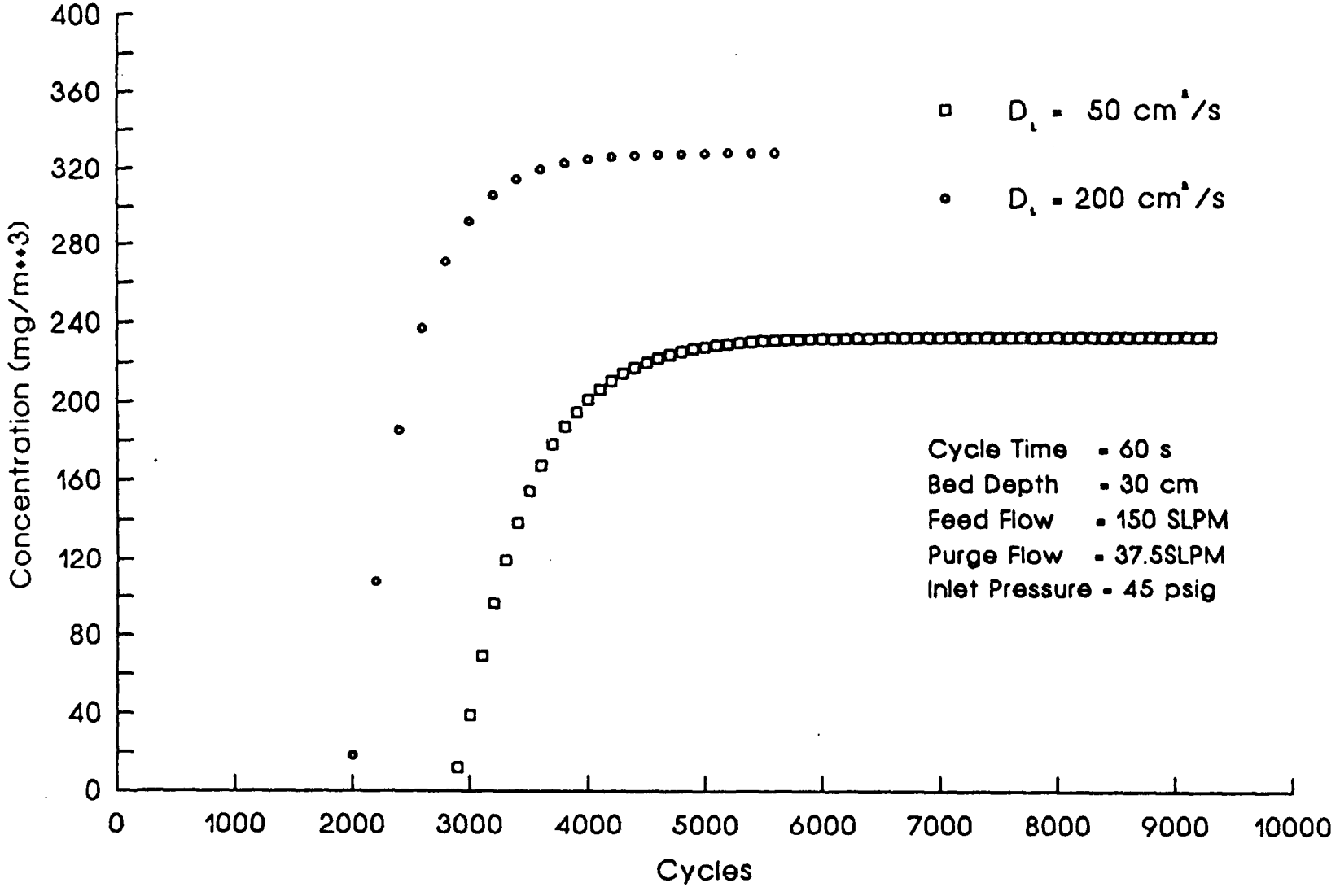

Figure 10. Effect of Cycle Time on Steady-State PSA Bed Profiles

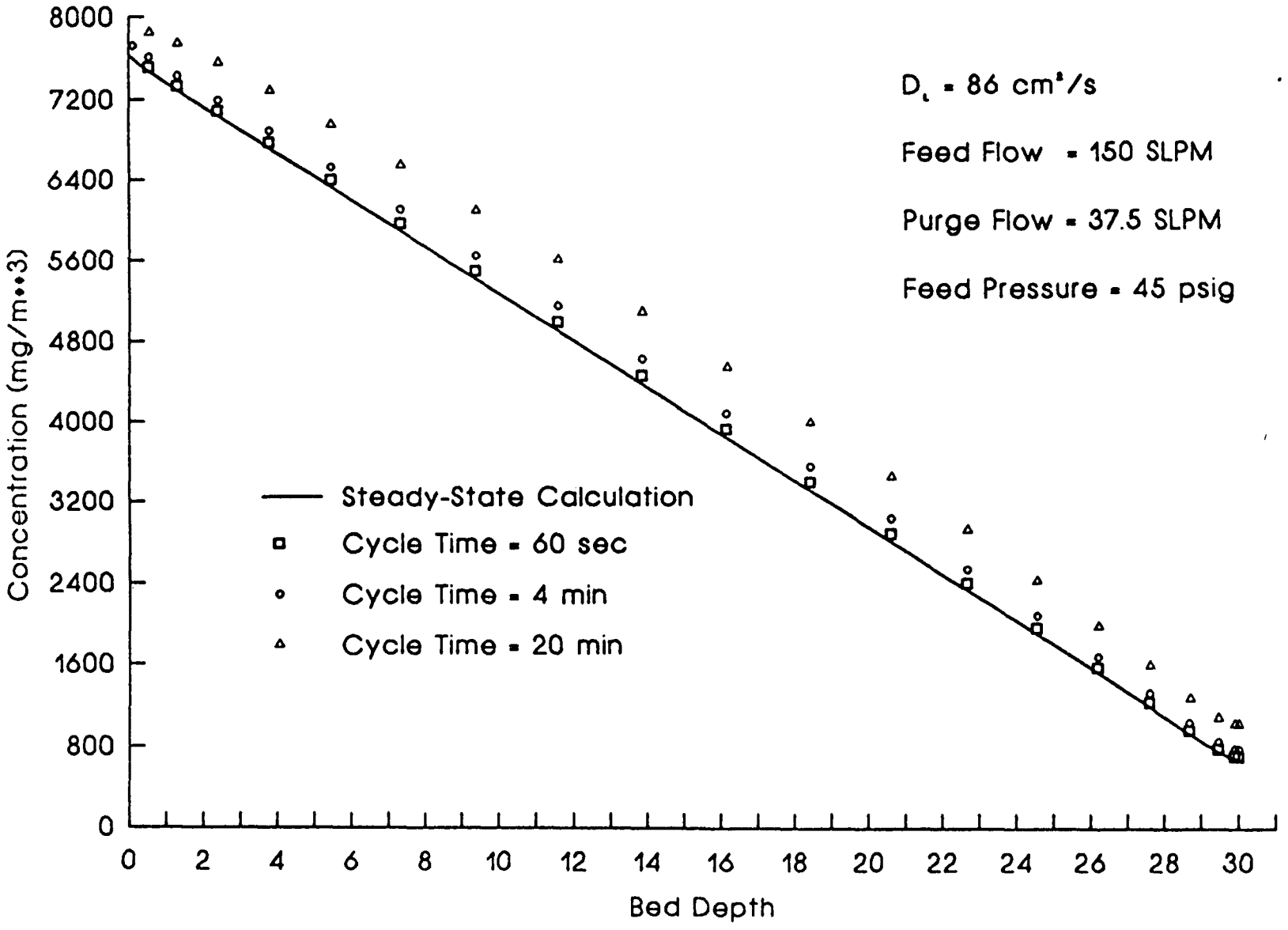

Blank

APPENDIX A

Axial Dispersion Effects on the Breakthrough Behavior of Favorably Adsorbed Vapors

by

John J. Mahle, U.S. Army, CRDEC,
Aberdeen Proving Ground, MD 21010-5423

and

David K. Friday, GEO-CENTERS, INC.,
Ft. Washington, MD 20744

Abstract

The design and optimization of adsorption-based separation and purification systems requires accurate adsorption equilibria and an understanding of the phenomena which determine the breadth of the adsorption wave. A mathematical model for an isothermal cylindrical fixed-bed adsorber is developed using both internal and external mass transfer rates and a Fickian diffusion term to describe axial dispersion. Adsorption equilibria and internal particle mass transfer rates for three chemical vapors, are measured on BPL activated carbon. Constant pattern breakthrough curves for each chemical are measured and compared with a mathematical model to evaluate the dispersion coefficient. The results show that the required dispersion coefficient is a function of the isotherm shape.

I. INTRODUCTION

The design and optimization of adsorption-based separation and purification systems require a quantitative understanding of the important adsorption equilibria relationships. For many applications, particularly those in which relatively low breakthrough concentrations are of interest, one must also have a quantitative understanding of the phenomena which determine the breadth of the adsorption wave. These phenomena include internal and external particle mass transfer rates and axial dispersion.

Numerous correlations (1-4) based on the Fickian model relate the axial dispersion coefficient to several operating parameters. However, no correlations have been developed which are appropriate for the systems under consideration, namely favorable adsorption equilibria. Chao and Hoelscher (5) found that axial dispersion coefficients were significantly larger for adsorbing systems, however they did not offer any explanation. Coppola and LeVan (6) showed that the constant pattern solution for an irreversible isotherm with a Fickian model for axial diffusion was always a shock, regardless of the value of the dispersion coefficient.

The significance of axial dispersion is demonstrated using an approach given by Costa and Rodrigues (7) in their analysis of a liquid phase adsorption process. Mass transfer rates are determined using available correlations to calculate the external particle mass transfer rate and a closed-loop batch uptake apparatus to

measure the internal particle mass transfer rates. All bed scale effects are lumped into a single parameter, D_L, which is determined from breakthrough experiments.

II. RESULTS AND DISCUSSION

II.1. Fixed-bed adsorber model

The system considered in this study is a constant feed concentration to an isothermal, cylindrical, fixed-bed adsorber. Both internal mass transfer resistances and axial dispersion are considered. The analysis treats a single adsorbable component with an inert carrier. The model consists of a material balance, two mass transfer rate expressions, and the appropriate adsorption equilibria. The material balance is given by

$$\rho_b \frac{\partial q}{\partial t} + \epsilon \frac{\partial c}{\partial t} + (1-\epsilon)\chi \frac{\partial c}{\partial t} + \epsilon v \frac{\partial c}{\partial z} = \epsilon D_L \frac{\partial^2 c}{\partial z^2} \qquad (1)$$

with the following boundary conditions,

$$D_L \frac{\partial c}{\partial z}\Big|_{z=0} = v(c - c_{feed}) \quad ; \quad \frac{\partial c}{\partial z}\Big|_{z=L} = 0 \qquad (2, 3)$$

Two mass transfer resistances are included in the model. The external particle resistance is expressed using a linear driving force approximation.

$$\rho_b \frac{\partial q}{\partial t} = k_f a (c - c^*) \qquad (4)$$

The internal particle resistance is represented using a distributed parameter expression, based on the adsorbed phase concentration,

$$\frac{\partial q_r}{\partial t} = D_e \left(\frac{\partial^2 q_r}{\partial r^2} + \frac{2}{r} \frac{\partial q_r}{\partial r} \right) \qquad (5)$$

where

$$q = \frac{3}{R_p^3} \int_0^{R_p} q r^2 dr \qquad (6)$$

with the boundary conditions of

$$q = q^*\,|_{r=R_p} \quad ; \quad \frac{\partial q}{\partial r}\Big|_{r=0} = 0 \qquad (7, 8)$$

The model requires that three parameters, D_E, D_L, and $k_v a$ and the adsorption equilibrium expression, $c^* = f(q^*)$, be determined from correlations and experiments.

II.2. Adsorption equilibria

Isotherms at 25C were measured for octofluorocyclobutane (PFCB), 1,1,2 trichloro, 1,2,2 trifluoroethane (CFC-113) and 1-hexanol on 16x18 mesh BPL carbon using a closed-loop apparatus. Figure 1 compares measured data for each chemical vapor with the least squares best fit of the ln(p) using the Toth isotherm (Eq. 9), where $\theta = q/q_{sat} = W/W_o$. The parameter values obtained from the correlation are shown in Table 1.

$$p = \left(\frac{b}{\theta^{-t} - 1} \right)^{1/t} \tag{9}$$

Table 1. Toth Isotherm Parameters

Chemical	b	t	W_o (cc/g)	q_{sat} (g/g)
PFCB	.7794	.2750	.7890	1.194
CFC-113	.2698	.2237	.9017	1.411
Hexanol	.0401	.4467	.6498	0.530

II.3. Parameter determination - $k_v a$

The external mass transfer rate coefficient, $k_v a$, is obtained from the Wakao and Funazkri (8) correlation given below.

$$Sh = 2.0 + 1.1 Re^{0.6} Sc^{1/3} \tag{10}$$

II.4. Parameter determination - D_E

The internal particle effective diffusivity, D_E, is determined from a batch-uptake experiment using a closed-loop system. A model was developed by combining a closed-loop material balance with the internal rate expression given in Equation 5. Figure 2 shows the measured batch-uptake data for CFC-113 compared to the closed-loop model results using three different values of D_E. From Figure 2, the value of D_E is approximately 6.0×10^{-7} cm^2/s. The values for PFCB and hexanol were determined in a similar manner and found to be 1.0×10^{-6} and 3.5×10^{-7} cm^2/s, respectively.

II.5. Parameter determination - D_L

Fixed-bed experiments may now be conducted with only one adjustable parameter, D_L, to be determined from measured breakthrough data. The model results presented in this section were obtained by developing collocation matrices in the z and r coordinates (see Ref. 9) and solving the resulting ordinary differential equations using a Gear's method integration package developed by Hindmarsh (10).

Table 2. Fixed-Bed Breakthrough Experiments

Adsorbent	BPL Carbon, 16x18 mesh (particle diameter = 0.1 cm)
Adsorbates	PFCB, CFC-113, and 1-hexanol
Feed Concentration	20 mmol/m^3
Temperature	298 K
Bed Depth	2 to 24 cm
Bed Diameter	1.1 cm

Figure 3 shows breakthrough curves for CFC-113 using a 1.1-cm diameter bed and several bed depths. These data are normalized by establishing the time when the effluent concentration reaches 1/2 of the feed concentration as zero time. The approach to constant pattern is clearly demonstrated from these results since the wave does not spread any perceptible amount from the 6-cm bed to the 9-cm bed. These same experiments were performed with PFCB and hexanol to establish a constant pattern bed depth. For PFCB constant pattern was established at a bed depth of 18 cm and for hexanol at a bed depth of 4 cm.

The axial dispersion effects on the breakthrough behavior of different adsorbates were investigated using bed depths obtained from the constant pattern study. Measured breakthrough data are compared to model results with a "fit" value of D_L and the value of D_L obtained from the correlation of Langer et al. (1). Shown in Figure 4, 5 and 6 are the constant pattern breakthrough data for each chemical vapor with the model results using the Langer (dashed lines) and "fit" (solid lines) D_L values. The "fit" values were obtained by finding the value of D_L which best matched the mid-height slope of the data. Given below is a summary of all the conditions and parameters used to obtain these results.

Table 3. Summary of Isotherm vs D_L Results

Chemical	R	Flow (SLPM)	Re_p	D_L (Fit) (cm^2/s)	D_L(corr) (cm^2/s)	D_E (cm^2/s)	Bed Depth (cm)
PFCB	0.424	1.95	21.2	39	13.8	1.0×10^{-6}	18
CFC-113	0.169	2.0	21.7	81	14.2	6.0×10^{-7}	12
Hexanol	0.032	1.73	18.8	1600	12.3	3.5×10^{-7}	4

The relationship between the isotherm shape and the axial dispersion coefficient can be seen by comparing the fit values of D_L with R. The value of R is 1 for a linear isotherm and 0 for an irreversible isotherm. There are two significant points. First, the fit value for D_L, even for the least favorably adsorbed vapor (closest to linear), PFCB, is larger than the correlated value, a trend noted by Chao and Hoelscher (5). Second, the difference between the correlated and "fit" values becomes larger the more favorable the isotherm to the point where the value of D_L required to fit the hexanol breakthrough data is unreasonably large. Also note in Figure 6 that the model does not adequately represent low breakthrough concentration behavior. The hexanol results are consistent with the constant pattern solutions of Coppola and LeVan (6). Differences between measured and model breakthrough concentrations are probably due to the

Figure 1 Isotherm Data for PFCB, CFC-113 and Hexanol on 16x18 mesh BPL Carbon at 25C

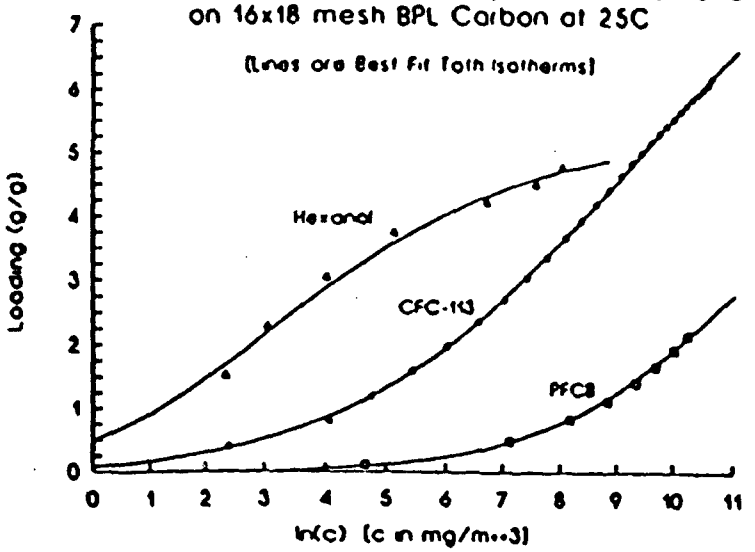

Figure 2 Batch Uptake Data for CFC-113 on 16x18 mesh BPL Carbon - Determination of D_E

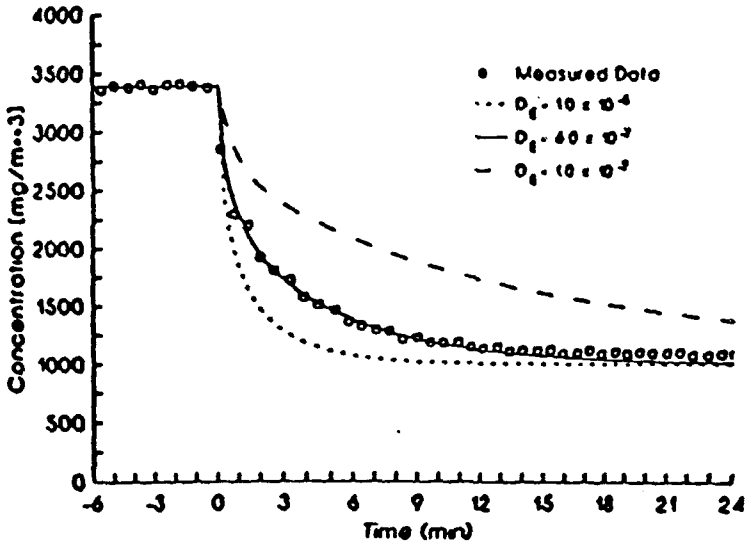

Figure 3 Breakthrough Data for CFC-113 on 16x18 mesh BPL Carbon - Using Four Bed Depths

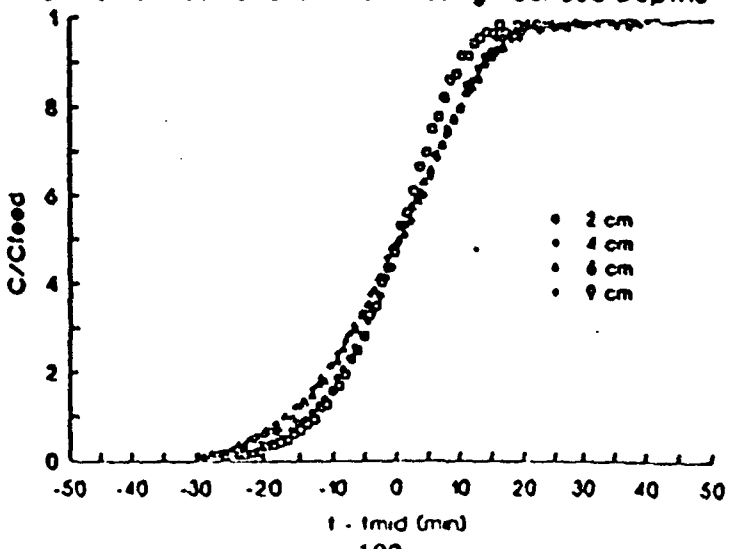

Figure 4 Breakthrough Data for PFCB on BPL Carbon and Model Results Using a Correlated and Fit Dispersion Coefficient

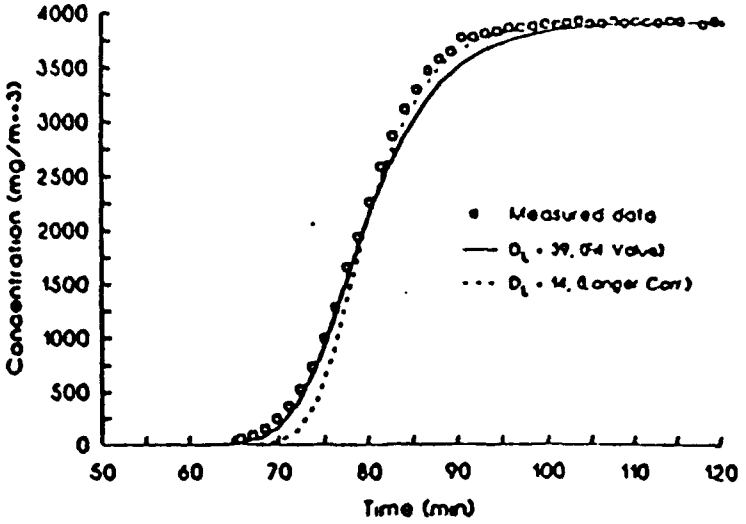

Figure 5 Breakthrough Data for CFC-113 on BPL Carbon and Model Results Using a Correlated and Fit Dispersion Coefficient

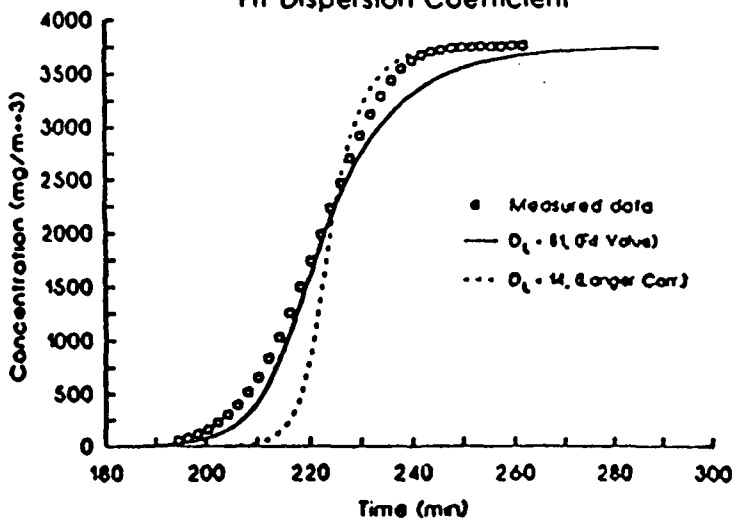

Figure 6 Breakthrough Data for Hexanol on BPL Carbon and Model Results Using a Correlated and Fit Dispersion Coefficient

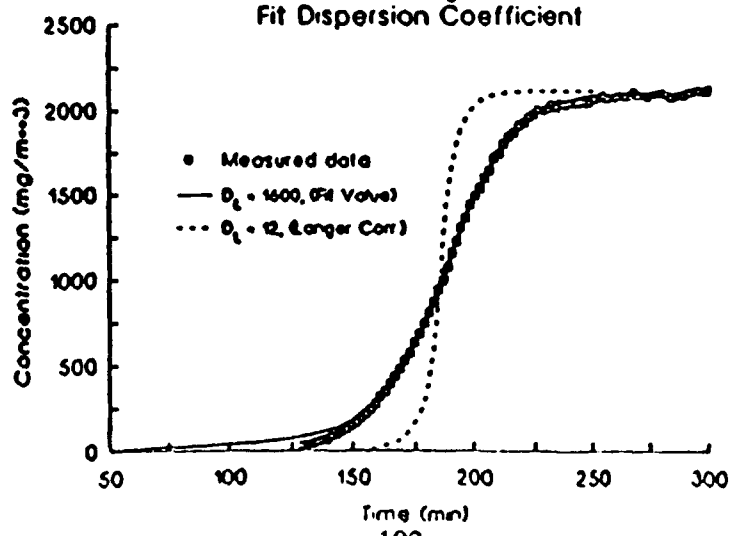

inability of the Fickian expression for axial dispersion to accurately represent the controlling physical phenomena (e.g. flow maldistributions). These results demonstrate the need for a more accurate mathematical description of fixed-bed phenomena when considering very favorably adsorbed vapors.

The results presented here cannot be attributed to heat transfer resistances. The adiabatic temperature rise for the experiment with the largest heat effect, hexanol, was calculated to be 0.01 K. In addition, during all experiments, both the inlet and outlet temperatures were monitored continuously to insure that no temperature changes occurred.

III. CONCLUSIONS

1. Axial dispersion can contribute significantly to the spreading of the adsorption wave even in deep beds.
2. The axial dispersion coefficient, D_L, is a function of the isotherm shape.
3. The Fickian model for axial dispersion begins to break down as the isotherm becomes irreversible.

IV. ACKNOWLEDGEMENTS

The authors gratefully acknowledge the experimental assistance of Bernardita Infiesto, Donna Carlile, and Amanda Brady.

References

1. Langer, G., Roethe,A., Roethe,P., and Gelbin,D.,"Heat and Mass Transfer in Packed Beds-III. Axial Mass Transfer", J. Heat and Mass Transfer, 21, p. 751, (1978).
2. Wen, C.Y., and Fan,L.T., "Models for Flow Systems and Chemical Reactors", Marcel Dekker, New York, 1975.
3. Gunn, D.J., "Axial and Radial Dispersion in Fixed Beds", Chem. Eng. Sci.,42, p. 363, (1987).
4. Suzuki, M., and Smith, J. M., "Axial Dispersion in Beds of Small Particles", Chem. Eng. J., 3, p. 256, (1972).
5. Chao, R. and Hoelscher, H. E., "Simultaneous Axial Dispersion and Adsorption in a Packed Bed", AIChE J., 12, p. 271, (1966).
6. Coppola, A. P. and LeVan M. D., "Adsorption with Axial Diffusion in Deep Beds", Chem. Eng. Sci., 38, p. 991, (1981).
7. Costa, C. and Rodrigues, A., "Design of Cyclic Fixed-Bed Adsorption Processes Part I: Phenol Adsorption on Polymeric Adsorbents, AIChE J., 31, p. 1645, (1985).
8. Wakao, N. and Funazkri, T.,"Effect of Fluid Dispersion Coefficients on Particle-To-Fluid Mass Transfer Coefficients in Packed Beds", Chem. Eng. Sci., 33, p. 1375, (1978).
9. Raghavan, N.S. and Ruthven, D.M., "Numerical Simulation of a Fixed-Bed Adsorption Column by the Method of Orthogonal Collocation", AIChE J., 29, p. 922, (1983).
10. Hindmarsh, A.C., "LSODE and LSODI, Two New Initial-Value Ordinary Differential Equation Solvers", ACM-SIGNUM Newsletter, 15(4), p. 10, (1980).

APPENDIX A-6

QUARTERLY PROGRESS REPORT

GC-PR-2194-06

REPORTING PERIOD:	11/1/91 - 1/31/92
REPORTING DATE:	2/15/92
CONTRACT NUMBER:	DAAA15-90-C-1056
CONTRACT TITLE:	Improved Filtration Materials and Modeling

I. Adsorption Equilibria

Single Component Measurements and Apparatus

The data base of chemicals has been expanded to include chlorodifluoromethane (R-22). Shown in Figure 1 are R-22 isotherms on BPL carbon at five temperatures. There are two interesting features found in the plot. The loading of R-22 at 75C and 100 mg/m^3 is extremely small (< 0.0002 g/g) and the ratio of loading at 5C and 75C at mg/m^3 is nearly 100:1. Thus, any adsorption-based air purification system will perform much better against vapors similar to R-22 by operating at the lowest possible temperature during the adsorption step. In addition, the data show that R-22 may easily be removed from BPL carbon using temperatures below 100C.

Shown in Figure 2 is a comparison of three chemicals on BPL carbon at 25C. For reference the boiling points of each chemical vapor shown in Figure 2 are : (1) CFC-113 = 47C, (2) PFCBa = -5C, and (3) R-22 = -40C. These results clearly show the effect of vapor pressure on adsorption capacity. Consider a vapor phase concentration of approximately 100 mg/m^3. It is quite interesting that the loading of CFC-113 is about an

order of magnitude larger than PFCBa which in turn is about an order of magnitude larger than R-22. These results imply that about 100 times more adsorbent is required to prevent R-22 from breaking through during the feed step of a PSA cycle. The steeper slope of the R-22 isotherm, as compared to the CFC-113 and PFCBa isotherms, means that R-22 will be much more efficiently desorbed during the purge step of a cycle. Therefore, one would expect that PSA system performance against R-22 will be much more sensitive to cycle time than CFC-113 or PFCBa.

Shown in Figure 3 are the same data from Figure 2 on a linear scale shown to give the reader a more recognizable isotherm shape. These results allow one to quickly assess that CFC-113 is the most favorable (most concave downward) isotherm and R-22 is the least favorable (almost linear) isotherm.

CFC-113 isotherm on 13X molecular sieve were measured this quarter. Shown in Figure 4 are some of the initial results at 25C. Some of the differences in the data may be caused by several factors, including effective water removal and not allowing enough time to reach equilibrium. For example, the first equilibrium point (lowest loading) measured for each experiment typically required up to 48 hours to reach equilibrium. Regardless of the reasons for the spread of the data, these results clearly indicate a leveling off of CFC-113 loading at about 0.1-0.15 g/g over a fairly wide range of concentrations (1,000 to 100,000 mg/m^3). This phenomena was not observed on BPL. The PSA design implication is that systems employing 13X may be overwhelmed at high feed concentrations, since the system capacity does not show any appreciable increase with increasing vapor phase concentrations.

Figure 5 compares CFC-113 and PFCBa adsorption isotherm data on 13X molecular

sieve. As with BPL carbon the loading of PFCBa is substantially lower that CFC-113, particularly at low concentrations.

Multicomponent Measurements and Apparatus

Temperature control remains a problem in the current multi-component system. In addition, the current system cannot adequately measure equilibria on strongly hydrophilic adsorbents such as 13X molecular sieve. A new system is being developed which employs a water-jacketed glass tube and a Cahn microbalance in a flow-through mode. Initial results indicate that even though the room temperature fluctuates as much as 10C, the circulating water is able to maintain the adsorbent temperature at 25C. A spiral loop containing Ni-Chrome wire surrounds the basket holding the adsorbent. By applying an electrical potential across this wire, desorption temperatures above 350C may easily be achieved. These temperatures are required to effectively remove the residual water for 13X experiments.

II. Breakthrough Studies

Previous reports have shown the significance of axial dispersion on the performance of a PSA system. An area that has not been addressed in the literature is pressure effects on dispersion. Since we are feeding at elevated pressures, we must correctly determine the axial dispersion coefficient, D_L for the feed step. Shown in Figure 6 are results of a breakthrough experiment for CFC-113 on BPL carbon at 45 psig. The solid line on the graph is the math model results for a dispersion coefficient of 100 cm^2/s and the dashed line are the model results for D_L = 200 cm^2/s. These data clearly show that the correct value of D_L is between 100 and 200, probably closer to 200. However, as reported in the paper entitled "Axial Dispersion Effects on the Breakthrough Behavior of Favorably Adsorbed Vapors" given in Appendix A of the previous quarterly report, the value of D_L

using the same linear velocity at atmospheric pressure was 81 cm^2/s. Therefore, these initial results show that we must consider pressure in any correlation we develop to predict D_L from operating conditions.

III. Pressure Swing Adsorption

Math Modeling

Shown in Figure 7 are PSA results for CFC-113 on BPL at conditions listed on the plot. The boxes are the in-bed concentrations measured at steady-state, or more correctly, periodic state. These data were measured at about 10 seconds into the feed step. The solid line in Figure 7 corresponds to the model results using a purge value for D_L of 10 cm^2/s. The dashed line corresponds to a purge value for D_L of 500 cm^2/s. The value of D_L for the feed step obtained from results shown in Figure 6 was 170 cm^2/s. It was attempted to independently measure the value for D_L during the purge step by pre-saturating a bed and subsequently feeding clean air in the opposite direction. However, these results proved inconclusive since a wide range of values for D_L gave approximately the same results. However, it appears from Figure 7, that for cyclic systems over many cycles, the purge value for D_L can significantly effect system performance.

Temperature fluctuations of more than 15C during the course of a PSA have been noted in the literature and measured in our laboratory. The PSA math model was modified to include an energy balance, but not include a pressurization and blowdown step. Shown in Figure 8 are the model results with and without an energy balance. There is no change in concentration profiles because the temperature profiles predicted do not vary by more than 0.1C. We must, therefore, include a pressurization and blowdown step in the math model to adequately predict temperature profiles during each cycle.

Experiments and Apparatus

In the previous quarterly report, we showed results for CFC-113 on BPL carbon using a purge to product ratio of 1:1. Those results showed a dramatic decrease in the periodic-state, plateau concentrations down the bed. Figure 9 shows the results for the same experiment except, the purge to product ratio is 1:2. The plateau concentrations still decrease with increasing bed depth, but the difference between these concentrations is relatively small. In addition, using the purge to product ratio of 1:2 produces shorter breakthrough times for each sample port as compared with the results from the 1:1 purge to product experiment. However, data shown in Figure 9 demonstrate that the breakthrough time for the 5-cm port is still greater than 200 minutes at a steady feed concentration of 2200 mg/m3, which corresponds to a total Ct > 440,000! Thus, the operation of PSA system in the field may need to use much less purge than that required to prevent breakthrough at the periodic state.

Software designed to control the PSA system was modified to allow the enhanced display of challenge concentration. This software was tested and found to operate properly. Shortly thereafter while trying to run this software on a different computer it was found to generate stack overflow errors. Efforts to isolate the cause proved elusive. After detailed examination of the software the problem was found to be caused by an attempt to print an error message from within an interrupt routine. DOS is not re-entrant and any calls made to it during an interrupt routine are not guaranteed to work. This error had not occurred previously and escaped detection. All PSA software is operational at this time.

IV. Data Acquisition and Control

In an effort to optimize available resources, the gathering of chemical data has been

automated as much as possible. While current software developed under independent contract meets required levels of functionality, the level of expertise needed to maintain or modify this software is inconsistent with current staffing. A search was initiated for a system whereby users with minimal software background could design, implement and maintain automated chemical experiments. It was determined that the National Instruments LabView 2 Instrumentation Software could fill this need. Consultation with engineering representatives from National Instruments confirmed this. Since this approach represented a major departure from current method of developing instrumentation software it was decided that an in house evaluation of the product would be made.

The first area to be examined was the ease of creating user friendly interfaces to the controlling software. Several different sample projects were designed and implemented to make use of a representative mixture of the available input and display capabilities of LabView. In all cases it was determined that systems could be built providing a comprehensive easy to use interface to the experiment being controlled. This area of exploration demonstrated that LabView could with a high level of confidence be expected to provide the necessary user interface to control any foreseeable experimental system.

The next area of interest was the underlying structures available to control an experiment. The LabView software provides a rich set of control constructs allowing the designer to graphically describe the sequencing of experiments. Sample systems were designed to exercise these various constructs. It was determined that labView provided sufficient capability to allow control of any foreseeable experimental system.

In any experiment the collected data must be collected, analyzed and stored. Each of these functions was examined individually. The LabView system allows the control of a wide variety of data acquisition hardware. The intuitive interface allows one to easily configure and utilize data acquisition hardware. A sample program was created which allowed the measuring the analog output from a HP 5890 Gas Chromatograph.

LabView contains a large collection of data analysis functions. These functions allow highly sophisticated manipulation of collected data to extract pertinent information. Sample experiments were designed which demonstrated such functions as frequency domain signal analysis, integration of input analog signals as well as least squares curve fitting to user defined functions.

Once data has been processed, it needs to be stored. LabView possesses the functionality to store collected data in any number of formats. Several tests were conducted to demonstrate the ability to store and recover experimental data.

Several areas remain to be explored. These include RS-232 communications, a thorough study of the IEEE.488-1(2) communications as well as a more detailed analysis of time constrained program sequencing. These studies will be conducted shortly.

V. Other

The following six papers were given at the CRDEC conference on November 19, 1991.

1. " Development of Air Purification Systems "
2. " Adsorption Equilibria for Simulant Vapors on 13X Molecular Sieve"

3. " Single Component Isotherm Measurement with the Cahn Microbalance"
4. " Prediction of Binary Vapor Adsorption for a Benzene/Water Mixture on Activated Carbon"
5. " Experimental Studies in Pressure Swing Adsorption"
6. " Pressure Swing Adsorption (PSA) Performance Prediction Model"

Figure 1. Isotherm Data for R-22 on BPL(10-90) 12x30 at 5, 15, 25, 50 and 75C

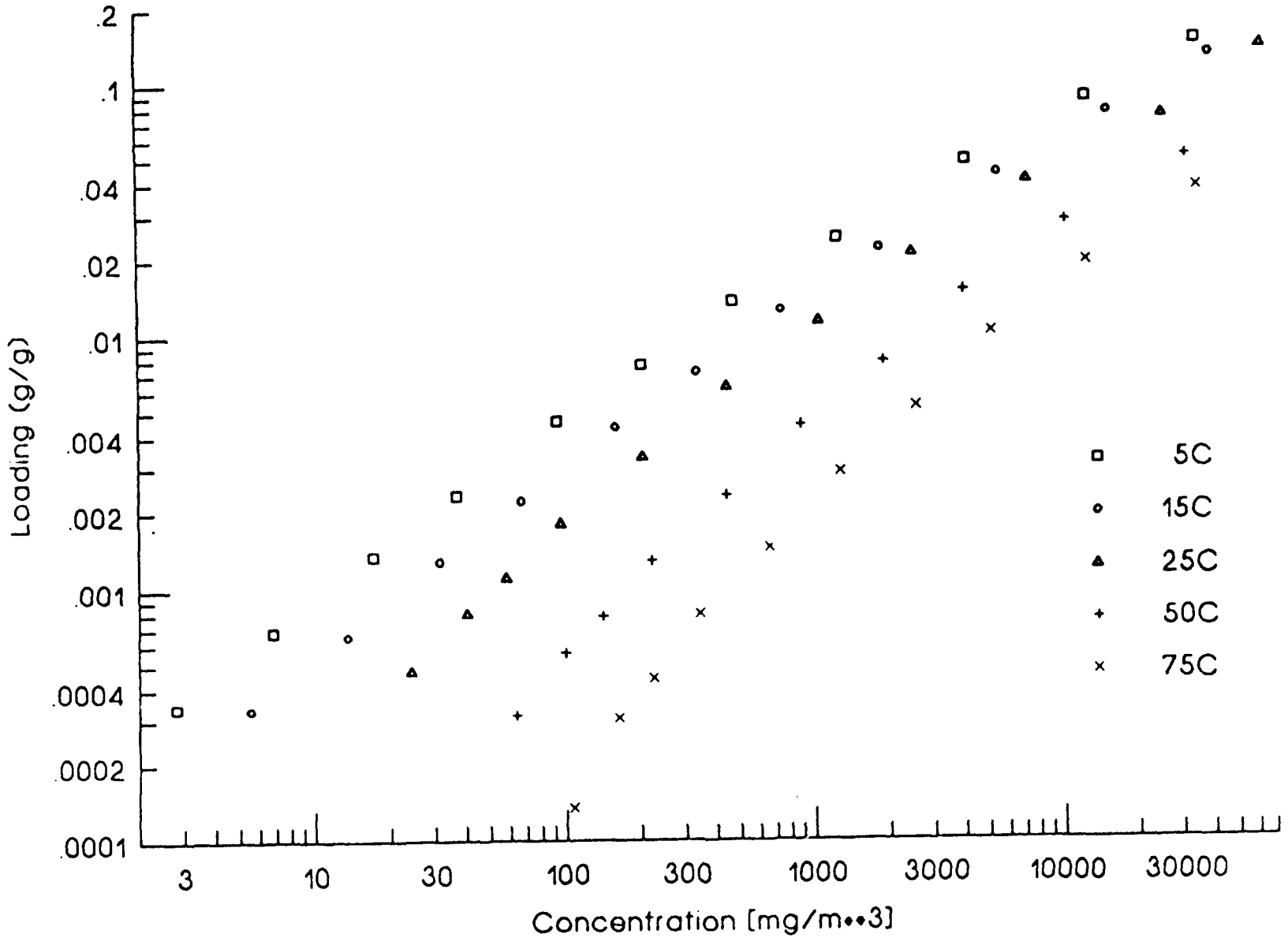

Figure 2. Comparison of Data for CFC-113, PFCBa and R-22 on BPL 12x30 at 25C

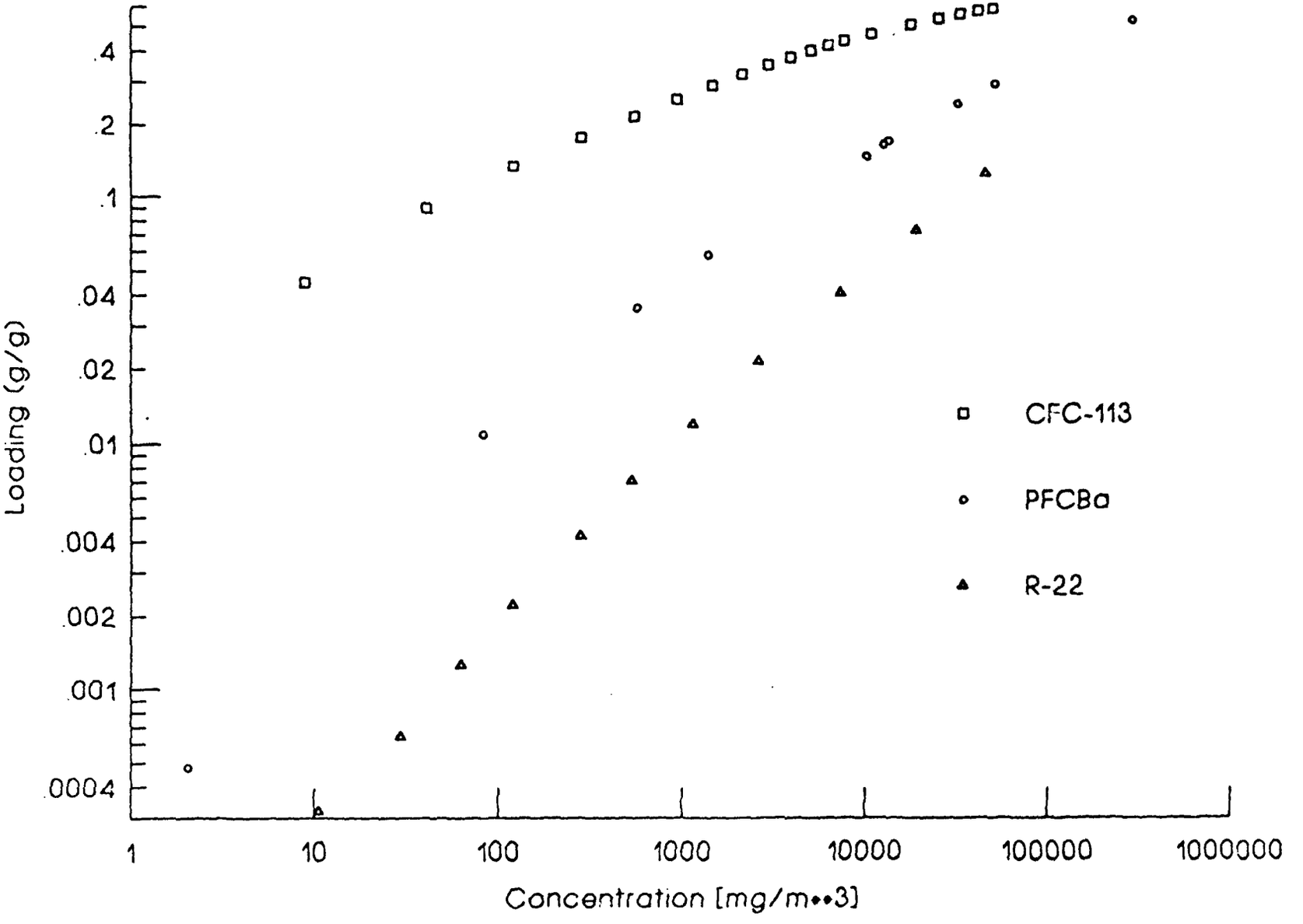

Figure 3. Comparison of Data for CFC-113, PFCBa and R22 on BPL 12x30 at 25C

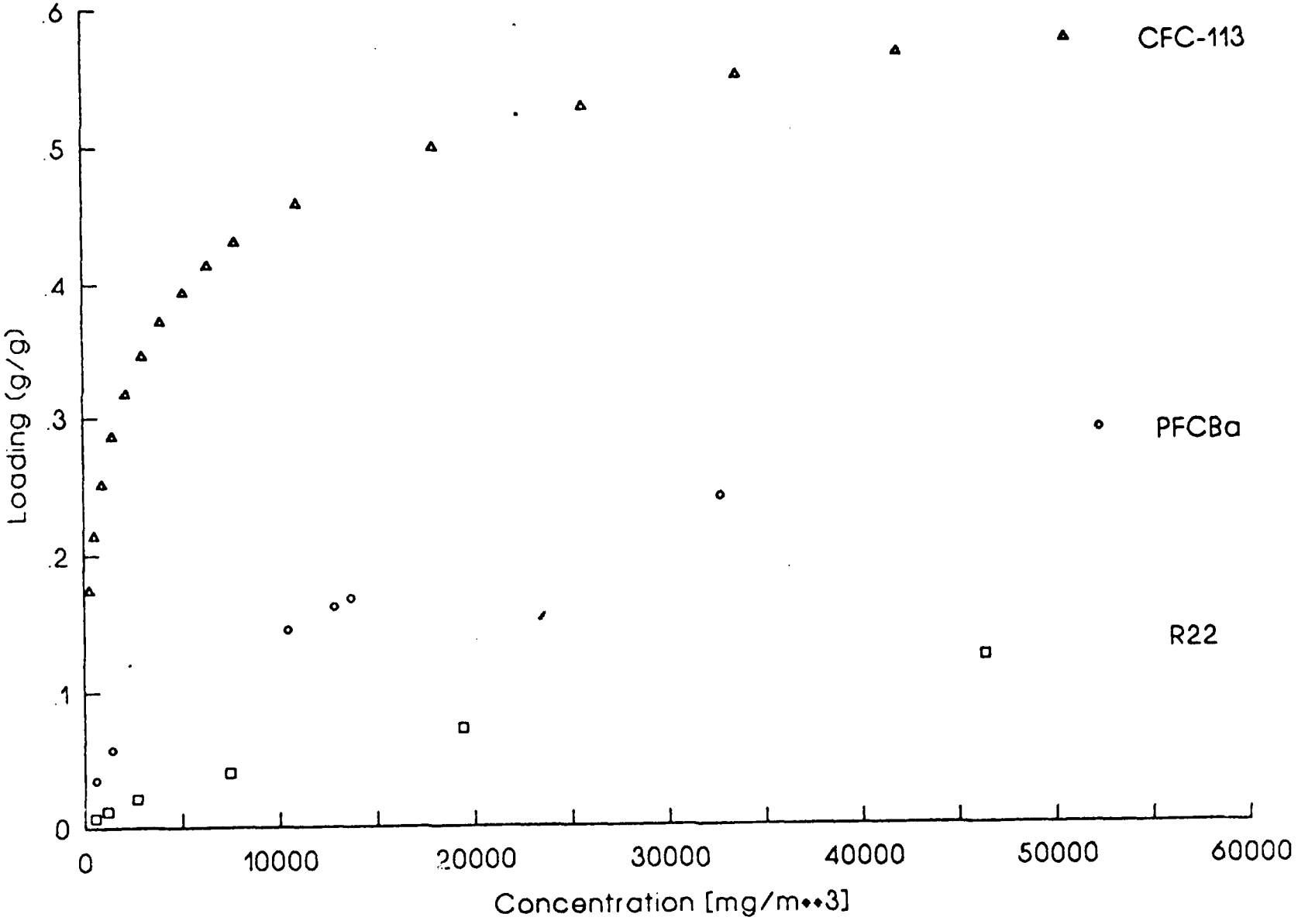

Figure 4. Isotherm Data for CFC-113 on 13X Molecular Sieve, at 25C

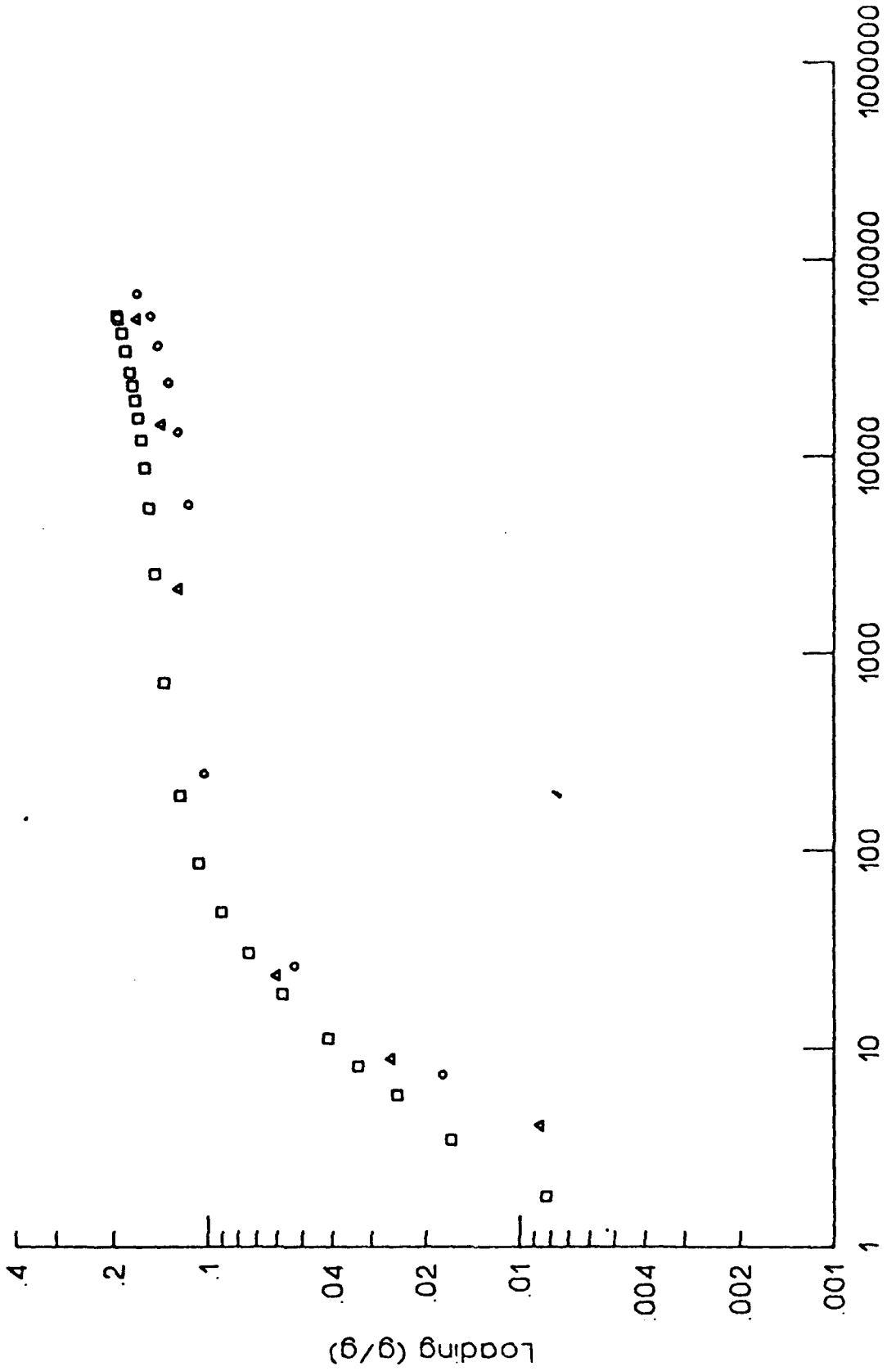

Figure 5. Isotherm Data for PFCBa and CFC-113 on 13X Molecular Sieve at 25C

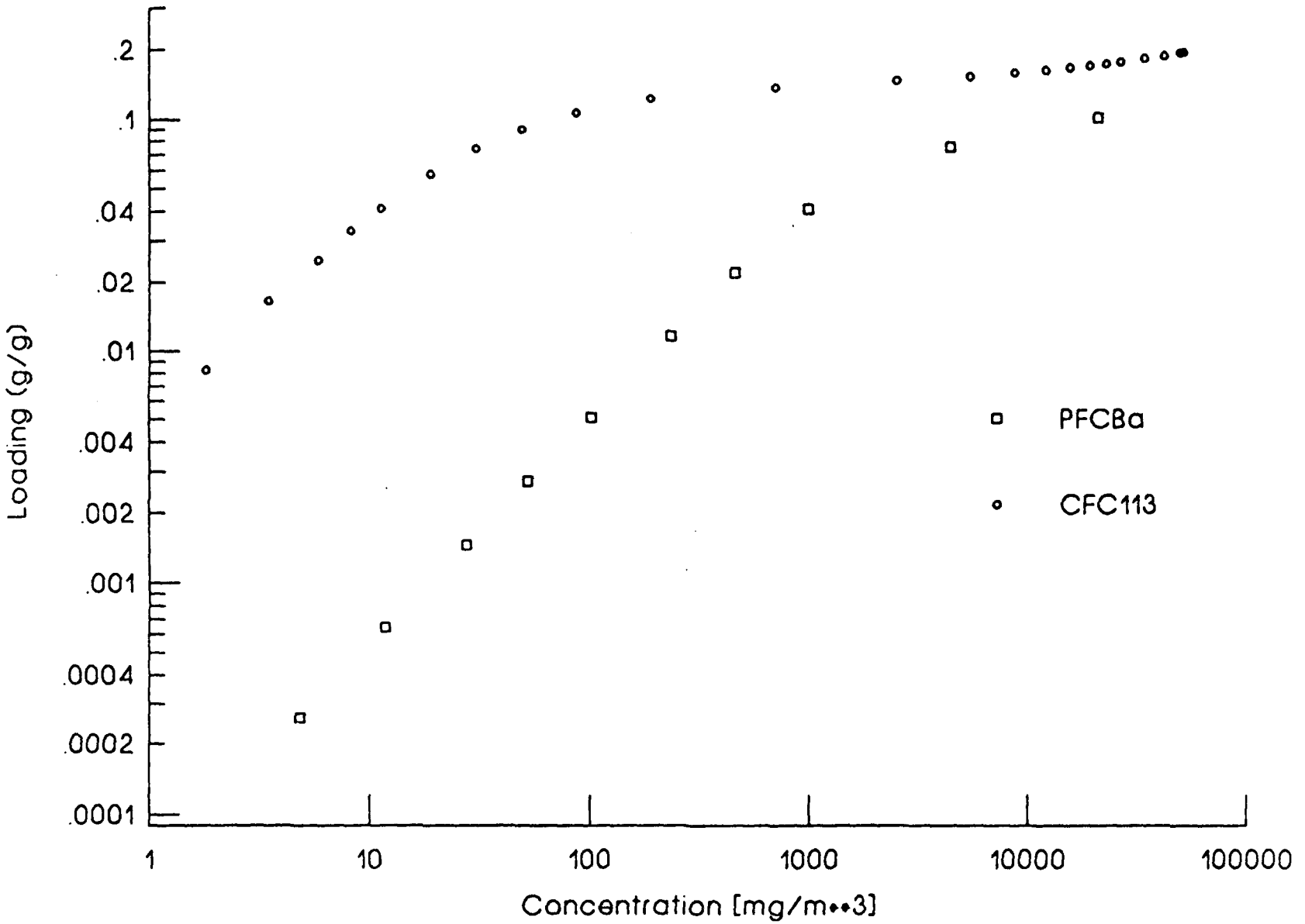

Figure 6. CFC-113 ON BPL CARBON HIGH PRESSURE BREAKTHROUGH

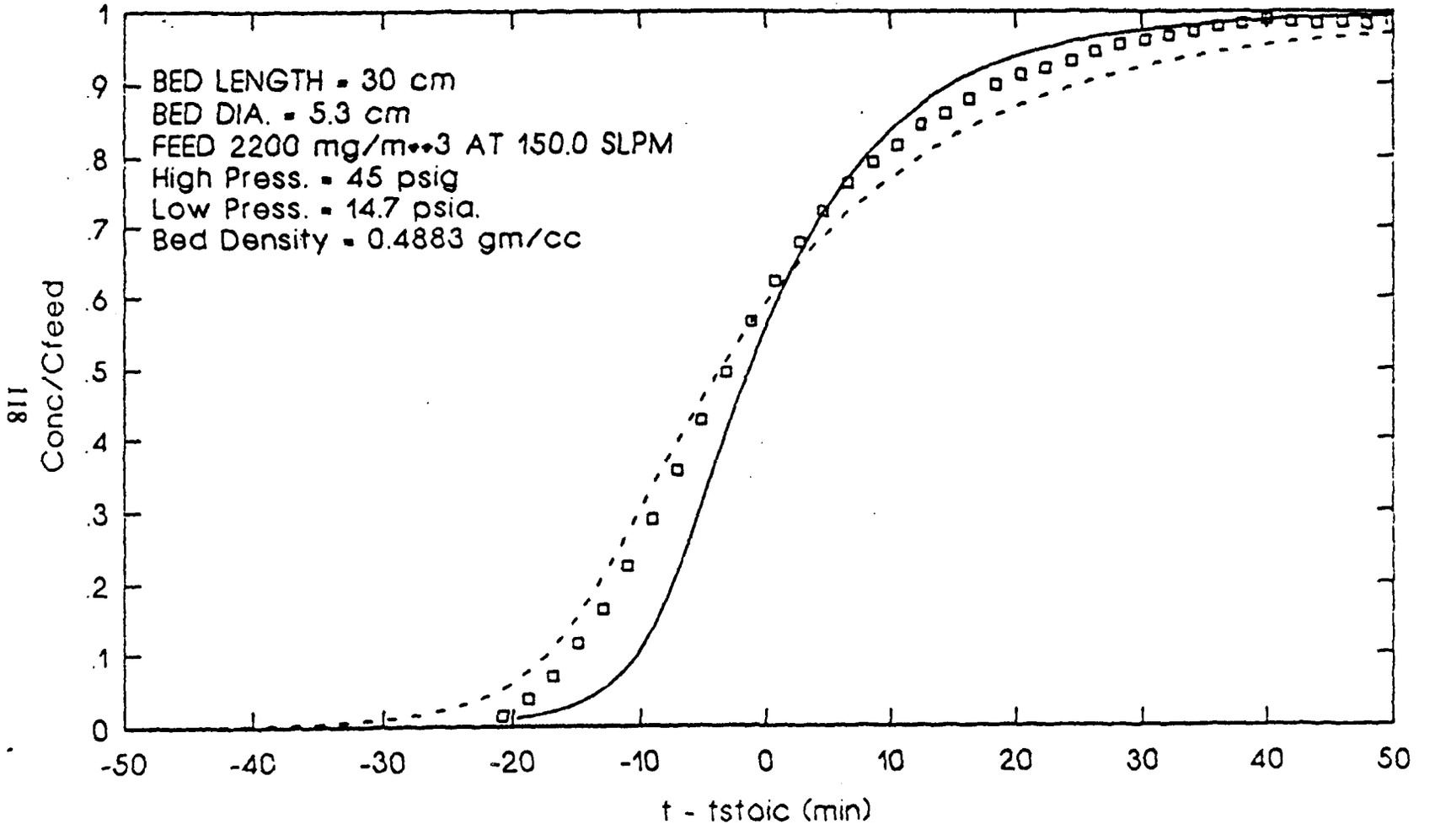

Figure 7 STEADY STATE PSA PROFILES: COMPARISON OF FICKIAN MODEL AND EXPERIMENT

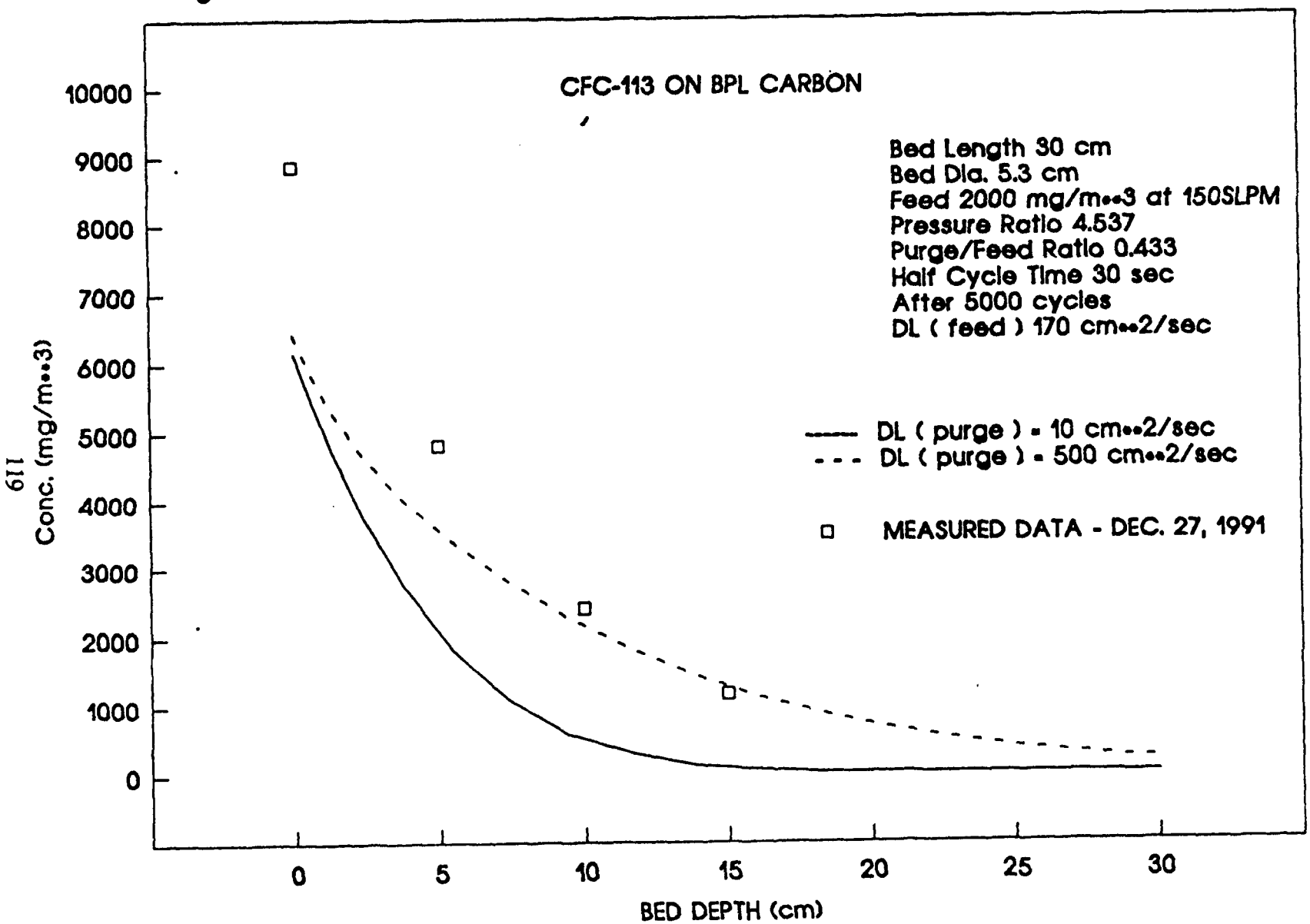

Figure 8. COMPARISON OF ISOTHERMAL AND NON-ISOTHERMAL SIMULATIONS

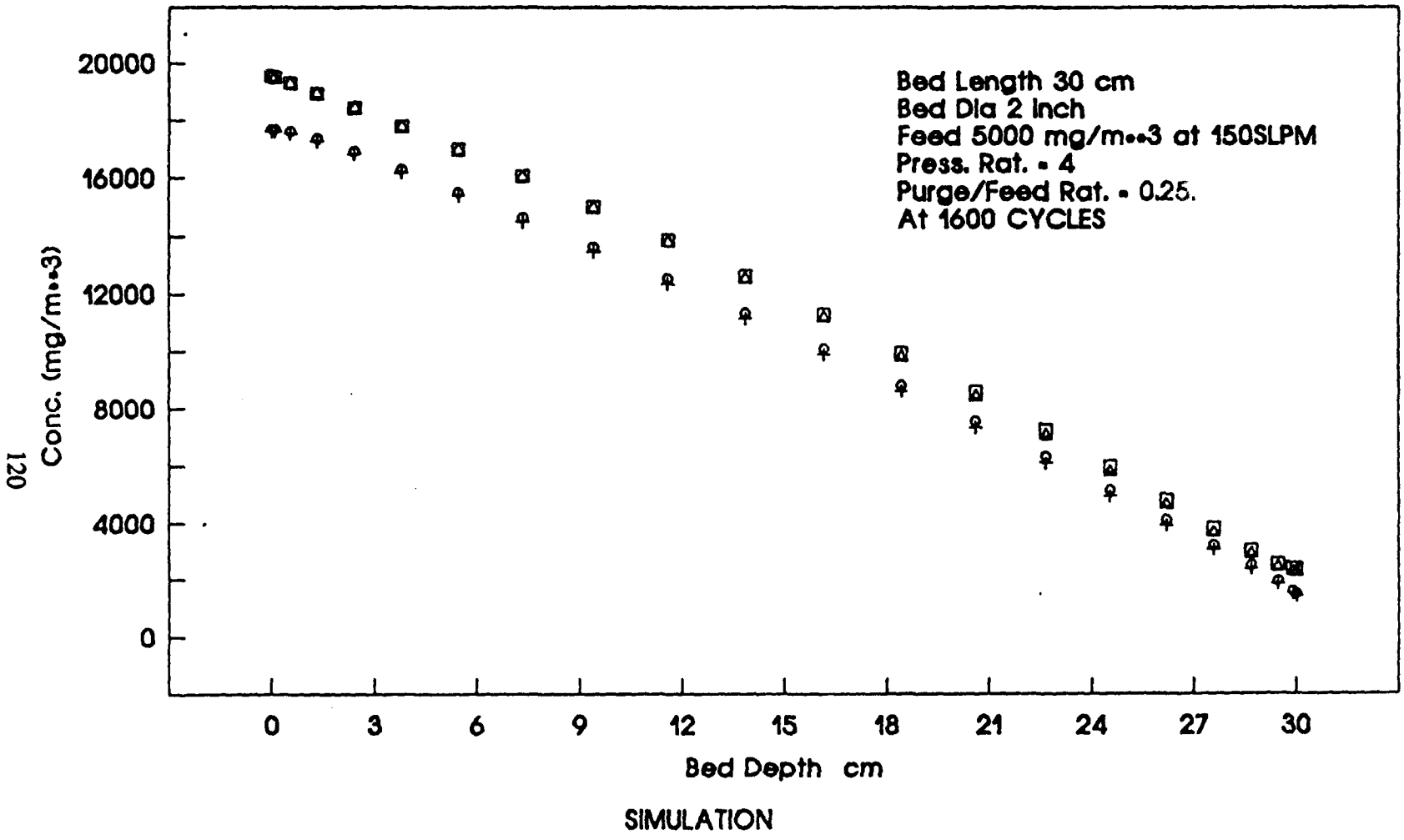

Figure 9. PSA Bed Profile for CFC113 on BPL Carbon
Product 101LPM Purge 54LPM

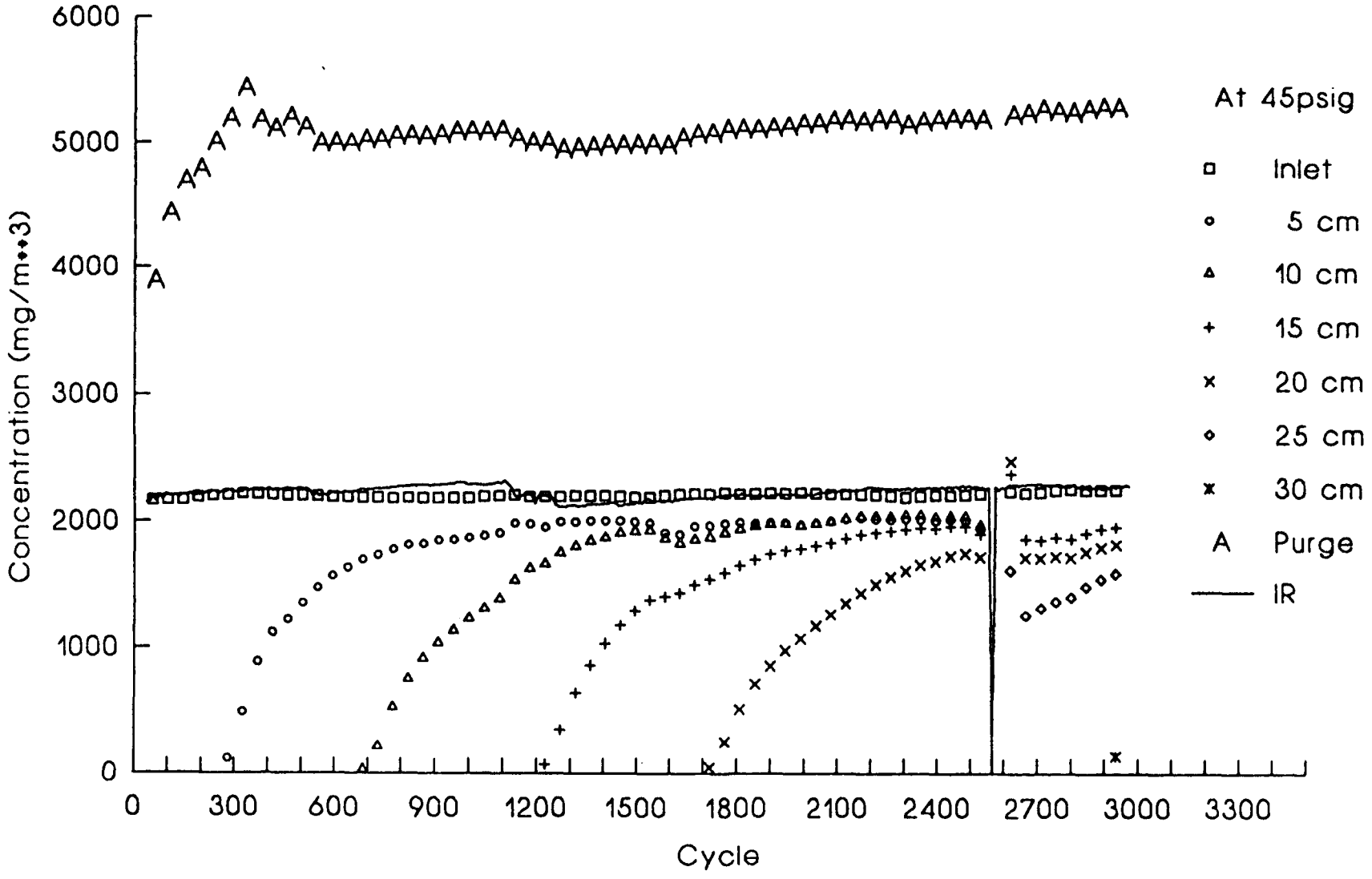

Blank

APPENDIX A-7

QUARTERLY PROGRESS REPORT

GC-PR-2194-07

REPORTING PERIOD:	2/1/91 - 4/30/92
REPORTING DATE:	5/15/92
CONTRACT NUMBER:	DAAA15-90-C-1056
CONTRACT TITLE:	Improved Filtration Materials and Modeling

I. Adsorption Equilibria

Single Component Measurements and Apparatus

Shown in Figure 1 are adsorption equilibria data for difluorochloromethane (R-22) on 13X molecular sieve measured at 25C, 50C, and 75C, plotted on a log-log scale to emphasize the lower concentrations. These data were obtained using the improved drying procedure discussed in a previous quarterly report. Figure 2 compares the 25C isotherm for R-22 on 13X with the 25C isotherm for R-22 on BPL carbon. These results show that the loadings of R-22 on molecular sieve is about 4-10 times larger than the corresponding loadings for R-22 on BPL carbon over the entire concentration range measured. For example, at a vapor phase concentration of 100 mg/m^3, the loading on 13X molecular sieve is about .018 g/g while the loading on BPL carbon is about .0018 g/g. When one also considers that the packing density of 13X molecular sieve is about 0.75 g/cm^3 and BPL carbon is about 0.5 g/cm^3, the relative capacities of R-22 on the two adsorbent on a volumetric basis are approximately 15:1 (13X to BPL carbon). The R-22 isotherm results are in reverse order to similarly measured isotherm data for CFC-113 (trichlorotrifluoroethane) and PFCBa (perfluorocyclobutane) on 13X and BPL carbon. An obvious reason for this reversal in adsorption capacity is that the R-22 is a polar molecule with much stronger electrostatic attractions than either CFC-113 or PFCBa. In addition, there may be some stearic problems with adsorption of the 2 and 4 carbon molecules, particularly with the size of the ring structure of PFCBa. These results demonstrate that

vapor pressure and molecule polarity are important for adsorption on 13X and suggest that using 13X in a layered bed configuration may be required to effectively remove volatile, polar, toxic chemical vapor threats.

II. Pressure Swing Adsorption

Math Modeling

Several significant modifications to the PSA model were developed this quarter in conjunction with Professor LeVan at the University of Virginia. The first major modification was to correctly model the feed and purge flow rates for our two-step PSA system with pressurization using the feed stream. The second modification is the incorporation of an energy balance. We have measured temperature profiles within the bed and found that the compression and decompression of the carrier gas (air) cannot give the magnitude of the temperature swings measured during a cycle. The next quarterly report will detail the current investigations on-going to resolve this issue.

Experiments and Apparatus

An experimental study was undertaken to investigate the effects of three important PSA parameters on the performance of CFC-113/BPL carbon system. A set of base-case conditions was defined (see Table 1).

The three parameters under investigation, namely, (1) feed pressure to purge pressure ratio, (2) purge to product ratio, and (3) cycle time were varied one at time from the base case. The values used in the experiments were,

1. Pressure ratio = 3:1, **4:1**, 5:1
2. Purge to product ratio = 1:2, **1:1**, 2:1
3. Cycle time = 20s, **60s**, 180s, 300s

where the values in bold correspond to the base-case conditions.

Table 1. Base Case Conditions

Adsorbent:	BPL Carbon, 12x30, fresh from drum
Chemical:	CFC-113
Feed RH:	3-5% @ ambient pressure
Feed Flow:	150 SLPM
Feed Temperature:	298 K
Feed Pressure:	45 psig
Feed Concentration:	4000 mg/m^3 @ 1 atm
Purge Flow:	75 SLPM
Cycle Time:	60 Seconds (1/2 cycle = 30 sec.)
Bed Diameter:	5.2 cm
Bed Depth:	25 cm

The results for the base-case experiment are given in Figure 3, plotted on a semi-log scale to display the low concentrations. These data demonstrate the importance and value of the in-bed sampling system and the general behavior of the PSA system. Note that the feed concentration remains constant throughout the experiment while each succeeding sample port down the bed reaches a lower plateau concentration. Also interesting is the time between successive port breakthroughs. For example, the 5-cm port begins to breakthrough at about 200 cycles, the 10-cm port begins to breakthrough at about 1000 cycles, the 15-cm port at about 2700 cycles, and the 20-cm port at about 5100 cycles. The reason these times are not equally spaced is the shape of the isotherm. Since the CFC-113 isotherm on BPL carbon is favorable (concave downward on a concentration versus loading plot), the relative capacity for CFC-113 at lower concentrations increases. This results in longer times for the lower concentrations to move down the bed. In fact, the spacing between port breakthroughs can be a direct measure of the isotherm shape. If a more favorably adsorbed material (e.g. hexanol) were used, the spacing between port

breakthroughs would be much farther apart, while for a more weakly adsorbed vapor such as PFCBa or R-22 on BPL carbon, the spacing would be more linear.

Effect of pressure ratio. The pressure ratio is defined as the feed pressure divided by the purge pressure. Shown in Figures 4 and 5 are the breakthrough data for pressure ratios (P_R) of 3 and 5, respectively. As with the base case results, the difference between port breakthrough times is governed by the concentration. These data are more easily interpreted by comparing the breakthrough behavior at a given port and the periodic concentration values. Shown in Figure 6 are the breakthrough data for the 15-cm port for each of the pressure ratio experiments. The differences between the times when material is first detected as the value of P_R is increased from 3 to 4 to 5 is about linear. For example, for P_R = 3, the first detected concentration occurred at about 800 cycles, for P_R = 4 at about 1100 cycles and P_R = 5 at about 1500 cycles. However, the effect of the pressure ratio on the plateau concentration at 15 cm is not linear. There is more than a 4-fold decrease, from about 3000 mg/m^3 to about 700 mg/m^3, in the plateau concentration when P_R is increased from 3 to 4 (an increase in P_R of 33%). A 2-fold decrease, from about 700 mg/m^3 to about 350 mg/m^3, occurs in the plateau concentration when P_R is increased from 4 to 5 (an increase in P_R of 25%).

Shown in Figure 7 are the periodic-state (plateau) concentrations for each pressure ratio. These data also demonstrate that for this system, the effect of the pressure ratio is much more pronounced for P_R between 3 and 4. For P_R = 3, there is very little separation (small differences in plateau concentration) achieved as the bed depth is increased. For P_R = 4 and 5, notice that the relationship between the periodic state concentration and bed depth for each experiment is logarithmic, with the slope of the line on a semi-log plot steeper for the higher pressure ratio. The design implication for military systems is that an optimum feed pressure exists. Lower values reduce the system size and energy, while higher pressures afford greater protection.

Effect of purge to product ratio. The purge to product ratio is the purge flow rate divided by the product flow. Shown in Figures 8 are the results for the high product, low purge flow experiment. These data show that the time (number of cycles) between the breakthrough of each port is about linear. The reason for this is that almost no separation (i.e., reduction in concentration) is being achieved using this low purge flow. Figure 9 shows the breakthrough data for the high purge, low product flow experiment. Note that this experiment was run almost 7000 minutes and the 20 cm port did not show any measurable concentration. Compare that to Figure 8 where the system reached periodic state in about 1750 minutes.

The in-bed concentrations at a bed depth of 15 cm as a function of time are plotted in Figure 10 for each purge to product ratio. The time to breakthrough as the purge to product ratio is increased from 1:2 to 1:1 goes from about 300 minutes to about 1000 minutes and then to about 2100 minutes for the 2:1 experiment. The plateau concentration, as the purge to product ratio is increased, shows a 6-fold to 7-fold decrease between experiments. Figure 11 displays the periodic state concentration versus bed depth results. As with the pressure ratio results, the periodic state concentration is reduced in a logarithmic fashion with increasing bed depth. Notice also the spread (difference in slope) between the 1:1 and 2:1 purge to product ratio results is much larger than for the pressure ratio experiments.

Effect of cycle time. Shown in Figures 12, 13 and 14 are the full in-bed results for the cycle time experiments. Once again the 15-cm port results for each cycle time are shown in Figure 15. There are two interesting features. The breakthrough times for the 180 and 300 second experiments are almost identical, while the separation at periodic state is approximately a factor of 2 better for the 180 second cycle time. Also, notice that the 20 second cycle time does not follow the trend of improved performance with reduced cycle time. The 20 second cycle time not only produces shorter times to breakthrough, compared to the 60 second cycle time, the plateau concentration is close to the 180 second result. The

periodic state results shown in Figure 16 also demonstrate that the best system protection performance is obtained using the 60 second cycle time. The three minute cycle time value at 25 cm has not reached periodic state. One possible explanation for the cycle time behavior can be traced to the type of two-step PSA cycle we are operating. During the pressurization phase of the feed step, contaminated air is entering the bed at high velocity. For the 20 second cycle time experiments, the fraction of time during each cycle where high velocity feed is entering the bed is enough to offset the advantage gained by a shorter cycle.

Summary of Results. It should be emphasized that the conclusions drawn from these data may be entirely different for a different adsorbent/adsorbate system. However, the qualitative effects of the three parameters investigated should hold true. One can visualize a design problem which requires size and power required by the filtration unit to be minimized, but still maintain some desired product flow. As the feed pressure is reduced, the power and size go down, but the protection time is decreased. If the purge to product ratio is increased to afford better protection, then the amount of product produced is reduced. One must then provide more feed air to generate enough product, thus increasing size and energy requirements. There is not a large effect of cycle time for the CFC-113/BPL carbon system. However, one would expect that for more weakly adsorbed species, this effect will become more pronounced. Future experiments with less strongly adsorbed species will determine if this is true.

III. Data Acquisition and Control

The single component system software was modified to address temperature control problems. Due to a drift in the D/A hardware, the system was unable to lock on to a precise temperature. The software was modified to include reset capability. Current operational results indicate the problem has been corrected.

National Instruments LabView 2 training classes were attended. Training was received in basic and advanced LabView techniques.

The TSA interim control software was developed in LabView 2. This software allows a user to control the interim TSA system. Parameters such as cycle time and amount of power applied can be set by the user. In addition, the software will acquire in-bed temperature profiles. The software was integrated with the existing hardware. An interim solution is required because available hardware does not allow the full implementation of the system. The full system will be implemented when additional GFE is supplied.

The TSA power controller hardware was designed and drawings were prepared. Assembly awaits the completion of another drawing and final fabrication.

Software and hardware were developed to allow the real time study of temperature profiles in an operating PSA bed. A SC-2070 interface was modified to bandwidth limit thermocouple signals. LabView 2 software was developed to input, present, and store the temperature data. Additional LabView software was developed to allow various methods of evaluating the collected data.

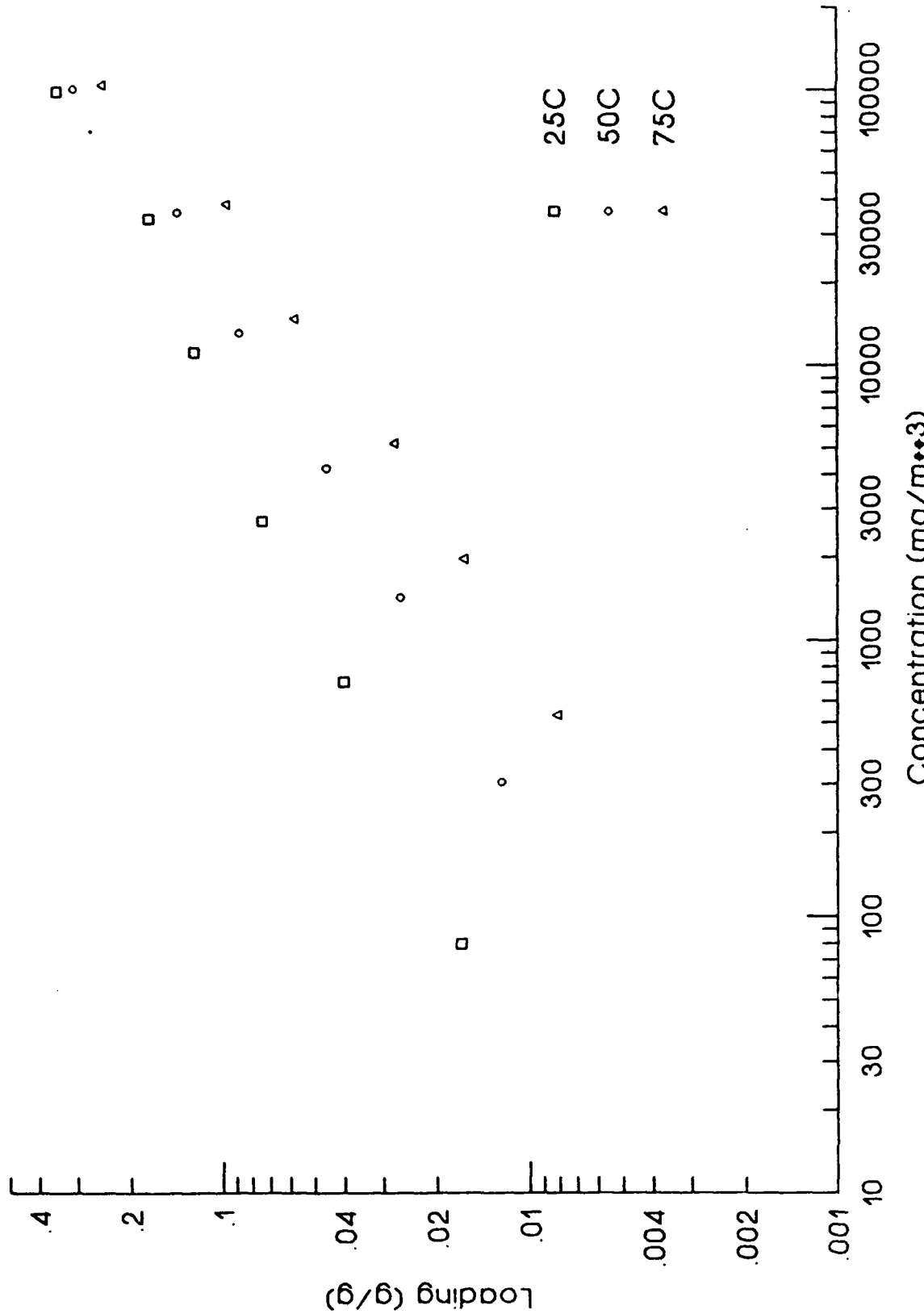

Figure 1. Isotherm Data for R-22 on 13X Molecular Seive at 25, 50 and 75C

Figure 2. Isotherm Data for R-22 on 13X Molecular Seive and BPL Carbon at 25C

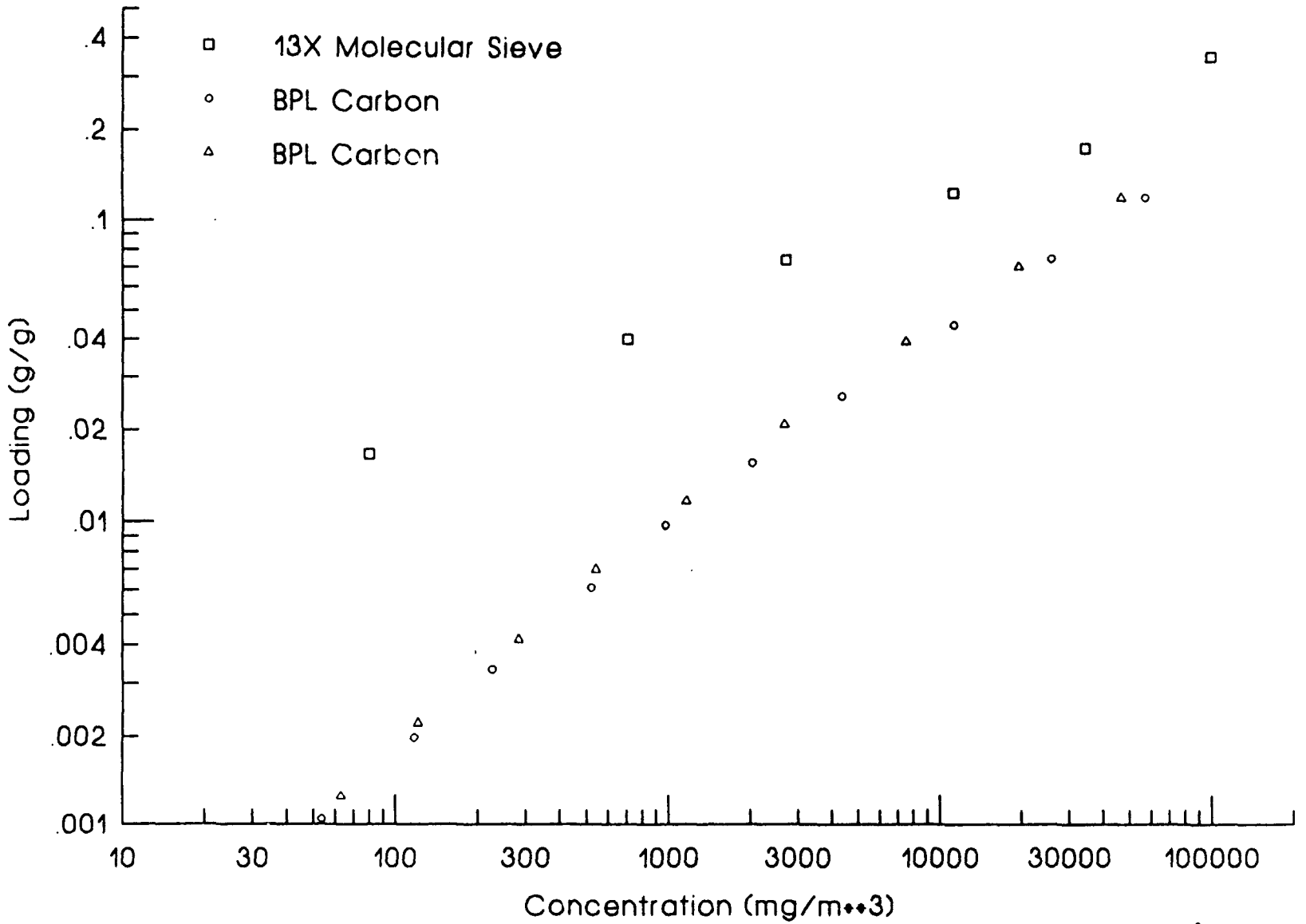

Figure 3. PSA Bed Profile for CFC113 on BPL Carbon
Base Case Conditions

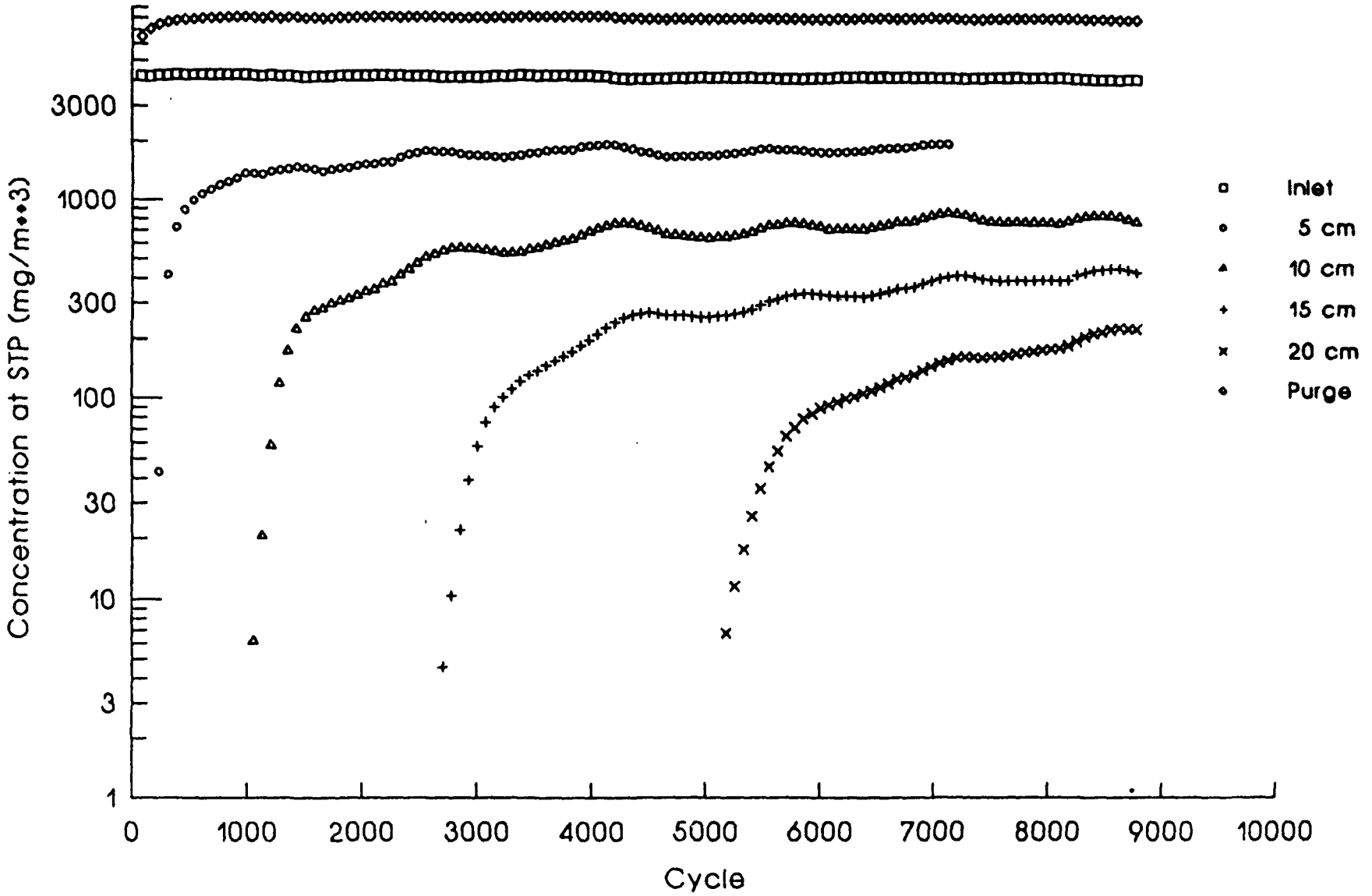

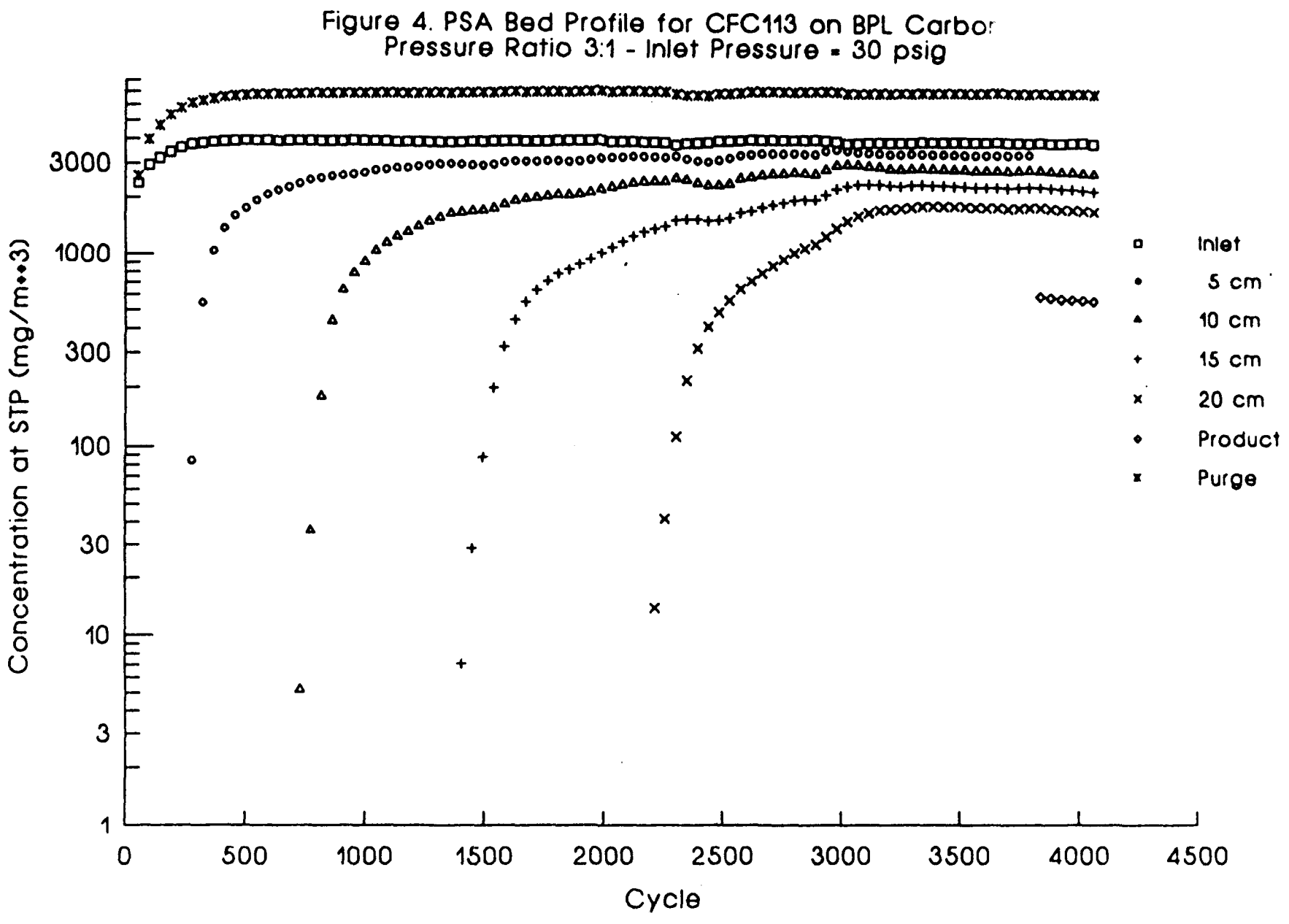
Figure 4. PSA Bed Profile for CFC113 on BPL Carbo
Pressure Ratio 3:1 - Inlet Pressure = 30 psig
Concentration at STP (mg/m**3)
3000
1000
300
100
30
10
3
1
0
500
1000
1500
2000
2500
3000
3500
4000
4500
Cycle
Inlet
5 cm
10 cm
15 cm
20 cm
Product
Purge

Figure 5. PSA Bed Profile for CFC113 on BPL Carbon
Pressure Ration 5:1 - Inlet Pressure = 60 psig

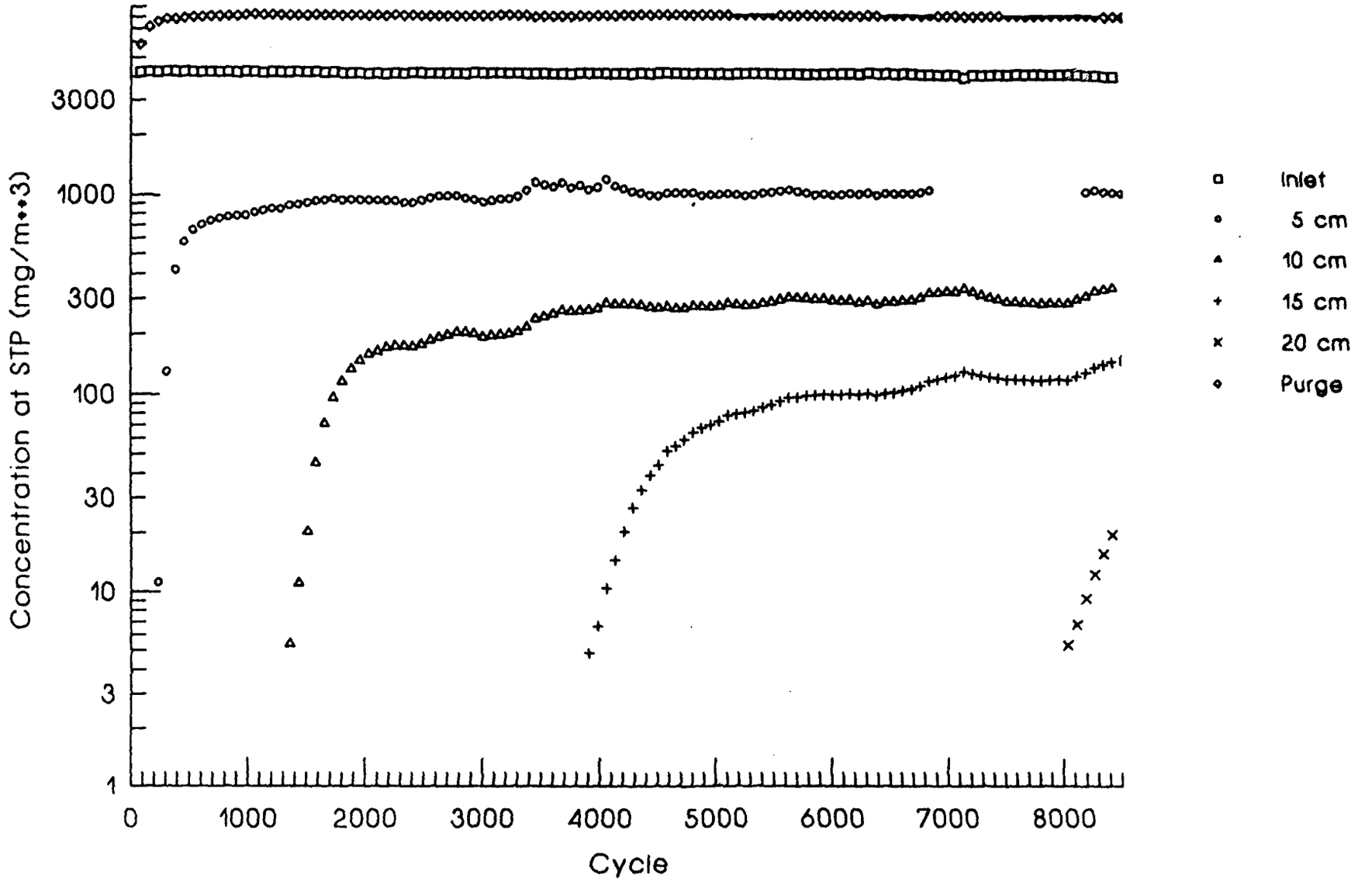

Figure 6. Concentration vs Time at 15cm
Effect of Pressure Ratio

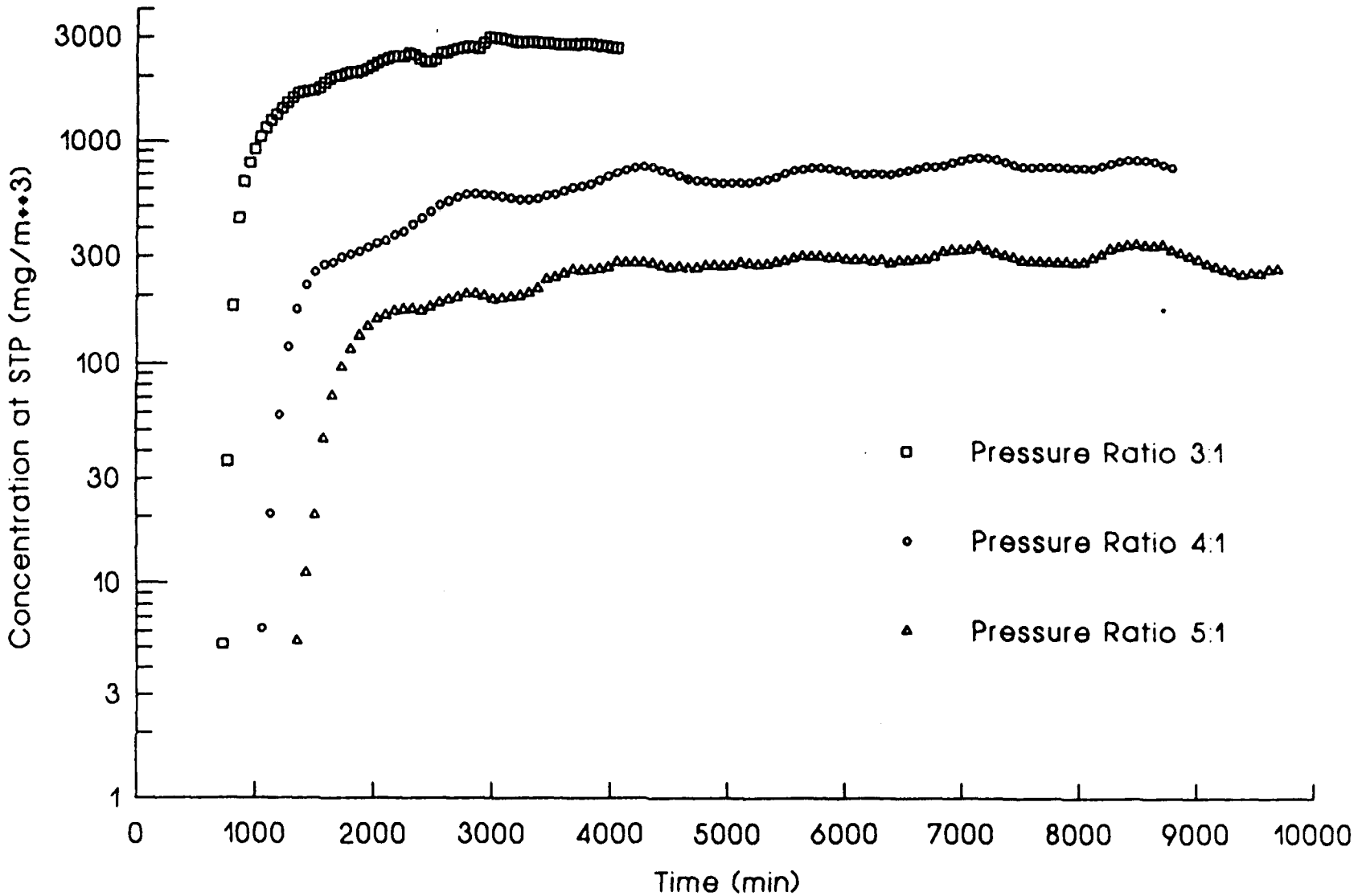

Figure 7. Concentration as a Function of Bed Length For CFC-113 on BPL Carbon

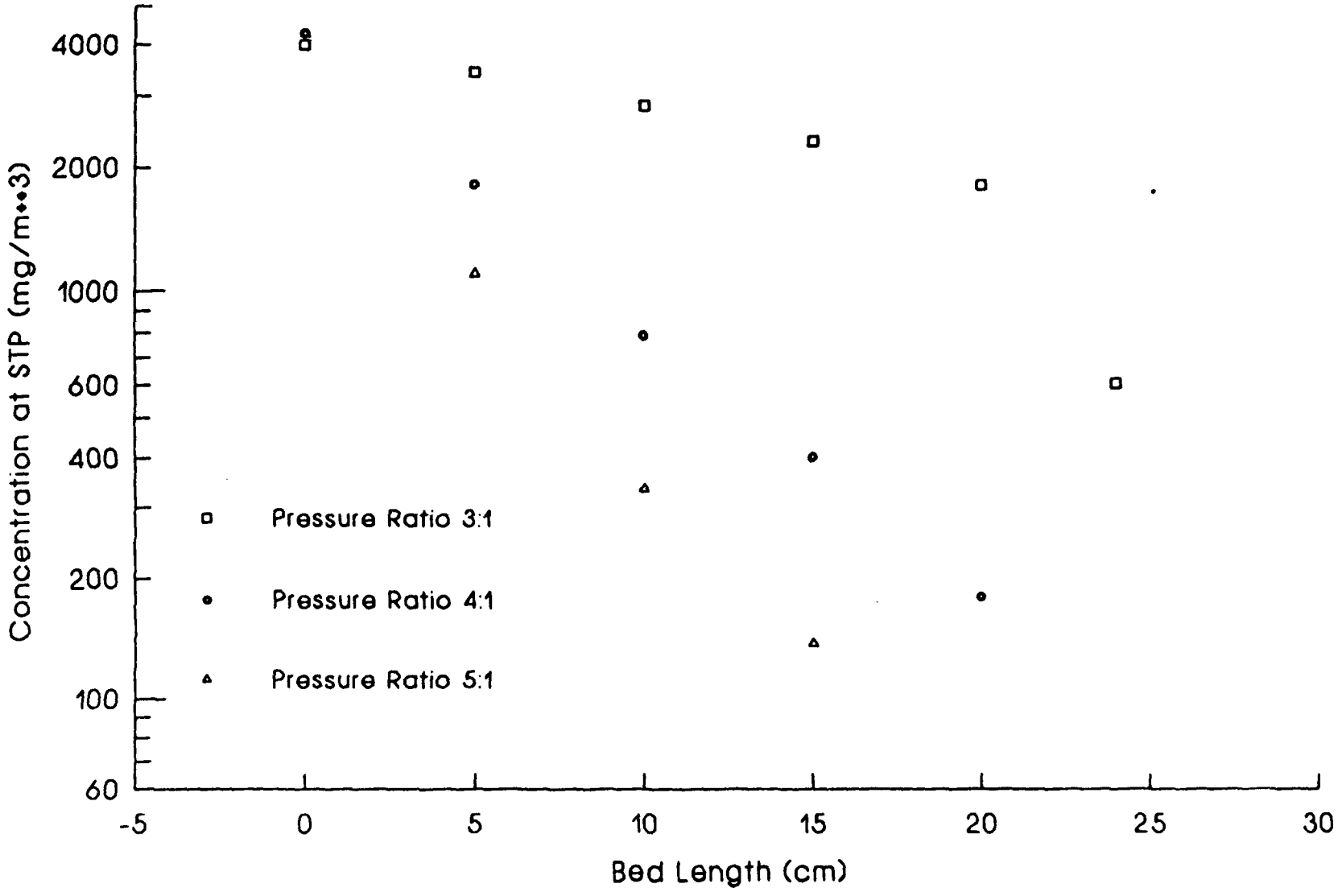

Figure 8. PSA Bed Profile for CFC113 on BPL Carbon
Purge to Product Ratio 1:2 - 50SLPM Purge

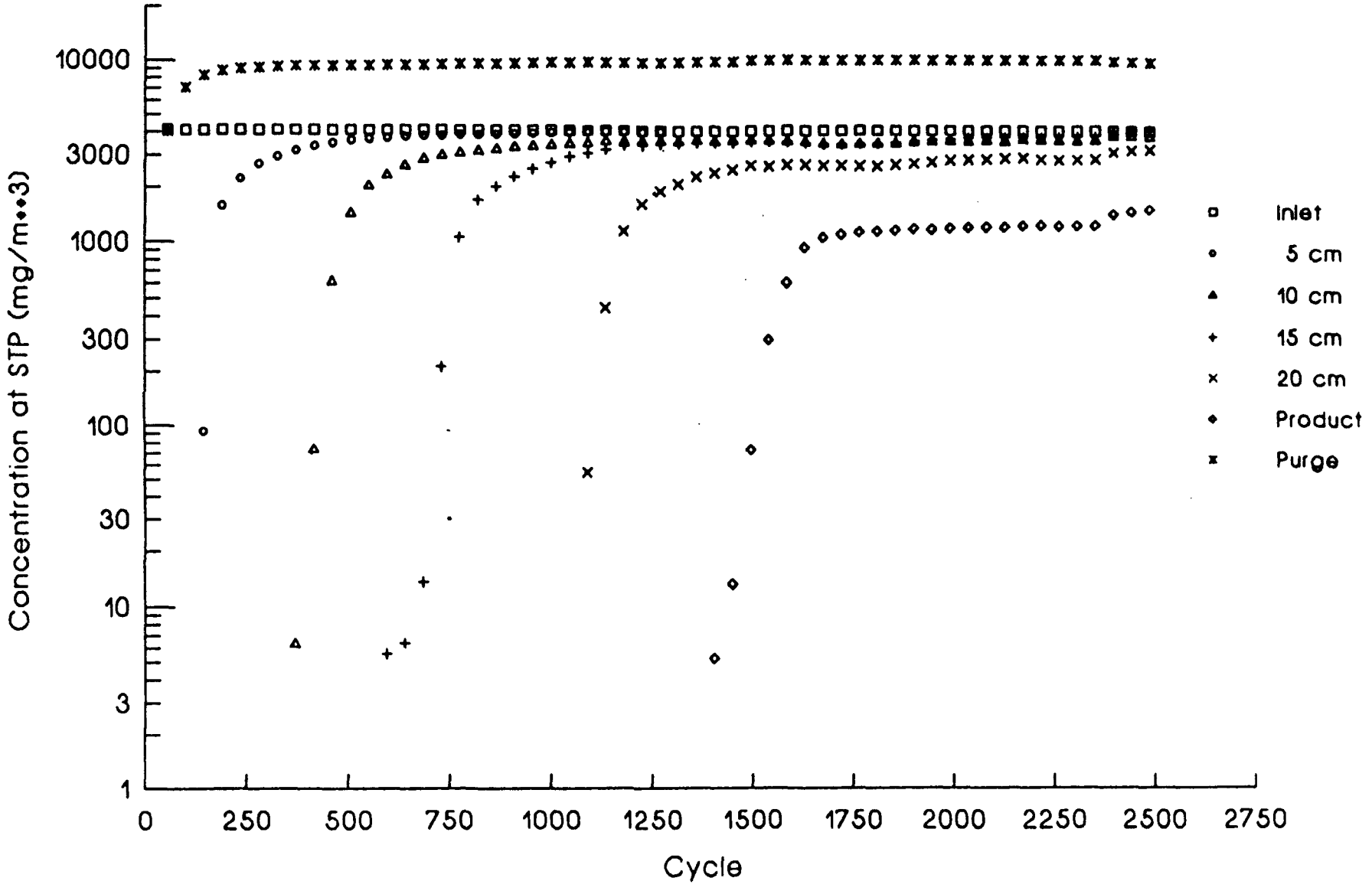

Figure 9. PSA Bed Profile for CFC113 on BPL Carbon
Purge to Product Ratio 2:1 - 50SLPM Product

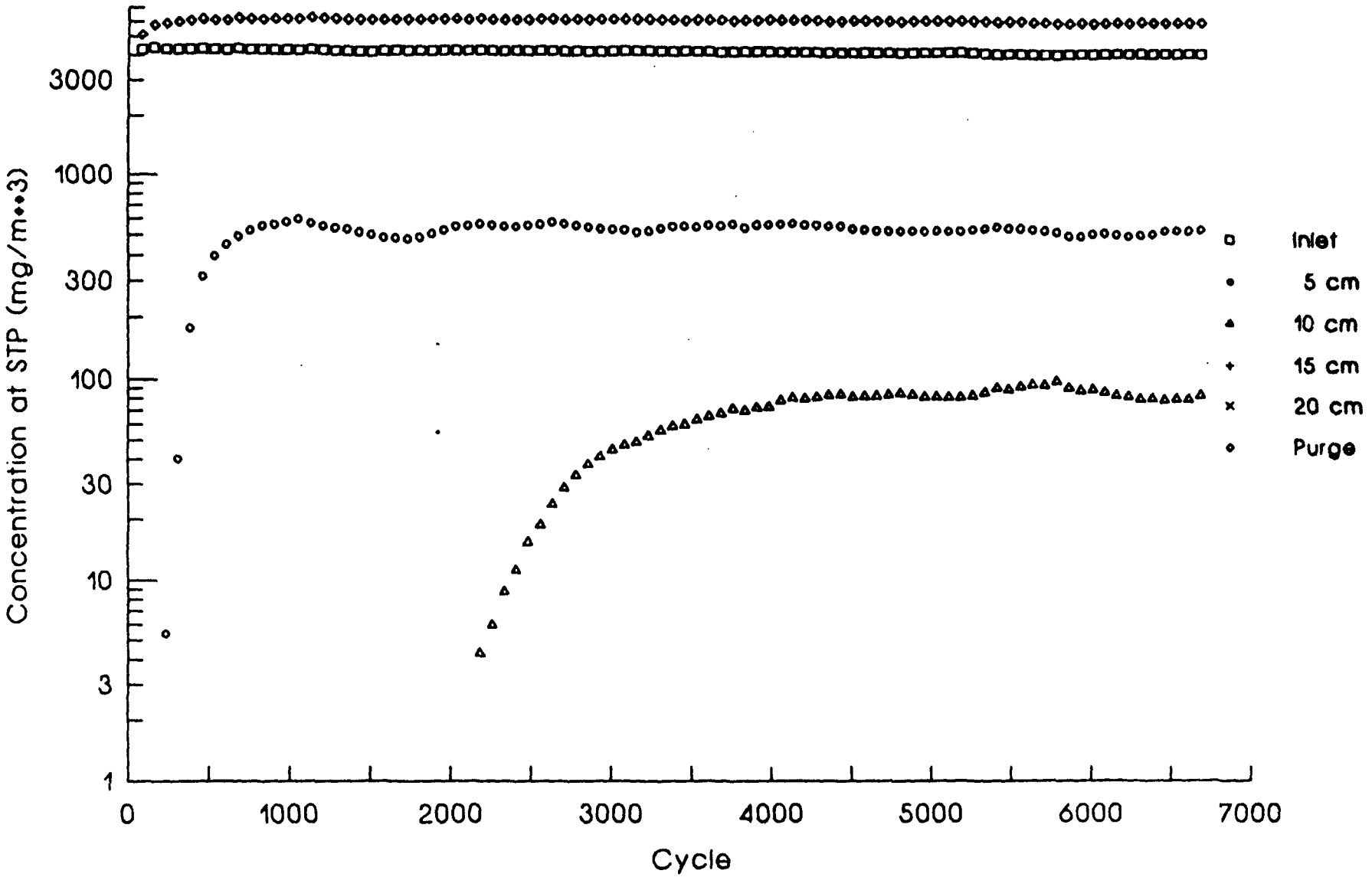

Figure 10. Concentration vs Time at 15cm
Effect of Purge to Feed Ratio

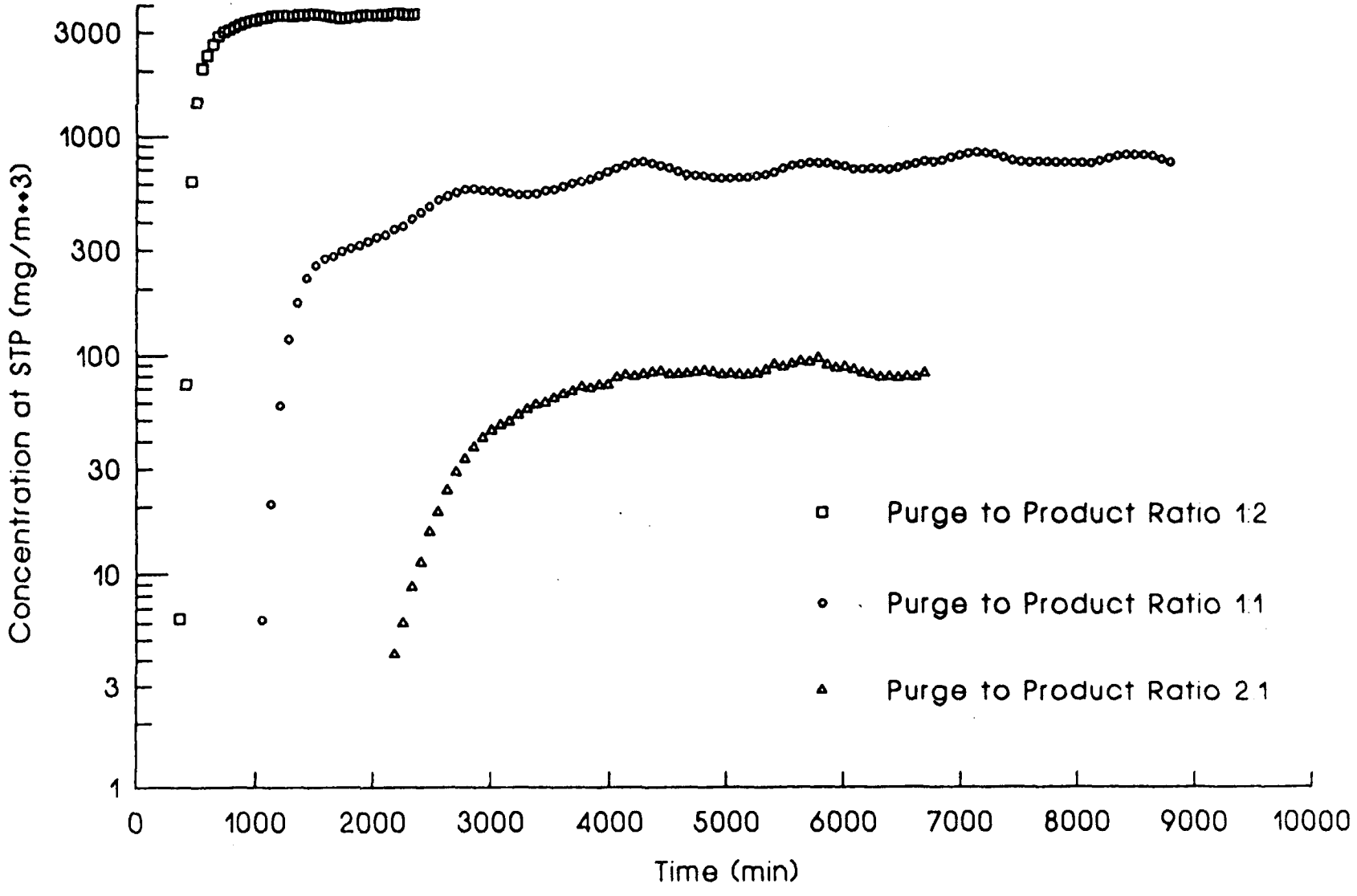

Figure 11. Concentration as a Function of Bed Length
For CFC-113 on BPL Carbon

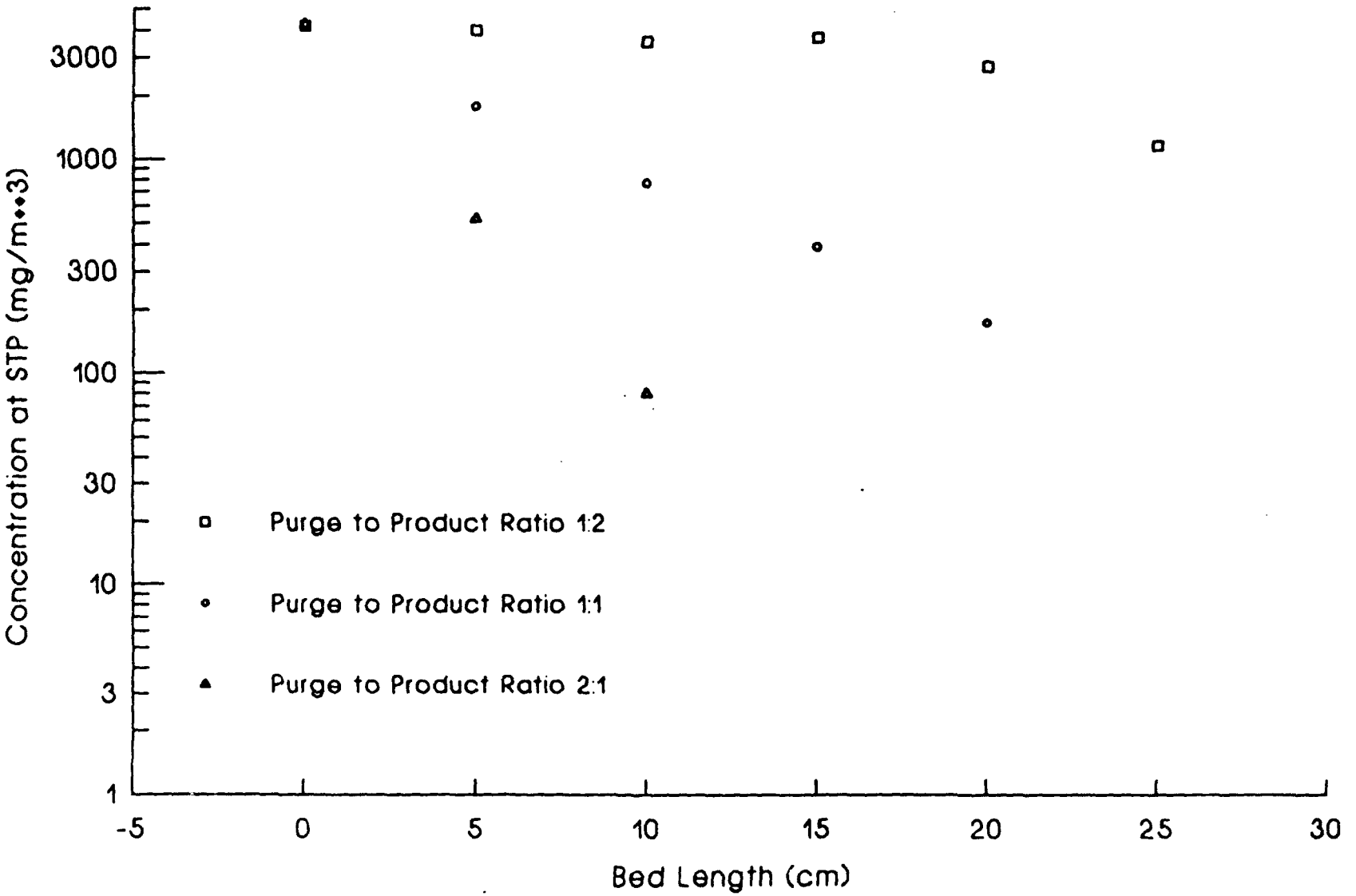

Figure 12. PSA Bed Profile for CFC113 on BPL CArbon
Cycle Time = 20 sec

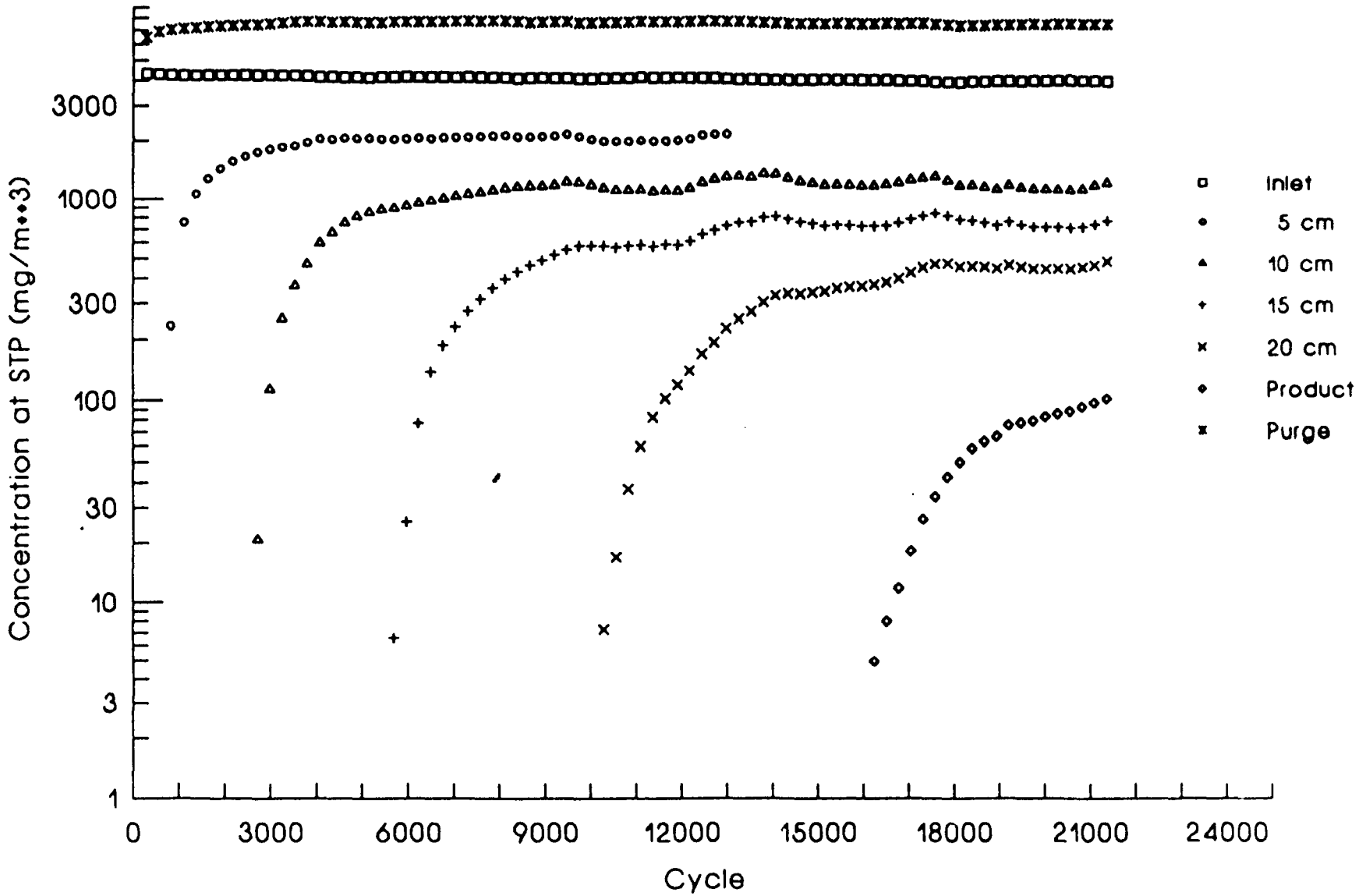

Figure 13. PSA Bed Profile for CFC113 on BPL Carbon
Cycle Time = 180 sec

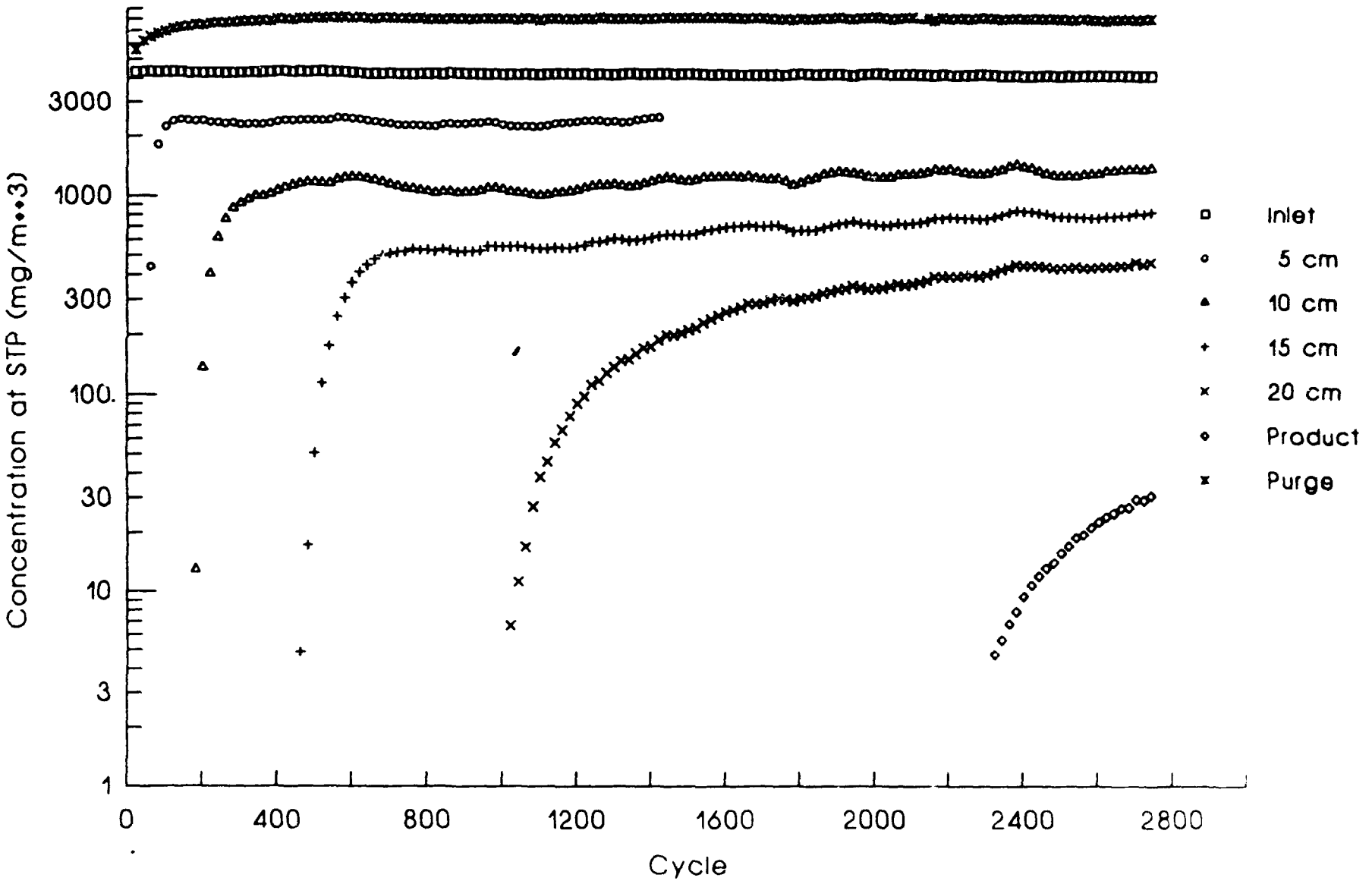

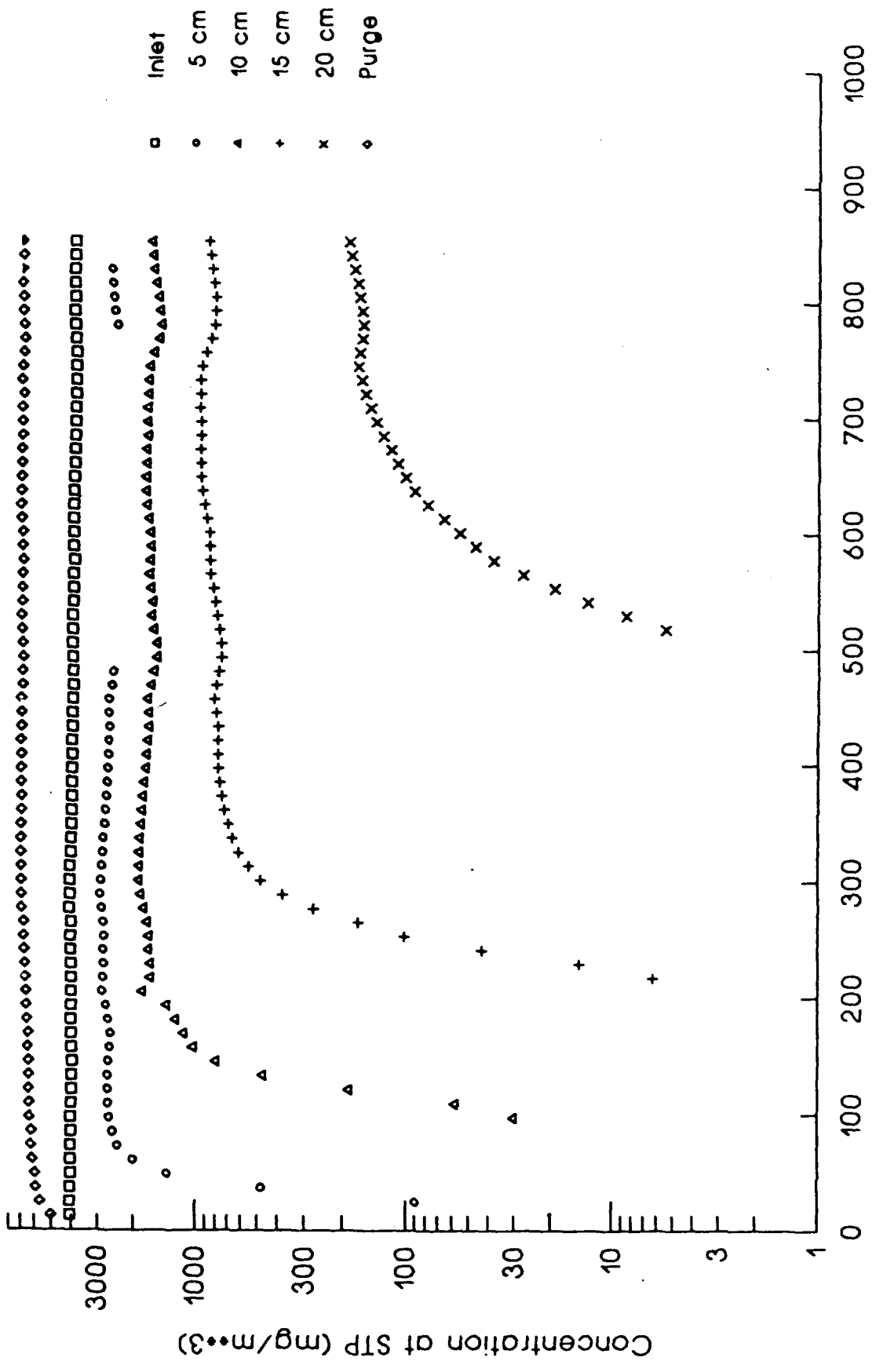
Figure 14. PSA Bed Profile for CFC113 on BPL Carbon
Cycle Time = 300 sec
Concentration at STP (mg/m**3)
3000
1000
300
100
30
10
3
1
0
100
200
300
400
500
600
700
800
900
1000
Cycle
Inlet
5 cm
10 cm
15 cm
20 cm
Purge

Figure 15. Concentration vs Time at 15cm
Effect of Cycle Time

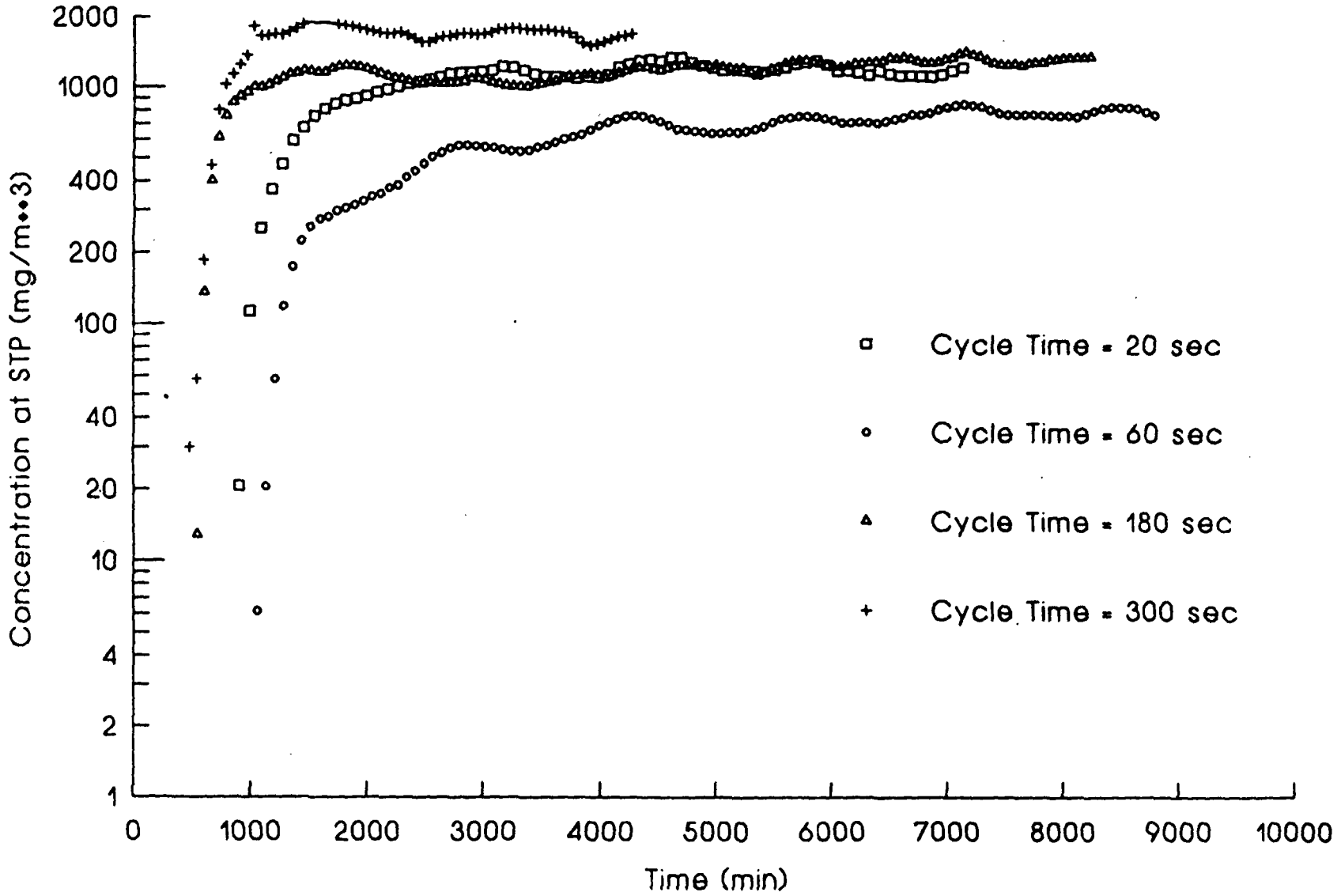

Figure 16. Concentration as a Function of Bed Length
For CFC-113 on BPL Carbon

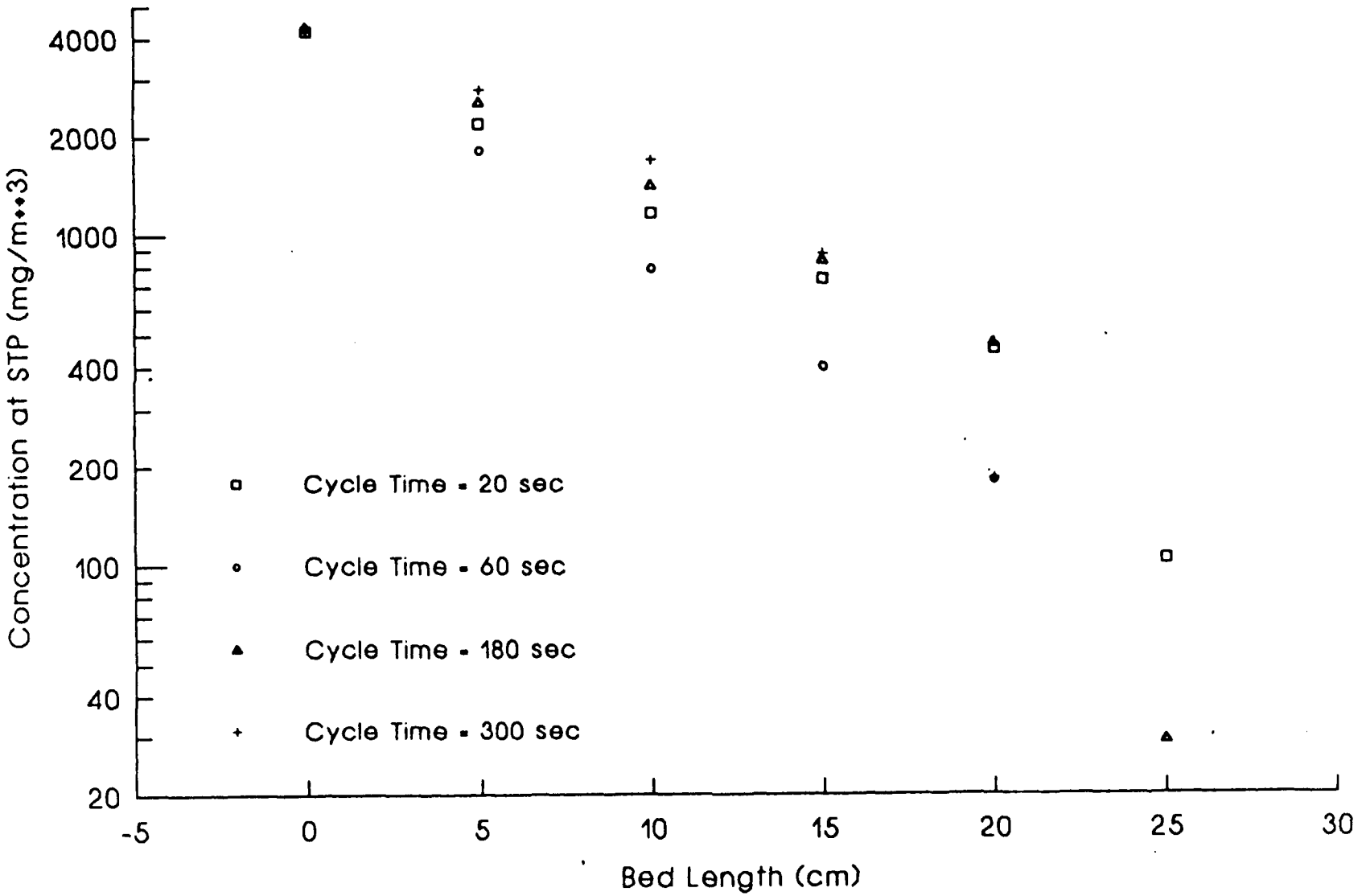

Blank

APPENDIX A-8

QUARTERLY PROGRESS REPORT

GC-PR-2194-08

REPORTING PERIOD:	5/1/92 - 7/31/92
REPORTING DATE:	8/15/92
CONTRACT NUMBER:	DAAA15-90-C-1056
CONTRACT TITLE:	Improved Filtration Materials and Modeling

I. Adsorption Equilibria

Single Component Measurements and Apparatus

Shown in Figure 1 are the measured adsorption equilibria for trichloro, fluoromethane (R-11) on 12x30 mesh BPL carbon at 25°C, 50°C, and 75°C. Data above about 10,000 mg/m^3 seem to exhibit unusually high loadings. We are trying to determine if the calibration data for R-11 is incorrect.

Multicomponent Measurements and Apparatus

The apparatus used to measure multicomponent adsorption equilibria was taken apart and rebuilt. Shown in Figure 2 is the current configuration of the system. Valves 4 and 5 have been installed to facilitate the calibration portion of the experimental procedure. It was necessary to rebuild the system to effectively trouble-shoot the system and to insure that valves are switched in the correct sequence when changing to the next step. Experiments performed where the valves were changed in the incorrect sequence produced erroneous results in measured loadings. Recently measured isotherm data for water on BPL carbon with correct valve change sequences have agreed with previously measured values. Single component octafluorocyclobutane (PFCBa) experiments have been initiated as the lead-in to experiments to measure PFCba and water co-adsorbed on BPL carbon.

II. Pressure Swing Adsorption

Math Modeling

There are three major mathematical modelling issues, (1) axial dispersion, (2) low concentration behavior, and (3) the observed temperature swings in the bed during cycles. Axial dispersion continues to be a critical phenomenon that needs to be accurately described in the model. Currently, we are using a Fickian diffusion model of the form $D_L * (\partial^2 c/\partial z^2)$ to represent and describe dispersion. We have found in a previous study (see GEO-CENTERS Quarterly Report, GC-PR-2194-05, November, 15, 1992) that the value of D_L required to accurately describe single-pass breakthrough data was considerably lower than the value obtained from available literature correlations. Further, this work also shows that the value of D_L is dependent on the "irreversibility" of the isotherm, i.e., the more favorable the isotherm, the greater the deviation between correlated and observed values for D_L.

The mathematical model developed to describe a PSA system uses the measured value for D_L from single-pass breakthrough data. The model results show that for a favorably adsorbed material (CFC-113 on BPL carbon) and a 30 second cycle time, the concentration at the bed inlet ($z = 0$) at the end of the feed step does not reach the feed concentration. This is ph cally incorrect, but it results mathematically as a consequence of using a diffusion model to describe phenomena controlled by hydrodynamics. This result is consistent with the observation of Coppola and LeVan (Chem. Eng. Sci., 38, 1991) that the Fickian model cannot be expected to represent dispersion in systems which exhibit irreversible adsorption equilibrium.

The second major issue is the behavior of the model at low concentrations. Model results for simulations of several adsorbates on several adsorbents have shown that

concentrations oscillate at low values, frequently becoming negative. This is a characteristic of solutions to partial differential equations using orthogonal collocation methods. For many applications these oscillations are not significant, however for very toxic vapors this is not the case. One may attempt to reduce the concentration where these oscillations occur by using more collocation points. However, the time required to achieve a solution goes up proportionally with each point. In addition, for each system, the benefit gained by using another collocation point becomes less and less as each point is added. The combination of the axial dispersion issue and the collocation solution which produces low concentration cycling has led us to consider alternative solution methods. During the next quarter, we will examine the stage model with some unique modifications to account for axial dispersion in hopes of addressing the first two issues.

The third issue is independent of the solution method. Data given in the next section demonstrates the thermal behavior of PSA during normal cycling and establishes the controlling mechanism as air adsorption and desorption. We are currently exploring several approaches to account for the adsorption and desorption of air during a PSA cycle and its subsequent effect on the temperature of the purge air. First, we need to determine how significant this effect is and, if required, put together an isotherm expression which will account for the adsorption behavior of air over many cycles.

Experiments and Apparatus

A series of experiments were performed to determine the mechanism for the magnitude of the temperature cycles measured during PSA operation. The following analysis demonstrates that the observed temperature changes of more than 10 °C cannot result from pressurization and blowdown.

Assuming no adsorption or desorption, the change in temperature from blowdown or pressurization may be approximated by,

$$\Delta T = - \Delta P / (\rho_s C_{ps} + \rho_f C_{pf})$$

where

ΔT = temperature change (K)

ΔP = pressure change (Pa)

ρ_s = solid phase density (g/m^3)

C_{ps} = solid phase heat capacity (J/gK)

ρ_f = fluid phase density (g/m^3)

C_{pf} = fluid phase heat capacity (J/gK)

Assume we wish to calculate the change in temperature for the expansion of air from 505 Kpa to 101 Kpa (5 atm. to 1 atm.). Assume we have a bed filled with activated carbon, where the heat capacity of carbon is 0.25 J/gK, and its packing density is 5.0×10^5 g/m^3. The heat capacity of air is about 0.25 J/gK and its density (from the ideal gas law at 298K) is about 1.2×10^3 g/m^3. Using the identity of 1 Pa = 1 J/m^3, the change in temperature may be calculated as:

$$\Delta T = - 4.04 \times 10^5 / (0.25 * 5.0 \times 10^5 + 0.25 * 1.2 \times 10^3) = - 3.2K$$

If one considers that the walls of the vessel must also be included in the solid phase heat capacity term and the environment can either warm or cool the bed during cycles, the temperature change can easily be less than 1 °C.

Shown in Figure 3 are the results for a series of experiments to demonstrate the accuracy of the calculation performed above. Four experiments were performed, namely; (1) 20%RH air/BPL carbon, (2) dry air/BPL carbon, (3) dry air/glass beads, and (4) He/BPL carbon. The results demonstrate that water adsorption does not affect the magnitude of the temperature swing. Also, compression and decompression are not mainly responsible for the observed 10-15 °C magnitude in the temperature swings. Only when an adsorbent (BPL carbon) and volatile adsorbate (air) are present do the temperature swings exceed more than about 1°C.

Shown in Figures 4, 5, and 6 are the results for series experiments at three different pressures using R-11 and BPL carbon. The conditions used for each experiment are given in Table 1.

Table 1. Conditions for R-11/BPL Carbon PSA Experiments
Bed diameter = 3.77 cm
Bed length = 24 cm
Feed flow rate = 75 SLPM
Feed concentration = 4.0 mg/lit
Product flow rate = 38 SLPM
Cycle time = 30 seconds

The effect of feed pressure observed for the CFC-113/BPL carbon system last quarter seems to hold true for the R-11/BPL system. Consider the product concentration in each

experiment. For the 30 psig experiment, breakthrough begins at about 1250 cycles (675 minutes) and reaches a periodic state concentration of about 1800 mg/m^3. The product concentration in the 45 psig experiment is first measured at about 2700 cycles and reaches a periodic state concentration of about 500 mg/m^3. The results of the 60 psig experiment show that the product concentration begins to breakthrough at about 4100 cycles and reaches a periodic state concentration of about 300 mg/m^3. The 15 psig increase from 30 to 45 psig shows a much larger improvement in the periodic-state product concentration than the same 15 psig increase to 60 psig.

Shown in Figure 7 is the concentration versus time data for the three experiments measured at a location 20 cm into the bed. As with the product concentration analysis, these results demonstrate that increasing the pressure from 30 to 45 psig improves the periodic-state separation considerably more than increasing the pressure from 45 to 60 psig.

The results for feed pressure studies using the R-11/13X molecular sieve are shown in Figures 8, 9, and 10. The conditions used for these experiments are given in Table 2.

Table 2. Conditions for R-11/13X Molecular Sieve PSA Experiments
Bed diameter = 3.77 cm
Bed length = 24 cm
Feed flow rate = 75 SLPM
Feed concentration = 4.0 mg/lit
Product flow rate = 38 SLPM
Cycle time = 30 seconds

These results are different than for the R-11/BPL carbon system. The pressure increase from 35 to 45 psig shows almost no improvement in the either the product breakthrough time or product periodic-state concentration. However, the experiment at 62 psig shows a large improvement in both areas. Figure 11 is a plot of the concentration versus time at 20cm for each of the three experiments. These results clearly show that the performance at 35 and 45 psig are almost the same, while the performance at 62 psig is about twice as good based on both breakthrough time and periodic-state concentration.

Figure 12 is a plot of the 20-cm port concentrations for the three R-11/BPL carbon experiments and the three R-11/13X molecular sieve experiments. The breakthrough time for the 30 psig BPL carbon system is longer than any of the 13X experiments, including the 62 psig experiment. The breakthrough times for the 45 psig and 60 psig BPL experiments are about 7 times longer than the corresponding 13X experiments. However, notice that the periodic-state concentrations for BPL and 13X at 45 psig and 60 psig are approximately the same.

III. Data Acquisition and Control

PSA temperature profile data was collected for various combinations of bed sizes, adsorbents and adsorbates. A program was developed to examine all the data files of a given experiment and generate a plot of the maximum temperature swings for each point in the bed versus time. Examination of this data allowed correlations to be made that demonstrated that changes in the adsorption capacity within the bed could be tracked by temperature. Further investigations will be made into details surrounding the shape of the temperature and temperature differential curves.

Construction of the TSA power control hardware is in progress. The design of the power monitoring hardware was modified to provide protection to external devices connected to the power controller. The voltage measurement is supplied via an opto-isolator and amplifier providing a 0-5 V signal representing the 0-150 VDC power supply output. Current measurement is now supplied by a Hal effect current loop and associated amplifiers providing a 0-5 V signal representing the 0-20 A output of the power supply. Both these outputs are completely isolated from potentially dangerous and damaging voltages and referenced to equipment ground.

In the process of taking preliminary temperature data from the interim TSA system, it was found that common mode signals repeatedly exceeded limits of the data acquisition system. At first thermocouples were installed which were grounded, sending large common mode voltages to the data acquisition board. This destroyed the multiplexor on the board and required repair by the manufacturer. Later, insulated non-grounded thermocouples were used, however, the 1-2 MΩ insulation provided was inadequate to protect the board. It was decided to purchase commercially available 5B modules which provide an optically-isolated (1500VRMS) 0-5 V signal representing the thermocouple output. These modules, in combination with the protected power monitoring equipment, should allow data acquisition without risk to the measuring equipment.

IV. Other

An invited paper entitled " PSA for Air Purification : Experiments and Modeling " was written and presented at the Fourth International Conference on the Fundamentals of Adsorption in Kyoto, Japan on May 18, 1992.

A patent was submitted entitled "PSA Performance Monitor" by David E. Tevault, David K. Friday, John J. Mahle, Leonard C. Buettner, and Charles Dawson.

FIGURE 1. Isotherm Data for R-11 on BPL Carbon at 25, 50 and 75C

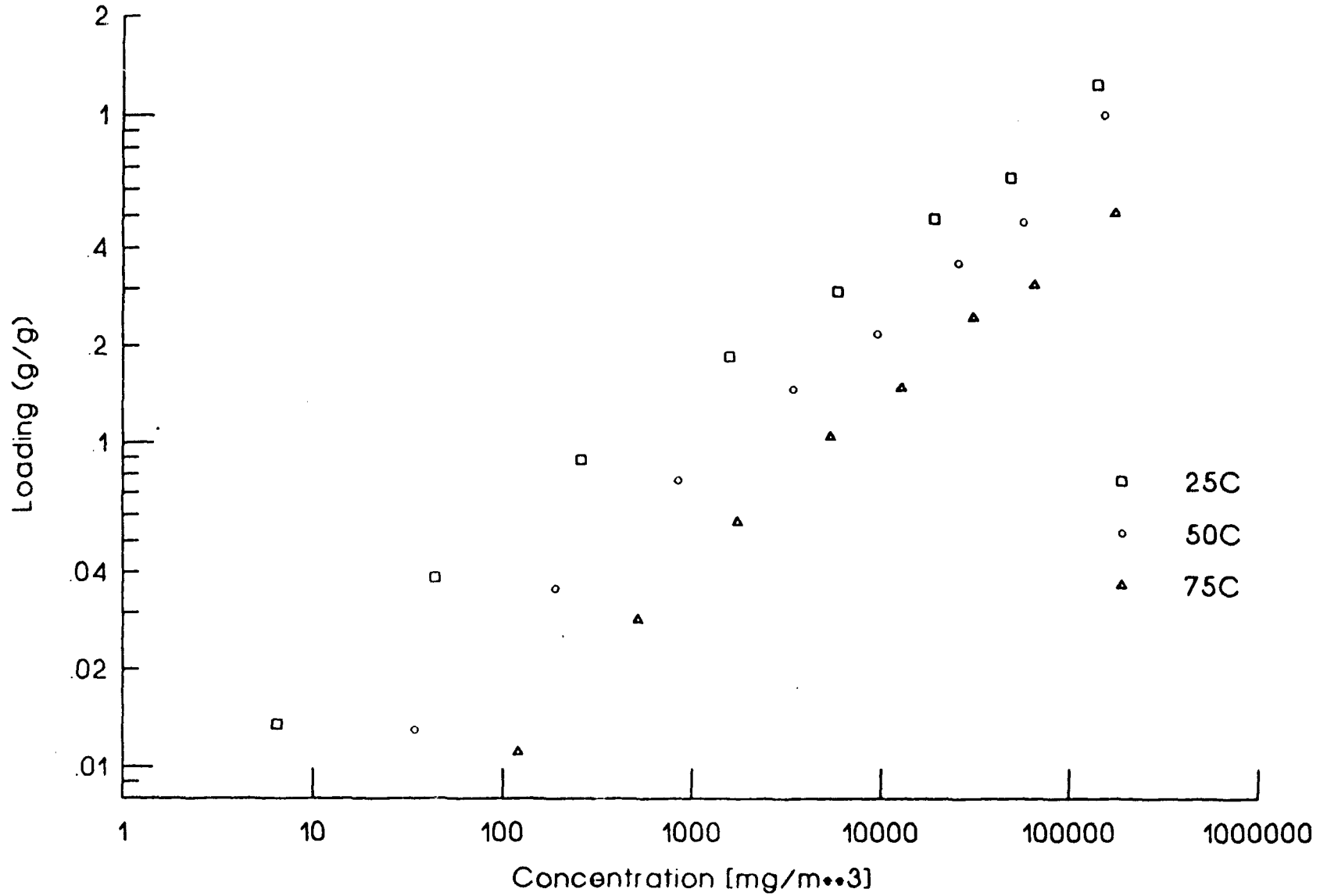

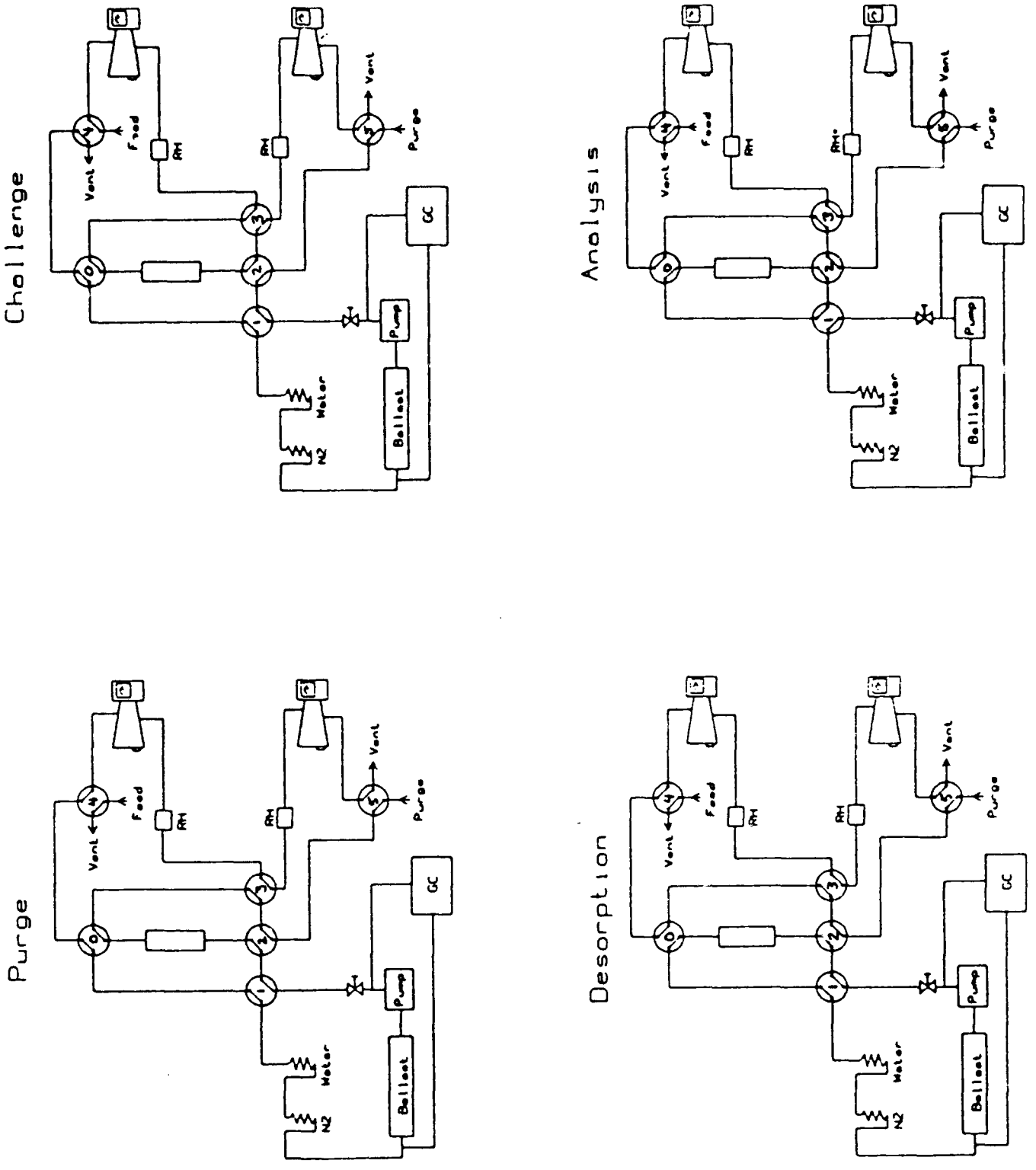

Figure 2. Multicomponent Isotherm Apparatus

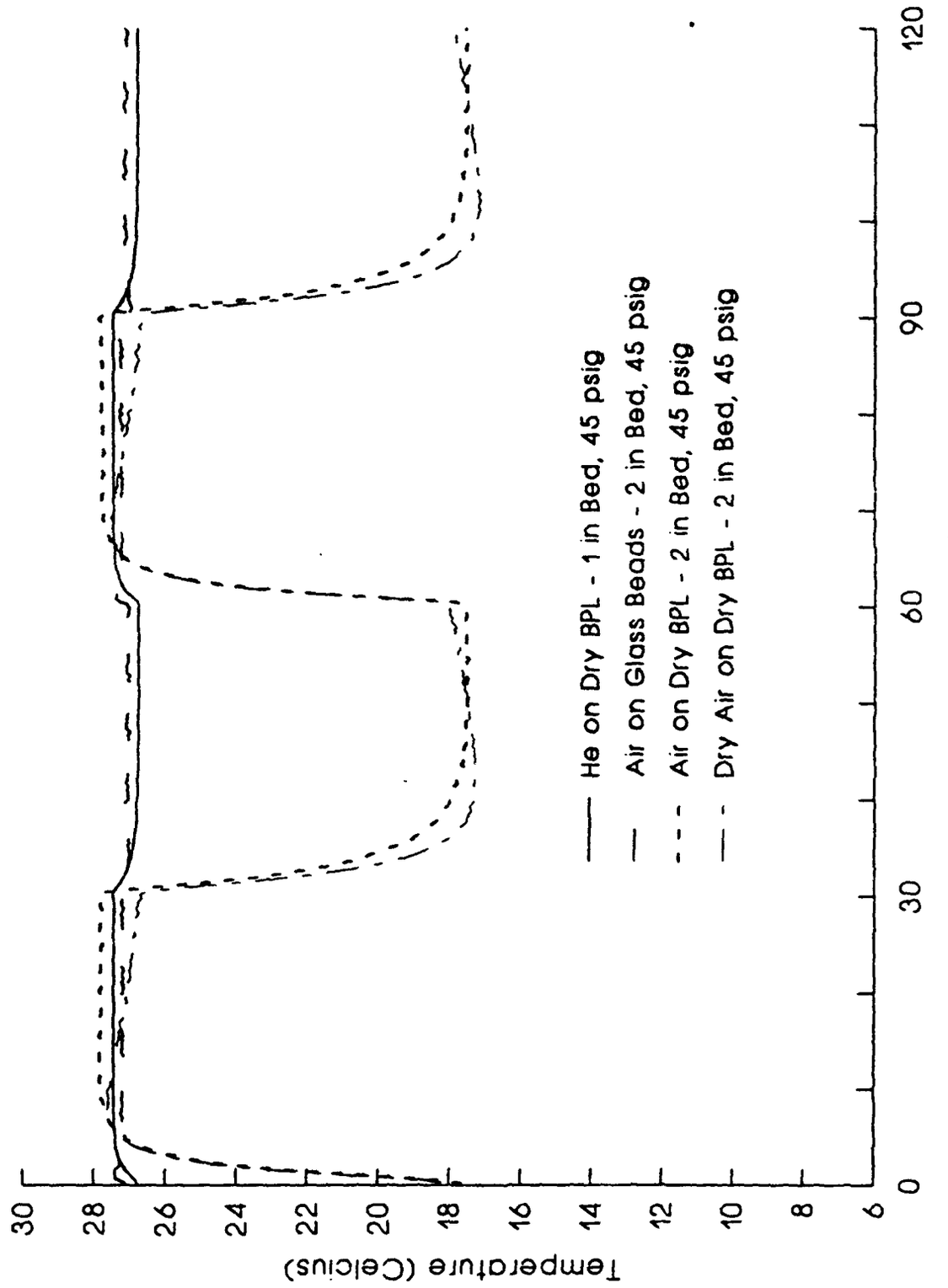

Figure 3. PSA Bed Temperature Profiles at 15 cm

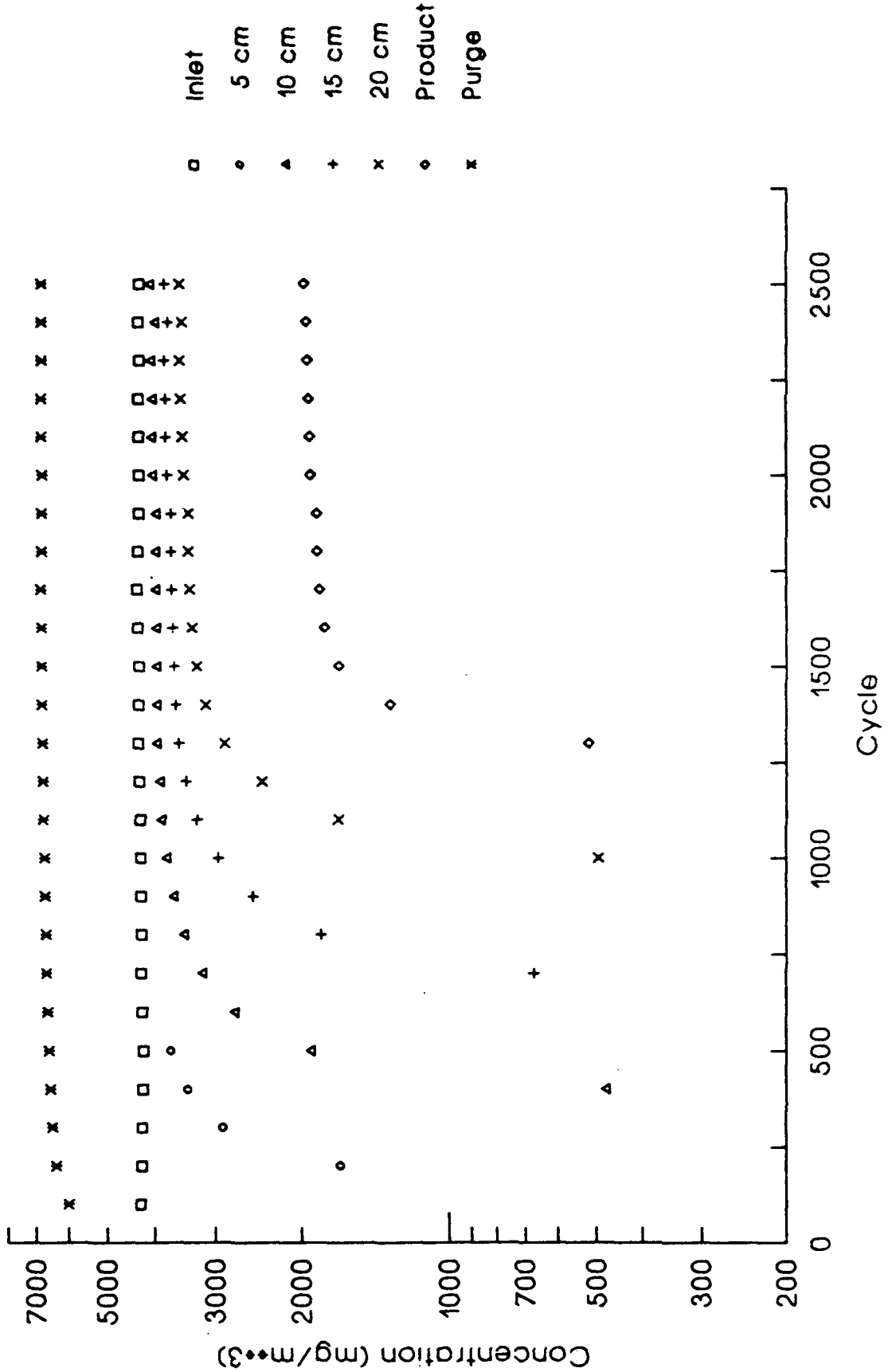

Figure 4. PSA Bed Profile for R11 on BPL Carbon
Bed Pressure at 30 psig

Figure 5. PSA Bed Profile for R11 on BPL Carbon
Bed Pressure at 45 psig

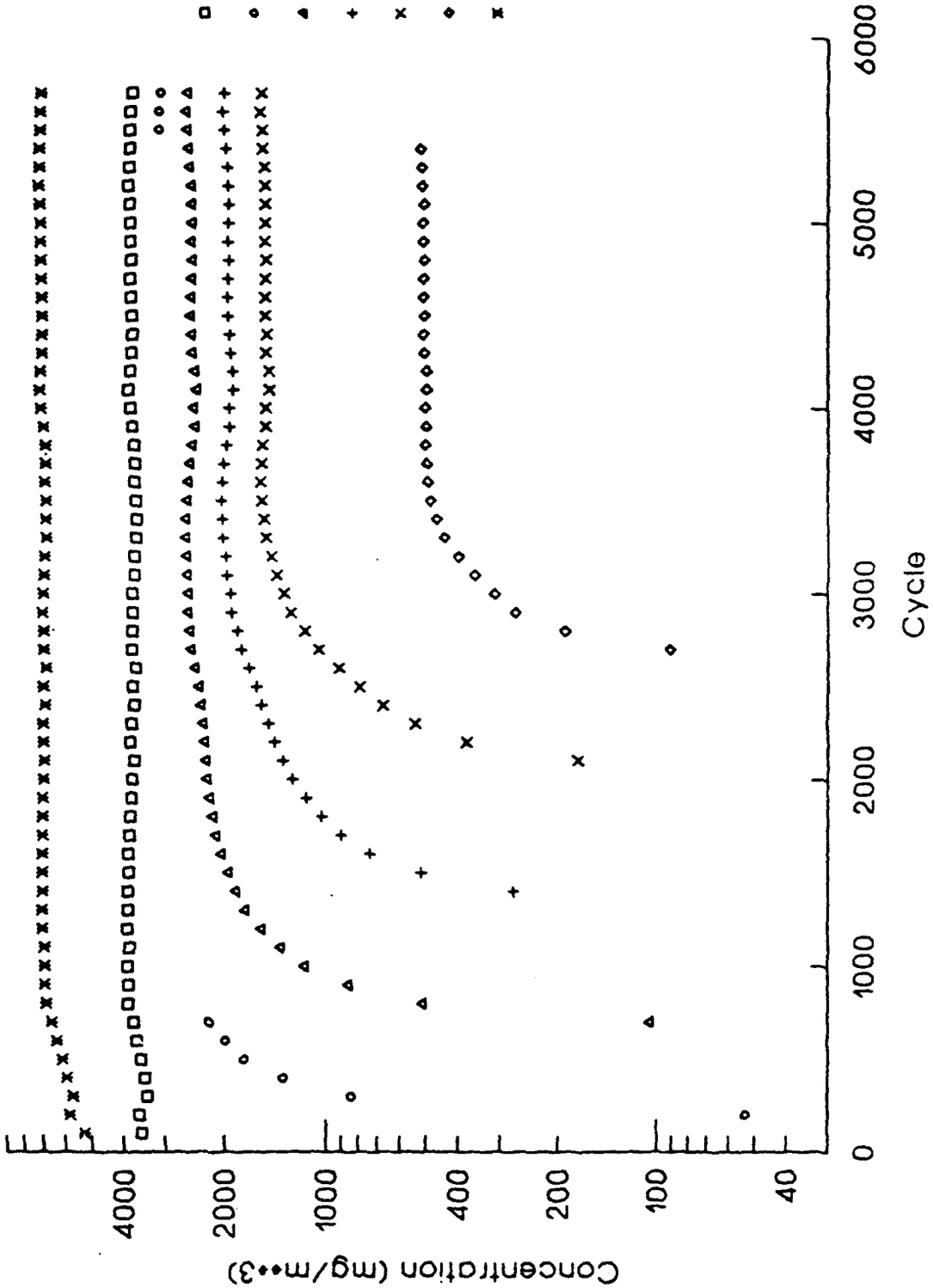

Figure 6. PSA Bed Profile for R11 on BPL Carbon
Bed Pressure at 60 psig

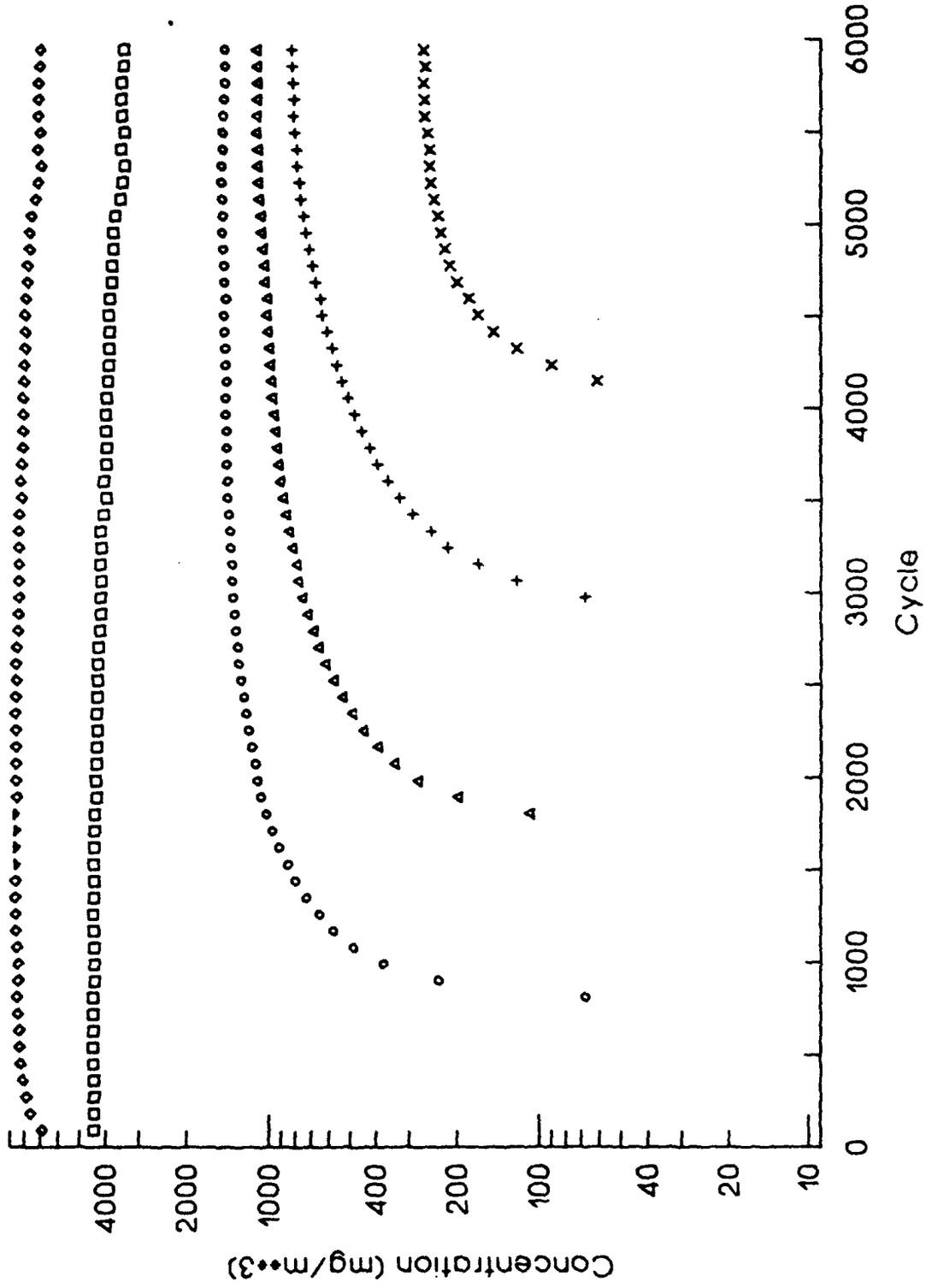

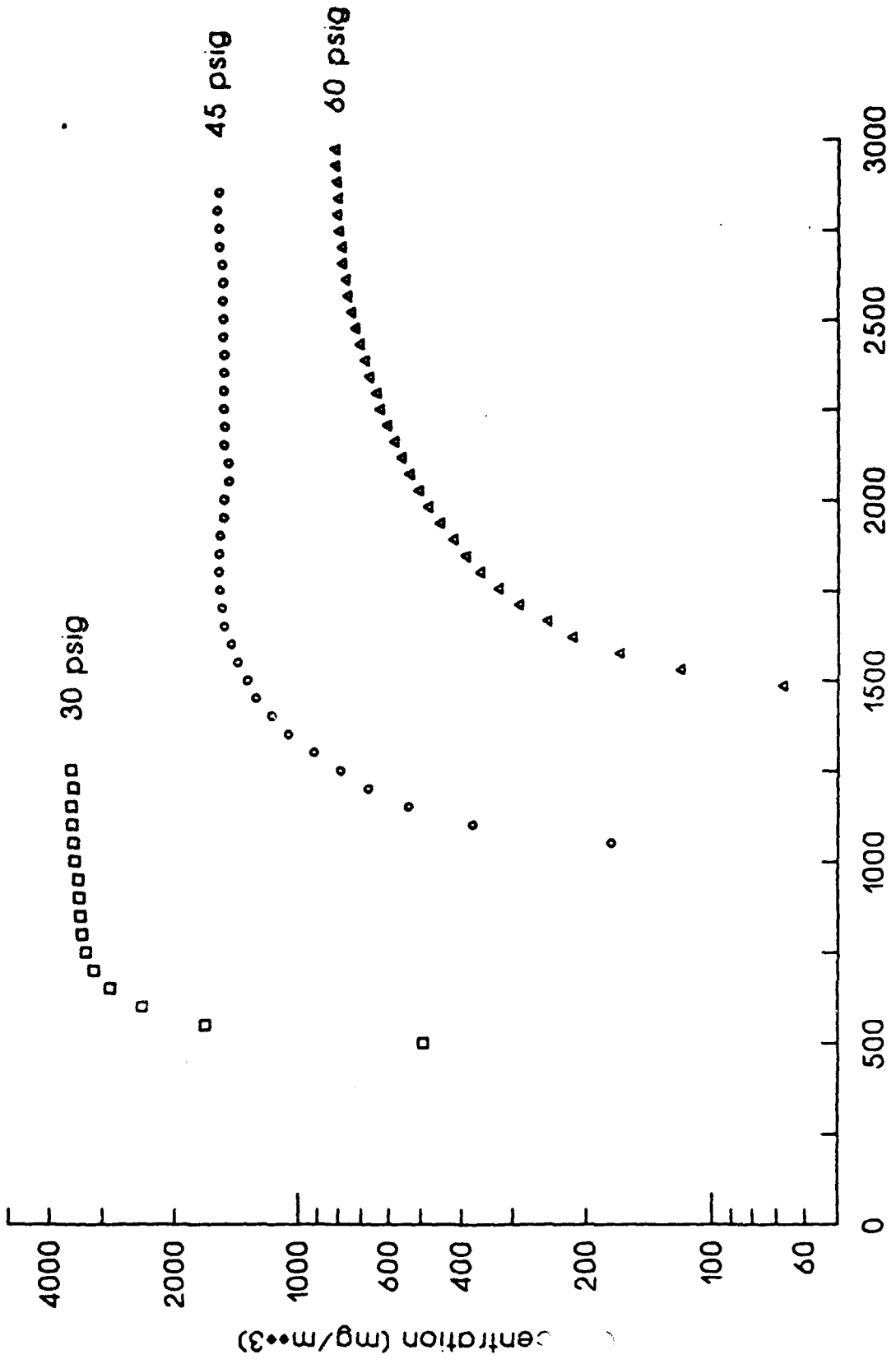

Figure 7. Transient Profiles at 20 cm for R11 on BPL Carbon Bed Pressure at 30, 45 and 60 psig

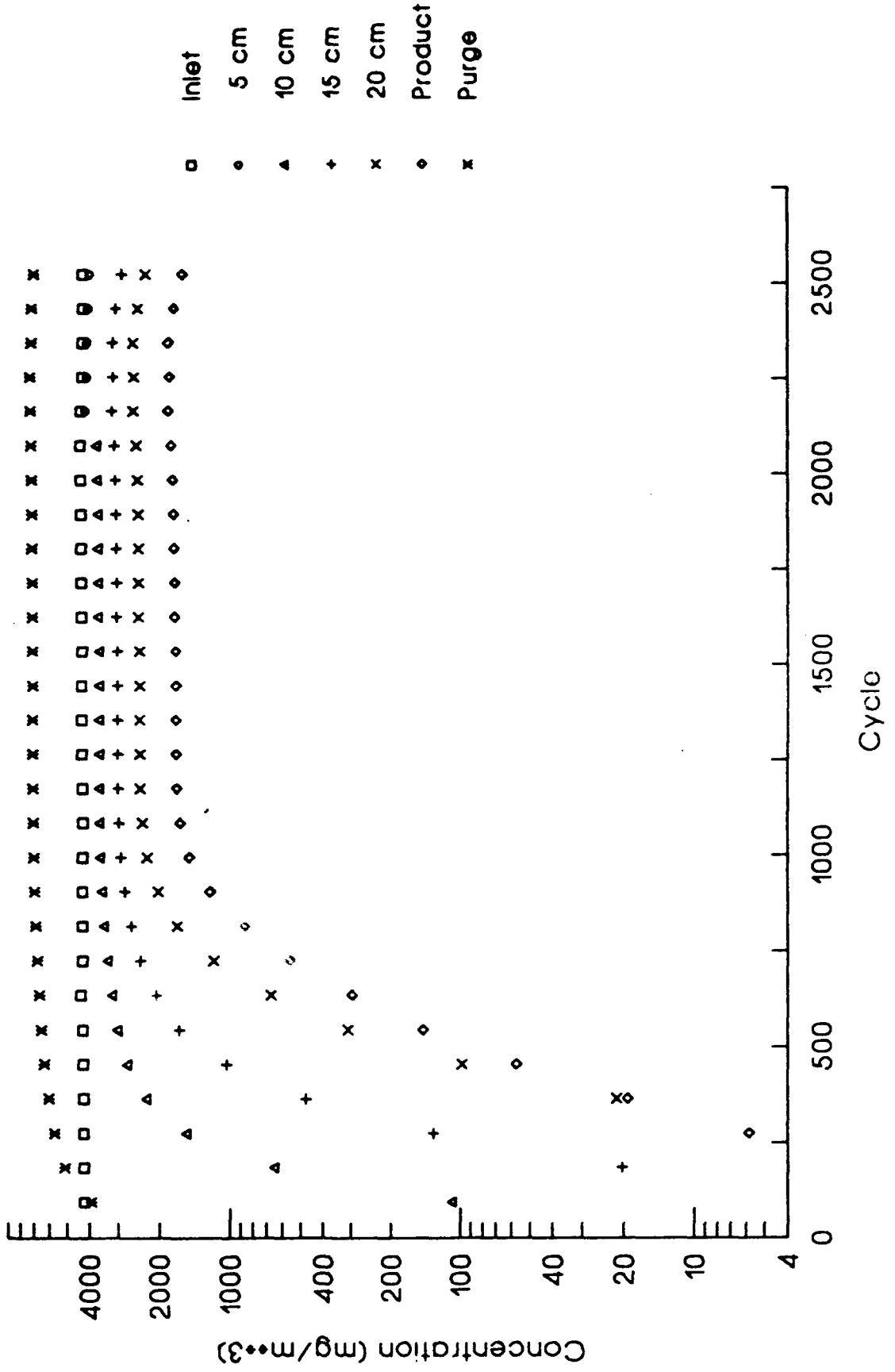

Figure 8. PSA Profile for R11 on 13X Mol Sieve
Bed Pressure at 35 psig

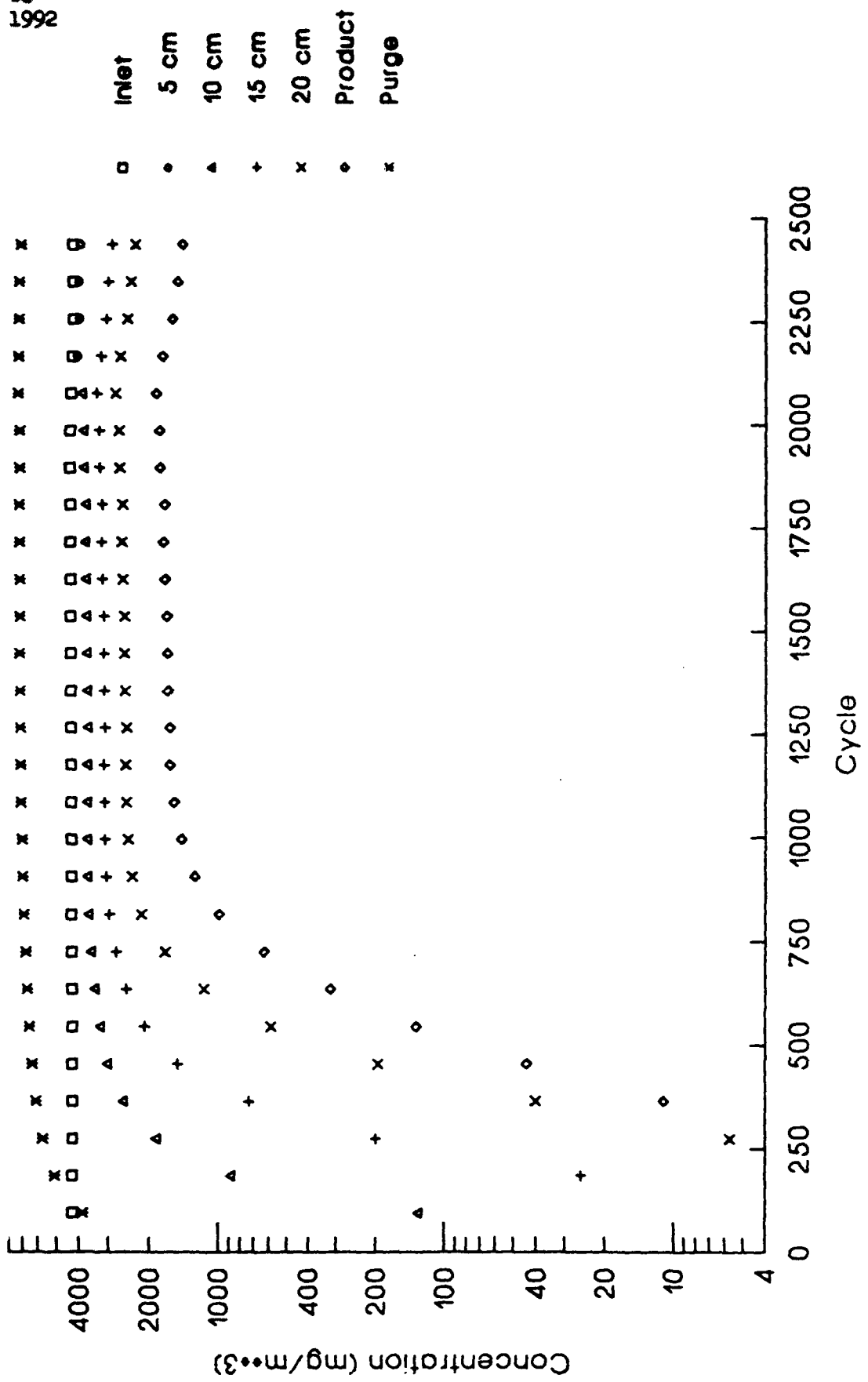

Figure 9. PSA Profile for R11 on 13X Mol Sieve
Bed Pressure at 45 psig

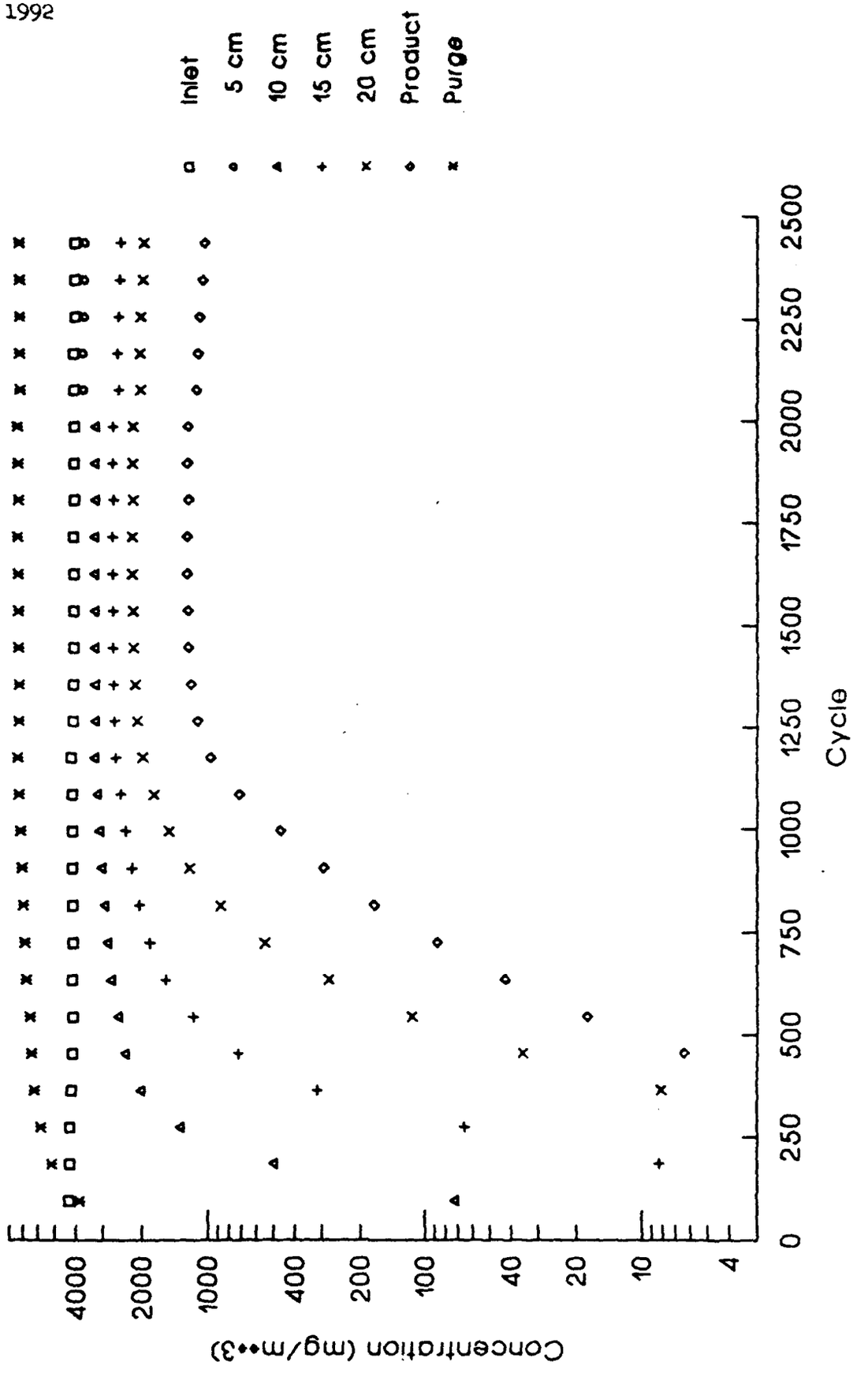

Figure 10. PSA Profile for R11 on 13X Mol Sieve
Bed Pressure at 62 psig

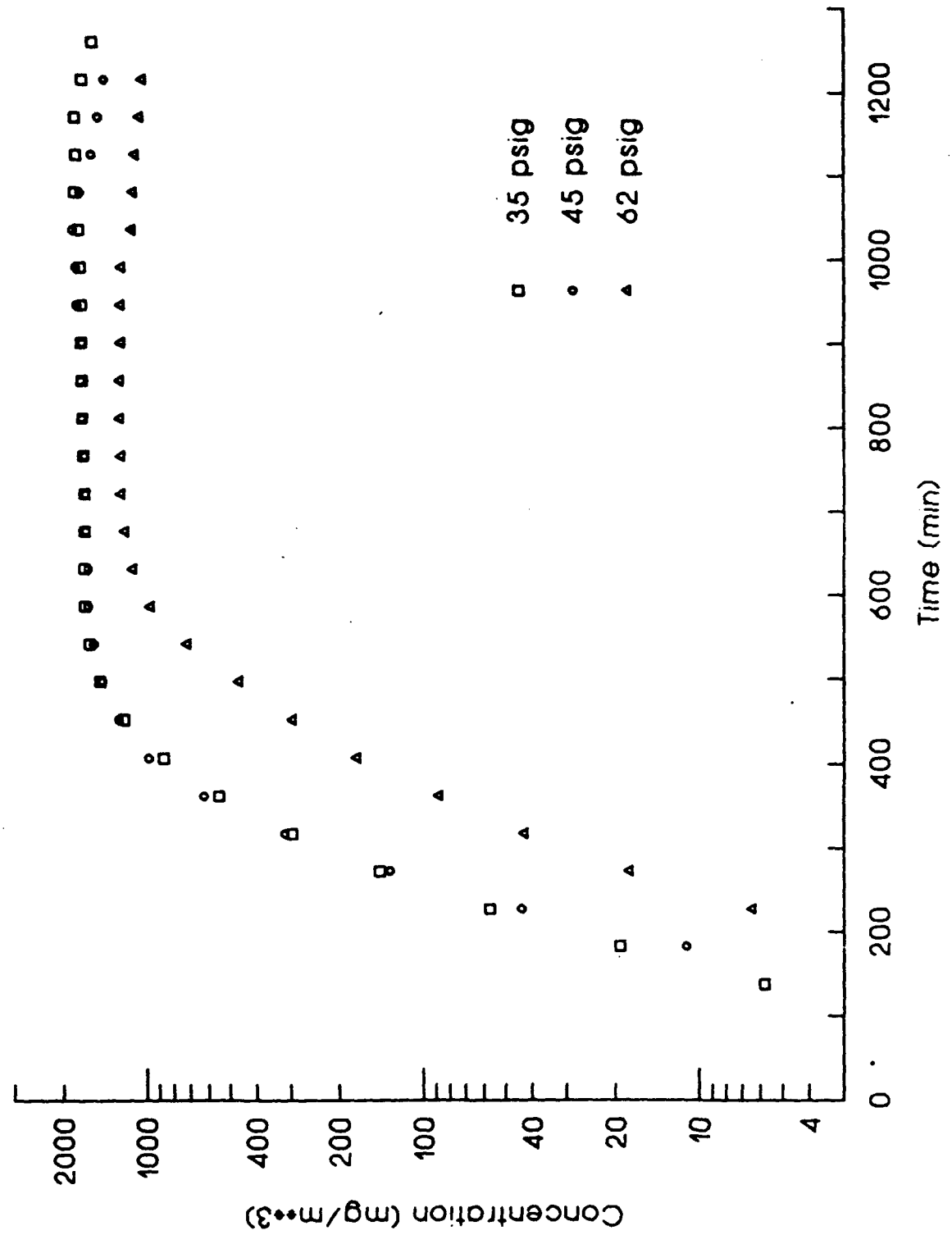

Figure 11. Transient Profiles at 20 cm for R11 on 13X Molecular Sieve Bed Pressure at 35, 45 and 62 psig

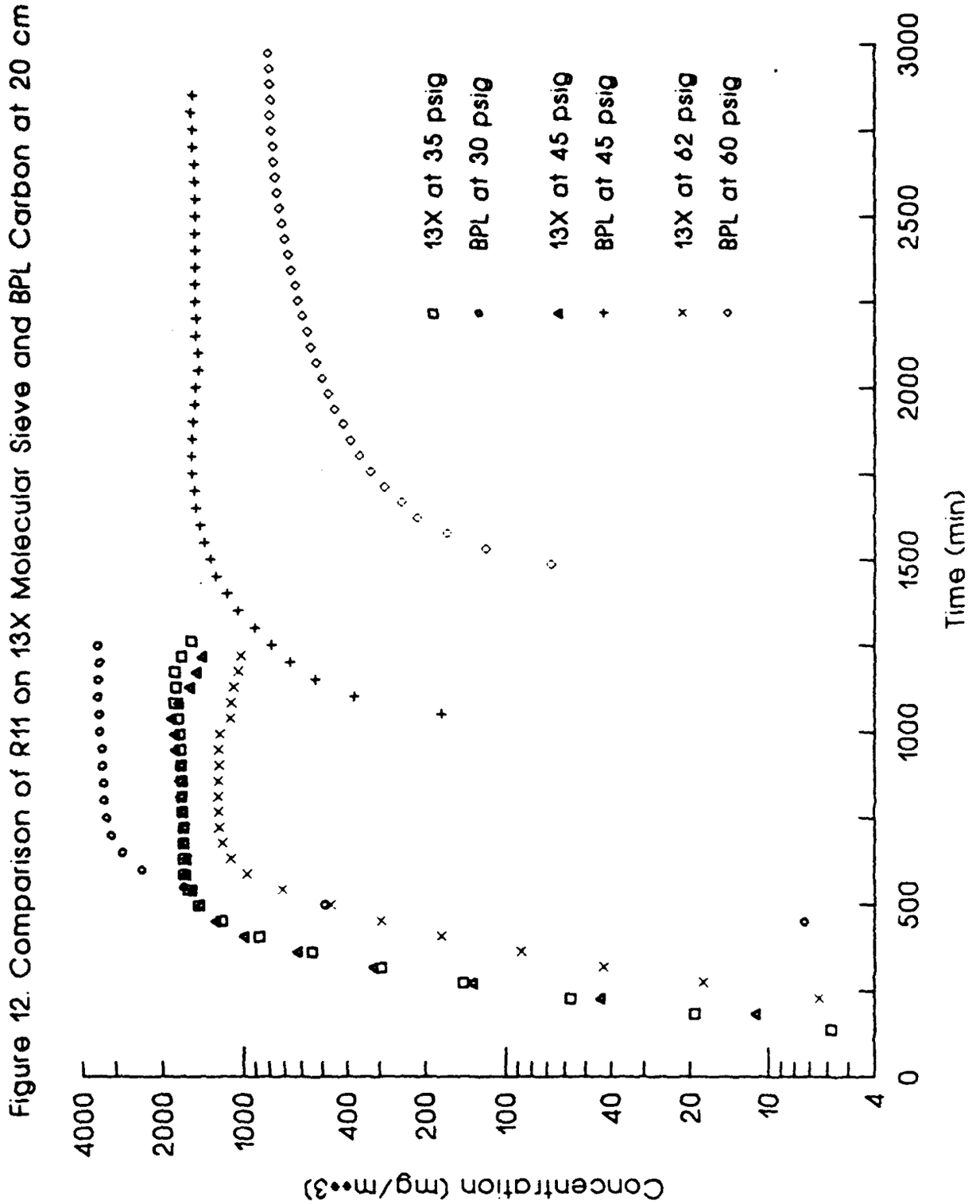
Figure 12. Comparison of R11 on 13X Molecular Sieve and BPL Carbon at 20 cm
Concentration (mg/m**3)
4000
2000
1000
400
200
100
40
20
10
4
0
500
1000
1500
2000
2500
3000
Time (min)
13X at 35 psig
BPL at 30 psig
13X at 45 psig
BPL at 45 psig
13X at 62 psig
BPL at 60 psig

Blank

QUARTERLY PROGRESS REPORT

GC-PR-2194-09

REPORTING PERIOD: 8/1/92 - 10/31/92

REPORTING DATE: 11/15/92

CONTRACT NUMBER: DAAA15-90-C-1056

CONTRACT TITLE: Improved Filtration Materials and Modeling

I. Adsorption Equilibria

Single Component Measurements and Apparatus

In the last quarterly report, unusually high loadings were measured for trichlorofluoromethane (R-11) on BPL carbon at concentrations above about 10,000 mg/m^3. We have determined that these high loadings are not real, rather they are a result of the unusual response of R-11 in a Flame Ionization Detector (FID). R-11 calibration response curves were generated using a system which reliably introduces known volumes of vapor at a known temperature and pressure into the closed-loop system. The result of the calibration effort is shown in Figure 1. For every chemical vapor we have studied to date, the detector response tends to become less sensitive at higher concentrations resulting in a concave downward response curve. Figure 1 indicates that for R-11, the response actually becomes more sensitive. The high loadings originally calculated for R-11 can now be attributed to the non-linear, concave up, FID response curve.

The explanation for the high R-11 loadings follows. Before each isotherm point is determined, the system is placed in the bypass mode, i.e., flow is around, not through the adsorbent. R-11 is injected into the system and the amount injected is calculated using the R-11 calibration curve. Since we were using a linear response curve, we were calculating that much larger amounts of R-11 were injected into the system than were actually injected. This in turn resulted in the unrealistic loadings calculated for R-11.

The laboratory data measured to this point using 13X molecular sieve as the absorbent has been obtained with Davison 13X. Systems designed by two contractors have used UOP 13X. PSA data measured using the two different 13X adsorbents showed dramatically different performances (PSA data will be shown later). These measured differences were suspected to result from different adsorption equilibria behavior of R-11 on each adsorbent. The results shown in Figure 2 indicate that the capacity of the UOP 13X is about 2 times greater than the Davison 13X over the range of concentrations used in PSA experiments. Therefore, it was concluded that the better separation and breakthrough performance measured for the UOP 13X was mainly due to the isotherm behavior.

Multicomponent Measurements and Apparatus

Multicomponent isotherms for perfluorocyclobutane (PFCBa) and water on BPL carbon at 298 K have been completed. Several significant improvements to the system were made to insure reproducible and accurate results. These include a new bed design which allows the bed to be heated to high desorption temperatures without any leaks forming and an experimental procedure to insure reproducible results which includes both daily calibration checks and a periodic change of the adsorbent bed.

The first phase of the multicomponent study is to verify the experimental system by measuring single component data for each chemical. Figures 3 and 4 show single component data for PFCBa and water, respectively, measured using the multicomponent system compared to the single component data for each chemical measured using the single component isotherm apparatus. Both the water and PFCBa measurements are consistent

using both systems, indicating that the multicomponent system is operating correctly.

Shown in Figure 5 are PFCBa isotherms measured at 25C under dry, 40% RH, 60% RH, and 80% RH conditions. The effect of co-adsorbed water is obvious from these data. For example, at a PFCBa vapor-phase concentration of 1,000 mg/m^3, the loading of PFCBa at 80% RH is only 0.0006 g/g, or about 100 times less than the loading of PFCBa under dry conditions. Even at 60% RH, the PFCBa loading is less than 1/5 of the dry PFCBa loading. These data demonstrate that PFCBa and similar compounds will be severely affected by the presence of adsorbed water. Systems which are designed to protect against these compounds must either reduce the RH to near 40% or use an adsorbent which performs better in humid conditions.

More information about the PFCBa-water adsorption behavior on BPL carbon can be obtained by measuring the amount of water adsorbed as a function of PFCBa and RH. Shown in Figure 6 are the water loadings versus vapor-phase PFCBa concentration at 40%, 60% and 80% RH. These data show that at 80% RH (triangles), the PFCBa is not able to displace the adsorbed water, even when the PFCBa concentration is increased above 10,000 mg/m^3. In addition, the water loadings measured for the 80% RH experiments are very close to the pure component water loadings (see Figure 4). Based on these data and those presented in Figure 5, it is clear that adsorbed water is greatly reducing the adsorption capacity for PFCBa. At 40% RH (boxes), there is also no obvious change in the water loading over about three orders of magnitude of PFCBa concentrations. However, since the PFCBa loadings are not very different from their pure component values, it is clear that at 40% RH and the range of PFCBa concentrations used, that each chemical is acting nearly

independent of the other. At 60% RH (circles), measured water loadings reveal an interesting situation. At low PFCBa concentrations (below 100 mg/m$^{3)}$, the water loadings are close the pure component water loading at 60% RH. From Figure 5, low PFCBa concentrations measured at 60% RH result in PFCBa loadings more than order of magnitude below the corresponding PFCBa loadings under dry conditions. As the PFCBa concentration is increased, Figure 6 shows that water is being displaced and near a PFCBa concentration of 10,000 mg/m^3, the water loading is only about 1/3 of its pure component value. This also reflected in the PFCBa loadings from Figure 5, where at high PFCBa concentrations and 60% RH, PFCBa loadings are nearly 1/2 of their pure component values.

II. Pressure Swing Adsorption

Experiments and Apparatus

In support of the mathematical modeling effort, lab-scale experiments are being performed under the identical conditions as full-scale experiments. During the course of this effort significant differences in PSA system performance were observed between lab-scale and full-scale units. This lead to the discovery that the 13X molecular sieve used in the lab-scale experiments (from Davison) was from a different vendor than the 13X used in the full-scale experiments (from UOP). Samples of 13X adsorbent from each vendor were used to measure the single component isotherms shown in Figure 2.

Shown in Figure 7 and Figure 8 are the results of PSA experiments using the operating and initial conditions given below and the 13X molecular sieve adsorbent from Davison and UOP.

Table 1. Base-Case Conditions for R-22/BPL Carbon Experiments

Feed RH:	3-5% @ 15 psig
Feed Flow:	36 SLPM
Feed Temperature:	298 K
Feed Pressure:	35-40 psig
Feed Concentration:	4.0 mg/lit @ 15 psig
Purge Flow:	18 SLPM
Cycle Time:	30 sec. (1/2 cycle = 15 sec.)
Bed Diameter:	2.57 cm
Bed Depth:	24 cm

Both the Davison 13X used to produce the results in Figure 7 and the UOP 13X used to produce the results shown in Figure 8 were dried at 350C overnight prior to use. The differences in performance between the two sources of adsorbent are dramatic. For the Davison 13X, there is almost an immediate breakthrough of R-22 at 10 cm, while for the UOP 13X, breakthrough at 10 cm does not occur until about 600 cycles (300 minutes). The breakthrough of R-22 in the product for Davison 13X occurs at about 450 cycles or 225 minutes. The breakthrough of R-22 for the UOP 13X does not occur until about 5500 cycles or 2775 minutes. These data demonstrate the importance of understanding and characterizing the adsorbent(s) to be used in a PSA system. Simply by using a different source of the same adsorbent, the breakthrough time was improved by more than 40 hours! Note also that the periodic-state concentration at 20 cm and in the product is about four to five times greater using the Davison 13X than the UOP 13X.

The dried UOP 13X performance shown in Figure 8 was much better (longer

breakthrough times and better separation) than the full-scale results. Since the full-scale data was obtained using the UOP 13X straight from the container, it was thought that residual adsorbed water could be the reason. To test this hypothesis, a third experiment using the conditions in Table 1 was performed using UOP 13X directly from the container. The results of this experiment are shown in Figure 9. The change in system performance is again dramatic. The breakthrough time for the product concentration for the UOP 13X as received is about 1/2 of the dried UOP. In general, it appears that the breakthrough time at each bed depth for the as received UOP 13X is approximately 1/2 of that measured using the dried UOP 13X.

The effect of water on the performance of a PSA system using 13X molecular sieve is obvious from the results shown in Figure 9. To further investigate the behavior of water in PSA systems, experiments were performed using only water as the feed chemical and measuring the water concentration using a Thermal Conductivity Detector (TCD). Shown in Figure 10 are the results for an experiment using the conditions given in Table 2.

Table 2. Conditions for Water/BPL PSA Experiments

Feed RH:	80% @ 45 psig
Feed Flow:	80 SLPM
Feed Temperature:	298 K
Feed Pressure:	35-40 psig
Feed Concentration:	292 K dew point
Purge Flow:	40 SLPM
Cycle Time:	60 sec. (1/2 cycle = 30 sec.)
Bed Diameter:	3.77 cm
Bed Depth:	25 cm

The results in Figure 10 demonstrate that water quickly reaches a periodic-state with BPL carbon and that the separation factor (ratio of feed concentration to the product concentration) at periodic state is more than ten. Shown in Figure 11 are the results from Figure 10 plotted as RH versus bed length at periodic state. These show that the feed RH is reduced below 40% somewhere between 5 and 10 cm of bed depth. If we refer back to the results given in Figure 5, one can use the results of Figure 11 to infer that the first 5 -7 cm of BPL will not provide any protection against PFCBa. However, it is also clear that BPL carbon dries the air as it passes through the system.

A second experiment using BPL carbon was performed using a feed concentration of water which corresponded to a dew point of about 274 K (RH = 20%) at pressure. The results of this experiment are shown in Figure 12. Once again the system reaches periodic-state very quickly with a clearly measurable level of separation. Figure 13 shows the RH versus bed depth plot for these data. Notice that the product RH is around 2%, corresponding to dew point of about 253K indicating that BPL carbon can produce dry air.

The conditions given in Table 2 were used for the water/UOP 13X molecular sieve experiments, except the feed pressure was 50 psig. These results are shown in Figure 14. There is no detectable water (below about 2 mg/m^3) even at 5 cm into the bed for a purge to product flow rate ratio of 1.0. At 2500 cycles into the experiment, the purge flow was changed to 20 SLPM, corresponding to a purge to product ratio of 0.5. About 500 cycles after the change, the 15 cm port began breakthrough. Eventually the bed became saturated with water. At about 4100 cycles the purge flow was increased to 30 SLPM, corresponding to a purge to product ratio of 0.6. The bed began to quickly clean up. Approximately 2500

cycles following the change, the only measurable water vapor concentration was at the 10 cm port. These results demonstrate the extreme sensitivity of water/13X systems to the purge to product ratio. Small changes in the purge flow rate produced dramatically different performances with respect to water concentration, which can in turn produce dramatically different performances against weakly adsorbed chemical threat vapors.

Because of the importance of water in the system and the need to streamline the multicomponent adsorption equilibria effort, a full parametric study of the behavior of water on both adsorbents will be conducted next quarter. In addition, 4-step experiments will be performed to attempt to simulate full-scale 4 step experiments to provide valuable scale-up information.

III. Data Acquisition and Control

Temperature Swing Adsorption (TSA) system power control hardware is complete. The power monitoring hardware was tested and calibrated. The interim TSA software was completed and tested with the hardware. Power control PID loops were tuned to the system and hydrocarbon analyzers were added to the system to measure chemical concentrations. Initial data was taken using CFC-113 to verify system performance. It was decided that the system was ready for use. A subsequent test without chemical resulted in an uncommanded thermal excursion. The control software was re-examined and minor modifications made. The system is now fully operational.

The PSA temperature profiler was modified to take unattended temperature profiles at periodic intervals. In addition, thermocouples were calibrated in preparation for future

experiments.

A paper entitled "Designing Experimental Control and Data Acquisition for Air Purification Systems " was presented at the Summit for Scientific Computing in Washington DC.

IV. Other

Temperature Swing Adsorption

A lab-scale TSA system has been fabricated and initial experiments have been conducted. This system uses direct electrical heating of the adsorbent bed by applying a controlled potential across the length of the bed. The adsorbent, in this case BPL carbon, is heated as a controlled amount of power is passed through the bed. The cycle operates as follows :

1. CFC-113 at 5.0 mg/lit is fed to the bottom of the bed at 75 SLPM for 5 minutes.
2. Valves are changed to feed 15 SLPM of clean purge to the top of the bed.
3. 500 watts of power is introduced to the bed for 30 seconds.
4. Power is turned off and 15 SLPM of purge is fed to the top of the bed for another 4 minutes and 30 seconds.

Shown in Figures 15 and 16 are some initial results from a simulated two-bed TSA cycle using a single bed. In-bed temperature probes were placed at 5, 10, and 15 cm from the bottom (feed end) of the bed. Figure 15 shows the temperatures within the bed during four full cycles and the associated power input. Figure 16 shows the same temperature profiles

compared to the concentrations of CFC-113 as measured by a hydrocarbon analyzer connected to the top (product, "clean end") and bottom (purge, feed, "dirty end") flow streams. These results indicate that the bed does not cool down to near ambient temperature before the start of the next feed step. As Figure 16 shows, the maximum concentration of CFC-113 measured in the product appears to be increasing from cycle to cycle. This occurs because the net bed temperature seems to be increasing slightly. Other important points to note are that the power control seems to be excellent and the amount of power required to heat the bed to 100C is relatively small.

Figure 1 R-11 Calibration Data

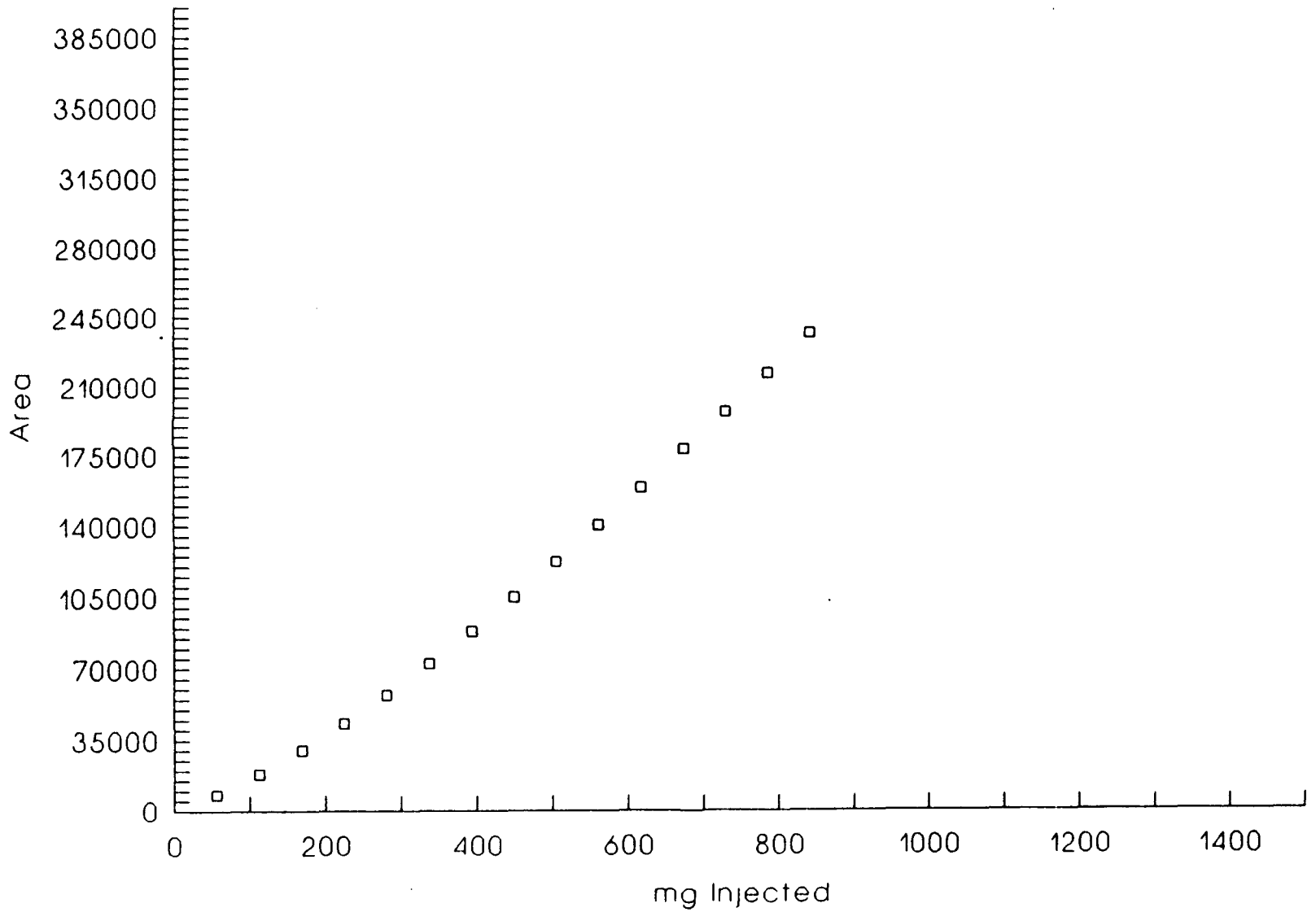

Figure 2 Isotherm Data for R-22 on Mol Seives at 25C

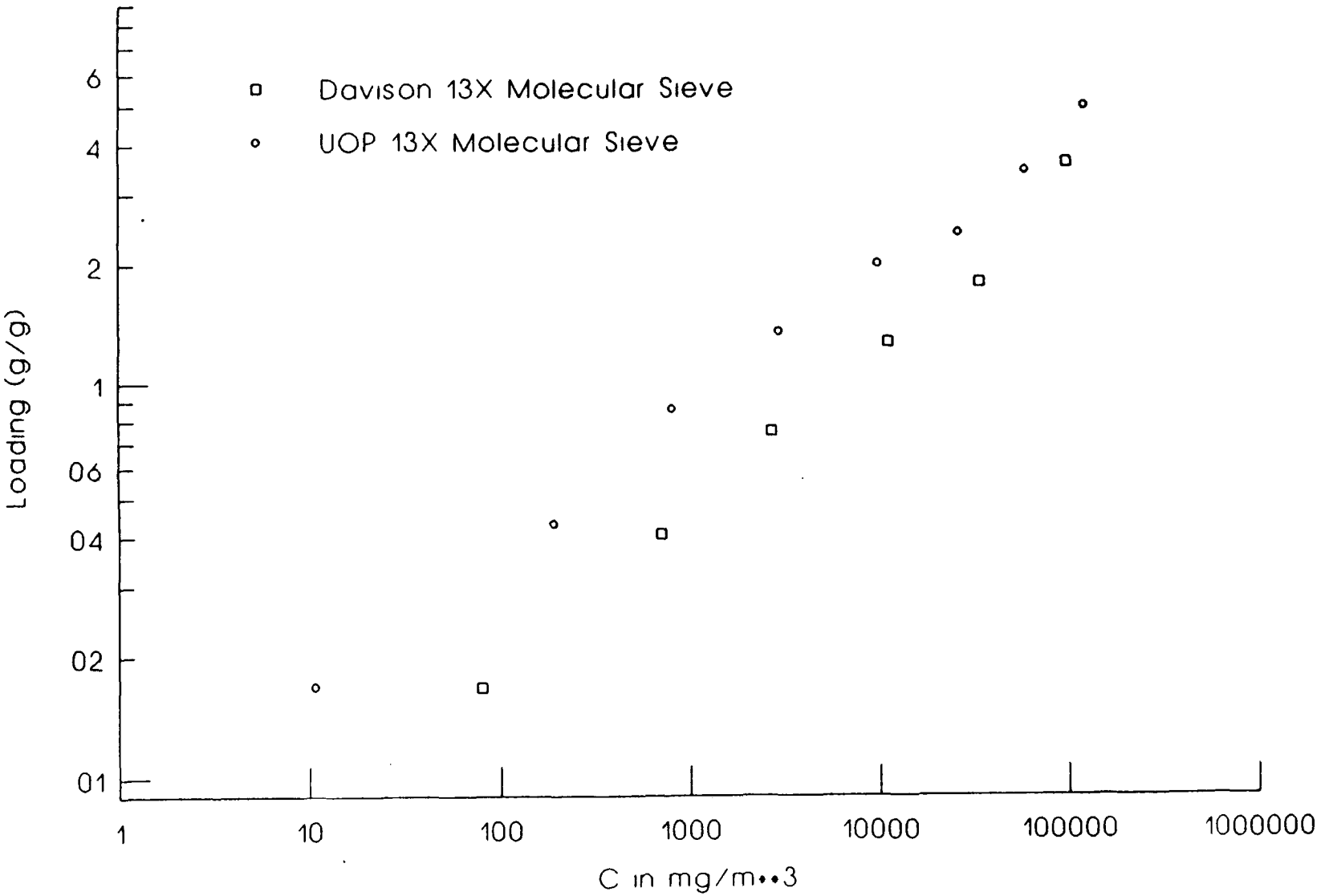

Figure 3. Comparison of Isotherm Data for PFCBa on 12x30 BPL Carbon Measured Using Single and Multicomponent Systems

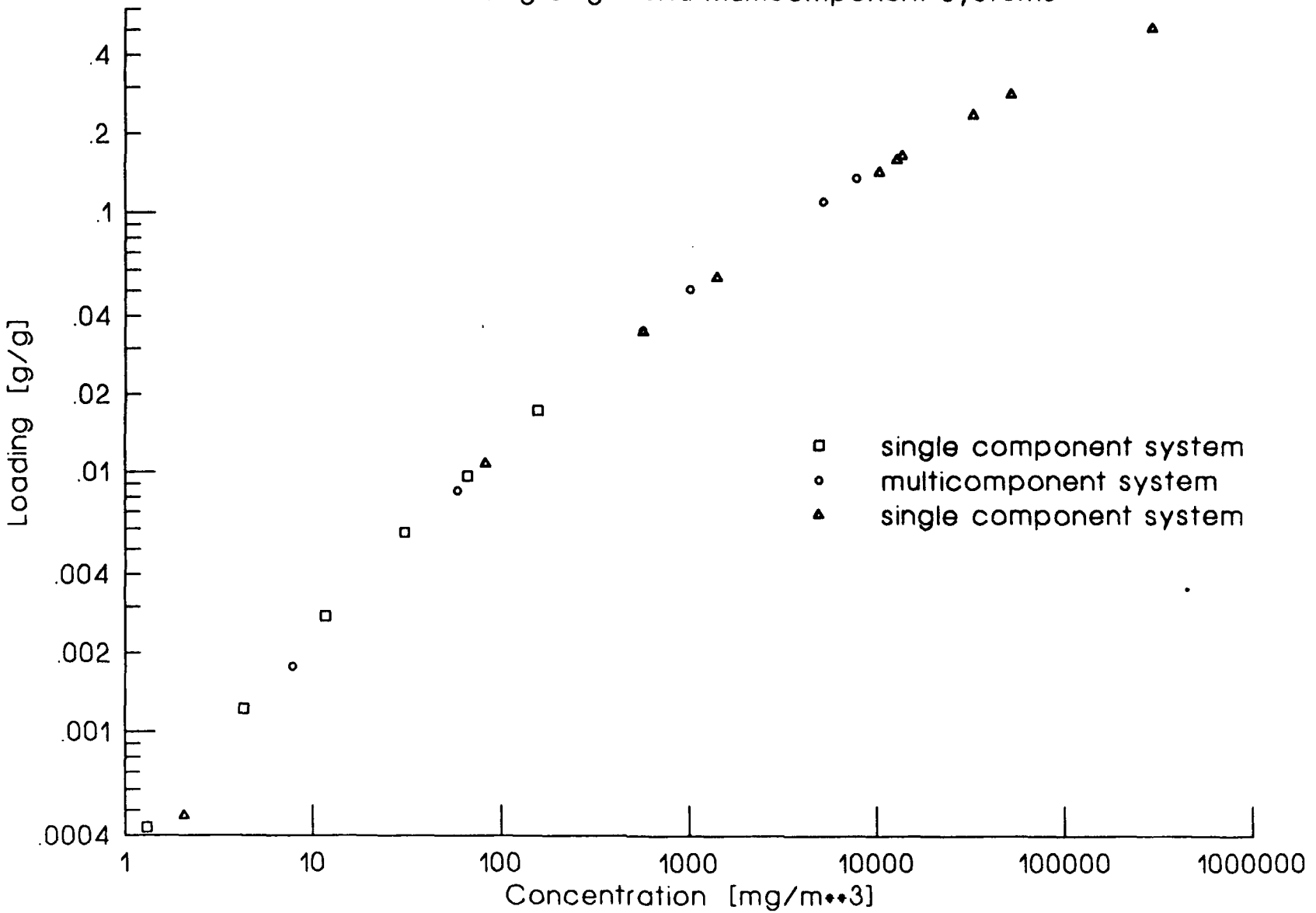

Figure 4. Water Isotherms for BPL Carbon Using Single Component and Multicomponent Systems

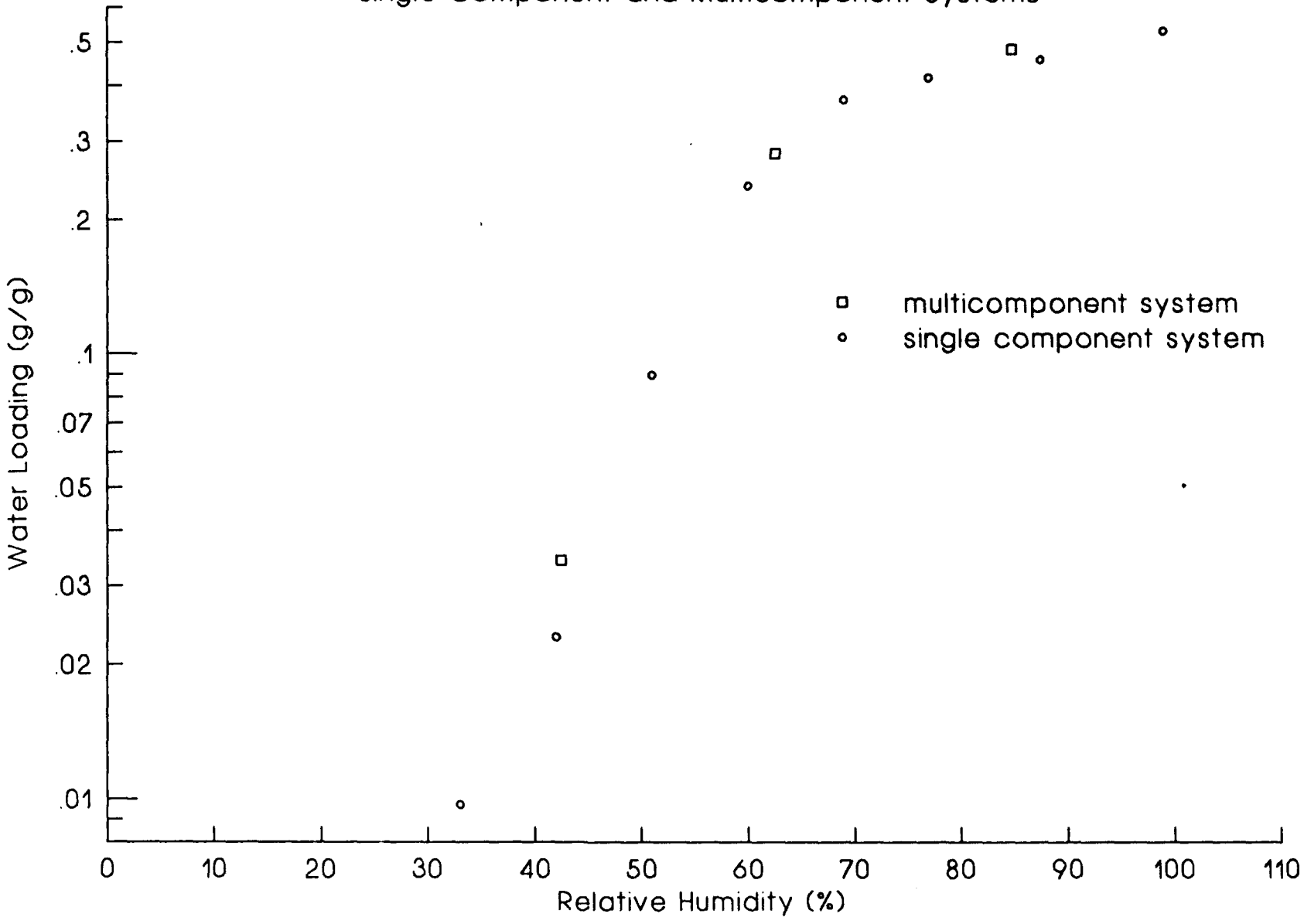

Figure 5. The Effects of Water on PFCBa Loading as a Function of RH at 25 C

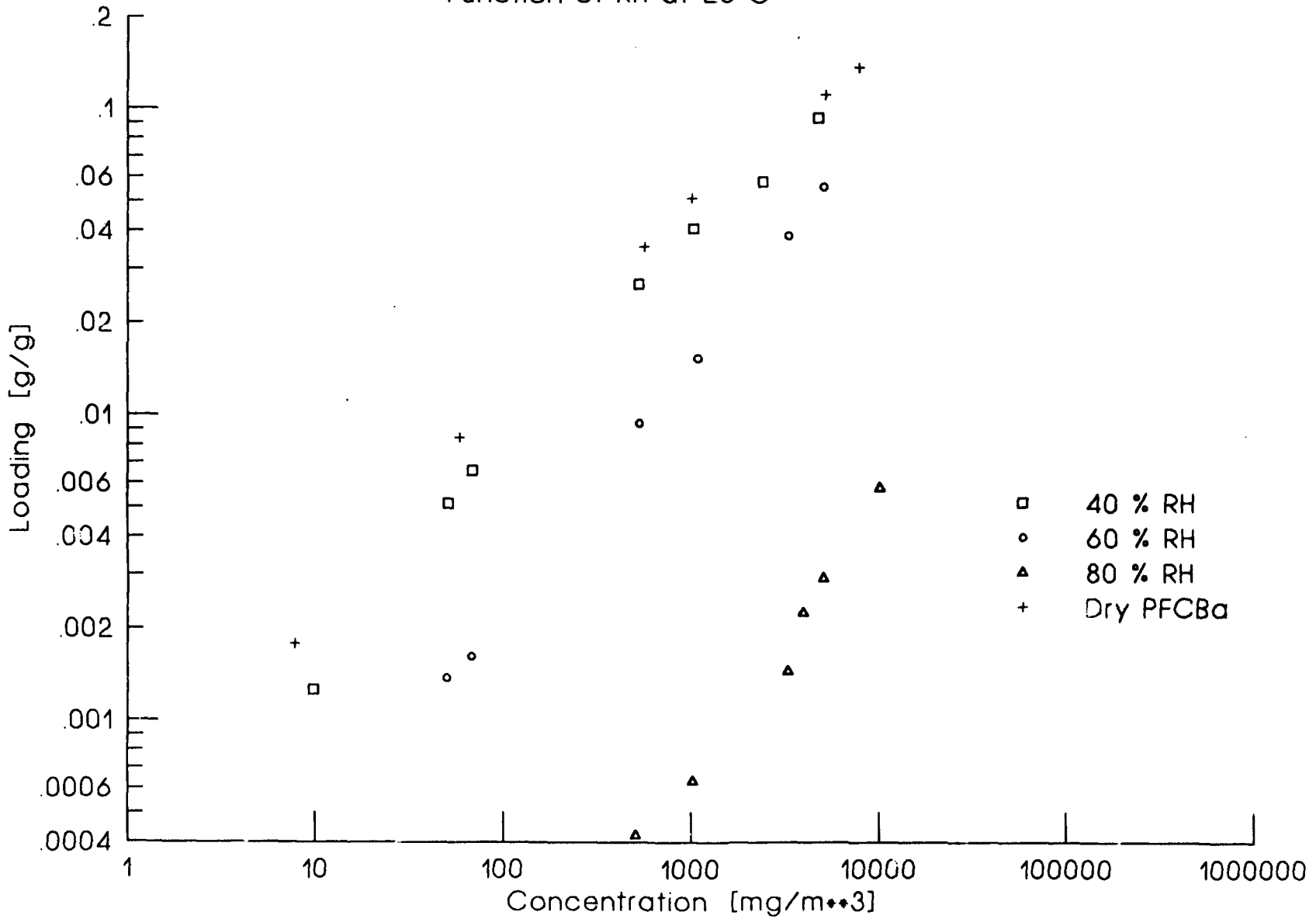

Figure 6. The Effects of PFCBa on Water Loading

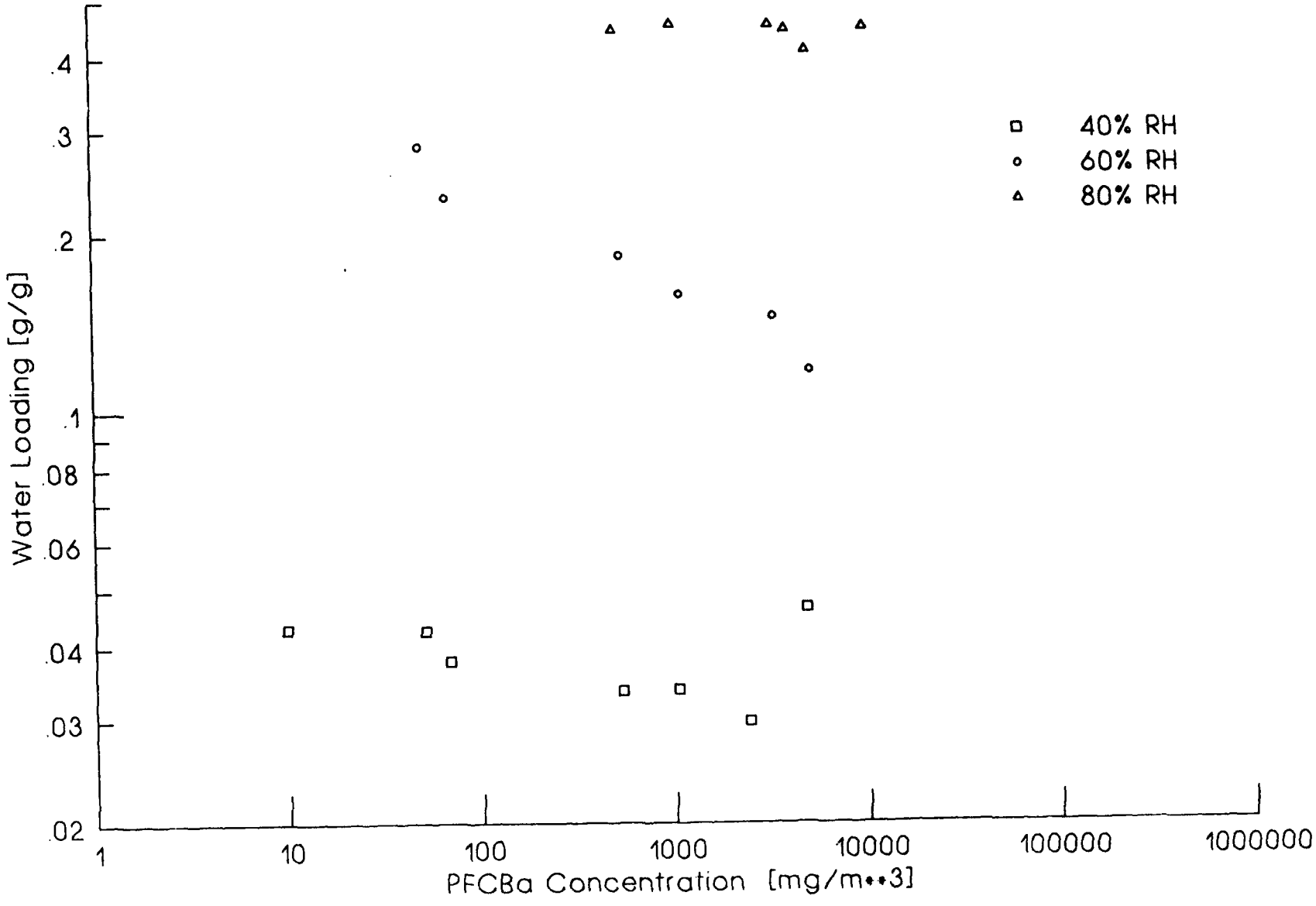

Figure 7. PSA Profile for R22 on Davison 13X Mol Sieve
(Sample Dried Overnight at 350C)

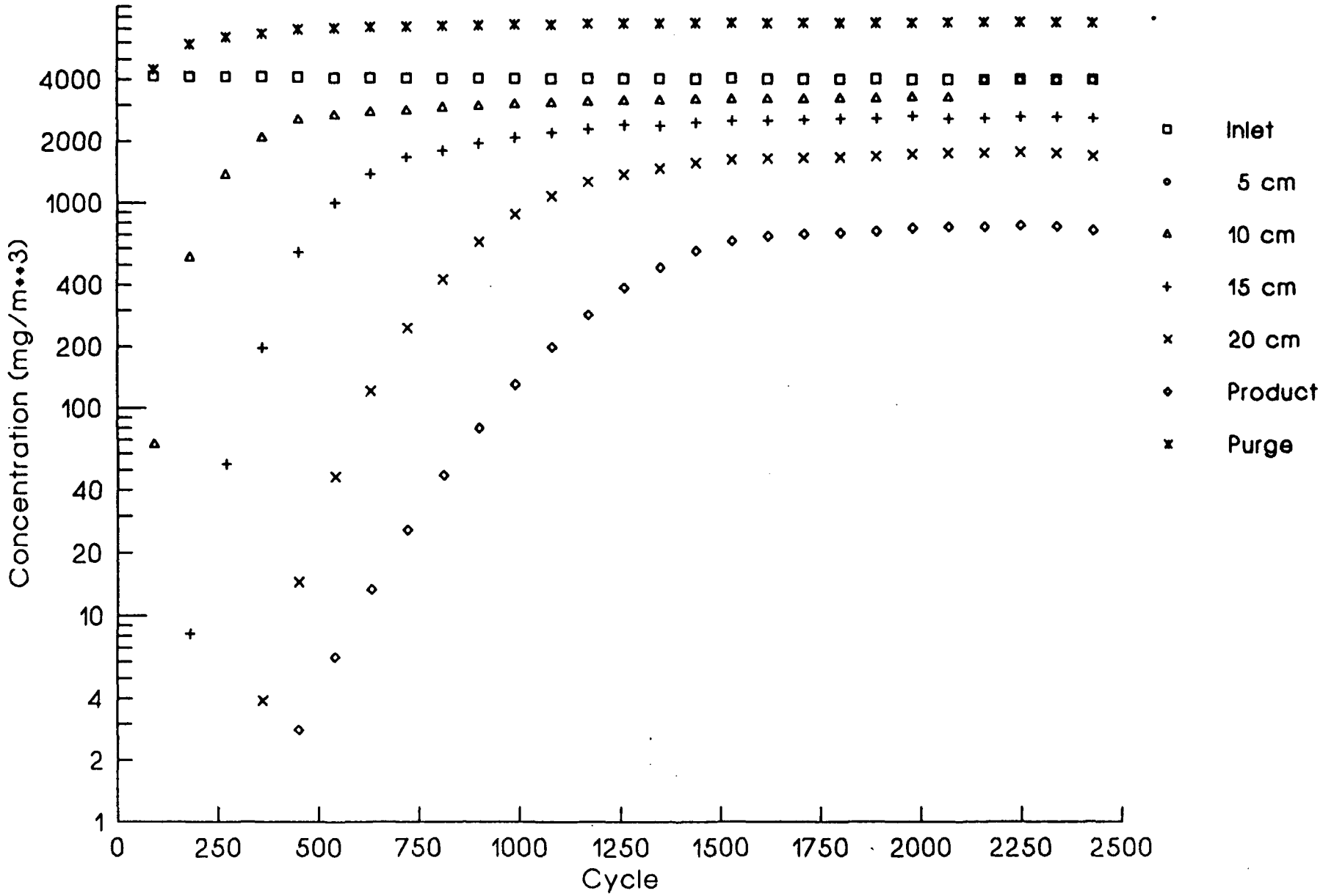

Figure 8. PSA Profile for R22 on UOP 13X Molecular Sieve
(Sample Dried Overnight at 350C)

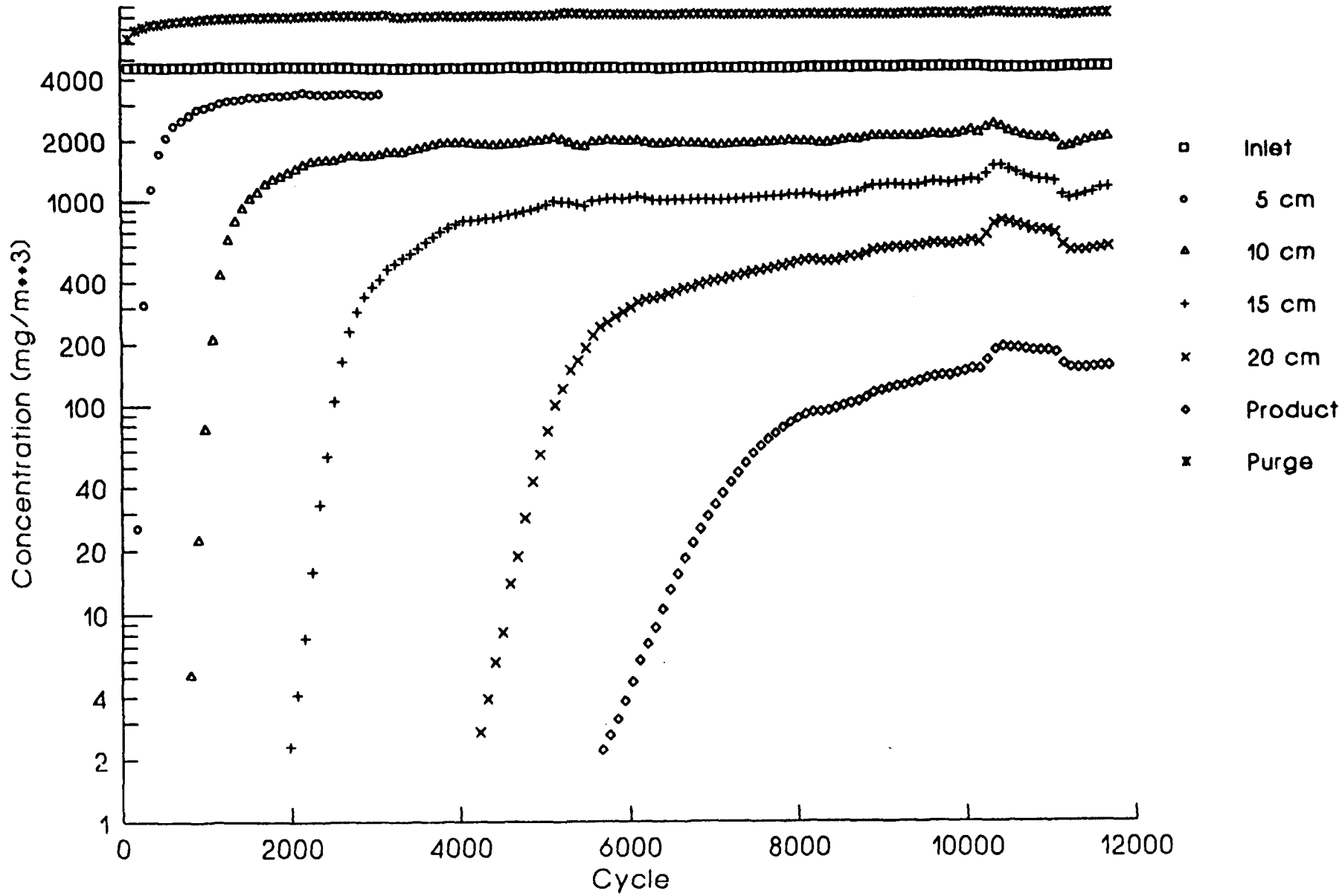

Figure 9. PSA Profile for R22 on UOP 13X Molecular Sieve
(Sample Taken Directly From Container)

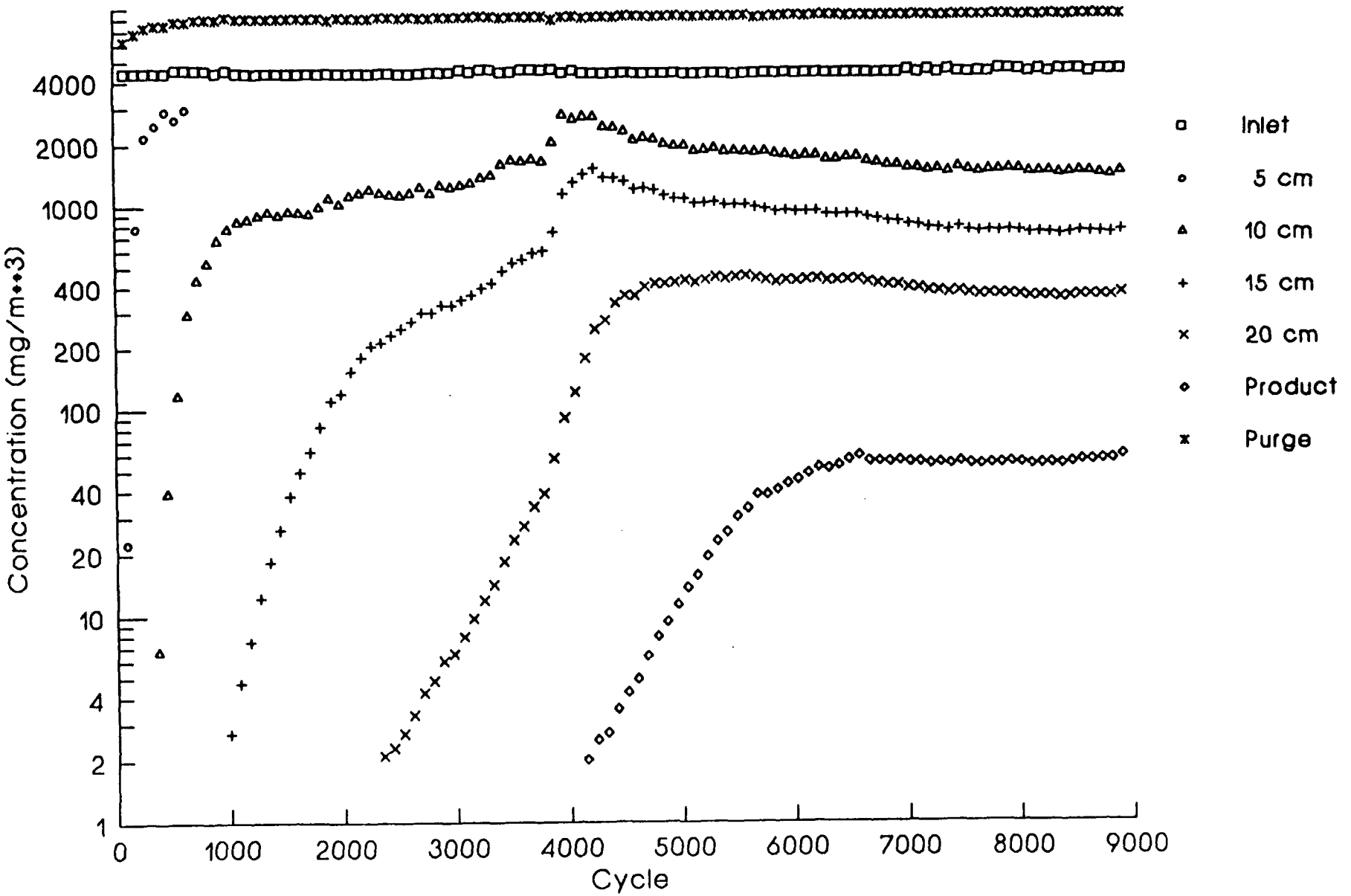

Figure 10. PSA Profile for Water on BPL Carbon
Feed Dew Point = 17C at Pressure

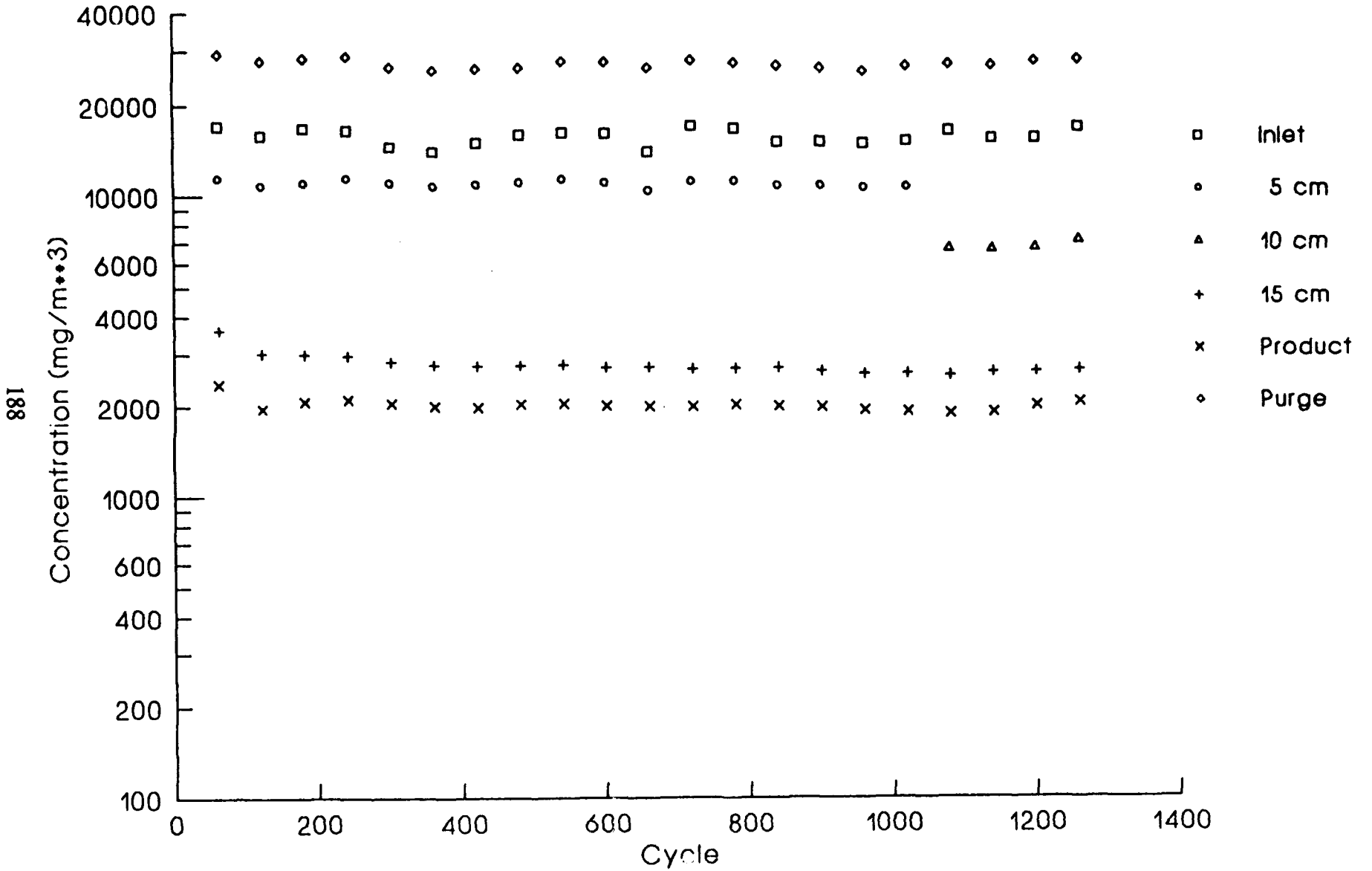

Figure 11. Relative Humidity as a Function of Bed Length

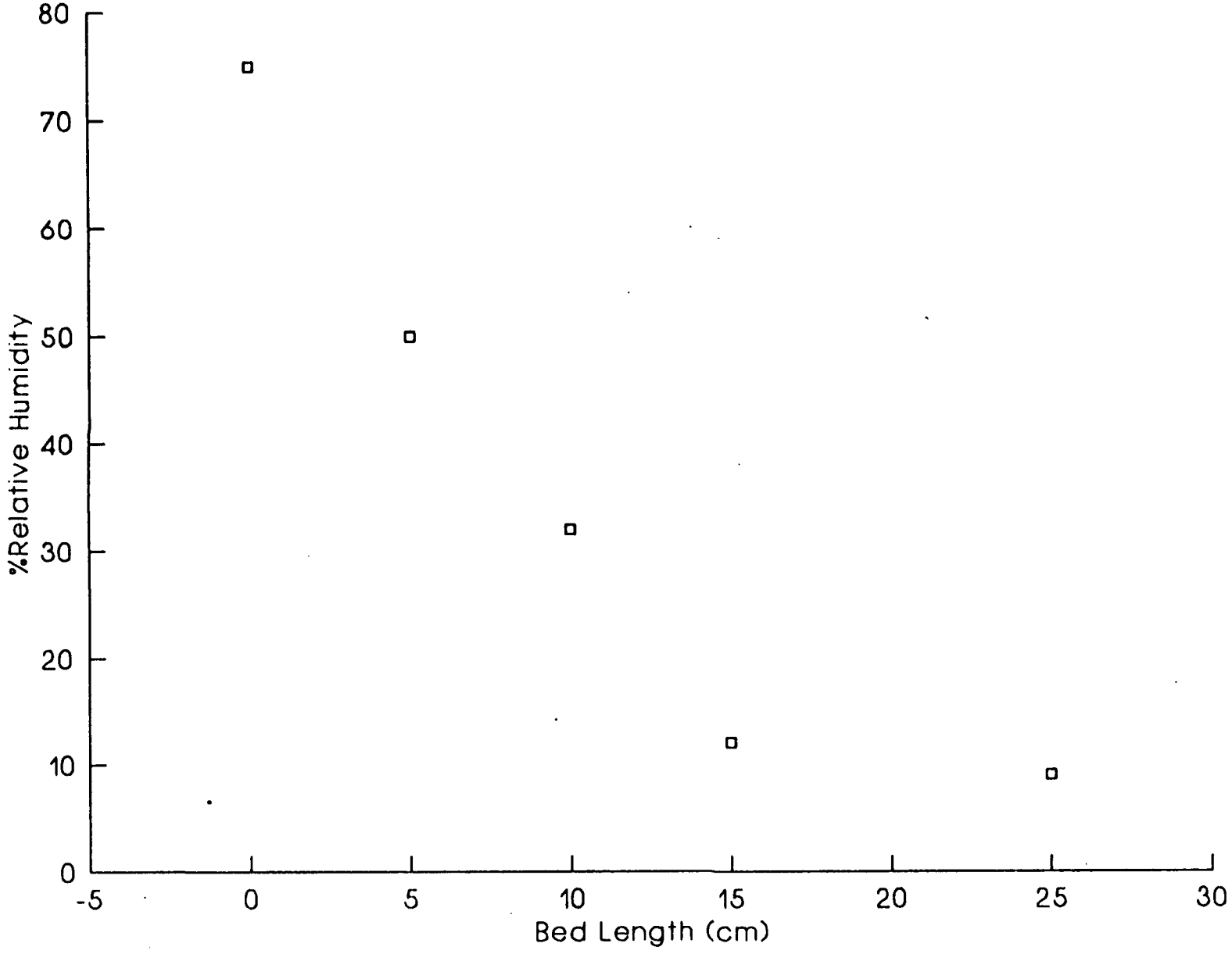

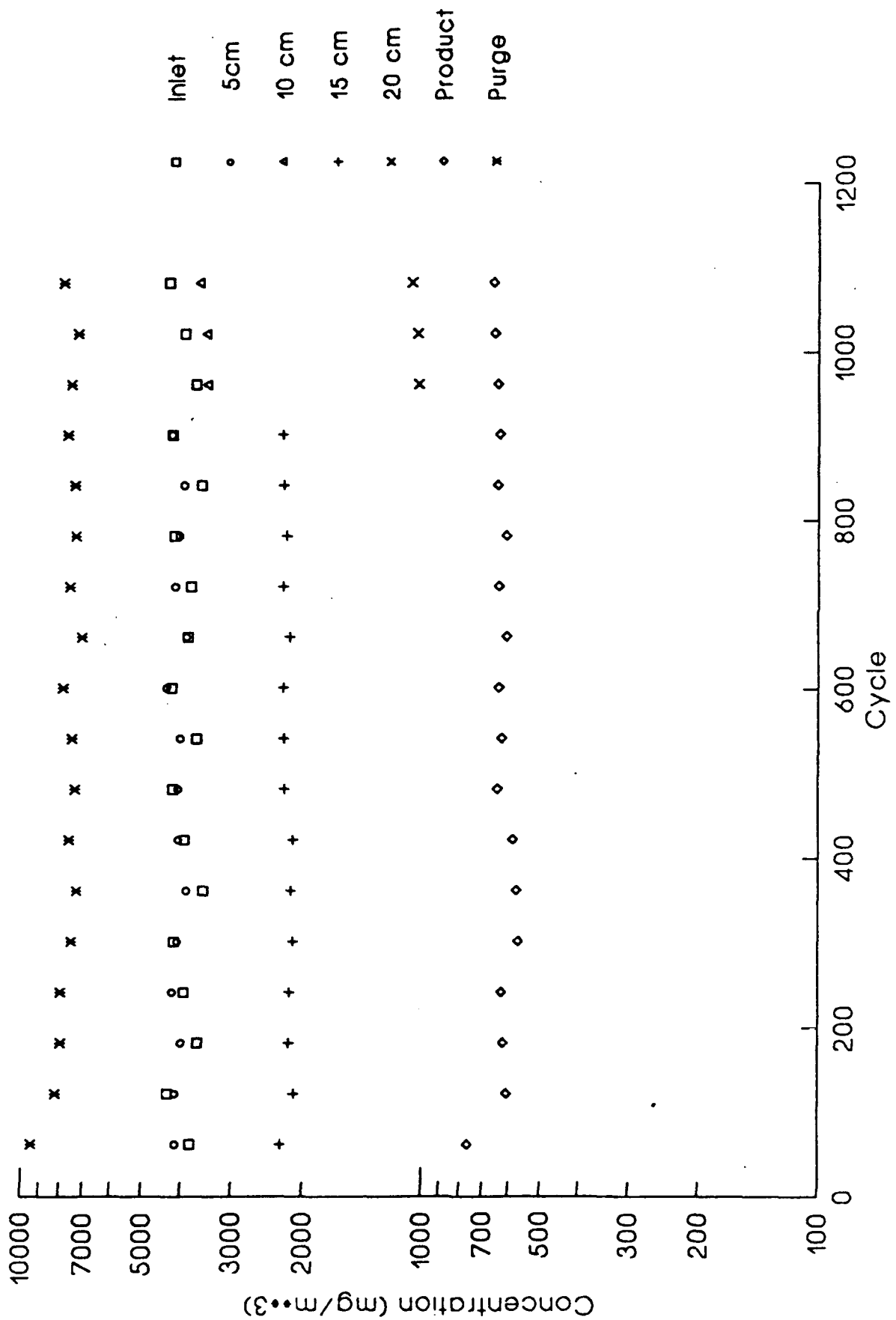

Figure 12. PSA Profile for Water on BPL Carbon
Feed Dew Point = 1C at Pressure

Figure 13. Relative Humidity as a Function of Bed Length

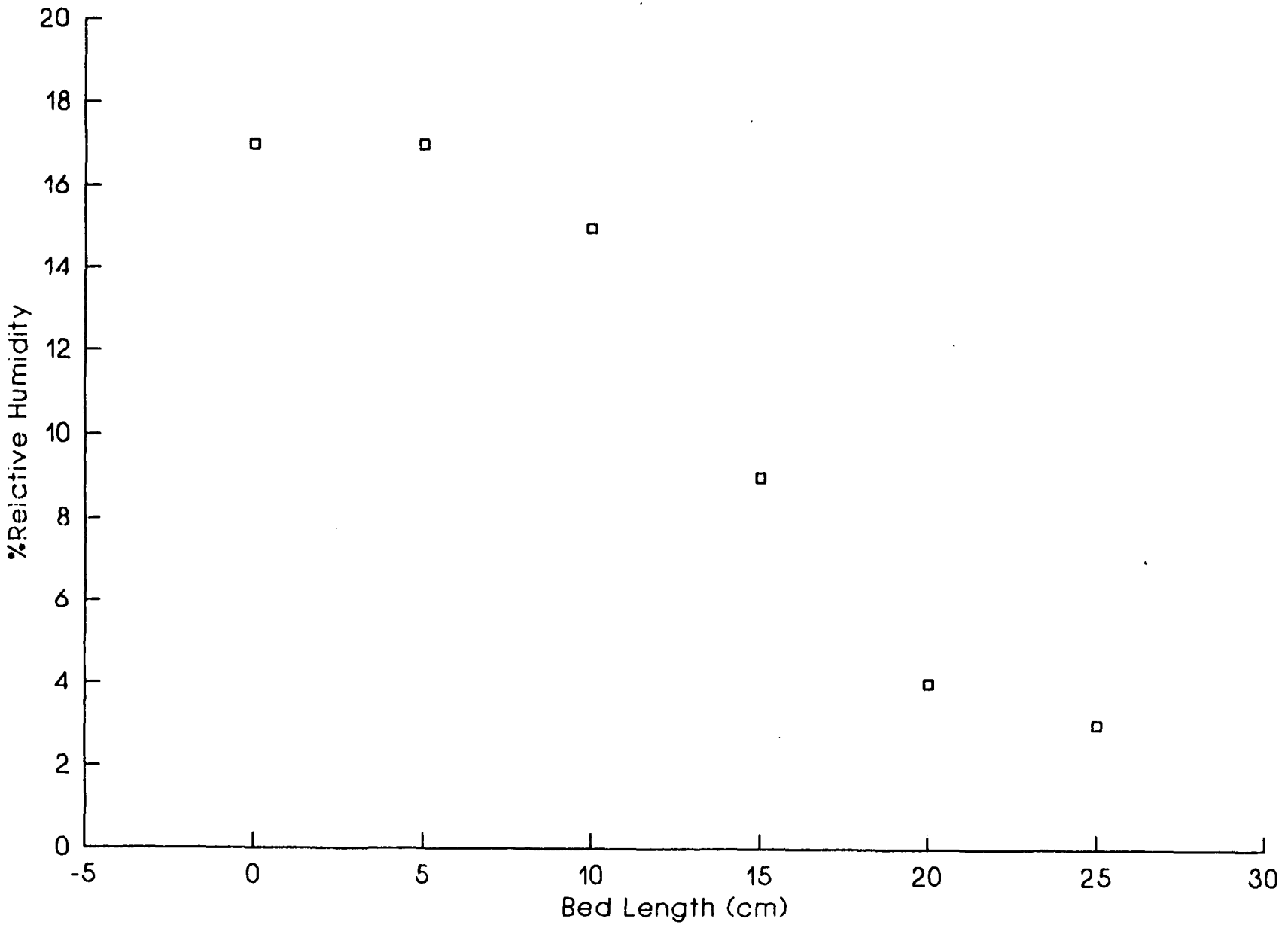

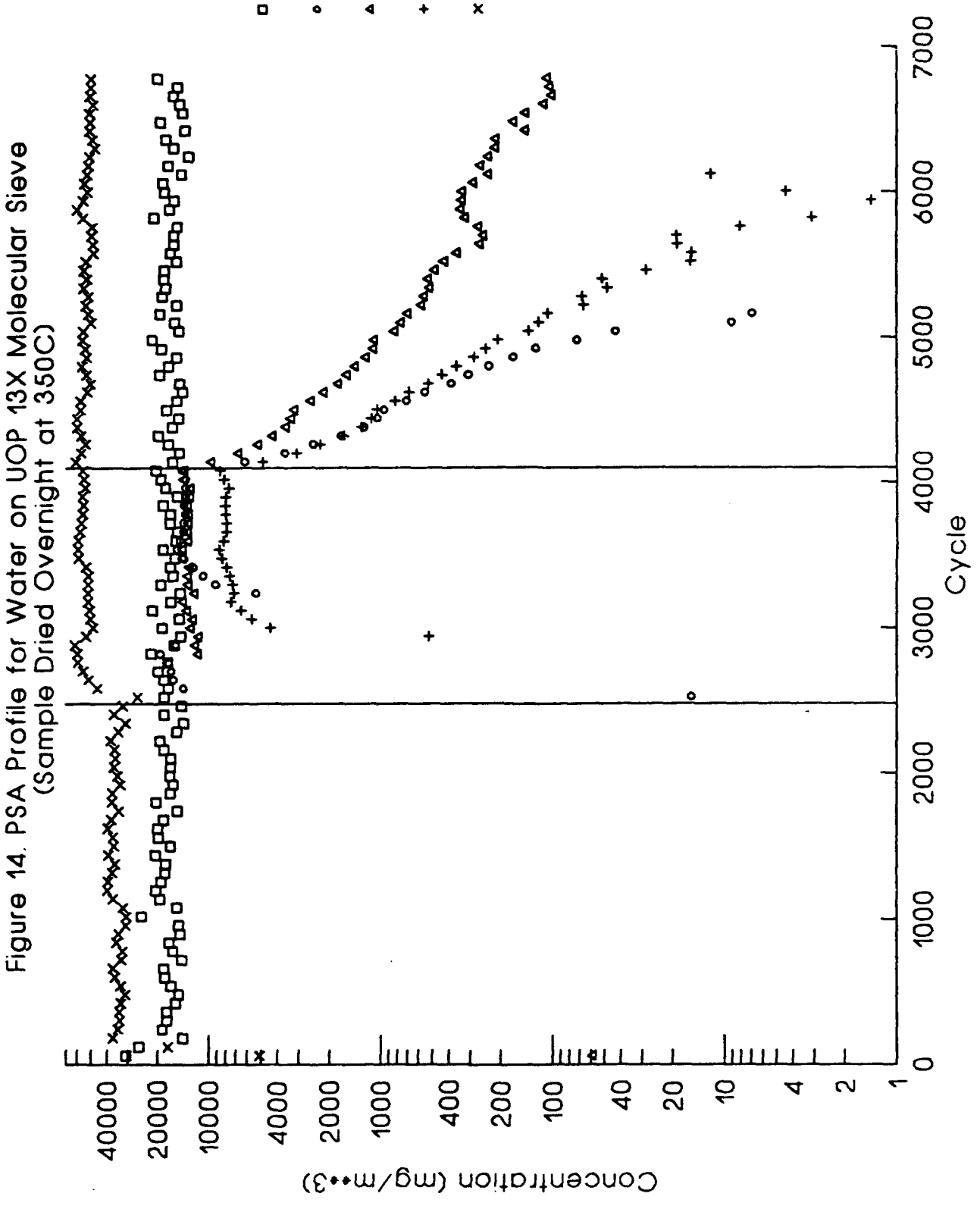
Figure 14. PSA Profile for Water on UOP 13X Molecular Sieve
(Sample Dried Overnight at 350C)
Inlet
5 cm
10 cm
15 cm
Purge
Concentration (mg/m**3)
40000
20000
10000
4000
2000
1000
400
200
100
40
20
10
4
2
1
0
1000
2000
3000
4000
5000
6000
7000
Cycle

Figure 15.

Temperature and Power Profiles for 10 minute TSA cycles simulated using a single bed

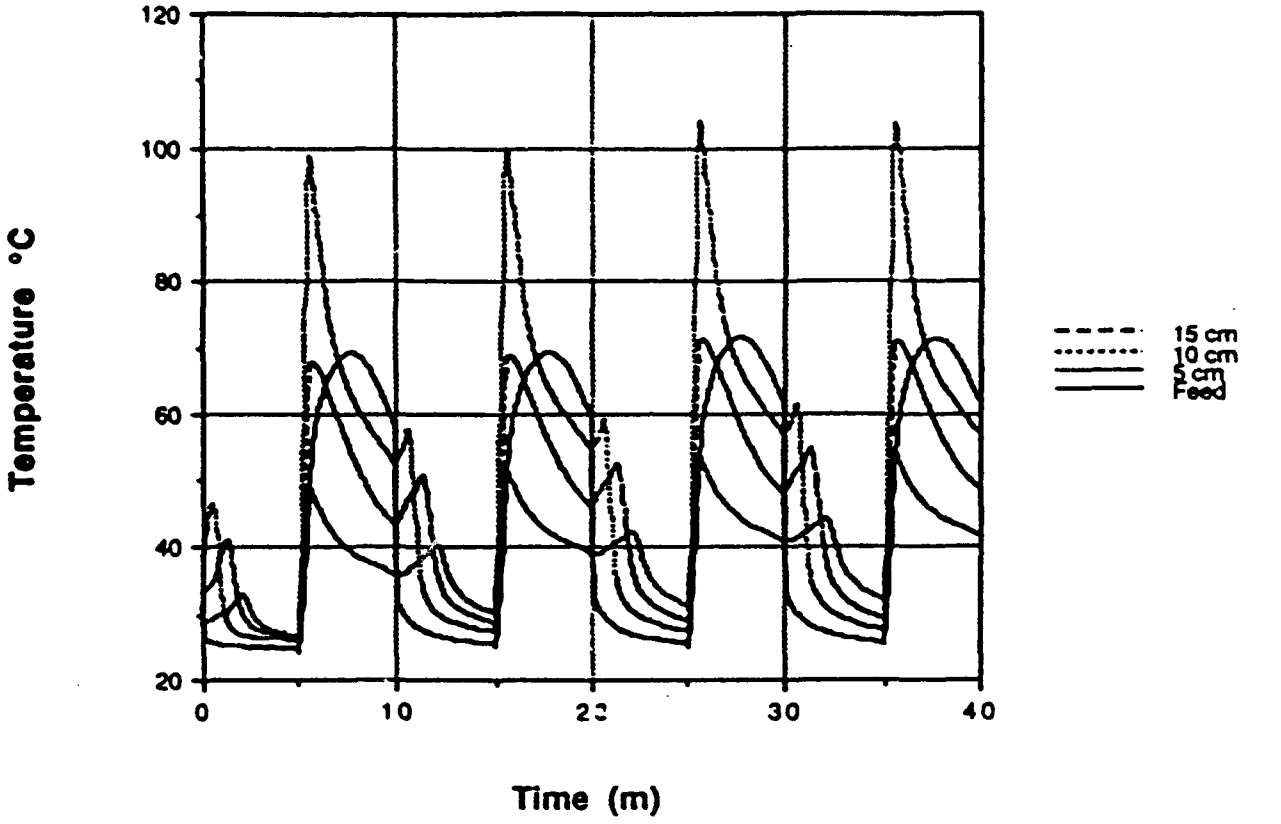

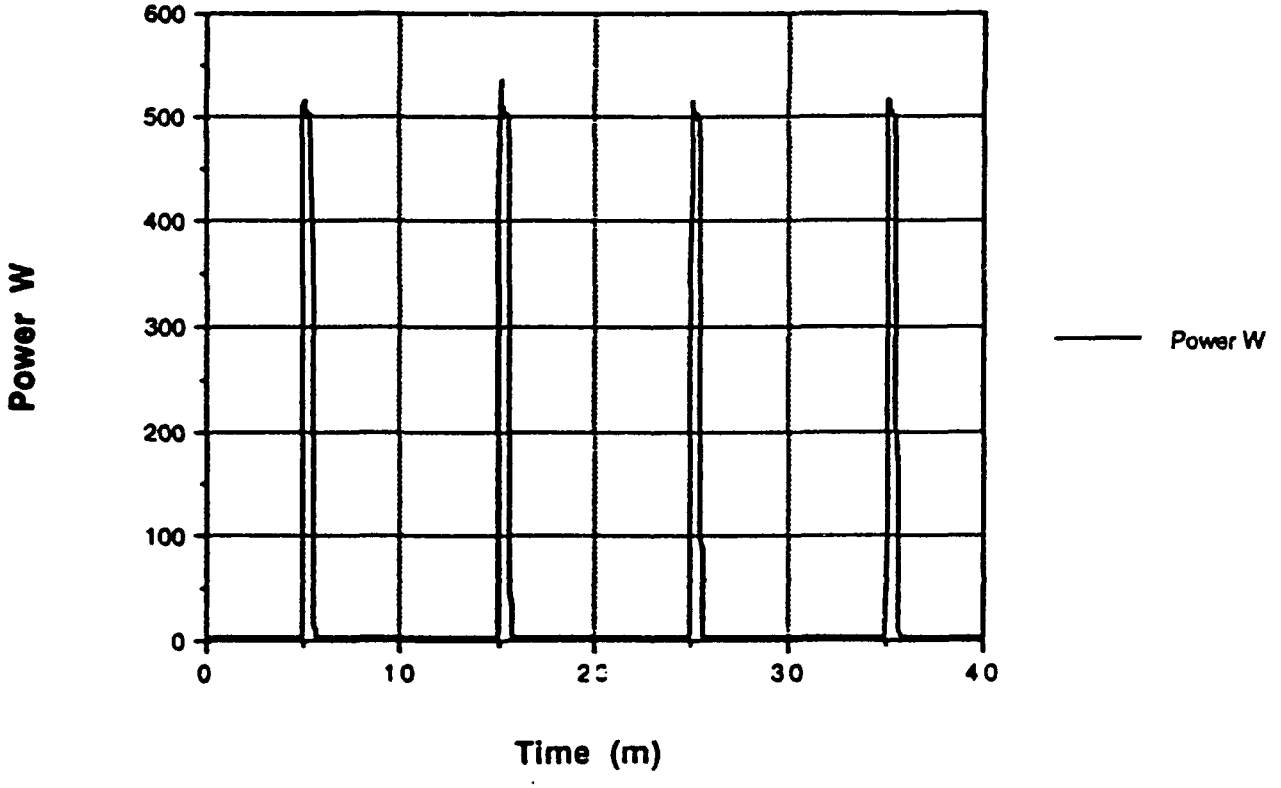

Figure 16.

Temperature and Concentration Profiles for 10 minute TSA cycles simulated using a single bed

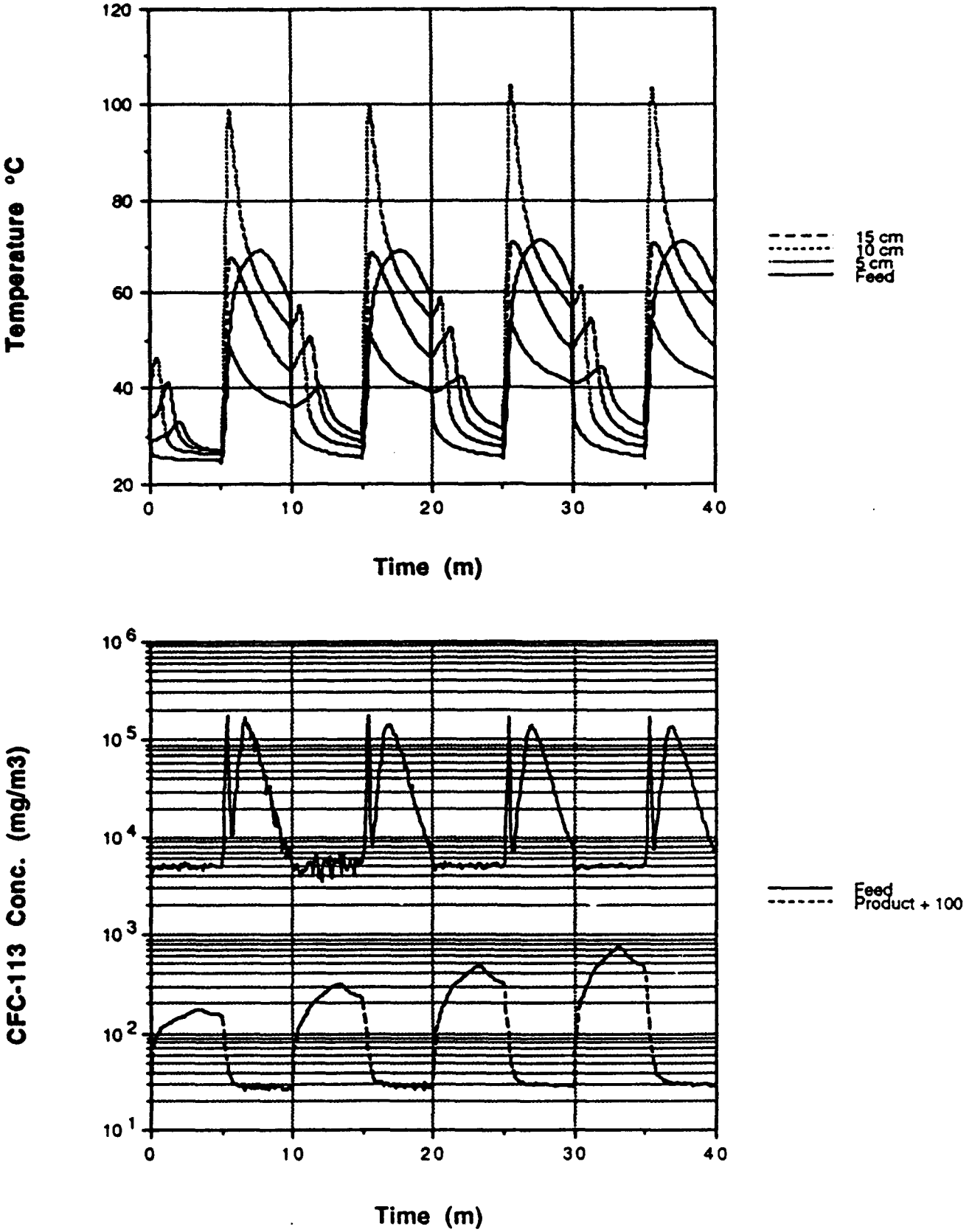

APPENDIX A-10

QUARTERLY PROGRESS REPORT

GC-PR-2194-10

REPORTING PERIOD: 11/1/92 - 1/31/93

REPORTING DATE: 2/15/93

CONTRACT NUMBER: DAAA15-90-C-1056

CONTRACT TITLE: Improved Filtration Materials and Modeling

I. Adsorption Equilibria

Single Component Measurements and Apparatus

Shown in Figure 1 are isotherms for trichlorofluoromethane (R-11) on BPL at 298K, 323K and 348K. These data span about four orders of magnitude in concentration and nearly two orders of magnitude in loading. The capability of the isotherm system to generate reproducible data is demonstrated by duplicate experimental results.

Multicomponent Measurements and Apparatus

Multicomponent isotherms for perfluorocyclobutane (PFCBa) and water on UOP 13X molecular sieve at 298 K have been initiated. Shown in Figure 2 are the data measured to date for PFCBa on 13X under dry (about -60°C dew point) conditions, 20% RH and 80% RH. PFCBa vapor-phase concentrations are between 500 and 10,000 mg/m^3. Isotherm points for PFCBa on 13X measured under dry conditions using the single component system are also presented for reference. This is the first part of this study. Lower concentrations of PFCBa will be used in the second part of this work. Dividing the work up this way was required since the IRs which monitor the feed and effluent of PFCBa concentration will have to be recalibrated and the volume of the

analysis loop will have to be reduced to obtain measurable quantities of PFCBa following desorption.

Figure 3 compares the results shown in Figure 2 with the isotherm data measured last quarter for PFCBa and water on BPL carbon. Several interesting observations may be made. The dry 13X and the dry BPL have about the same capacity above 1000 mg/m^3. The 13X dry point measured at about 500 mg/m^3 shows a large reduction in capacity. This point will be confirmed when the low PFCBa concentration experiments are performed next quarter. Another interesting feature is that the two adsorbents have about the same capacity for PFCBa under 80% RH conditions. The most important difference in the two adsorbents is shown by comparing the data for BPL at 40% RH and 13X at 20% RH. The BPL capacity at 40% RH is nearly the same as dry BPL, while the adsorption capacity for PFCBa on 13X at 20% is about an order of magnitude smaller than under dry conditions. It is this strong affinity for water at low RH's which makes 13X impractical for use in military systems unless other adsorbents are used to remove water.

II. Pressure Swing Adsorption

Experiments and Apparatus

An experimental study was performed to determine the phenomenon responsible for the measured temperature swings during PSA system operation. Results of the experiments and discussion are given in the ERDEC paper in Appendix A. The major conclusion drawn from this effort is that air adsorbing during pressurization and

desorbing during blowdown accounts for about 90% of the total swing in temperature (work to compress and decompress the air provides the rest).

The effect of water on the adsorption capacity of 13X molecular sieve for PFCBa at low RH's was shown in Figure 3. A study of PSA performance using water/13X was conducted to determine if higher pressures (about 60 psig) afforded significant improvement. The feed concentration of water corresponded to about 80% RH at pressure (about a 2°C dew point at ambient pressure). The bed depth for this experiment was approximately 18 cm , the bed diameter was 3.77 cm and the feed flow rate was 165 SLPM. The purge to product ratio (Pu/Pr) was set to 1.0 (corresponding to a purge and product flow of about 82.5 SLPM) and the system was allowed to reach periodic state. The concentration of water was measured in the feed, product, and at 5 cm, 10 cm and 15 cm into the bed. After the system reached a periodic state, Pu/Pr was set to 0.8. Measured water concentrations for these two purge to product ratios are shown in Figure 4. The concentration at 5 cm increases rather quickly when the purge flow is reduced. However, there is no measurable water concentration present at 10 cm even using Pu/Pr = 0.8. Temperature profiles were also measured at periodic state for both purge to product ratios and are shown in Figures 5 and 6, respectively. At 5 cm for Pu/Pr = 1.0 (Figure 5), there is only about 2-3°C temperature swing indicating that water has saturated the bed to that point. There is, however, a temperature swing at 10 cm of about 14°C for both Pu/Pr = 0.8 and 1.0. The Pu/Pr was set to 0.6 and the progression of the water through the bed was measured and shown in Figure 7. Water appears at 10 cm at about 22000 cycles and then falls off during the next 6000 cycles. The reason for this is not clear. One explanation may be the increase in system pressure

from 60 psig to 66 psig. Shown in Figure 8 are the corresponding temperature profiles for Pu/Pr = 0.6. The results indicate that the bed is contaminated past 15 cm, although there is a noticeable swing in temperature at 15 cm. Most importantly, this results shows that measurable quantities of water and loss of bed capacity are not necessarily coincident when 13X molecular sieve is used. There are two possible reasons for this observed behavior. First, the measurable water concentration is about 5 mg/m^3 and the water isotherm is so favorable on 13X that concentrations below 5 result in relatively large adsorbed water concentrations. The second explanation could be the presence of a CO_2 wave in front of the water wave, since 13X also adsorbs CO_2 (but not nearly as strongly as water, preferentially to 0_2 and N_2). Figures 9 through 14 show the concentration and temperature profiles for Pu/Pr = 0.5, Pu/Pr = 0.4, and Pu/Pr = 0.35. For Pu/Pr = 0.35, Figure 13 results show that the bed is essentially saturated with water, which is clearly demonstrated in Figure 14 where there is virtually no change in temperature during a cycle anywhere in the bed.

The results of the entire purge to product ratio study are shown in Figure 15. Periodic-state concentration profiles are plotted for each purge to product ratio. These results plotted on a semi-log graph show that at a Pu/Pr = 0.35 and 0.4, the majority of the water separation is being performed at the end of the bed between 15 cm and product (18 cm). For Pu/Pr = 0.5 a logarithmic decrease in water concentration is observed. Shown in Figure 16 are the same data plotted as concentration versus purge to product ratio. These results also show that a purge to product ratio of 0.5 or below is too small to keep water from contaminating the bed.

III. Temperature Swing Adsorption (TSA)

A program to control the operation of the lab-scale TSA system was written using LabView software. Some of the features added to this program during the past quarter include : (1) an overall material balance calculation for each cycle, (2) an improved power control algorithm and (3) data reduction programs to compile large amounts temperature and power data into a form which may be interpreted more easily.

Data reduction programs were written to : (1) extract the maximum and minimum temperatures at relevant parts of the cycle and (2) reduce the amount of power data and save the bed resistance as function of time. Shown in Figure 17 is an example of the output of the latter program. Notice that the bed resistance over the course of 24 hours is increasing. The reason for this behavior is not known at this time.

Experiments were performed to simulate both two-bed and three-bed TSA operation using a single bed. The details of the cycle are given in the last GEO-CENTERS quarterly report. Shown in Figures 18 through 21 are maximum and minimum temperatures at specific locations in the bed for a simulated two-bed TSA system compared with a simulated three-bed system. There are three steps in the cycle, namely; (1) feed, (2) heat, and (3) cool-down. The three-bed cycle has 5 minutes of feed, 30 seconds of heating and 9.5 minutes of cool-down while the two-bed cycle has only 4.5 minutes of cool-down. These experiments were performed without chemical feed because the hydrocarbon analyzers were not reliable. They are currently being replaced with IR's. However, these results show that the extra cool-down time may be important by comparing the maximum temperature in the bed during the feed step. At 5

and 15 cm the two-bed maximum temperature during the feed step was about 62°C, while for the three-bed cycle the maximum temperature was only about 43°C. This is important because higher bed temperatures during feed could carry contaminants toward the product end of the bed. Notice also that the maximum temperature at 25 cm during the feed step was about 14°C higher for the two-bed cycle (53°C compared to 39°C)

IV. Other

A. Publications

A CRDEC technical report entitled "1,1,2 Trichloro, 1,2,2 Trifluoroethane (CFC-113) and Water Isotherm Measurements on Impregnated and Unimpregnated Activated Carbons" by D.K. Friday and D.C. Carlile.

B. ERDEC Conference papers included the following :

Brady, A.B., Dawson, C.L., and Friday, D.K., "Measurement of In-Bed Temperature Profiles During Pressure Swing Adsorption Cycles", 1992 ERDEC Conference given Nov 17, 1992.

Friday, D.K., Brady, A.B., Mahle, J.J., and Buettner, L.C., "A Parametric Study of PSA for Air Purification Applications", 1992 ERDEC Conference given Nov 17, 1992.

Farris, M.M., Dawson, C.L. and Friday, D.K., "Multicomponent Adsorption Equilibria for Perfluorocyclobutane (PFCBa) and Water on BPL Carbon", 1992 ERDEC Conference given Nov 17, 1992.

Mahle, J.J., Friday, D.K., Sundaram, N., and LeVan, M.D., "Non-Isothermal Behavior of PSA for Air Purification", 1992 ERDEC Conference given Nov 17, 1992.

Carlile, D.C., Buettner, L.C., Tevault, D.E., and Friday, D.K., "CFC-113 Adsorption Equilibrium Data on ASC Whetlerite and BPL Carbon", 1992 ERDEC Conference given Nov 17, 1992.

Sundaram, N., Friday, D.K., Buettner, L.C., and Mahle J.J. "Development of a Pore-Filling Adsorption Equilibrium Model", 1992 ERDEC Conference given Nov 17, 1992.

Mahle, J.J., Friday, D.K., Mann, R. and Yousef, H., "Interpretation of Adsorption Isotherm Hysteresis for an Activated Charcoal Using Stochastic Pore Networks", CRDEC-TR-407, September 1992.

C. ERDEC Poster

Dawson, C.L., "Designing Experimental Control and Data Acquisition for Air Purification Systems" , 1992 ERDEC Scientific Conference on Chemical Defense Research.

FIGURE 1. Isotherm Data for R-11 on BPL Lot 7816-V

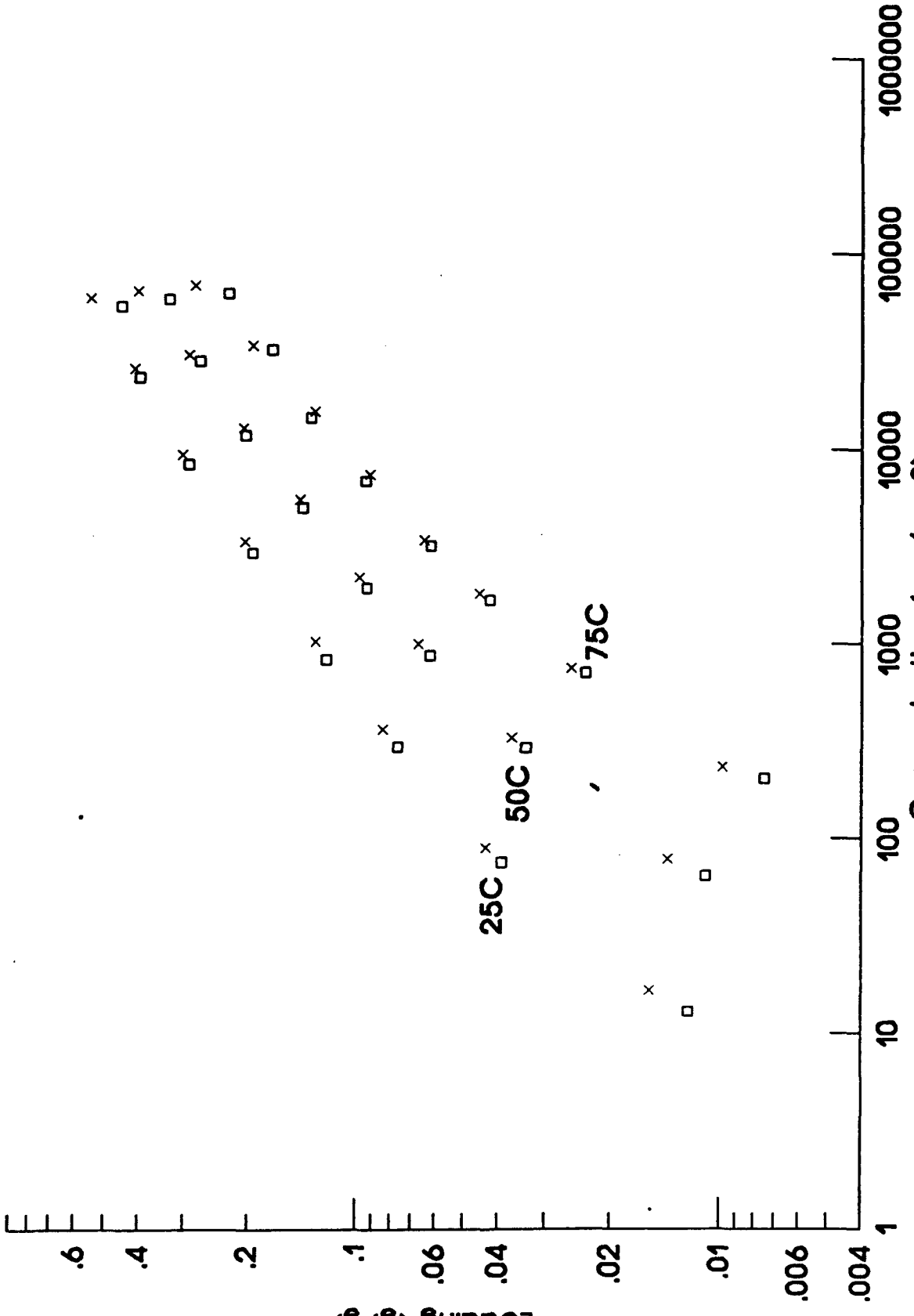

Figure 2: PFCBa Isotherms on 13X Molecular Sieve as a Function of RH

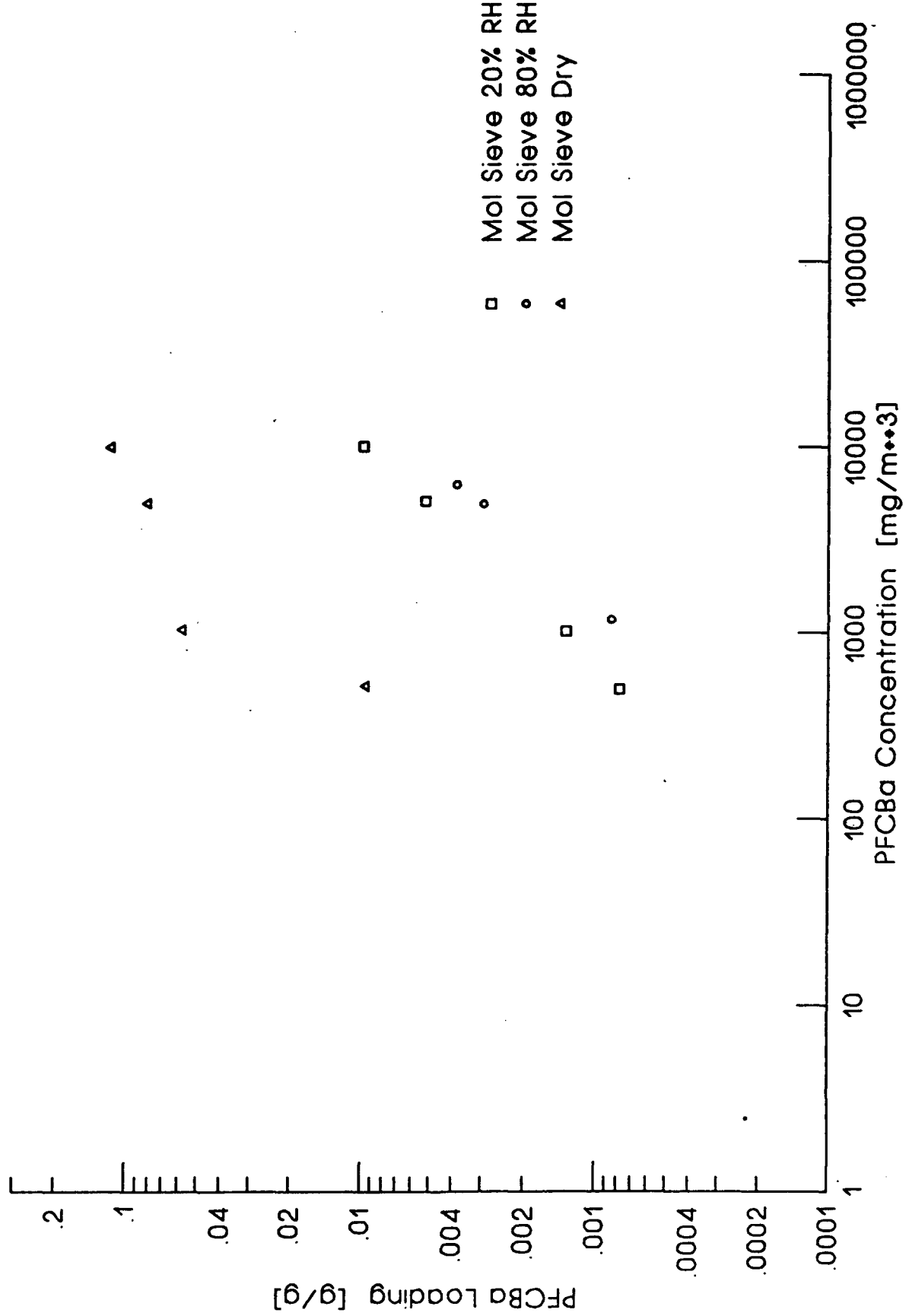

Figure 3: Comparison of PFCBa Adsorption on 13X Molecular Sieve And 12x30 Mesh BPL Carbon

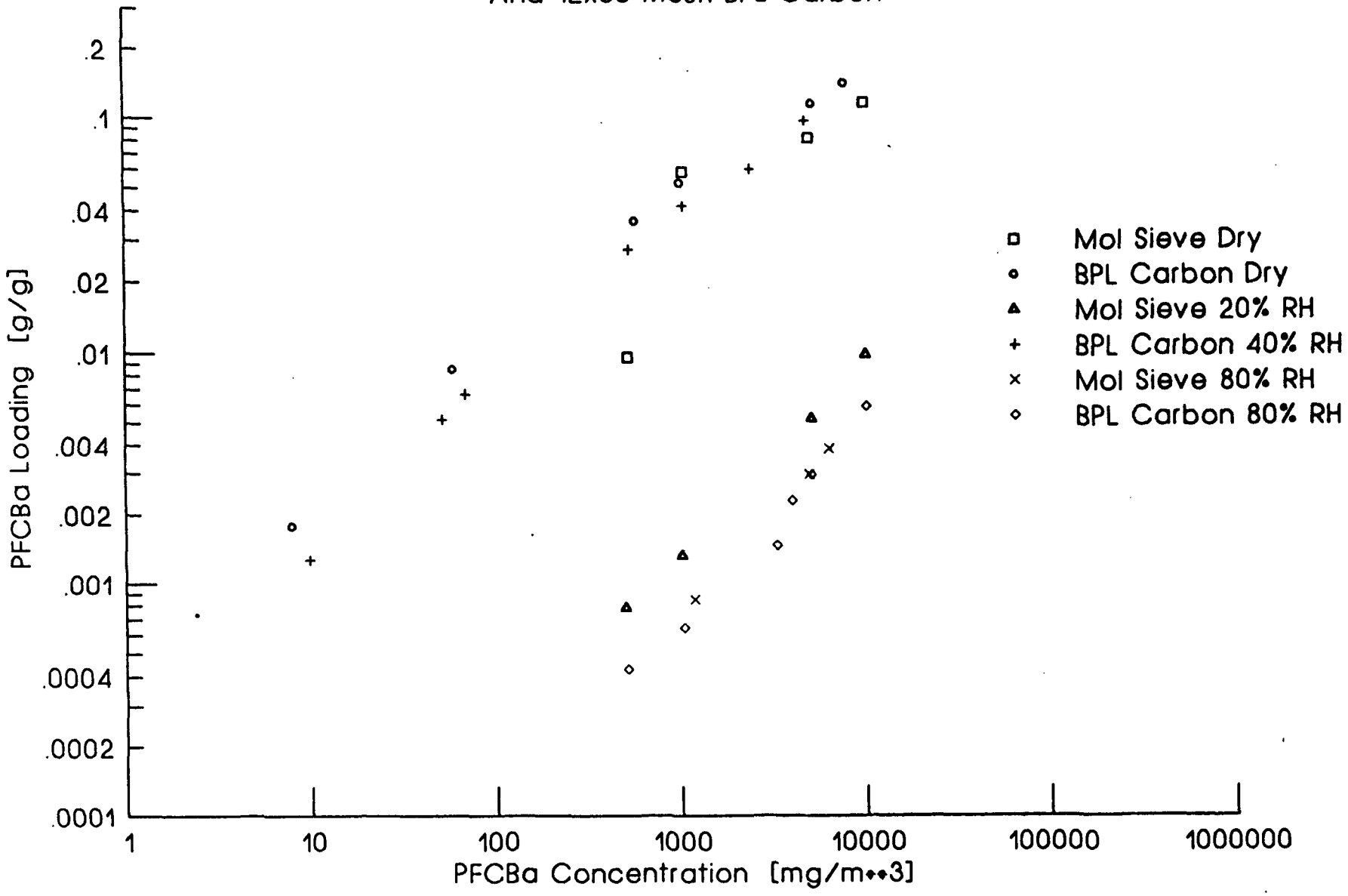

Figure 4. PSA Profile for Water on UOP Molecular Sieve
18 cm Bed, 30 sec Cycle Time

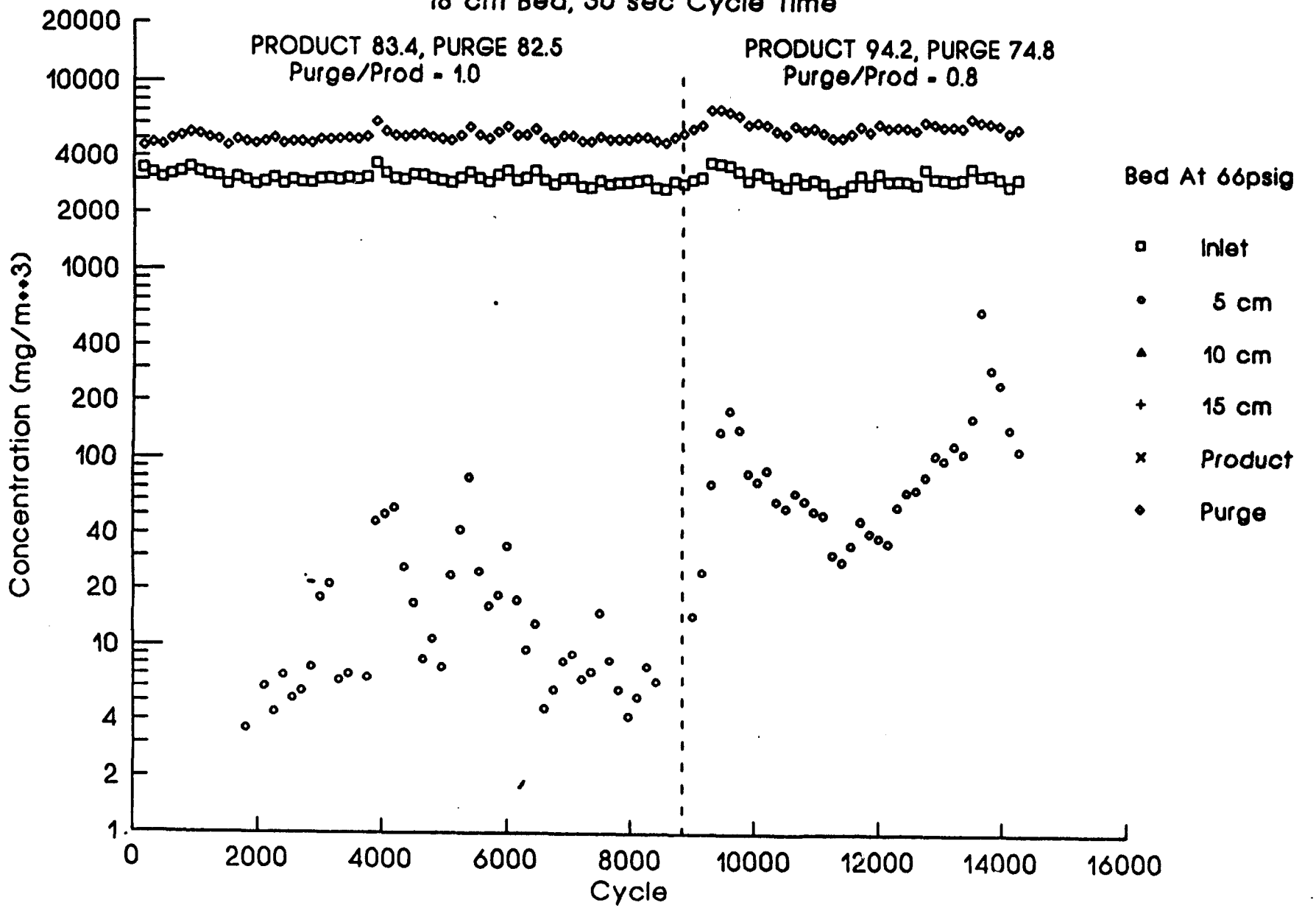

Figure 5. In-Bed Temperature Profile for Water on UOP Molecular Sieve
Periodic State #1, Purge/Product Ratio = 1.0

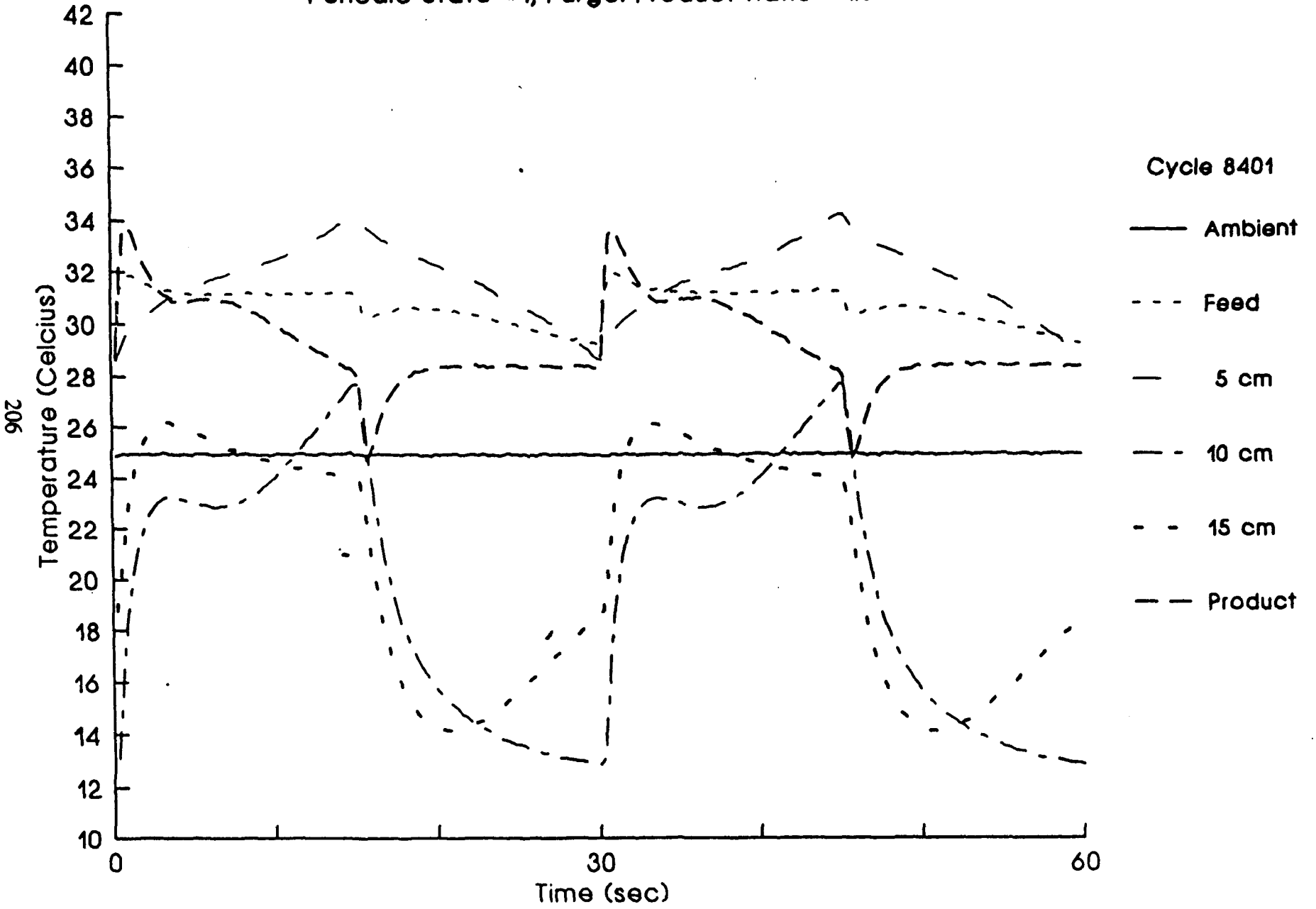

Figure 6. In-Bed Temperature Profile for Water on UOP Molecular Sieve
Periodic State #2, Purge/Product Ratio = 0.8

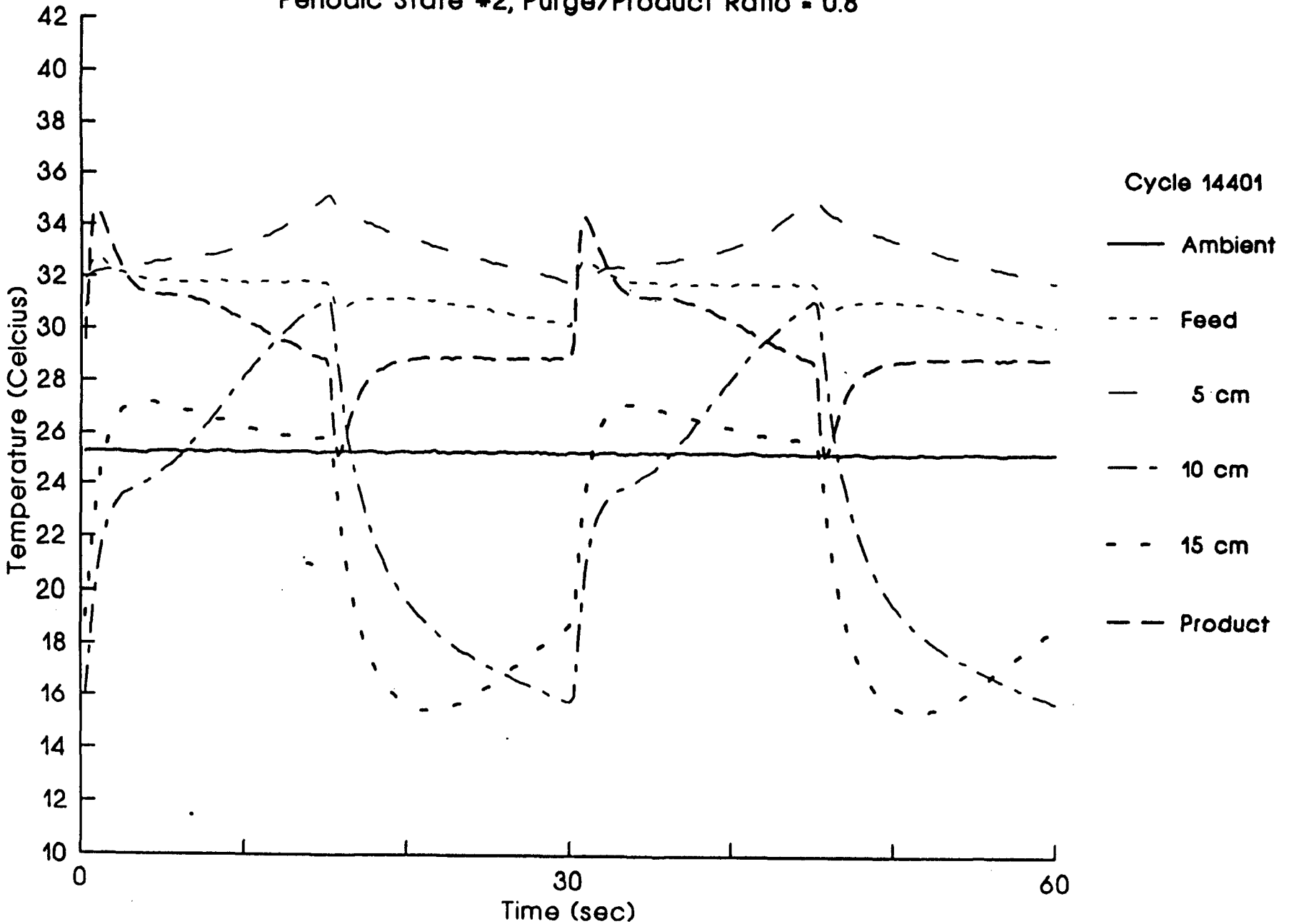

Figure 7. PSA Profile for Water on UOP Moleculer Sieve
Product 107SLPM Purge 63SLPM, Purge/Prod = 0.6
18 cm Bed, 30 sec Cycle Time

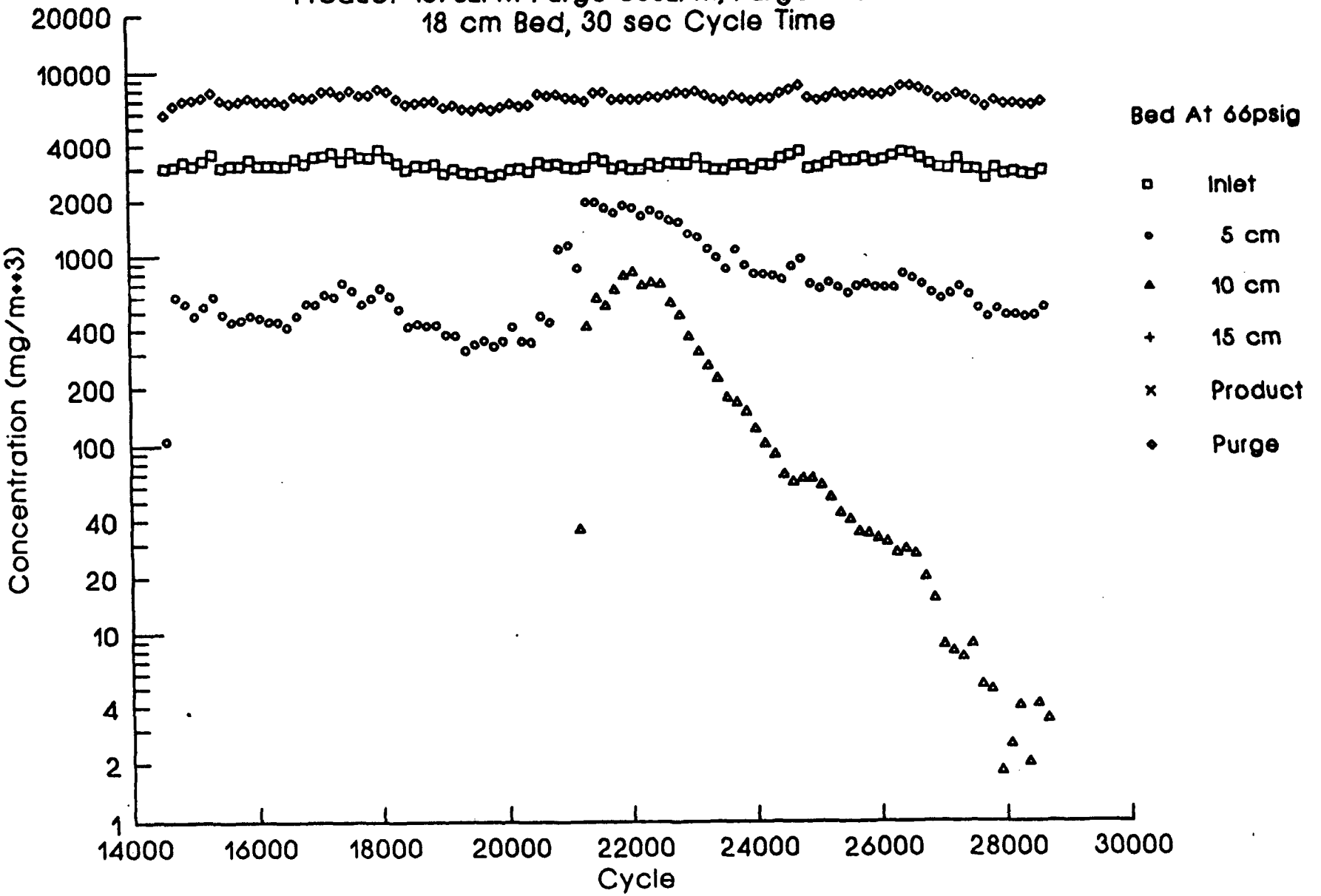

Figure 8. In-Bed Temperature Profile for Water on UOP Molecular Sieve
Periodic State #3, Purge/Product Ratio = 0.6

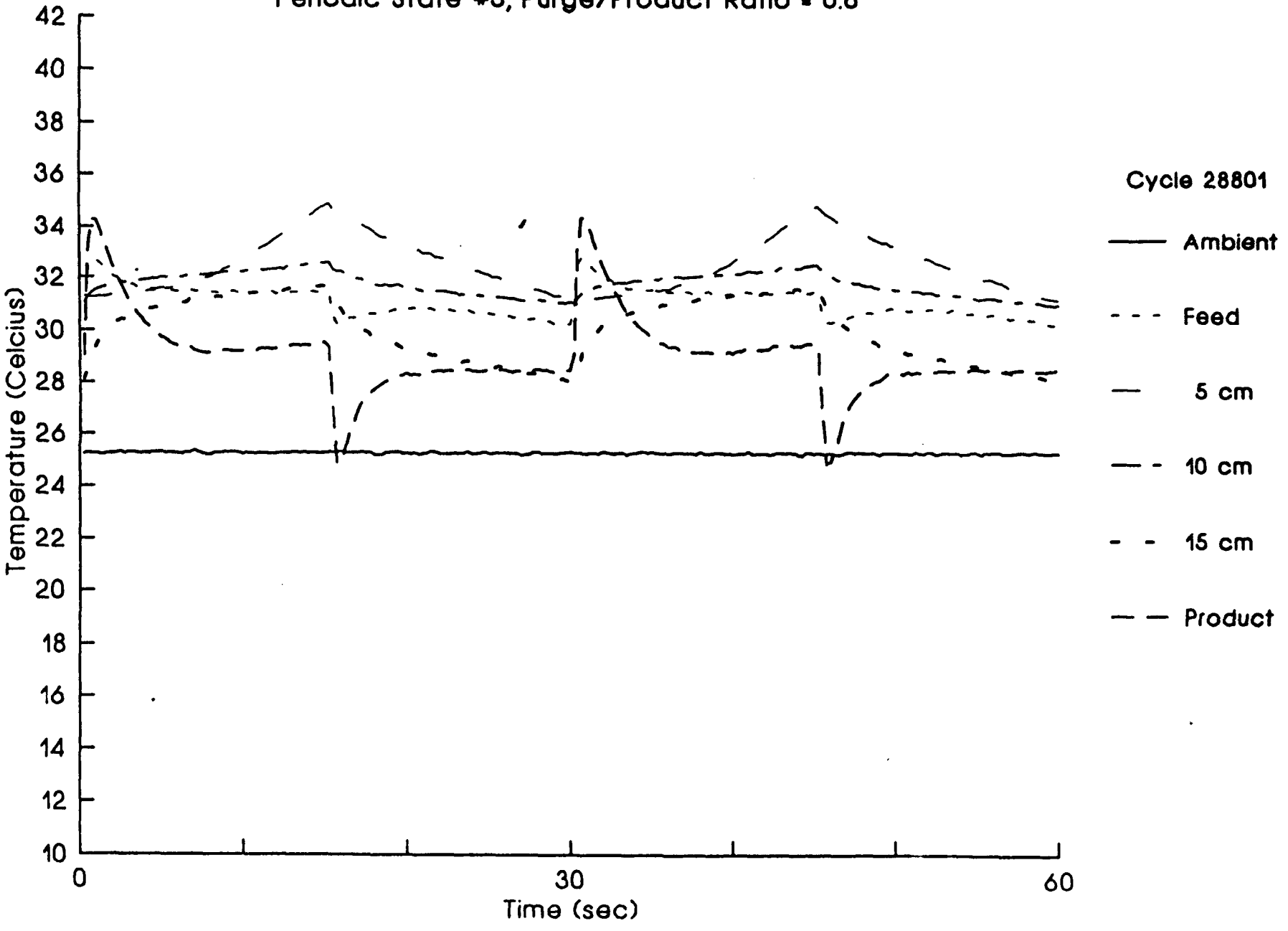

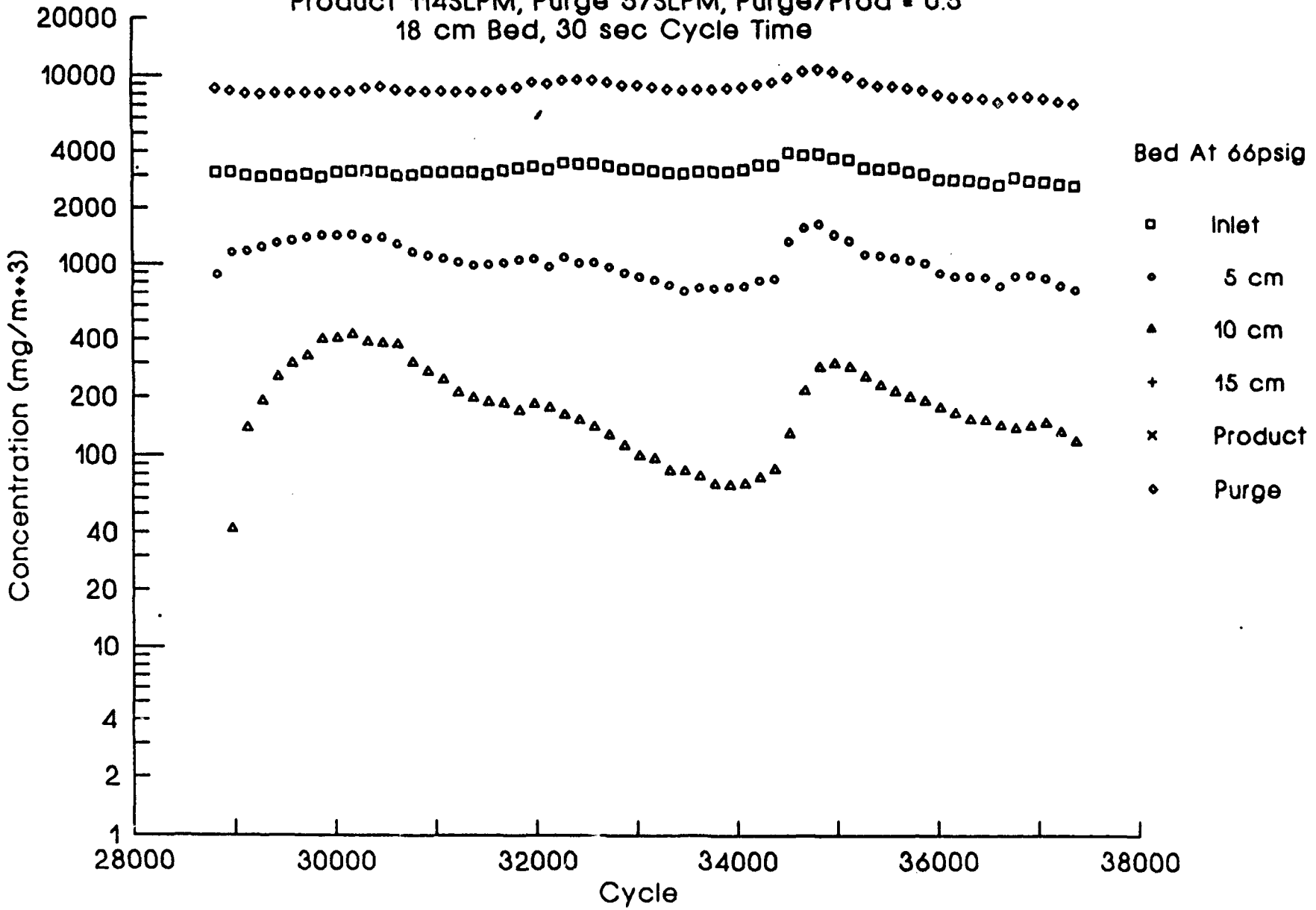
Figure 9. PSA Profile for Water on UOP Molecular Sieve
Product 114SLPM, Purge 57SLPM, Purge/Prod = 0.5
18 cm Bed, 30 sec Cycle Time
Concentration (mg/m**3)
20000
10000
4000
2000
1000
400
200
100
40
20
10
4
2
1
28000
30000
32000
34000
36000
38000
Cycle
Bed At 66psig
Inlet
5 cm
10 cm
15 cm
Product
Purge

Figure 10. In-Bed Temperature Profile for Water on UOP Molecular Sieve
Periodic State #4, Purge/Product Ratio = 0.5

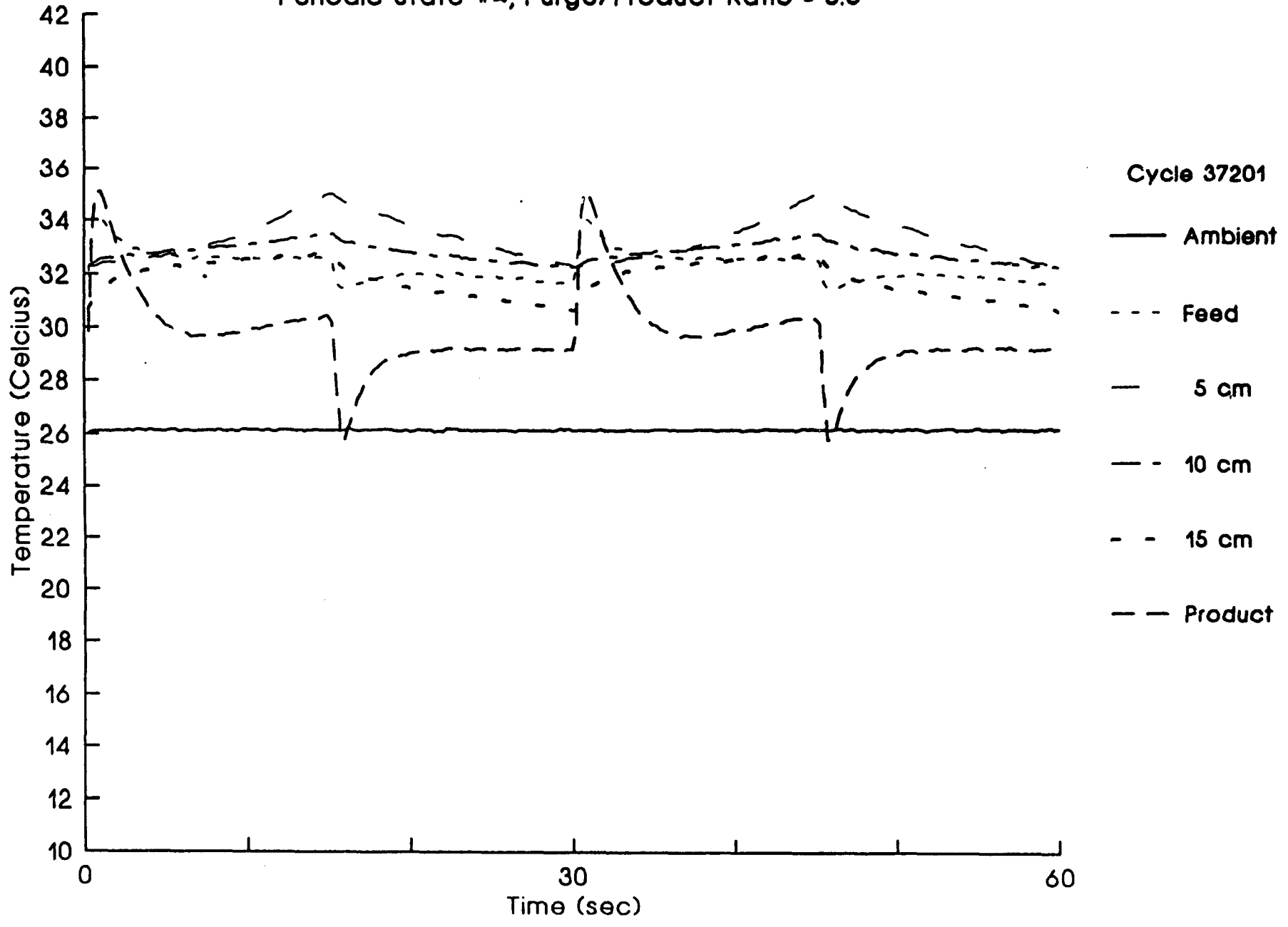

Figure 11. PSA Profile for Water on UOP Molecular Sieve
Product 120SLPM, Purge 49SLPM, Purge/Prod = 0.4
18 cm Bed, 30 sec Cycle Time

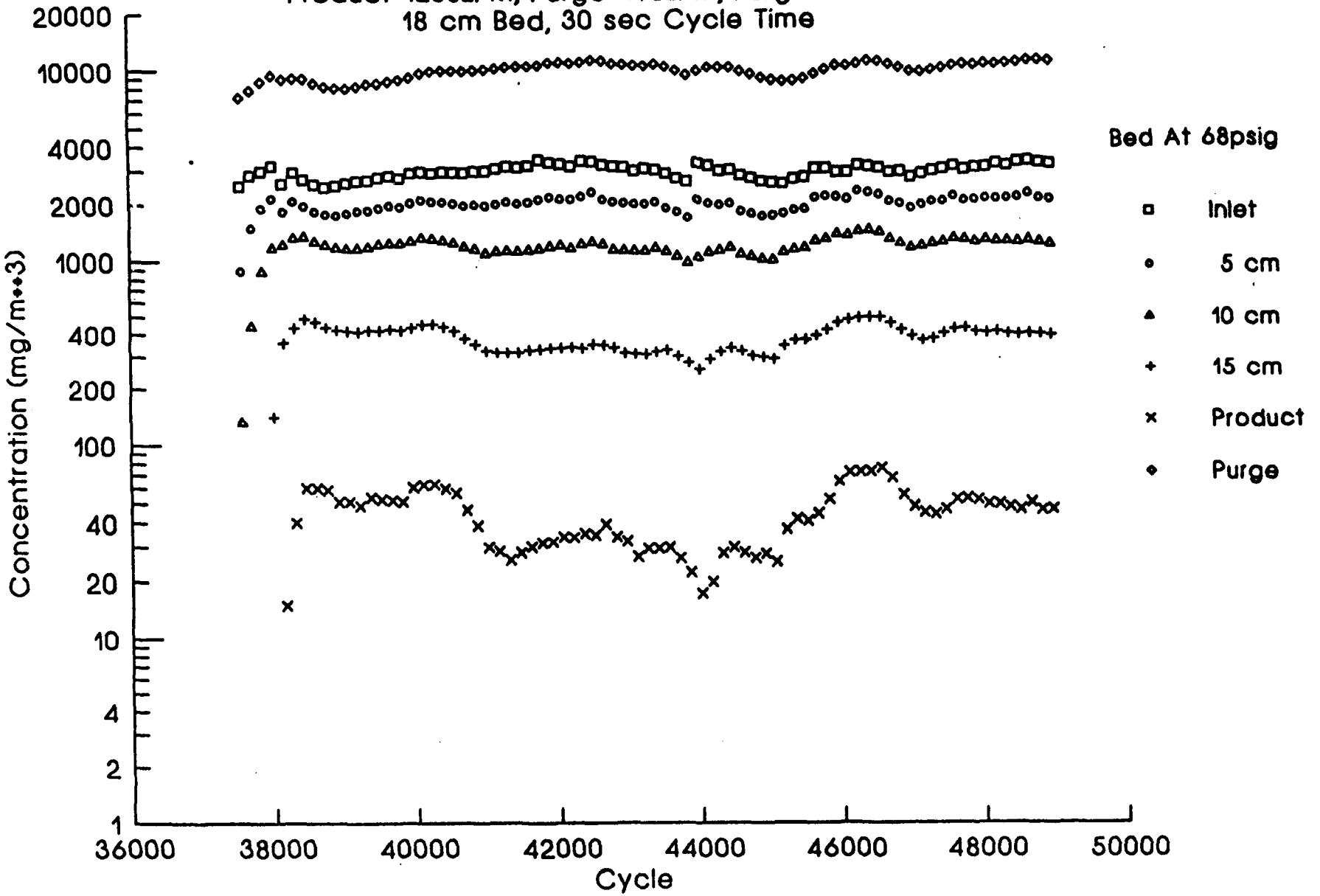

Figure 12. In-Bed Temperature Profile for Water on UOP Molecular Sieve
Periodic State #5, Purge/Product Ratio = 0.4

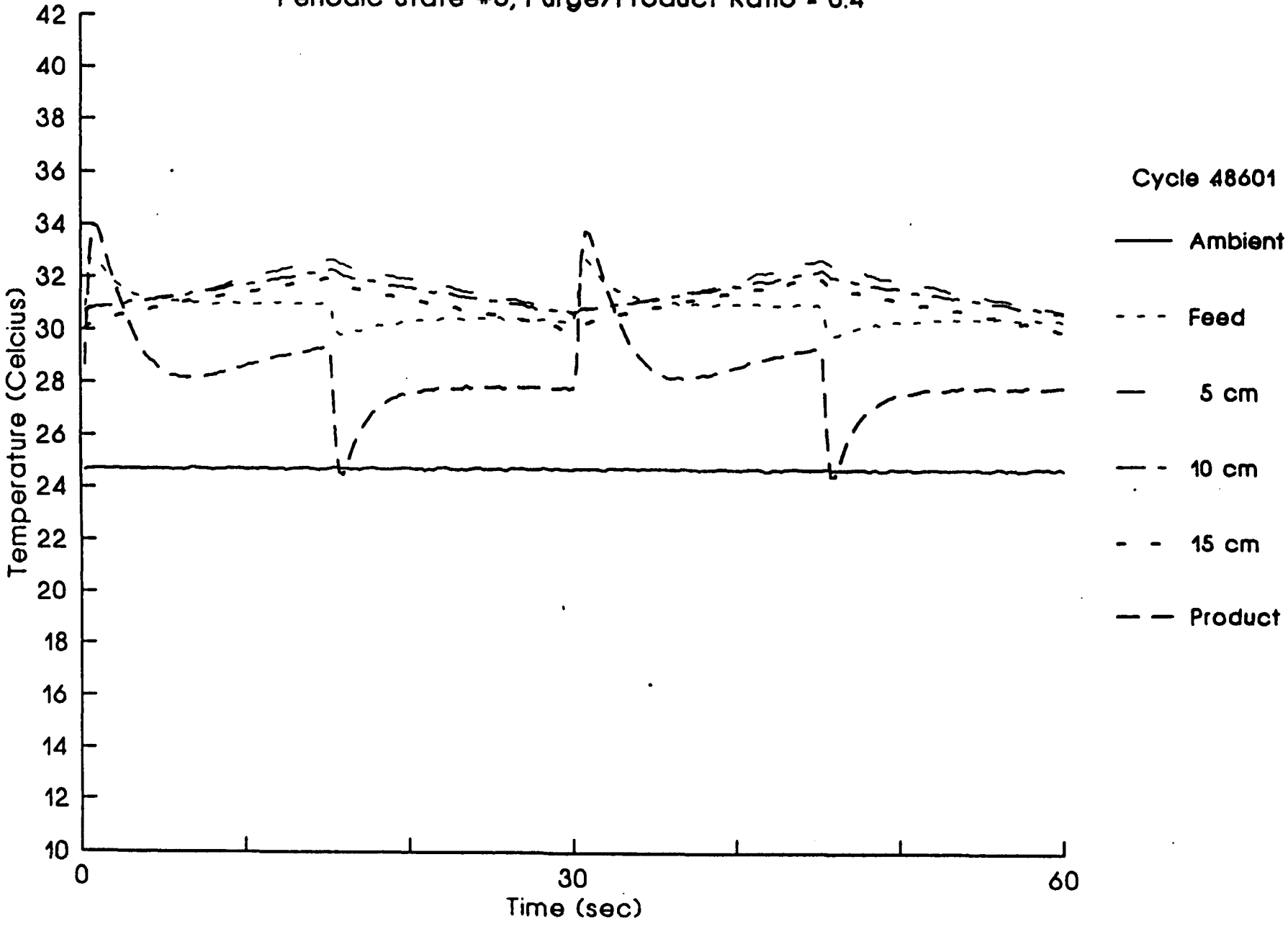

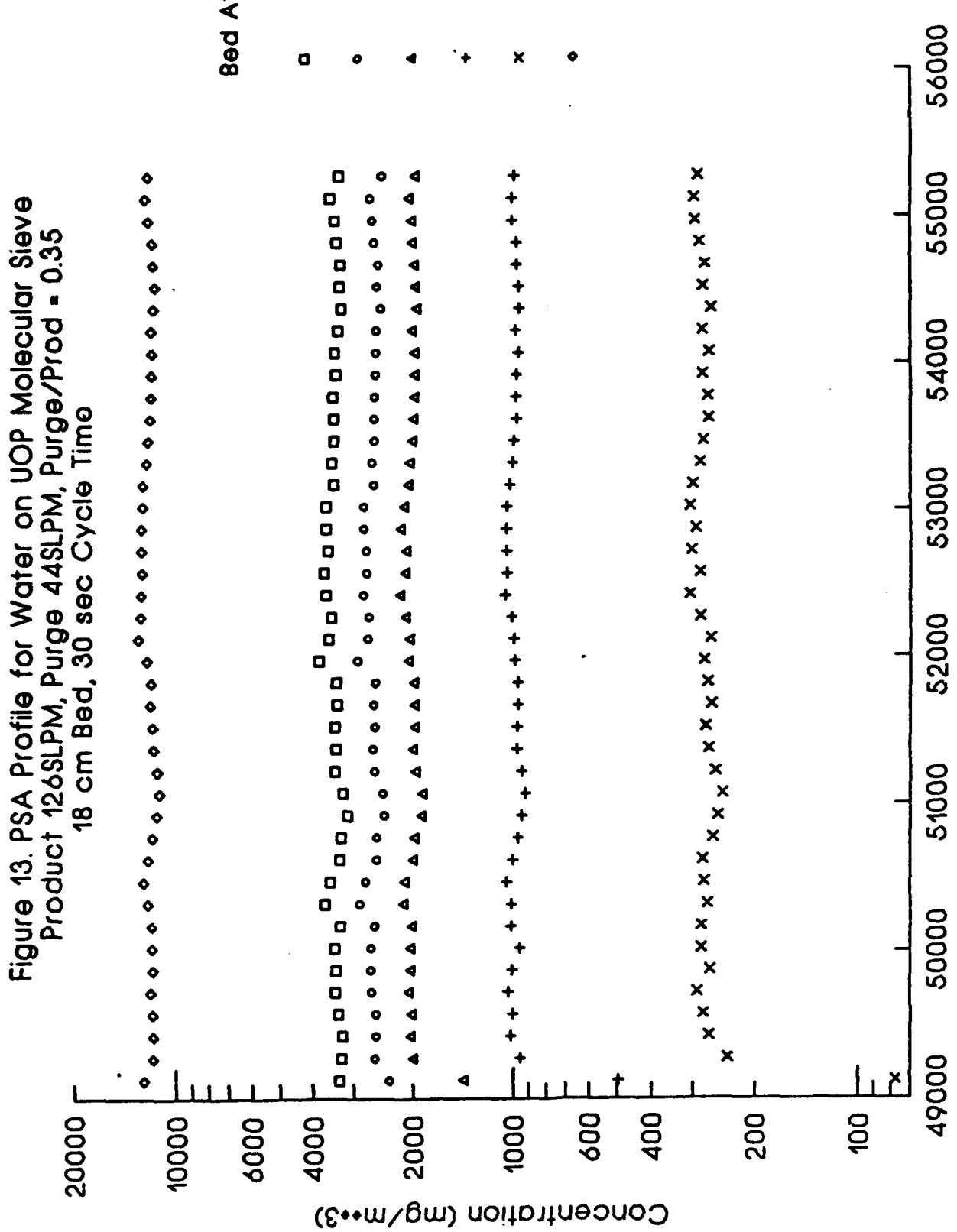
Figure 13. PSA Profile for Water on UOP Molecular Sieve
Product 126SLPM, Purge 44SLPM, Purge/Prod = 0.35
18 cm Bed, 30 sec Cycle Time
Bed At 66psig
Inlet
5 cm
10 cm
15 cm
Product
Purge
Concentration (mg/m**3)
20000
10000
6000
4000
2000
1000
600
400
200
100
49000
50000
51000
52000
53000
54000
55000
56000
Cycle

Figure 14. In-Bed Temperature Profile for Water on UOP Molecular Sieve
Periodic State #6, Purge/Product Ratio = 0.35

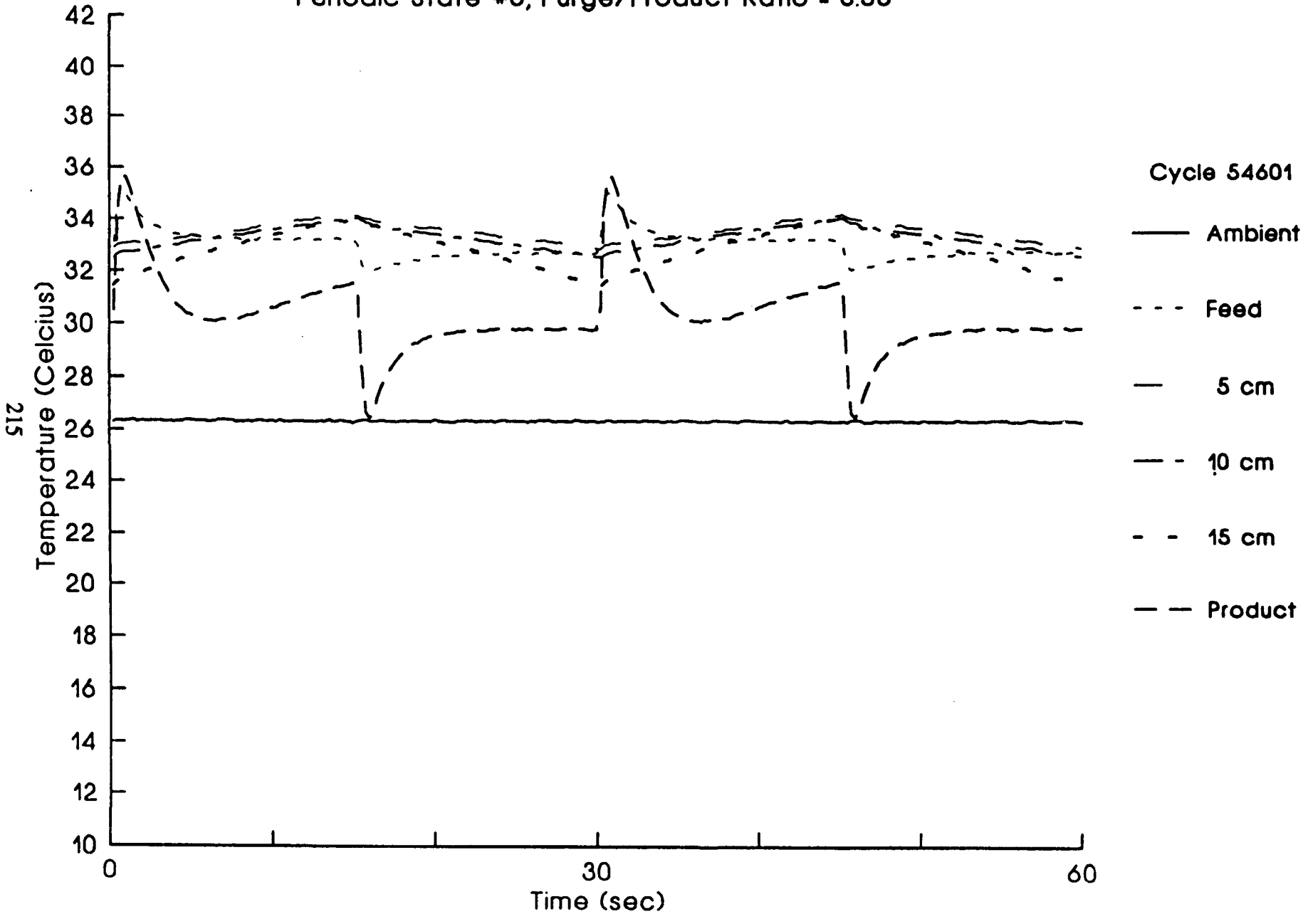

Figure 15. In-Bed Concentration Profiles for Water on UOP Molecular Sieve
Dependence on Purge/Product Ratio

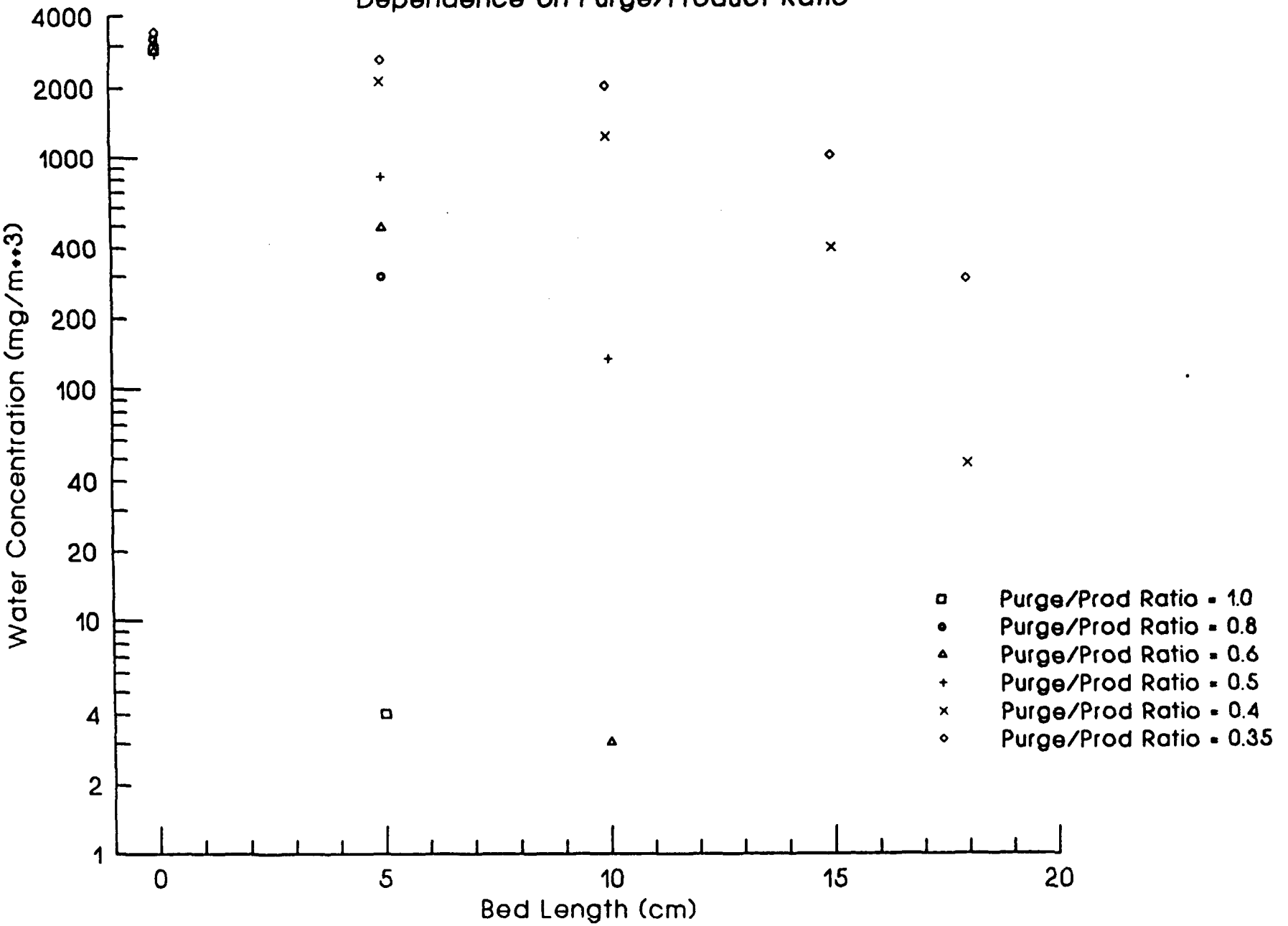

Figure 16. In-Bed Concentration Profiles for Water on UOP Molecular Sieve
Dependence on Purge/Product Ratio

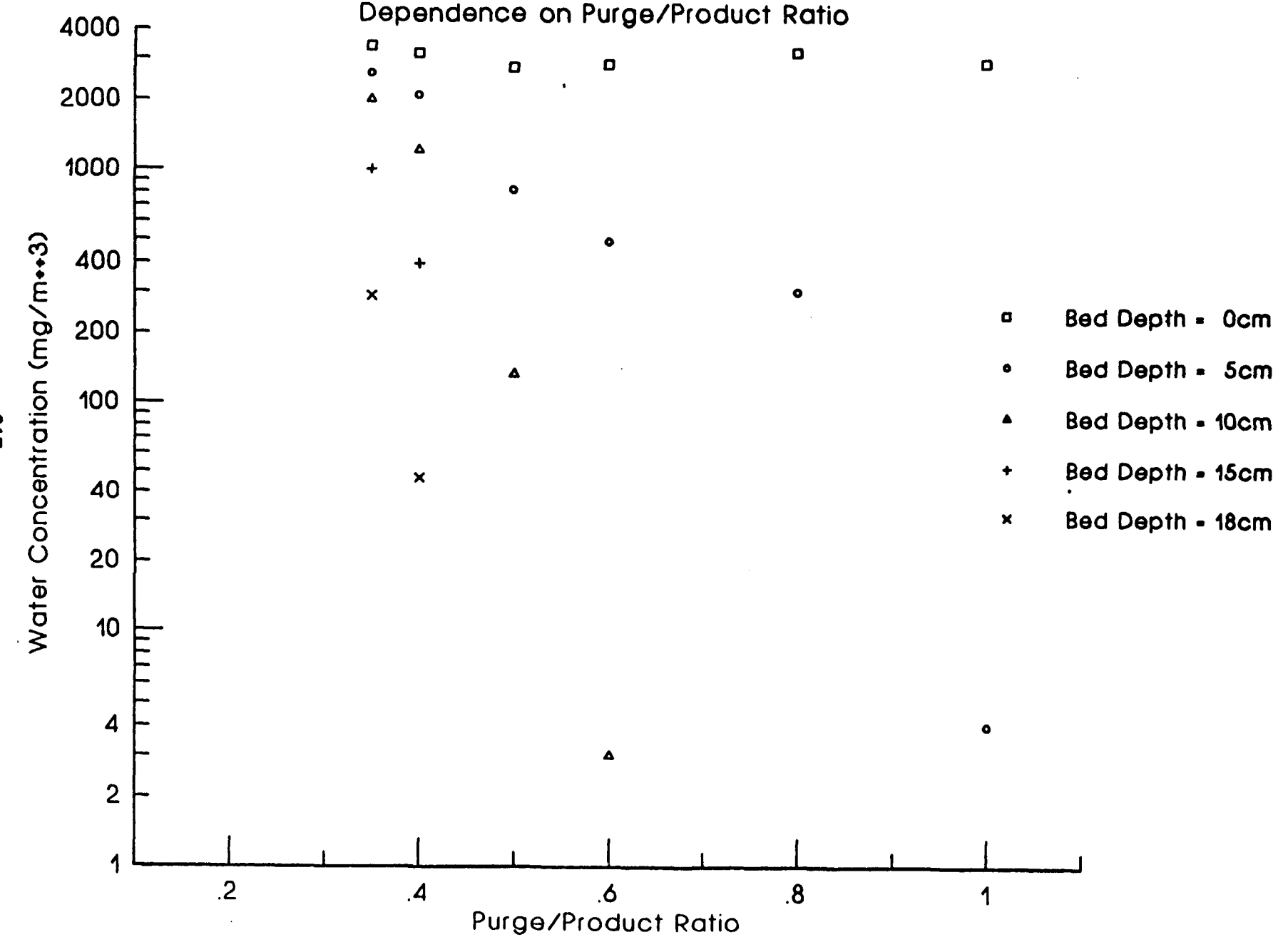

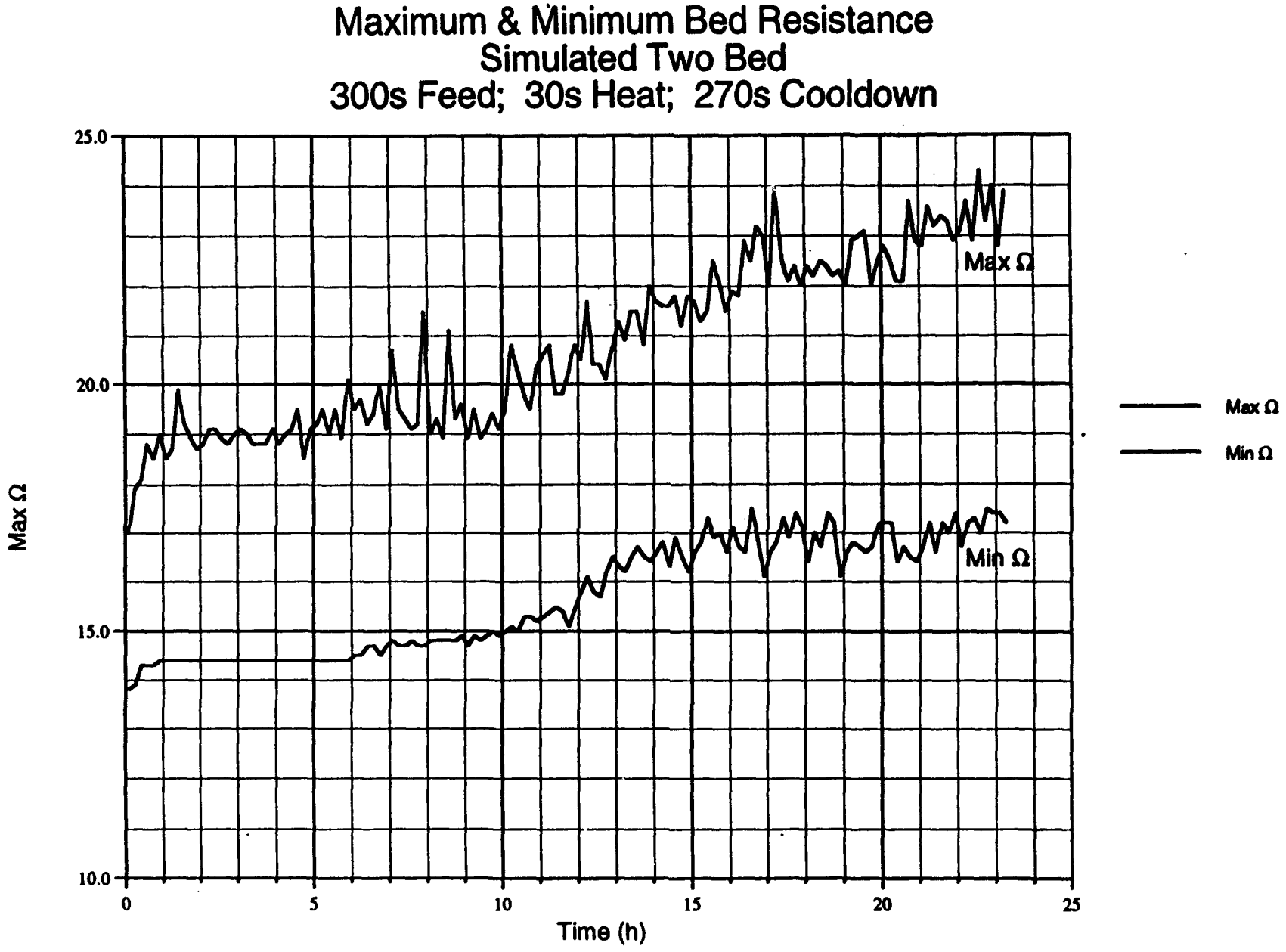
Maximum & Minimum Bed Resistance
Simulated Two Bed
300s Feed; 30s Heat; 270s Cooldown
25.0
20.0
15.0
10.0
Max Ω
0
5
10
15
20
25
Time (h)
Max Ω
Min Ω
Max Ω
Min Ω

Figure 17

Temperature Profiles Feed

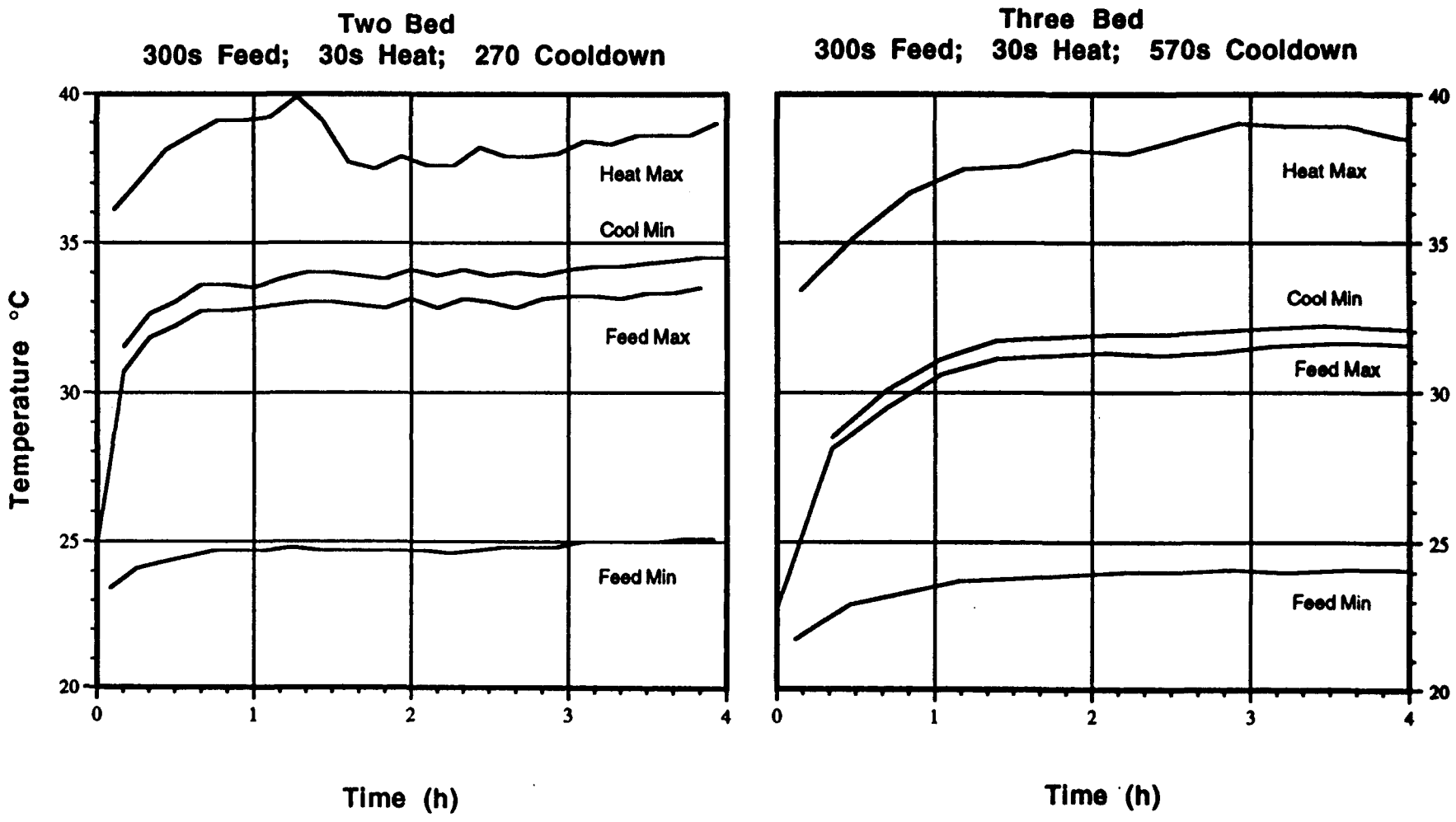

Figure 18

Temperature Profiles 5 cm

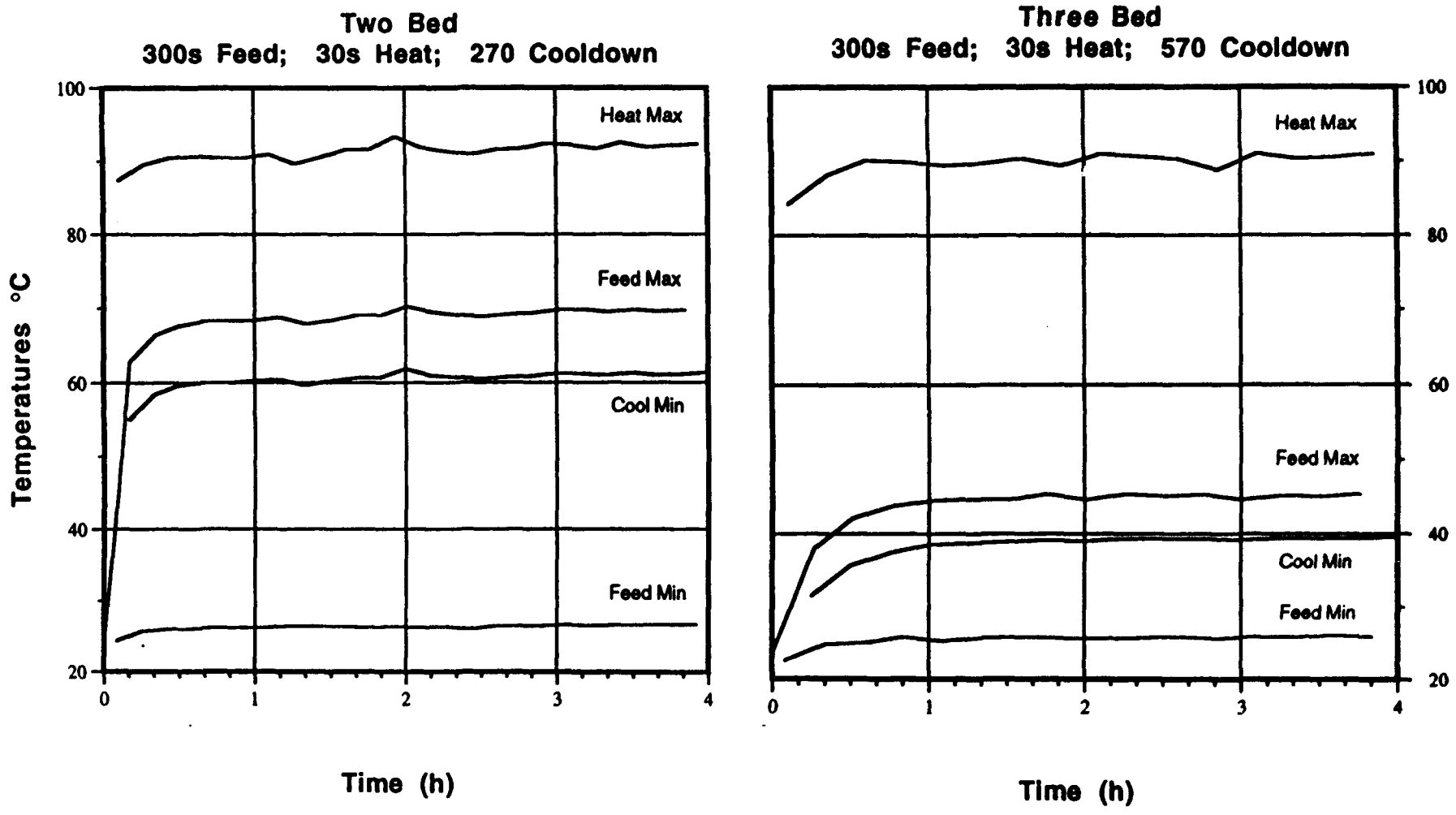

Figure 19

Temperature Profiles 15 cm

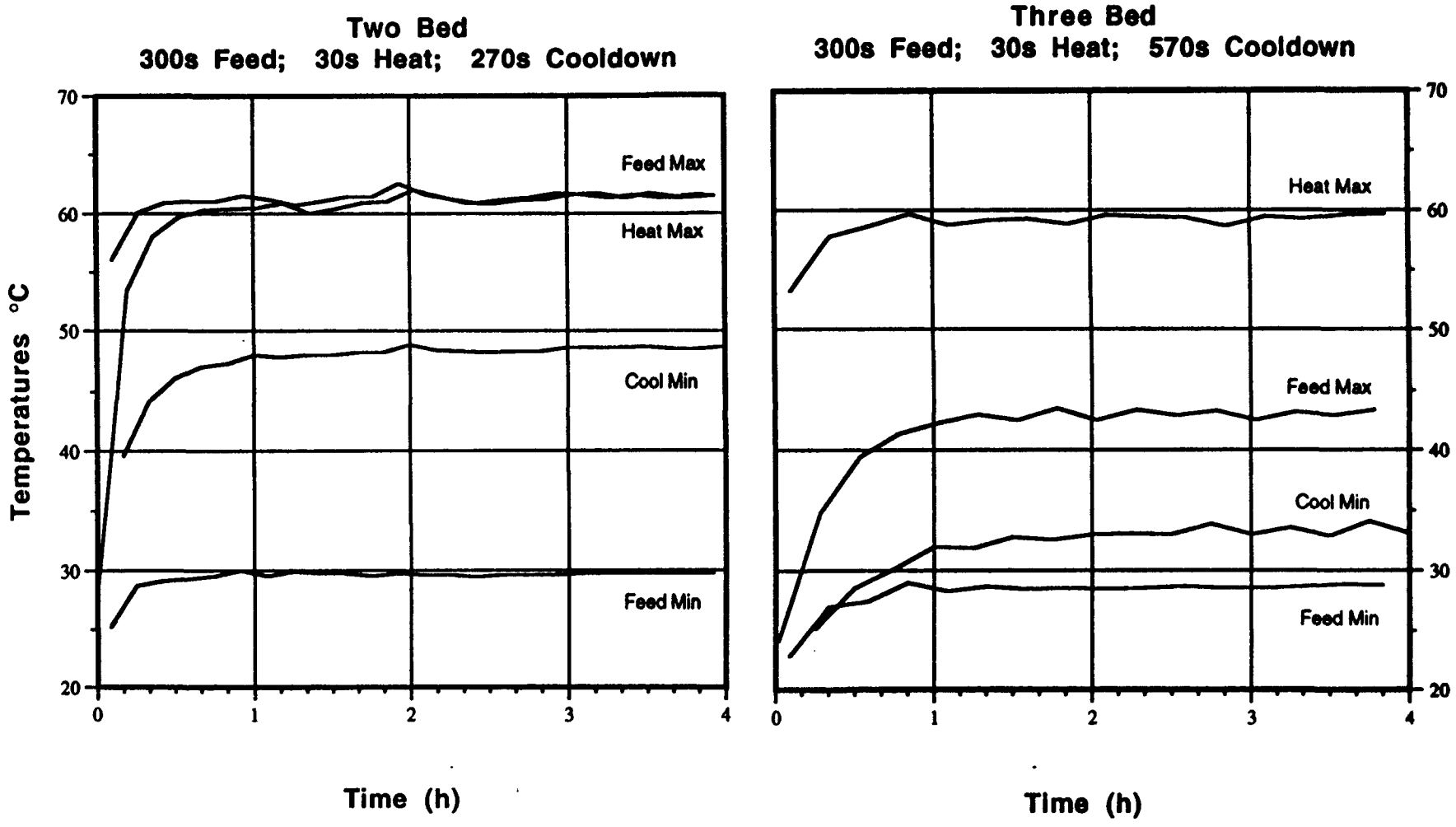

Figure 20

Temperature Profiles 25 cm

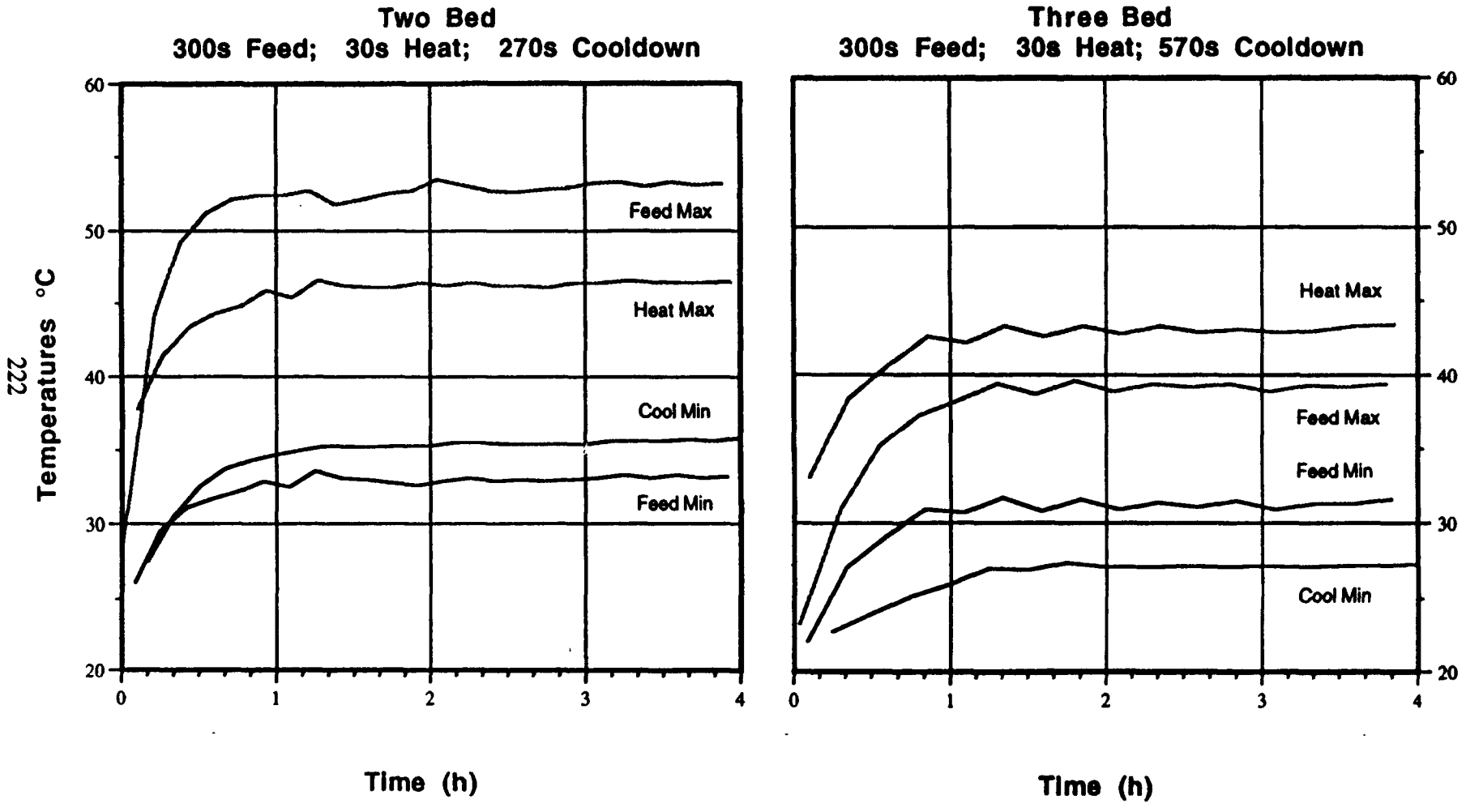

Figure 21

APPENDIX A

MEASUREMENT OF IN-BED TEMPERATURE PROFILES DURING PRESSURE SWING ADSORPTION CYCLES

Amanda B. Brady, David K. Friday, Charles L. Dawson III
Geo-Centers, Inc.
10903 Indian Head Highway
Fort Washington, MD 20744

Leonard C. Buettner
U.S. Army Edgewood Research Development and Engineering Center
Aberdeen Proving Ground, MD 21010-5423

ABSTRACT

Pressure swing adsorption (PSA) is a technology currently being investigated for military and industrial applications. In order to design and build PSA units which meet specific application requirements, it is important to understand the phenomena which control system performance.

Both lab-scale and full-scale systems operating against a chemical challenge exhibit temperature swings between 10°C and 15°C during the course of a cycle. In this study temperature profiles obtained from the following systems are measured using in-bed temperature probes: air in an empty bed, air on glass beads, humid air on BPL carbon, dry air on BPL carbon, nitrogen on BPL carbon, and helium on BPL carbon. The temperature profiles indicate that the adsorption and desorption of air is largely responsible for the cyclic temperature swings observed in the lab-scale and full-scale PSA systems.

INTRODUCTION

Pressure swing adsorption (PSA) is a technology currently being investigated for military and industrial applications. In order to design and build PSA units which meet specific application requirements, it is important to understand the phenomena which control system performance.

Both lab-scale and full-scale systems operating against a chemical challenge exhibit temperature swings between 10°C and 15°C during the course of a PSA cycle. The objective of this study was to determine those phenomena responsible for the measured temperature swings. In-bed temperature profiles were measured under a variety of different conditions to explore the effects of different gases and adsorbents.

APPARATUS

A schematic for the apparatus used for these experiments is shown in Figure 1. The PSA system is a modification of the PSA system used by Friday et. al., [1]. The supply gases used in these experiments were air, with a dew point of -60°C, provided in-house by a compressor and Ballston PSA drier, ultra high purity (UHP) helium and UHP nitrogen from Matheson Gas Products. The Miran infrared analyzers were not used in this study. An Apple IIci computer was used to obtain the temperature profiles using a National Instruments termination bread board, and 1/32" type T ungrounded quick connect sub miniature probes by Omega, (time constant = 2.85 sec.).

Table 1. List of Experiments

Experiment	Gas	Adsorbent
1 (Base Case)	Dry Air	BPL Carbon
2	Nitrogen	BPL Carbon
3	Humid Air	BPL Carbon
4	Dry Air	Empty Bed
5	Dry Air	Glass Beads
6	Helium	BPL Carbon

RESULTS AND DISCUSSION

The results take two forms, transient data and periodic-state data. Figures 3 through 5 are examples of transient data from the base case conditions (dry air on BPL). After the transient data has been discussed, the periodic state data for each case will be examined.

Figure 3 shows temperature profiles from the beginning of the Air/BPL experiment. The first 15 seconds are the pressurization and feed step, while the 15 to 30 second phase represents the blowdown and purge phases. At the beginning of the experiment, all in-bed temperatures were approximately the same. During the first cycle, all of the measured

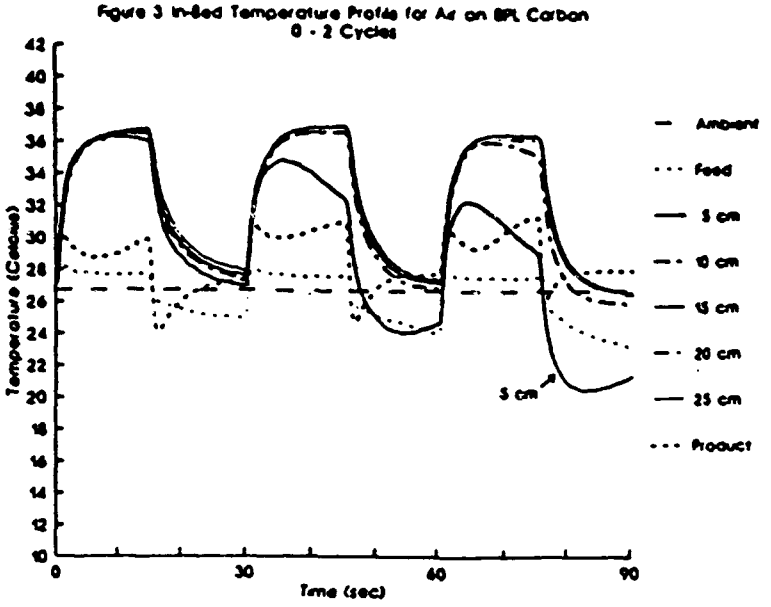

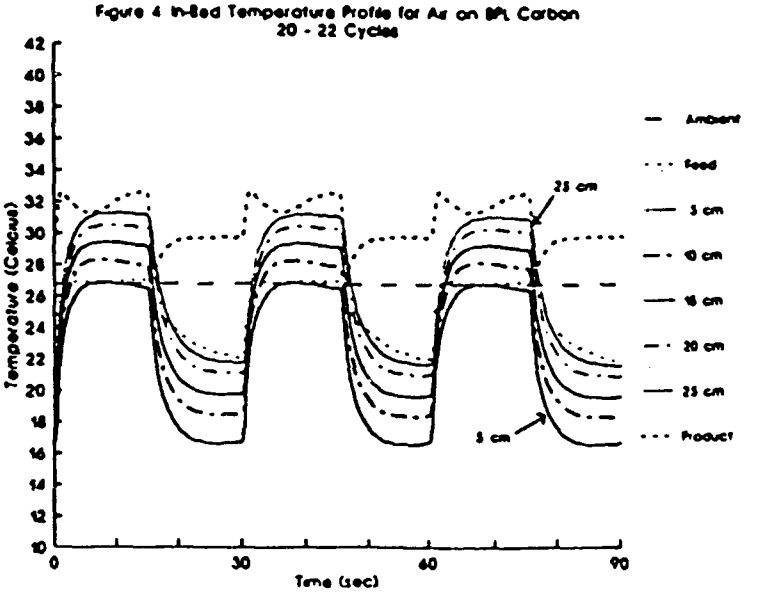

temperatures swing between 27°C and 37°C. However, a rapid cooling of the bed is observed at 5 cm during the second and third cycles. There is also some noticeable cooling beginning to occur at 10 cm during the third cycle.

Figure 4 shows the same experiment after 20 cycles. Although the same magnitude is seen in the temperature swings, there has been a significant amount of cooling in the bed. At 5 cm, the coldest point in the bed, the low temperature is 16°C, which is 10° cooler than ambient.

At 240 cycles, as shown in Figure 5, temperature profiles during each cycle have the same shape as at 20 cycles. The temperature at the front of the bed is only about a half degree cooler than at 20 cycles. However, there is additional cooling at the product end of the bed. After the system has completed 100 cycles there is no additional change to the temperature profiles of the system, indicating that the system is operating at periodic-state. For this system, periodic-state is reached when

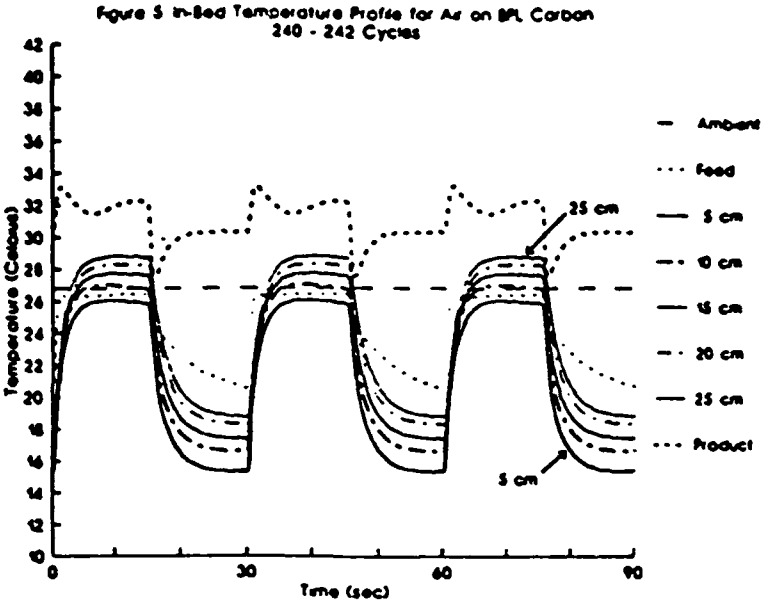

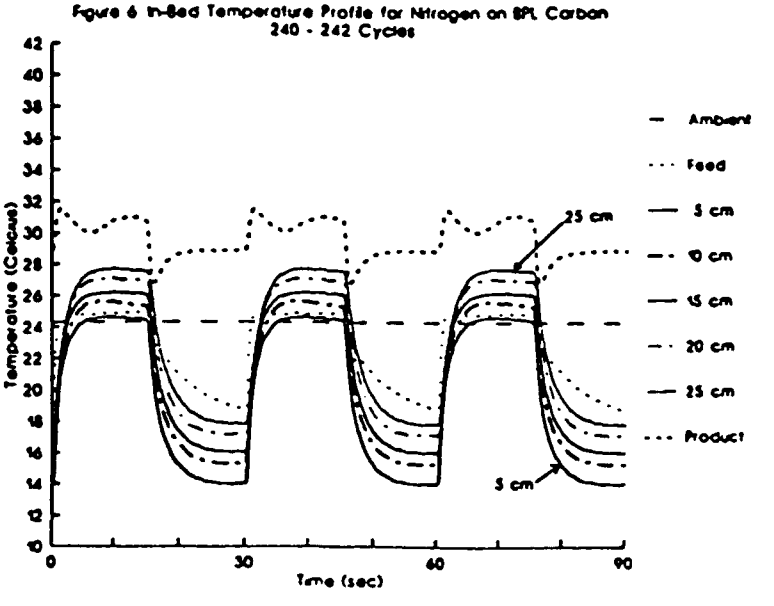

the temperature at each point in the bed follows the same path during the course of successive cycles.

The periodic-state results of nitrogen on BPL, shown in Figure 6, are very similar to the results for air on BPL, (Figure 5). The lowest measured temperatures using nitrogen are slightly lower than those observed for air, but the changes can be attributed to the fact that the room temperature was 2° lower during the nitrogen experiment. The temperature swings at each point in the bed, however, are very close to those of air.

Figure 7 shows the results of humid air on BPL carbon. The shapes of the curves are similar to those of dry air on BPL, but the temperature swings at each point in the bed are between 1° and 1.5°C less than for dry air. This is due to the reduced capacity for nitrogen and oxygen adsorption due to the presence of adsorbed water.

The temperature profiles for air in an empty bed are shown in Figure 8. The swings are the largest of all of the experiments because

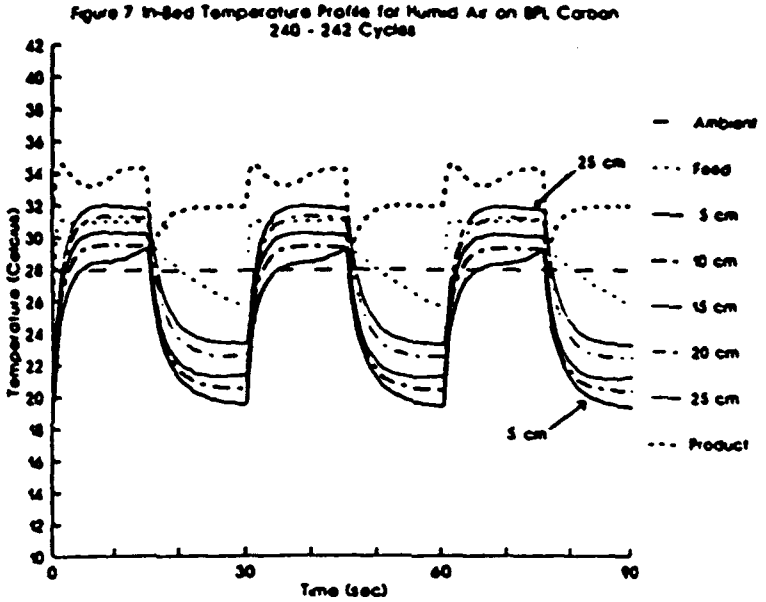

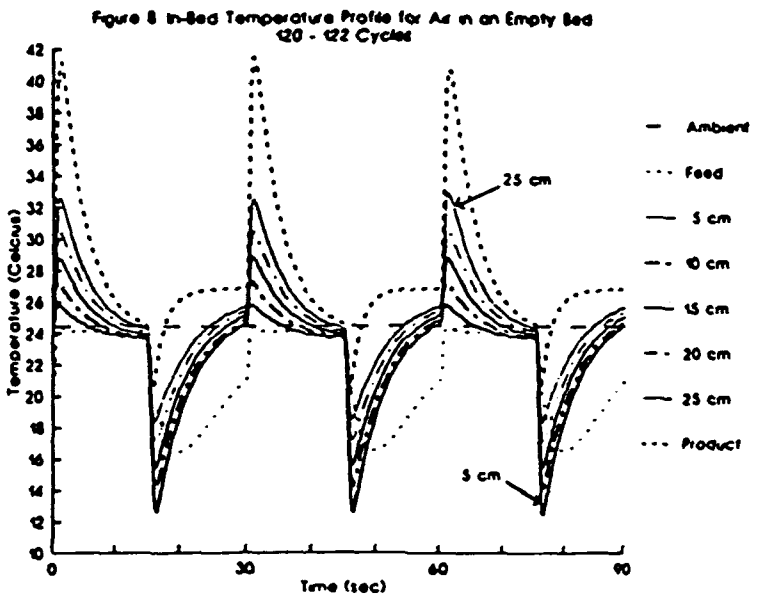

there is no heat capacity in the bed to dampen out the swings. Heating is due to compression, and cooling is a result of expansion.

Figure 9 shows the temperature profiles for air on glass beads. These results show the effects of packing the bed with an inert material, i.e. has no adsorption capacity. In Figure 8 temperature swings of 13 to 14°C are measured using an empty bed. However, in Figure 9, due to the heat capacity of the glass beads, temperature swings of only 1/2° C are measured at periodic-state.

Finally, Figure 10 shows the results of helium on BPL. Again the temperature swings observed in the bed are minimized by the heat capacity per unit volume of the BPL. Consequently, temperature swings of only 1°C are seen in the bed during the course of a cycle. The observed swings are larger than those for air on glass beads because the heat capacity per unit volume for glass beads is two to three times that of BPL. Hence, in the two experiments showing only the effects of compression and decompression, the larger

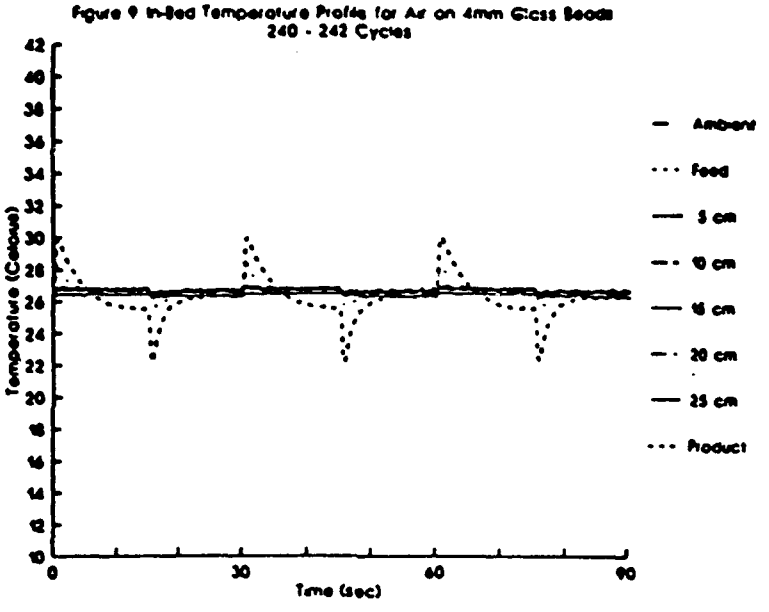

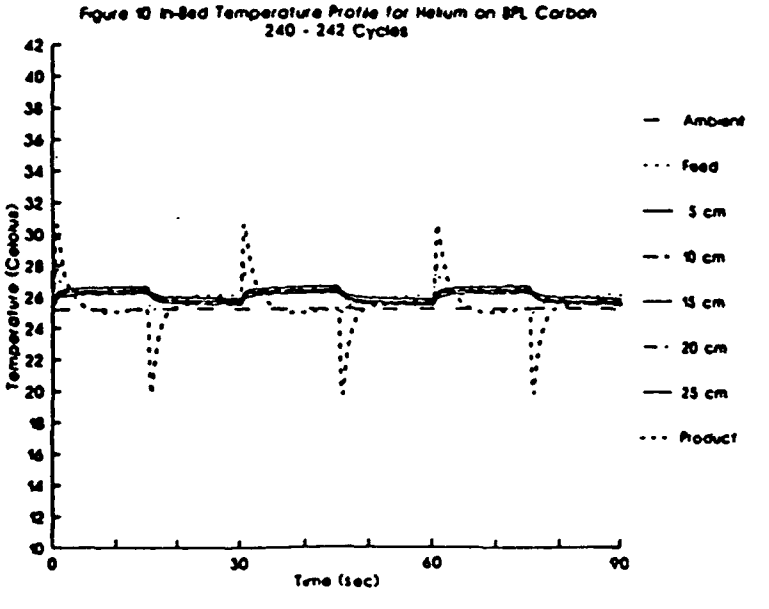

Table 2. Maximum Temperature Swings Observed During a Cycle

Experiment	Feed	5 cm	10 cm	15 cm	20 cm	25 cm	Product
BPL/Air	5.9	10.8	10.5	10.3	10.0	10.0	5.6
BPL/N_2	6.2	10.6	10.3	10.2	9.9	9.9	4.7
BPL/Humid Air	5.5	9.8	9.0	9.0	8.8	8.6	5.1
Empty Bed/Air	7.9	13.3	13.0	13.4	13.4	14.2	20.9
Glass Beads/Air	2.8	0.3	0.3	0.4	0.4	0.3	7.8
BPL/He	3.0	0.8	0.9	0.8	0.9	0.8	10.8

temperature swings are observed in the system with less heat capacity per unit volume.

When comparing the results of air on BPL with those for helium on BPL, the effects of adsorption and desorption of air become obvious. The maximum temperature swings observed in the inert system, helium on BPL, were only 1°C. Whereas the temperature swings for air on BPL were an order of magnitude higher. This also explains the cooling effects observed in the transient data. The adsorption and subsequent desorption of air in the front of the bed is responsible for the rapid cooling measured at 5 cm in Figure 3. Net cooling results because twice as many standard column volumes of air are passed through the bed in the feed step compared to the purge step. The amount of energy liberated during adsorption of air (pressurization & feed) and consumed on desorption of air (purge & blowdown) are equal. However, since more standard liters of gas are passed through the bed on the feed step than during the purge step, a net cooling is achieved during one cycle.

SUMMARY

The in-bed temperature profiles of air on BPL carbon are very similar to those for nitrogen on BPL. Humid air on BPL shows a slight reduction in magnitude of the temperature swings. The largest swings are observed with air in an empty bed resulting from compression and expansion. Glass beads and BPL carbon both act to effectively dampen the magnitude of the temperature swings due to the heat capacity of the packing materials. The results for glass beads show the smallest temperature swings because the glass beads have a higher heat capacity per unit volume than BPL carbon. The temperature effects of the adsorption and desorption of air can clearly be seen by comparing the temperature profiles from the air on BPL experiment with the results for helium on BPL.

CONCLUSION

The temperature swings of 10° to 15° C observed in the bed during the course of a PSA cycle are due to the adsorption and desorption of air.

REFERENCES

[1] Friday, D. K., Brady, A. B., Mahle, J. J., and Buettner, L. C., "A Parametric Study of PSA for Air Purification Applications", Proceedings of the 1992 U. S. Army ERDEC Conference on Chemical Defense Research.

APPENDIX A-11

QUARTERLY PROGRESS REPORT

GC-PR-2194-11

REPORTING PERIOD: 2/1/93 - 4/30/93

REPORTING DATE: 5/15/93

CONTRACT NUMBER: DAAA15-90-C-1056

CONTRACT TITLE: Improved Filtration Materials and Modeling

I. Adsorption Equilibr[illegible]

Single Compone[illegible] Measurements and Apparatus

Shown in Figure 1 are isotherms for trichlorofluoromethane (R-11) on 13X molecular sieve at 298K, 323K and 348K. We are checking several reasons for the scatter in the data. One possible problem that is currently being investigated is the temperature control algorithm.

Multicomponent Measurements and Apparatus

A significant problem developed during the quarter. Experiments where PFCBa/H_2O isotherms were measured on 13X molecular sieve showed erratic and unrealistically large water loadings. Several possible sources for this behavior were explored. After several weeks, it was determined that an internal leak in a four-way valve was most likely responsible. This was a very difficult problem to isolate since the system meets the pressure test.

The explanation for the large water loadings is as follows. During the desorption step, the bed is heated to remove the chemical vapors from the adsorbent. A pump is used to circulate the vapor around the closed-loop. The location of the four-way valve is up-

steam of the pump, and therefore at a slightly lower pressure. The pump, in effect, pulls some ambient vapor into the closed-loop and a cryogenic trap subsequently collects the water carried by the ambient vapor.

The stems on the four-way, flow direction valves were tightened to try to alleviate the leak problem. We are currently running tests to determine if this was successful.

II. Pressure Swing Adsorption

Experiments and Apparatus

A new air compressor was installed in the building. Some significant problems developed which caused the pressure to drop below the feed pressure needed for PSA experiments. The compressor was sent back to the factory for repairs. In spite of these problems, PSA experiments were successfully conducted which demonstrate that temperatures may be used to infer concentration.

An experimental study was performed with R-11 on BPL carbon to correlate the magnitude of the temperature swing during a cycle at a given axial position in the bed with the vapor-phase concentration at that position. The conditions for the experiment are given in Table 1.

Table 1. Conditions for R-11/BPL Carbon PSA Experiment

Adsorbent	12x30 mesh BPL Carbon
Feed Pressure	46 psig
Feed Flow Rate	100 SLPM
Feed Concentration	3.2×10^3 mg/m^3
Product Flow Rate	48 SLPM
Purge Flow Rate	52 SLPM
Bed Diameter	3.8 cm
Bed Depth	24 cm
1/2 Cycle Time	15 sec.
Cycle Type	2-step

R-11 was continuously fed to a bed of BPL activated carbon for approximately 8000 full cycles (2.8 days). In-bed vapor-phase concentration profiles were measured every 90 cycles (45 minutes). In-bed temperatures were sampled 4 times a second for 2 full cycles commencing 5 cycles prior to the start of each in-bed concentration profile measurement. The minimum temperature during the two full cycles was subtracted from the maximum temperature during the same two cycles to obtain the maximum temperature difference.

The maximum temperature difference and the vapor-phase concentrations are plotted versus the number of cycles and shown in Figure 2. As each concentration port breaks through, the maximum temperature difference decreases to about 4 C. A very interesting and new result can also be observed. There is a noticeable rise in the temperature difference several hundred cycles prior to the peak and subsequent fall. This rise starts about 100-200 cycles prior to the first measured concentration. Examine the behavior the vapor-phase concentrations and the maximum temperature difference at 10 cm, 15 cm, and 20 cm and this trend holds true. These results demonstrate the potential for temperatures to be used as an in-bed measure of the position of a contaminant mass transfer front. More importantly, the rise in temperature differences provides information well ahead of the concentration measurement. Note that the concentration measurement is sensitive to several mg/m^3.

III. Temperature Swing Adsorption (TSA)

The hardware and software controlling the TSA system was modified by incorporating the National Instruments SCXI Signal Conditioning System. The system is modular in its design, and represents a significant improvement in laboratory automation.

Hardware includes a chassis and plug-in modules for both analog and digital I/O. Special modules for temperature and pressure measurements may also be used. Each module requires careful examination of the manuals to understand the method by which it

needs to be integrated into the data acquisition system. In most cases jumpers had to be configured to match the board to the desired task. The SCXI hardware has its own multiplexing capability, and needs to be integrated with any multiplexing operations performed by the host computer. These concerns were addressed, and the SCXI hardware is currently in use.

The National Instruments software for the TSA system was revised to incorporate the new hardware. Coordination with the factory was required to find the correct combination of old and new drivers which correctly controlled both the new and old hardware.

TSA experiments were performed using the newly installed SCXI hardware and modified software.

Table 2. Conditions for CFC-113/BPL Carbon TSA Experiment

Adsorbent	12x30 mesh BPL carbon
Chemical	CFC-113
Feed Flow Rate	75 SLPM
Target Feed Conc.	4.0×10^3 mg/m^3
Feed Time	300 sec.
Purge Flow Rate	15 SLPM
Cool-Down Time	270 sec.
Power Input	500 watts
Heat Time	30 sec.
Cycle Type	3-step

MIRAN 80 infrared detectors (IR's) were used to monitor the purge, product and feed stream CFC-113 concentration. The product IR was calibrated for the lowest concentration range possible, about 5-400 mg/m^3. Besides the in-bed temperature sampling at 5-cm intervals, an overall material balance was calculated.

The objective of the experiment was to determine if TSA cycle times of the order of 10 minutes, as opposed to several hours, could be successfully used. Cycle time is important because, in general, the longer the cycle time, the bigger the beds need to be to prevent breakthrough of light gases during the feed step. Cycle times of an hour or more are probably not feasible for most military applications because of size constraints. The hypothesis for this experiment, and for TSA operation in general, is that the cycle times may be significantly reduced by starting the next feed step while a portion of the bed remains warm. Previous studies have required that the entire bed be cooled close to ambient (or below) temperature. This required an extended cool-down period.

Shown in Figures 3-7 are the maximum and minimum temperatures at each point in the bed for the entire 48-hour experiment. At 5cm (Figure 3), the highest temperature achieved in the bed is during the heating step, about 60 C initially, and about 52 C by the end of the experiment. The other three temperatures describe the behavior during the feed step. For simplicity, consider only the last 18 hours of the experiment. At the start of the feed step, the temperature is about 40 C (cool-min.). Sometime during the feed step it warms up to 47 C, because of the warmer carbon which is between the bed inlet and 5cm. At the end of the feed step the 5 cm point in the bed is back down to the feed air temperature of 25 C.

Figure 7 demonstrates what happens at the product end of the bed during a cycle. During the heating step (after 30 hours), the maximum temperature is 32 C. The bed cools back down to about 29 C during the cool-down step (cool-min). During the feed step, the temperature wave at the front of the bed is pushed through, resulting in a maximum temperature of about 38 C at the product end. The product end then is cooled at the end of the feed step back down to 27 C (feed-min).

The product IR showed no chemical during the entire 48-hour experiment. Shown in Figure 8 is an overall material balance calculation using integrated feed and purge

concentration profiles which shows that the system is at a periodic state. The difference between the two values is probably a calibration error which will be investigated. These results show that the TSA system may be successfully operated using the feed air to perform the final cooling of the bed, without "leakage" of the contaminant with the feed step temperature wave.

IV. Other

An effort has been initiated to perform the peak integration from the HP GC-5890 using LabView software. Currently, the GC information is obtained from the integrator by reading in the report table. The major problem is that the integrator communications is not robust. Any error in the communications can lock-up the integrator and shut-down sampling. Even running out of paper for the integrator can shut the sampling down. Special hardware was purchased from National Instruments to monitor the ChemStation-GC communications link to remove the source of system failure. The goal is to have LabView communicate with the GC (starts, stops, etc.), and subsequently perform peak integration. It appears that the communications protocol can be duplicated, and that the GC's may be controlled using existing Macintosh-based laboratory automation systems.

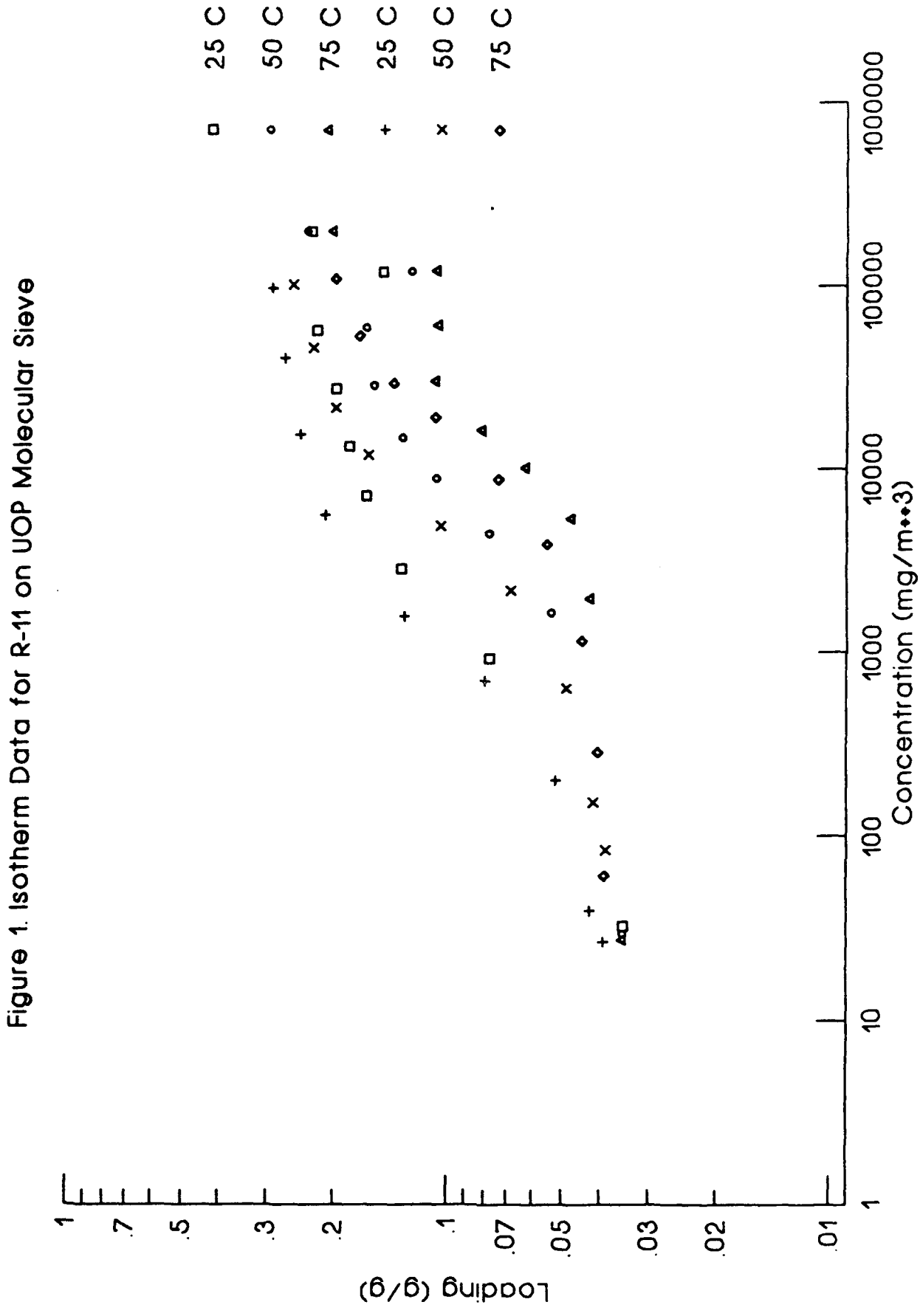

Figure 1. Isotherm Data for R-11 on UOP Molecular Sieve

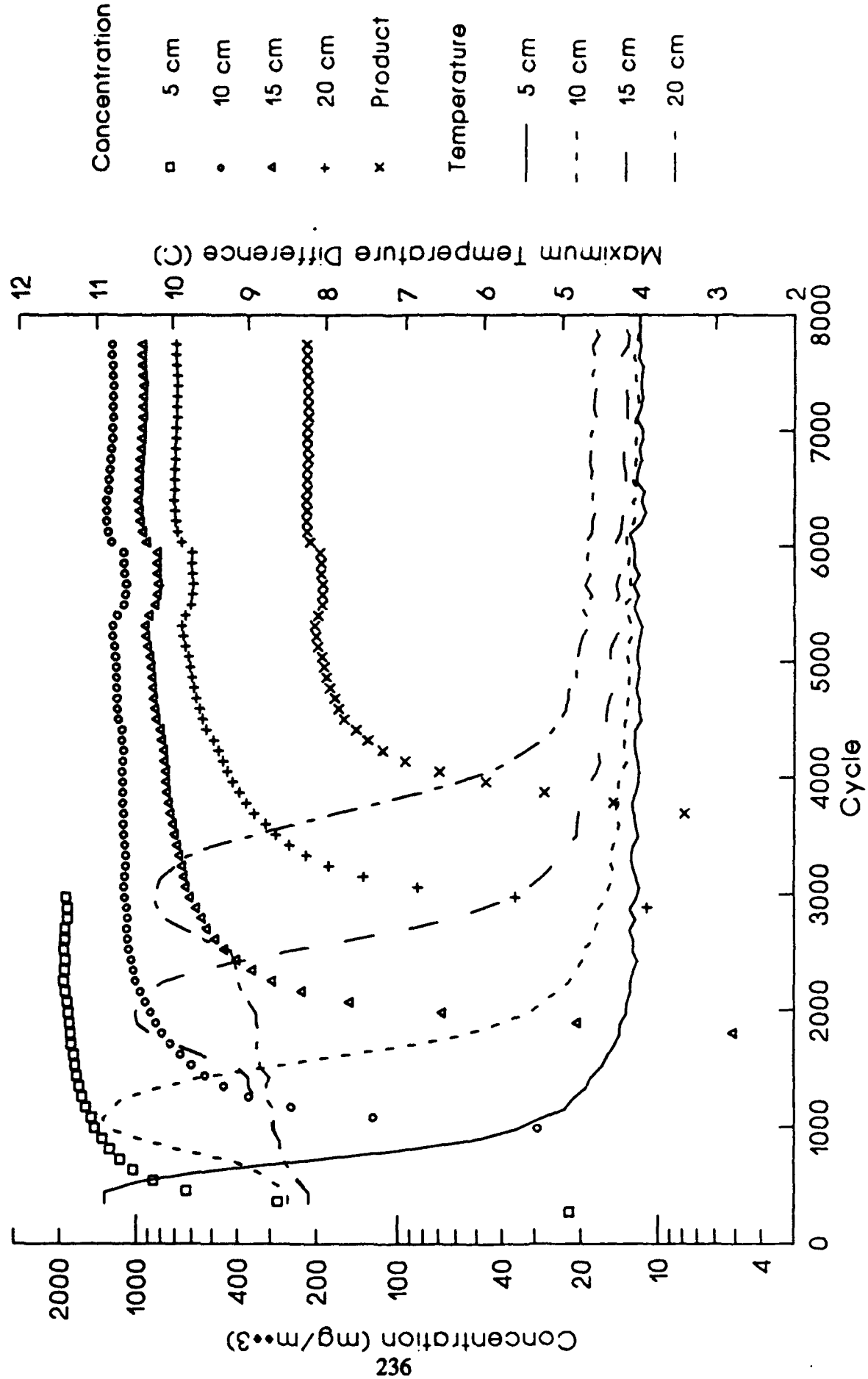

Figure 2. PSA Profile for R11 on BPL Carbon
Maximum Temperature Differences and In-Bed Concentrations

Figure 3

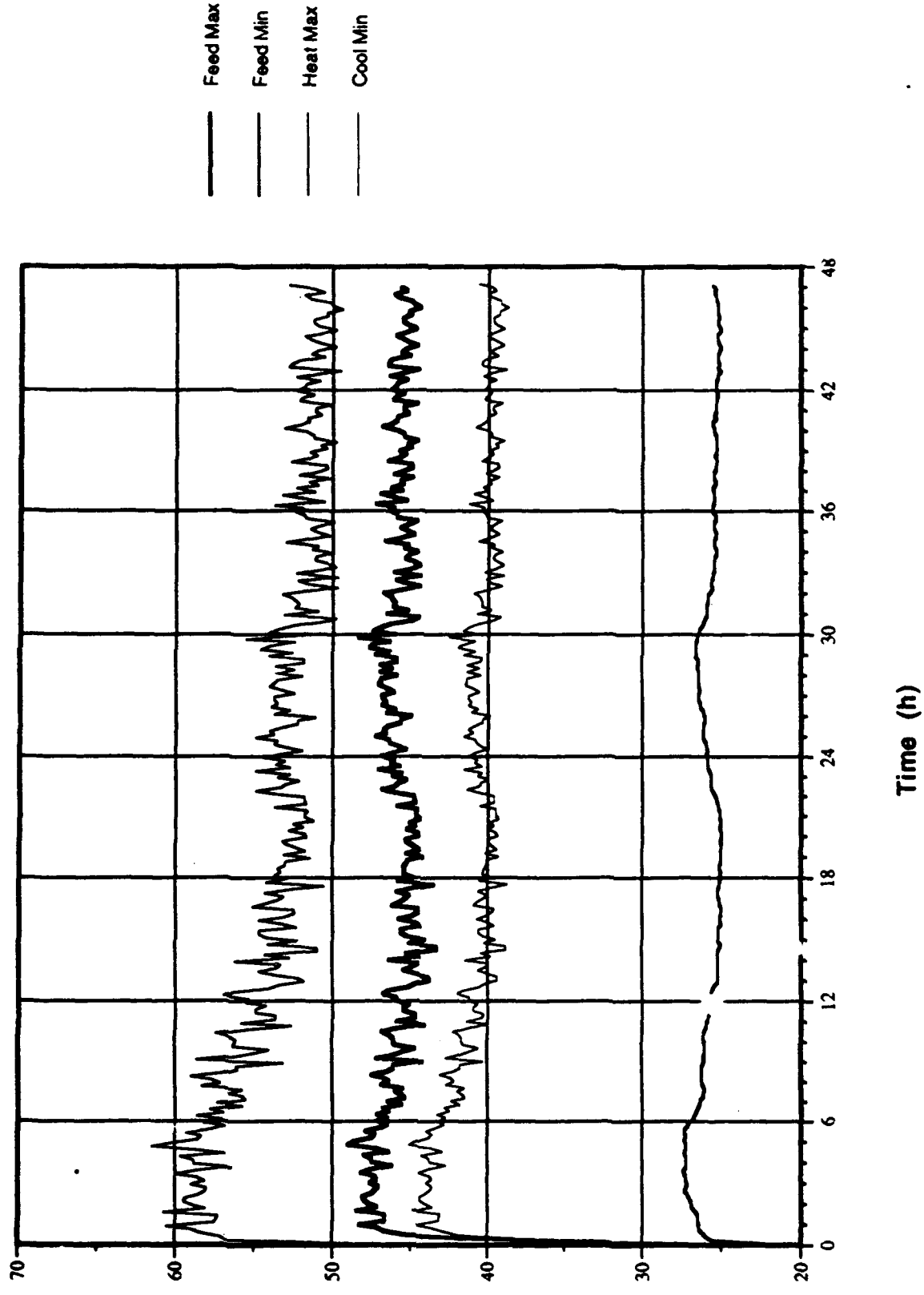
Simulated Two Step 5cm 051193
R-113
300s Feed; 30s Heat; 270s Cooldown
Feed Max
Feed Min
Heat Max
Cool Min
70
60
50
40
30
20
0
6
12
18
24
30
36
42
48
Time (h)

Figure 4

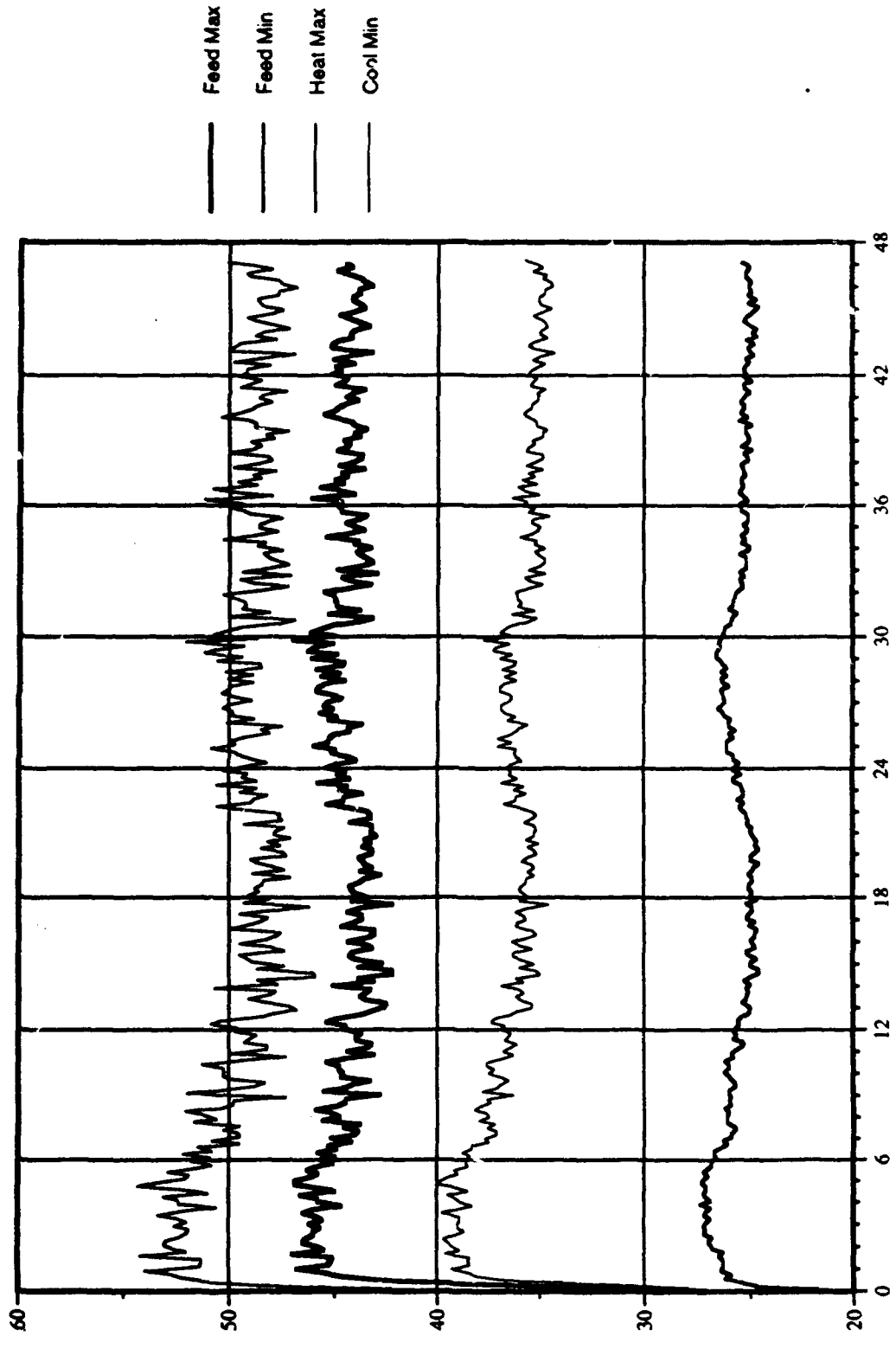
Simulated Two Step 10cm 051193
R-113
300s Feed; 30s Heat; 270s Cooldown
Feed Max
Feed Min
Heat Max
Cool Min
60
50
40
30
20
0
6
12
18
24
30
36
42
48
Time (h)
C°

Figure 5

Simulated Two Step 15cm 051193
R-113
300s Feed; 30s Heat; 270s Cooldown

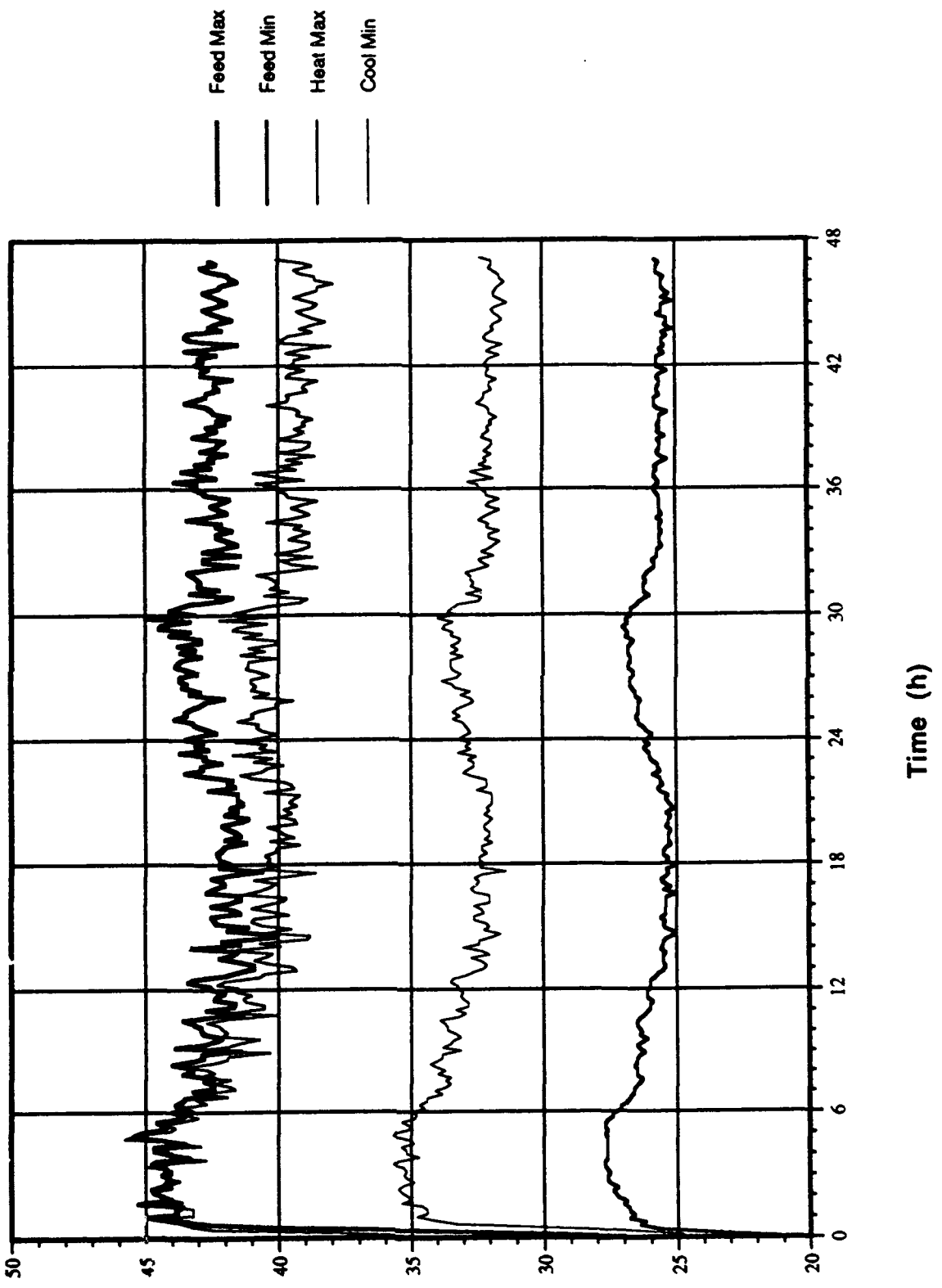

Figure 6

Simulated Two Step 20cm 051193
R-113
300s Feed; 30s Heat; 270s Cooldown

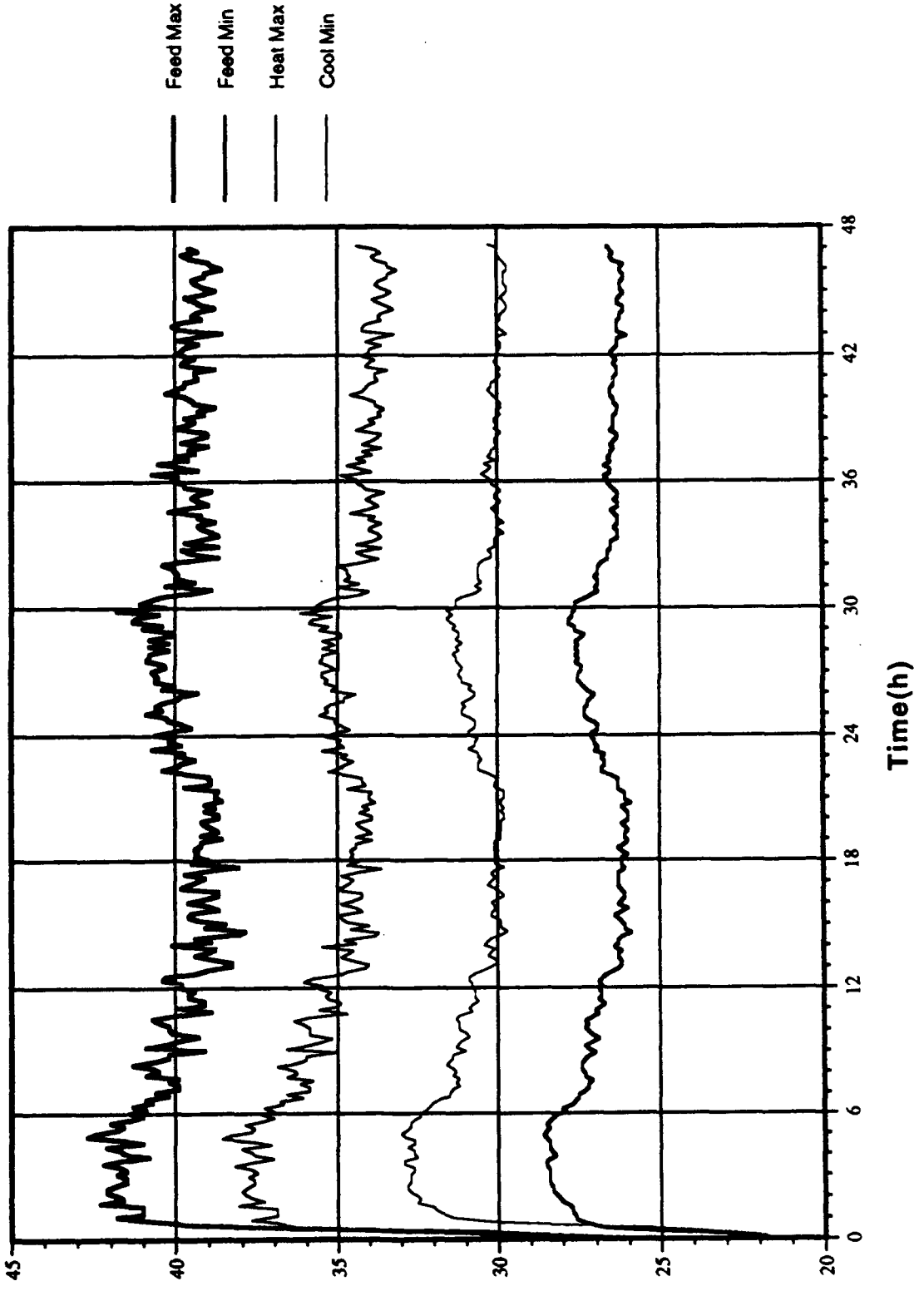

Figure 7

Simulated Two Step 25cm 051193
R-113
300s Feed; 30s Heat; 270s Cooldown

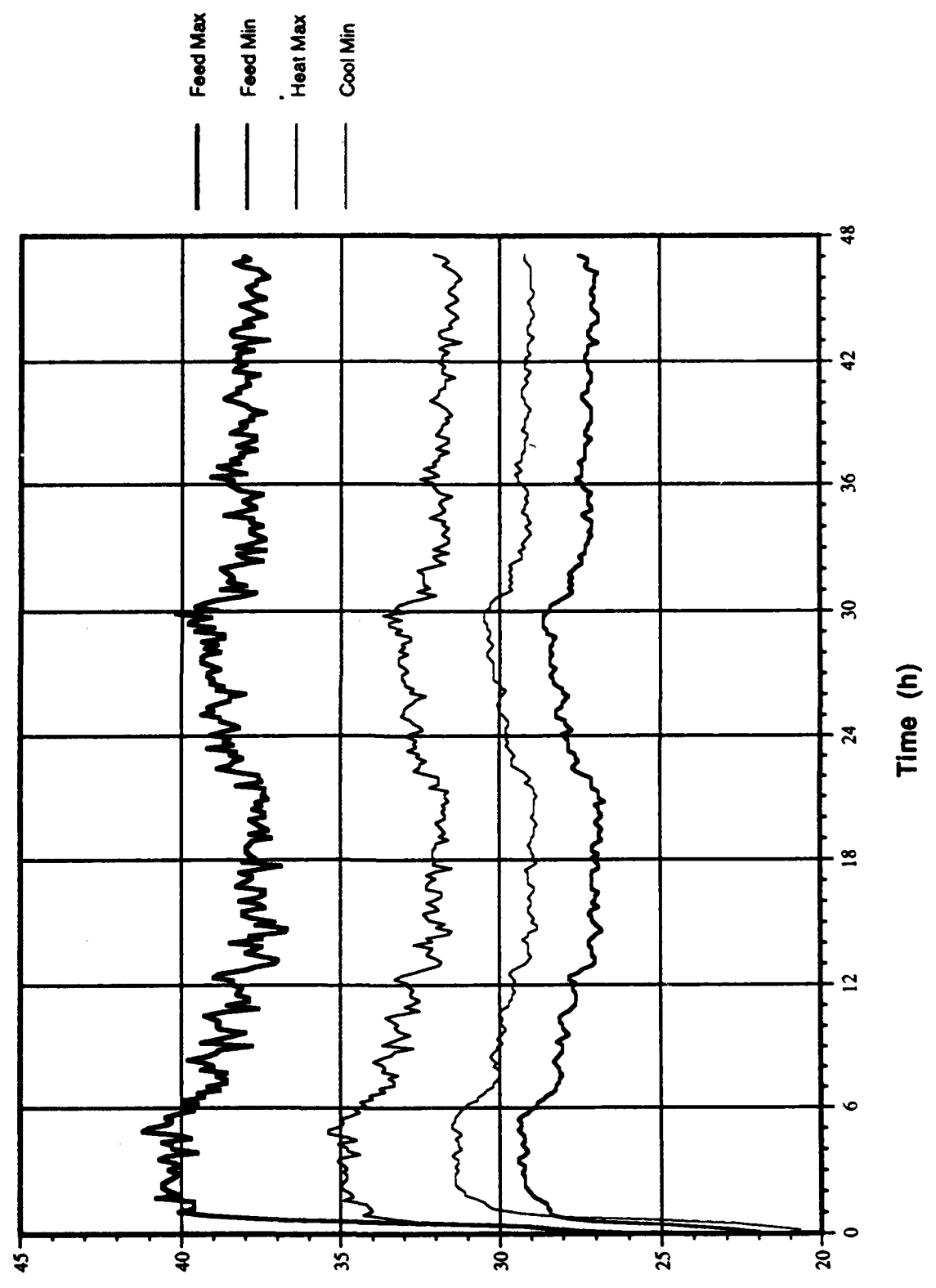

Figure 8

Feed and Purge Material 051193